

AD-A100 306

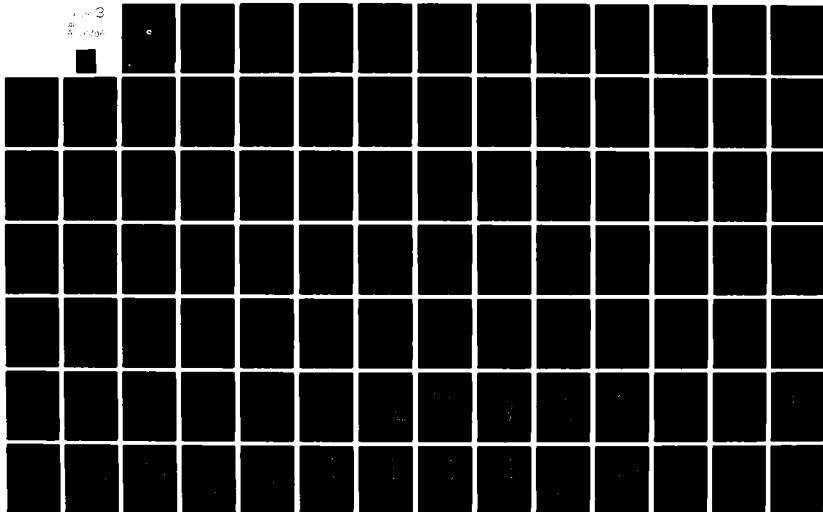
CALIFORNIA UNIV BERKELEY DEPT OF NAVAL ARCHITECTURE F/G 20/4
MODEL TESTS AND NUMERICAL SIMULATION OF SHIP CAPSIZING IN FOLLO--ETC(U)
JAN 80 W J FALLON, Y. HWANG, J L LIGUORI DOT-CG-64601-A

USCG-D-08-81

NL

UNCLASSIFIED

3
Page



REPORT NO. USCG-DH-88-81

LEVEL 12

MODEL TESTS AND NUMERICAL SIMULATION OF SHIP
CAPSIZING IN FOLLOWING SEAS.

AD A100306

William J. Fallon
Yuh-Lin Hwang
Jose Lescaut Liguori
J. R. Paulling
Gregg Visineau
Paul D. Wood

Department of Naval Architecture and Offshore Engineering
University of California, Berkeley, CA 94720

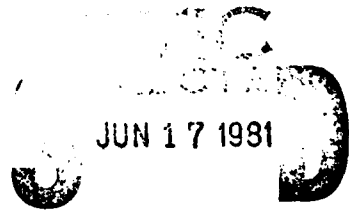


FINAL REPORT FOR PERIOD

December 1976 - October 1979,

January 1980

Document is available to the U.S. Public through the
National Technical Information Service,
Springfield, Virginia 22161



DIC FILE COPY

PREPARED FOR

A

U.S. DEPARTMENT OF TRANSPORTATION

UNITED STATES COAST GUARD

OFFICE OF RESEARCH AND DEVELOPMENT

WASHINGTON, D.C. 20590

JUN 17 1981
406 218

81 6 15 133

NOTICE

This document is disseminated under the sponsorship of the Department of Transportation in the interest of information exchange. The United States Government assumes no liability for its contents or use thereof.

The contents of this report do not necessarily reflect the official view or policy of the Coast Guard; and they do not constitute a standard, specification, or regulation.

This report, or portions thereof may not be used for advertising or sales promotion purposes. Citation of trade names and manufacturers does not constitute endorsement or approval of such products.

1. Report No. CG-D-08-81	2. Government Accession No. A100306	3. Recipient's Catalog No.	
4. Title and Subtitle Model Tests and Numerical Simulation of Ship Capsizing in Following Seas		5. Report Date January 1980	6. Performing Organization Code
		8. Performing Organization Report No.	
7. Author(s) Fallon, Hwang, Lescaut, Paulling, Visineau, Wood		10. Work Unit No. (TRAIS)	
9. Performing Organization Name and Address Department of Naval Architecture University of California Berkeley, CA 94720		11. Contract or Grant No. DOT-CG-64601-A <i>new</i>	
		13. Type of Report and Period Covered Final Report December 1976 - October 79	
12. Sponsoring Agency Name and Address Department of Transportation United States Coast Guard Washington, D.C.		14. Sponsoring Agency Code	
		15. Supplementary Notes	
16. Abstract <p>This report presents some comparisons of experimental data and computational simulations of the severe roll motion and capsizing of ships operating in following seas. Earlier reports have described experiments conducted using radio-controlled ship models in San Francisco Bay for the purpose of studying the phenomenon of ship capsizing and the initial development of a computer simulation of the same phenomenon. The present report describes experiments conducted in the towing tank using three models: a <u>Mariner</u> class cargo ship, a model of the <u>SL7</u> container ship, and a west coast crab fishing boat. The principal objectives of these experiments was to provide data with which to test the simulator program. In addition to these experiments, the report describes some studies made using a simple one-degree-of-freedom simulator program. A final Appendix contains a description of the simulator program and instructions for its use.</p>			
17. Key Words Ship Stability Capsizing Model Tests Computer Simulation		18. Distribution Statement Document is available to the public through the National Technical Information Service, Springfield, Virginia 22151	
19. Security Classif. (of this report) Unclassified	20. Security Classif. (of this page) Unclassified	21. No. of Pages	22. Price

METRIC CONVERSION FACTORS

Approximate Conversions to Metric Measures

Symbol	When You Know	Multiply by	To Find	Symbol
LENGTH				
in	inches	2.5	centimeters	cm
ft	feet	30	centimeters	cm
yd	yards	0.9	meters	m
mi	miles	1.6	kilometers	km
AREA				
sq ft	square inches	6.5	square centimeters	cm ²
sq ft	square feet	0.09	square meters	m ²
sq yd	square yards	0.8	square meters	m ²
sq mi	square miles	2.6	square kilometers	km ²
acres	acres	0.4	hectares	ha
MASS (weight)				
oz	ounces	28	grams	g
lb	pounds	0.45	kilograms	kg
	short tons (2000 lb)	0.9	tonnes	t
VOLUME				
teaspoon	teaspoons	5	milliliters	ml
tablespoon	tablespoons	15	milliliters	ml
fluid ounce	fluid ounces	30	milliliters	ml
cup	cups	0.24	liters	l
pint	pints	0.47	liters	l
quart	quarts	0.96	liters	l
gallon	gallons	3.8	liters	l
cu ft	cubic feet	0.03	cubic meters	m ³
cu yd	cubic yards	0.76	cubic meters	m ³

TEMPERATURE (exact)

°F	Fahrenheit temperature	5/9 (after subtracting 32)	Celsius temperature	°C
----	------------------------	----------------------------	---------------------	----

Symbol	When You Know	Multiply by	To Find	Symbol
LENGTH				
mm	millimeters	0.04	inches	in
cm	centimeters	0.4	inches	in
m	meters	3.3	feet	ft
km	kilometers	1.1	yards	yd
		0.6	miles	mi
AREA				
cm ²	square centimeters	0.16	square inches	sq in
m ²	square meters	1.2	square yards	sq yd
km ²	square kilometers	0.4	square miles	sq mi
ha	hectares (10,000 m ²)	2.5	acres	acres
MASS (weight)				
g	grams	0.035	ounces	oz
kg	kilograms	2.2	pounds	lb
t	tonnes (1000 kg)	1.1	short tons	short tons
VOLUME				
ml	milliliters	0.03	fluid ounces	fl oz
l	liters	2.1	pints	pt
l	liters	1.06	quarts	qt
l	liters	0.26	gallons	gal
m ³	cubic meters	35	cu ft	ft ³
m ³	cubic meters	1.3	cubic yards	yd ³
TEMPERATURE (exact)				
°C	Celsius temperature	9/5 (then add 32)	Fahrenheit temperature	°F



* In a 2.54 exactly. For other exact conversions and more detailed tables, see NBS Misc. Publ. 286, Units of Weight and Measure, Price \$2.25, SD Catalog No. C13.1U 286.

TABLE OF CONTENTS

INTRODUCTION	1
II. <u>THE CAPSIZE SIMULATOR</u>	5
Numerical simulation of the motion in astern seas.	7
Formulation of the problem.	7
Newton's second law for a rigid body.	7
Coordinate systems.	8
Time domain integration.	12
Computation of force and moment.	15
Wave diffraction, added mass and damping.	18
Steering system.	20
Thrust-resistance force.	22
Wind force and moment.	22
Other forces.	23
III. <u>TOWING TANK MODEL EXPERIMENTS</u>	25
MARINER model.	25
Motion restraints.	26
Experimental measurements and parameters.	26
Experimental results and observations.	28
Comparison of simulations with MARINER experiments.	31
Simulation results for the MARINER.	32
Factors which influence results.	33
Effect of roll damping.	34
Effect of suppression of surge, sway and yaw.	36
SEA LAND 7 containership model.	36
Comparison of simulation with SL-7 experiments.	38
Experimental observations.	40
Pacific Crab Boat model.	41
Experimental results and observations.	43
Comparison of simulations with experiments.	46
IV. <u>A ONE DEGREE-OF-FREEDOM MODEL OF THE NONLINEAR ROLLING MOTION OF A SHIP IN WAVE GROUPS</u>	110
One degree-of-freedom equation of rolling motion in oblique seas.	110
Determination of the damping coefficient.	112
Determination of the righting moment of a ship in waves.	113
Numerical solution to the problem.	114
CONCLUSIONS	123
REFERENCES	126
Appendix A: Principal Dimensions, Body Plans, Table of Offsets	128
Appendix B: Motion Restraint Mechanism, Model Arrangement, Instrumentation	B-1

Appendix C: Inclining Experiment Procedure, Table of Measured Metacentric Heights, Procedure for Measuring Moments of Inertia	C-1
Appendix D: Initial Conditions for Capsize Simulator	D-1
Appendix E-I: User Manual for Program CAPSIZE	E-1
Appendix E-II: CAPSIZE Program Description	E-33

FIGURES

Figure II-1: Coordinate Rotations	10
Figure III-1: Mariner 77.7 and American Challenger Righting Arm Curves	66
Figure III-2: Mariner 77.7 and American Challenger Righting Moment	67
Figure III-3: CAPSIZE: Integration Time Step	68
Figure III-4: CAPSIZE: Offsets	69
Figure III-5: MARINER CAPSIZE RUN 0901-41A	70
Figure III-6: MARINER CAPSIZE RUN 0901-41A	71
Figure III-7: MARINER CAPSIZE RUN 0905-55J3	72
Figure III-8: MARINER CAPSIZE RUN 0905-55J3	73
Figure III-9: MARINER CAPSIZE RUN 0905-55J3	74
Figure III-10: MARINER CAPSIZE RUN 0911-79B1	75
Figure III-11: MARINER CAPSIZE RUN 0911-79B1	76
Figure III-12: CAPSIZE: GM	77
Figure III-13: CAPSIZE: WAVE AMPLITUDE	78
Figure III-14: MARINER ROLL DECAY	79
Figure III-15: MARINER ROLL DECAY	80
Figure III-16: MARINER ROLL DECAY	81
Figure III-17: MARINER ROLL DECAY	82
Figure III-18: CAPSIZE RUN 0901-41A SIX DEOF	83
Figure III-19: CAPSIZE RUN 0901-41A SIX DEOF	84
Figure III-20: CAPSIZE RUN 0901-41A SIX DEOF	85
Figure III-21: CAPSIZE RUN 0901-41A SIX DEOF	86
Figure III-22: SEA LAND 7 CONTAINER VESSEL Righting Arm Curves	87
Figure III-23: SL7 CAPSIZE RUN 0409-46LQ 3 DEOF	88
Figure III-24: SL7 CAPSIZE RUN 0409-63LQ 3 DEOF	89

Figure III-25:	SL7 CAPSIZE RUN 0409-45LQ 3 DEOF	90
Figure III-26:	SL7 CAPSIZE RUN 0409-45LQ 3 DEOF	91
Figure III-27:	SL7 CAPSIZE RUN 0409-61LQ 3 DEOF	92
Figure III-28:	SL7 Roll Decay 3 DEOF	93
Figure III-29:	SL7 Roll Decay 3 DEOF	94
Figure III-30:	Pacific Coast Crab Boat Righting Arm Curves 100GM/B = 7.5	95
Figure III-31:	Pacific Coast Crab Boat Righting Arm Curves 100GM/B = 4.0	96
Figure III-32:	Pacific Coast Crab Boat Righting Arm Curves 100GM/B = 3.5	97
Figure III-33:	Pacific Coast Crab Boat Righting Arm Curves 100GM/B = 2.5	98
Figure III-34:	Crab Boat Model Free Roll Decay	99
Figure III-35:	Crab Boat Model Free Roll Decay	100
Figure III-36:	Crab Boat Model Free Roll Decay	101
Figure III-37:	Crab Boat Model Free Roll Decay	102
Figure III-38:	Crab Boat Model Free Roll Decay	103
Figure III-39:	Crab Boat Model Free Roll Decay	104
Figure III-40:	Crab Boat Model Run #7	105
Figure III-41:	Crab Boat Model Run #8	106
Figure III-42:	Crab Boat Model Run #20	107
Figure III-43:	Crab Boat Model Run #7 (15 DEG)	108
Figure III-44:	Crab Boat Model Run #7 (20 DEG)	109
Figure IV-1:	Coordinate Systems	116
Figure IV-2:	Mariner Run 0918-41A (1 DEOF)	117
Figure IV-3:	Mariner Run 0918-42A (1 DEOF)	118
Figure IV-4:	Mariner Run 0901-45A (1 DEOF)	119
Figure IV-5:	Mariner Run 0901-41A (1 DEOF)	120
Figure IV-6:	Capsize Run 0901-41A (1 DEOF)	121
Figure IV-7:	Capsize Run 0905-55J3 (1 DEOF)	122
Figure A-1:	American Challenger: Body Plan	A-2
Figure A-2:	Modified Mariner: Mariner 77.7 Body Plan	A-3
Figure A-3:	Modified Mariner: Mariner 77.7 Body Plan	A-4
Figure A-4:	SL7 Body Plan (100%)	A-10
Figure A-5:	Ship Plans and Profiles (no scale)	A-18
Figure A-6:	Pacific Coast Crab Boat Body Plan	A-19

Figure B-1:	Mariner 77.7 Model General Arrangement	B-4
Figure B-2:	Mariner Model	B-5
Figure B-3:	Towing Arrangement	B-5
Figure B-4:	Forward Restraint	B-6
Figure B-5:	After Restraint	B-6
Figure B-6:	Mariner 77.7 Model Deck Attachment	B-7
Figure C-1:	Mariner Model (1/96) Inclining Experiment	C-3
Figure E-1:	Block Diagram Showing Principal Segments of of Program CAPSIZE	E-50
Figure E-2:	Block Diagram of Principal Segments of Subroutine Systems COEFS	E-52
Figure E-3:	Block Diagram Showing Principal Segments of Subroutine System CAPSIZ	E-53

TABLES

Table III-1:	Summary of Mariner Experimental Runs	50
Table III-2:	Summary of SL7 Experimental Runs	54
Table III-3:	Pacific Coast Crab Boat Speed and Wave Parameters	63
Table III-4:	Pacific Coast Crab Boat Model Frequencies of Encounter	64
Table III-5:	Pacific Coast Crab Boat Summary of Experimental Runs	65
Table A-1:	Principal Dimensions of the Mariner and American Challenger	A-1
Table A-2:	Mariner - Full Table of Offsets	A-6
Table A-3:	Mariner - Partial Table of Offsets	A-8
Table A-4:	Principal Dimensions - SEALAND 7	A-9
Table A-5:	SEALAND 7 Full Table of Offsets	A-11
Table A-6:	SEALAND 7 Partial Table of Offsets	A-14
Table A-7:	Pacific Coast Crab Boat - Principal Dimen.	A-15
Table A-8:	Pacific Coast Crab Boat - Test Conditions	A-16
Table A-9:	CRAB BOAT - Table of Offsets	A-17
Table B-1:	Instrumentation	B-8
Table C-1:	Mariner 77.7 Measured Metacentric Height (GM)	C-4
Table D-1:	Mariner 77.7 Initial Conditions for Capsize Simulator	D-2

Table D-2: Initial Conditions for Capsize Simulator for the SL7	D-3
Table D-3: Pacific Coast Crab Boat Initial Conditions for Capsize Simulator	D-4

I. INTRODUCTION

A ship operating in a quartering or longitudinal seaway, where the waves are moving in a direction parallel to the ship longitudinal centerline, experiences a fluctuation of transverse stability above and below the still water value as a result of

- (a) variation of the geometry of the immersed hull as waves pass
- (b) variation of the water pressure distribution on the hull caused by water particle motion in waves [1]*.

This fluctuation of transverse stability has important consequences for certain ship forms. The most important geometric characteristics of the ship in determining the magnitude of this effect are freeboard and vertical location of the center of gravity. Consider a longitudinal seaway with wave lengths equal to the ship length. A wave crest at amidships causes a reduction and a trough at amidships causes an increase of the transverse stability. Righting arm curves for two vessels in calm water and statically poised on a wave are shown in figure III-1. Two possible consequences of this reduction in stability are:

1. Static capsizing if the reduction in transverse stability is sufficient. This may occur for example, if the ship operates in very high, steep following waves with a speed such that she remains on the wave crest for a sufficiently long time interval.
2. If the ship and wave speeds differ, the waves may slowly overtake the ship, or vice versa, resulting in a time-varying roll restoring moment. Under these circumstances, a phenomenon termed "autoparametric excitation" can occur which may result in severe resonant rolling. This is most likely to occur at ratios of the natural roll frequency to wave encounter frequency in the vicinity of $1/2$, 1 , $3/2$, and so on. In the extreme case, this may build up to such magnitude as to cause capsizing [2].

*[] indicates reference at end of text.

In order to visualize this latter effect, consider a ship operating in following waves of length equal to the ship length, and traveling at a ship speed such that the wave encounter frequency is twice the natural frequency of roll. Now, let the ship be heeled to starboard when a wave trough is at midship. In this position the righting moment is greater than the still water value. The ship consequently tends to roll back toward the port side. As it passes the upright position, as a result of the relative speed of ship and waves a crest now moves into the amidships position. The righting moment on the ship, when passing through the upright position, is consequently smaller than the still water value and may even be negative as shown in figure III-2. If it is small enough, the roll motion to the port side will meet with little resistance and a large roll to port may ensue. With the ship rolled to port a wave trough now moves into the amidships position and the ship is accelerated back to starboard. This sequence of events may continue through several cycles until either:

1. the roll amplitude has grown enough to cause capsizing,
2. a steady-state roll amplitude is reached and maintained,
3. the ship moves into waves of different frequency so that resonant roll is no longer being excited and the roll amplitude dies out.

Model experiments have shown the second mode of capsizing due to resonant rolling can occur if the following conditions are fulfilled:

1. the wave length is in the range of three-quarters to one-and-one times the ship length,
2. the wave height to length ratios of about thirty or steeper,
3. the ship is operating in quartering or following seas,
4. the ship encounters two to six consecutive, nearly regular waves having the characteristics of (1), (2), (3) above.

It follows that this type of capsizing occurs only in extreme sea conditions and the necessary combination of events has a very low probability of occurrence. The proper combination of circumstances may, however, occur in nature, and the conditions for its

occurrence may be encountered by a ship during the course of her lifetime.

For several years, the University of California's Department of Naval Architecture has been studying the capsizing of ships in quartering and following seas through a program sponsored by the United States Coast Guard. The goals of the program are:

1. make qualitative observations of model tests to determine what parameters are important in leading to a capsize,
2. develop an analytic technique for predicting a capsize. This has taken the form of a computer program which simulates the six degrees of ship motion up to the point of capsizing,
3. provide experimental verification of the program and documentation for the capsize simulator.

From 1970 to 1974 free running ship model tests were conducted in San Francisco Bay [2], [6], [10]. Two models of somewhat different form were used. The first was an eighteen foot long, 1/30 scale model of the American Challenger class cargo ship and the second, a seventeen foot long, 1/55 scale model of the Sea Land 7 class container ship. Following the physical understanding of the capsizing phenomenon, as a result of the experiments, several computer programs were developed which have coalesced to the final version called CAPSIZE, a ship motions simulator with six degrees of freedom.

The purpose of experiments described in the present report is to provide experimental verification of the predictions. CAPSIZE simulates ship motions in the time domain, and, in order to obtain complete comparisons of simulated motions with measured motions it is necessary to record not only the model motions, but also the waves which cause those motions. For practical reasons, the wave data in the San Francisco Bay model tests were collected only on a statistical basis in the general vicinity of the experiments. Thus, the average conditions at the time of test (and capsize) were known but not the specific waves in which the model was operating. In order to test the simulator program, however, it is necessary to have the exact wave profile at the

model location and this requires model tests which are conducted under more controlled conditions than were possible in the open waters of San Francisco Bay. The essential quantities to be recorded in the model tests are considered to be:

1. the ship motions with emphasis on roll,
2. the wave profile along the length of the model or wave measurements at one or more longitudinal positions such that the profile can be reconstructed.

A prerequisite to an experimental test of the program is the ability to control the generated waves. In this way, one may test the model in a predetermined seaway which may consist of anything from simple sinusoidal waves to more complex patterns obtained by the superposition of two or more sinusoidal waves. The limiting case is the complete random wave system having a predetermined spectral content.

To meet these requirements, model tests were conducted at the University of California's ship model towing tank. For practical reasons, a complete duplication of all conditions encountered in San Francisco Bay could not be attained. The principal restraint was imposed by the dimensions of the towing tank. As a result, the conditions under which the tests were conducted involved certain restrictions on the freedom of model motions. The essential features influencing large roll motion and capsizing were, however, preserved.

the motion variable of principal interest is rolling in following or quartering seas, and therefore, the experimental investigation reported in a later section of this report is concentrated on the measurement of roll motion. The validity of the program's simulation of pitch, yaw, surge, heave, and sway in following seas is not thoroughly investigated nor are sea directions other than dead astern. The restriction of experimental studies to following seas is, of course, a consequence of the towing tank proportions.

Numerical solution of the equations of motion in the time domain makes the program versatile. It is relatively easy to add other effects to the simulation, for example, anti-roll tanks or damping coefficients having a complex dependence on motion.

PRECEDING PAGE BLANK-NOT FILLED

Numerical Simulation of the Motion in Astern Seas.

Formulation of the problem.

A complete analytical solution for the motion of a ship in waves requires first that the hydrodynamic forces acting on the ship be found. Solutions of the hydrodynamic problems have heretofore been obtained only under the assumption of small motion amplitudes, in which case the forces acting on the ship differs but little from its mean position. Such an assumption cannot be used in the present case where large deviations in position from the mean are an essential feature of the phenomenon. Instead, we observe that, at high speed in following and quartering seas, the frequency of wave encounter will be low and the ship motion will be determined largely by the hydrostatic forces. This enables us to retreat from the necessity of determining the hydrodynamic forces with great precision but to concentrate instead on the hydrostatic forces which may be computed for the exact position of ship and waves. These forces, plus additional external forces representing, e.g., the steering and controls, plus a simplified approximation to the relatively unimportant hydrodynamic terms then are used as the right hand side of the rigid body equations of motion. A standard numerical procedure is employed to integrate the equations of motion leading to a step-by-step approximation of the vessel's motion.

Newton's second law for a rigid body.

The ship is assumed to behave as a rigid body having six degrees of freedom. Newton's second law may be written for the body in the form

$$\frac{d}{dt} m \dot{y} = f \quad (1)$$

and

$$\frac{d}{dt} I \dot{\theta} = g \quad (2)$$

where

t = time
 m = mass of the body (ship),
 \mathbf{v} = velocity vector of the mass center,
 \mathbf{f} = force vector,
 \mathbf{I} = inertia matrix,
 $\mathbf{\omega}$ = angular velocity vector, and
 \mathbf{g} = moment of the force about the mass center.

The force and moment result from the gravitational force acting at the mass center and the interaction between the ship and the sea. The force and moment, in general, depend on the time history of the position of the ship in the sea. Under appropriate circumstances, however, this history may be characterized by the instantaneous position, velocity, and acceleration of the ship. The general problem is nonlinear in the motion variables in that the force and moment are nonlinear functions of the motion of the ship, and the rate of change of angular momentum in equation (2) contains nonlinear terms. As noted previously, we shall focus on an exact computation only of the hydrostatic part of the force.

Coordinate systems.

Since large amplitude motions are to be computed, it is necessary to clearly define the relationships between several coordinate systems to be used in describing the ship and water motion. The coordinate systems described below are right hand Cartesian systems.

A Newtonian reference frame is formed by the $\bar{O}\bar{x}\bar{y}\bar{z}$ system which is fixed in space so oriented that the $\bar{x}\bar{z}$ -plane is the equilibrium sea surface, and the \bar{y} -axis is directed upwards.

A body coordinate system $Gxyz$ is fixed in the ship such that the origin, G , coincides with the center of gravity of the ship. In a ship of usual form, the x -axis is parallel to the baseline and directed forward, the xy -plane is parallel to the centerplane of the ship, the y -axis is directed upward and the z -axis to starboard.

The position of the ship mass center, G, may be specified in the fixed coordinate system by

$$\begin{aligned}\bar{x} &= x_G \\ \bar{y} &= y_G \\ \bar{z} &= z_G\end{aligned}$$

This may be represented by the vector

$$\bar{\mathbf{x}} = \begin{Bmatrix} x_G \\ y_G \\ z_G \end{Bmatrix} \quad (3)$$

The velocity of the mass center is represented by the vector

$$\bar{\mathbf{v}} = \frac{d}{dt} \bar{\mathbf{x}} = \begin{Bmatrix} \frac{d}{dt} x_G \\ \frac{d}{dt} y_G \\ \frac{d}{dt} z_G \end{Bmatrix} \quad (4)$$

Any rotation of the ship coordinate system is uniquely defined by the modified set of Eulerian angles described below. These angles are similar to the ones given by Blagoveshchensky in [2], but differ from the ones used by Euler. The angles are defined as follows.

Consider the ship coordinates in a position before rotation with the x, y, and z-axes parallel to the fixed \bar{x} , \bar{y} , \bar{z} -axes. This is the orientation of $Gx_1y_1z_1$ in figure II-1. Rotate the triad about the y_1 -axis to the yaw angle ϕ . This positions the frame as $Gx_2y_1z_2$ in the figure. Next, rotate about the z_2 -axis to the pitch angle ψ . The figure shows the yawed and pitched orientation as Gxy_3z_2 . The final rotation is about the x-axis to the roll angle θ . The orientation of the ship coordinates, $Gxyz$, is indicated in the figure.

The Eulerian angles ϕ , ψ and θ are represented by the vector

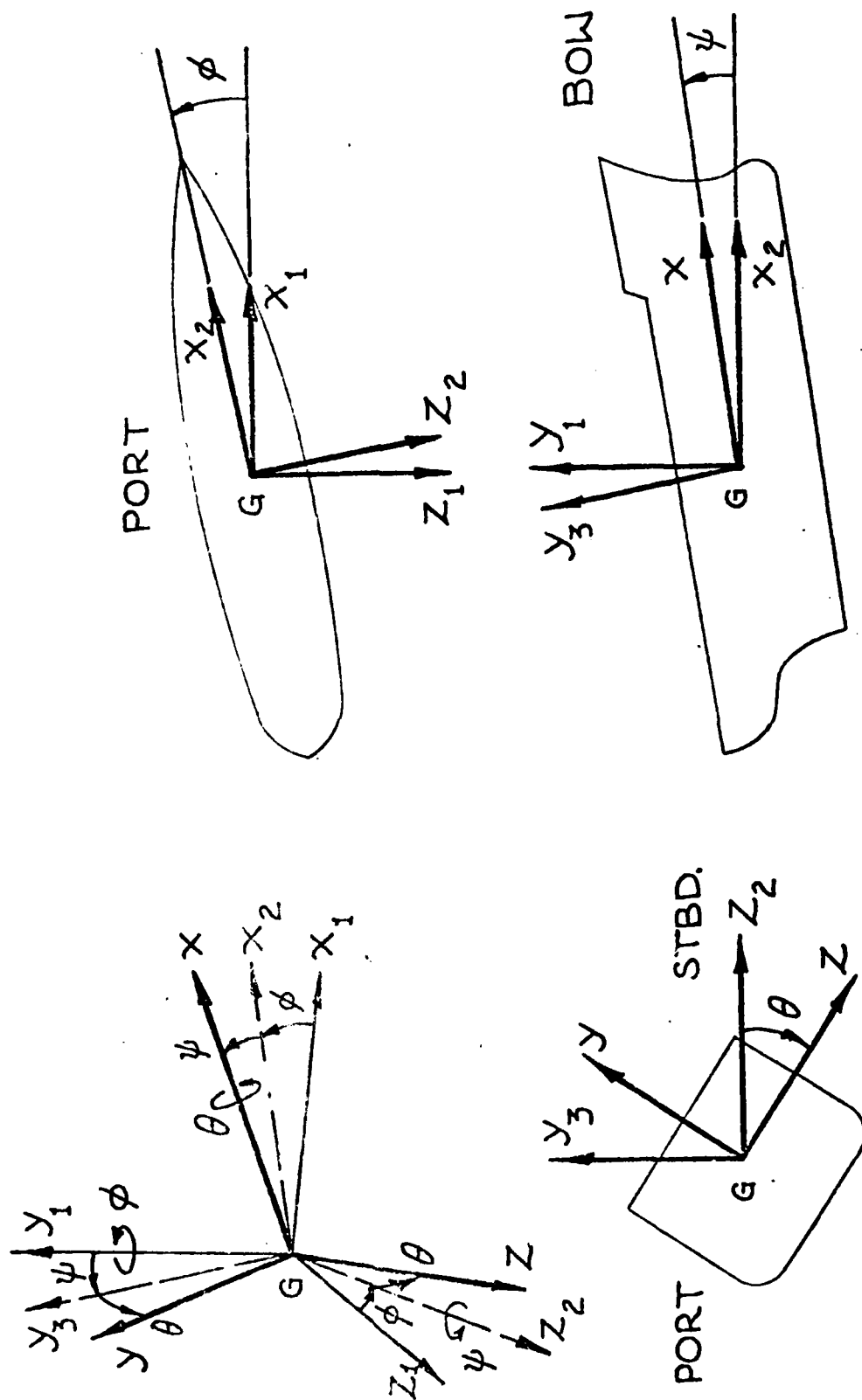


Figure II-1 Coordinate Rotations

$$\alpha = \begin{Bmatrix} \theta \\ \phi \\ \psi \end{Bmatrix} \quad (5)$$

The angular velocities about the ship coordinate axes are denoted by p, q, and r corresponding to components of the angular velocity vector along the x, y, and z-axes. These angular velocities may be expressed in terms of the Eulerian angles and their derivatives:

$$\begin{aligned} p &= \frac{d\theta}{dt} + \frac{d\phi}{dt} \sin \psi \\ q &= \frac{d\phi}{dt} \cos \theta \cos \psi + \frac{d\psi}{dt} \sin \theta \\ r &= \frac{d\psi}{dt} \cos \theta - \frac{d\phi}{dt} \sin \theta \cos \psi \end{aligned} \quad (6)$$

The notation is simplified by representing the angular velocities by the vector

$$\omega = \begin{Bmatrix} p \\ q \\ r \end{Bmatrix} \quad (7)$$

If we define the matrix

$$B = \begin{bmatrix} 1 & \sin \psi & 0 \\ 0 & \cos \theta \cos \psi & \sin \theta \\ 0 & -\sin \theta \cos \psi & \cos \theta \end{bmatrix} \quad (8)$$

and note that

$$\frac{d\alpha}{dt} = \begin{Bmatrix} \frac{d\theta}{dt} \\ \frac{d\phi}{dt} \\ \frac{d\psi}{dt} \end{Bmatrix} \quad (9)$$

then equations (6) are represented by

$$B \frac{d\alpha}{dt} = \omega \quad (10)$$

The moments and products of inertia in the angular momentum equation (2) are represented by the matrix

$$\underline{I} = \begin{bmatrix} I_{xx} & -I_{xy} & -I_{xz} \\ -I_{xy} & I_{yy} & -I_{yz} \\ -I_{xz} & -I_{yz} & I_{zz} \end{bmatrix} \quad (11)$$

The moments of inertia are defined as

$$\begin{aligned} I_{xx} &= \Sigma m' (y^2 + z^2), \\ I_{yy} &= \Sigma m' (z^2 + x^2), \end{aligned} \quad (12)$$

and

$$I_{zz} = \Sigma m' (x^2 + y^2),$$

where the summations are taken over all particles of mass m' comprising the ship. The products of inertia are

$$\begin{aligned} I_{xy} &= \Sigma m' xy, \\ I_{xz} &= \Sigma m' xz, \end{aligned} \quad (13)$$

and

$$I_{yz} = \Sigma m' yz.$$

These moments and products of inertia are constants in the moving ship coordinate system, $Gxyz$.

In the $Gxyz$ coordinate system, the rate of change of angular momentum is given by

$$\frac{d}{dt} \underline{I} \underline{\omega} = \underline{I} \frac{d}{dt} \underline{\omega} + \underline{\omega} \times \underline{I} \underline{\omega} \quad (14)$$

Time domain integration.

The equations of motion are solved by numerical integration in the time domain. In order to perform the integration using standard algorithms, the equations of motion are rewritten as first order ordinary differential equations.

The position of the ship's center of gravity is determined by the linear momentum equation (1). This equation and equation (4) are rewritten as

$$\frac{d}{dt} \vec{v} = \frac{1}{m} \vec{f} \quad (15)$$

and

$$\frac{d}{dt} \vec{x} = \vec{v} . \quad (16)$$

In equations (15) and (16) the vectors are referred to the Newtonian reference frame, \overline{Oxyz} .

The rotations of the ship are governed by the angular momentum equation (2). Combining equations (2) and (14) and re-writing equation (10) give

$$\frac{d}{dt} \vec{\omega} = \vec{I}^{-1} [\vec{g} - \vec{\omega} \times \vec{I}\vec{\omega}] \quad (17)$$

and

$$\frac{d}{dt} \vec{\alpha} = \vec{B}^{-1} \vec{\omega} . \quad (18)$$

In equation (17) the moment vector is referred to the ship coordinate system, $Gxyz$.

The vector equations (15), (16), (17), and (18) form a system of twelve simultaneous first order ordinary differential equations which may be integrated by standard numerical procedures. The original version of the program used a fifth-order Adams type predictor-corrector algorithm developed by Glauz (1960). This features a variable time step to control integration error and an interpolation procedure to avoid the calculation of derivatives at the times chosen for the output of results. At each time step in the integration, the algorithm predicts values for the instantaneous position of the ship and its velocity. The remainder of the program is devoted to the computation of the force and moment used to evaluate (15) and (17). The integration routine collects the position and velocity based on the values of the derivatives (15) through (18), but if the error is small these derivatives are not recomputed.

The time step is decreased whenever the relative error between the predicted and corrected values of any of the dependent variables exceeds a specified value. If the relative error is significantly smaller than this specified tolerance, the step size is increased. The increase in step size reduces the number of time steps required for the time domain integration, and computer time is minimized when everything goes well. The step size reduction can effectively avoid numerical instabilities if a proper error tolerance is selected. Unfortunately, the algorithm also tends to reduce the step size for any instabilities in the system, including physical instabilities. Capsizing is the result of a physical instability. This seems to cause the algorithm to select excessively small time increments in some situations.

The present version of the program uses a simple fourth-order Runge-Kutta integration with a fixed step size which is selected by the user. When a series of simulations are run, the Runge-Kutta routine allows a larger effective time step to be used than the average value that the Adams routine would automatically select. The effective time step for the fourth order Runge-Kutta method is one-half the specified step since the equations (15) and (16) are evaluated four times at the beginning, midpoint and end of each time step.

For computational purposes, equations (15) and (17) are combined. The generalized force vector includes both force and moment:

$$\tilde{f} = \begin{Bmatrix} f_1 \\ f_2 \\ f_3 \\ g_1 \\ g_2 \\ g_3 \end{Bmatrix} = \begin{Bmatrix} f_1 \\ f_2 \\ f_3 \\ f_4 \\ f_5 \\ f_6 \end{Bmatrix} \quad (19)$$

The changing angular momentum in the rotating ship coordinates is included in

$$\vec{f}' = \begin{pmatrix} f_1 \\ f_2 \\ f_3 \\ g_1' \\ g_2' \\ g_3' \end{pmatrix} \quad (20)$$

where the moment components are

$$\vec{g}' = \begin{pmatrix} g_1' \\ g_2' \\ g_3' \end{pmatrix} = \vec{g} - \vec{\omega} \times \underline{I} \vec{\omega} .$$

In (19) and (20) the first three elements are components of force in ship coordinates, and the last three are components of the moment. The generalized acceleration vector is

$$\vec{a} = \frac{d}{dt} \begin{pmatrix} u \\ v \\ w \\ p \\ q \\ r \end{pmatrix} . \quad (21)$$

The inertia of the ship is represented by the matrix

$$\underline{A'} = \begin{bmatrix} m & 0 & 0 & 0 & 0 & 0 \\ 0 & m & 0 & 0 & 0 & 0 \\ 0 & 0 & m & 0 & 0 & 0 \\ 0 & 0 & 0 & I_{xx} & -I_{xy} & -I_{xz} \\ 0 & 0 & 0 & -I_{xy} & I_{yy} & -I_{yz} \\ 0 & 0 & 0 & -I_{xz} & -I_{yz} & I_{zz} \end{bmatrix} \cdot \quad (22)$$

Using this notation the momentum equations (15) and (17) may be written:

$$\underline{A'} \underline{\ddot{a}} = \underline{f'} \cdot \quad (23)$$

After determining the force, this may be solved for the acceleration, $\underline{\ddot{a}}$. For the integration, the first three components of $\underline{\ddot{a}}$, the linear accelerations, are transformed into the fixed coordinate system to provide velocity derivatives (15), and the derivatives of the angular velocity (17) are the last three elements of $\underline{\ddot{a}}$.

Computation of force and moment.

The present version of the computer program for the time-domain simulation of large amplitude ship motions assumes that the force and moment acting on the ship may be modelled using an accurate computation of the hydrostatic or Froude-Krylov forces plus approximations to the hydrodynamic forces.

Since large amplitude motions and finite amplitude waves are assumed, the hydrostatic restoring and coupling coefficients computed for the equilibrium position cannot be used. It has been shown by Paulling in [11] and others that there can be significant variations in the roll restoring moment as a wave progresses along the ship's length as well as the change in this moment caused by large amplitude roll angles. The Froude-Krylov force that is computed by the numerical simulator includes both the motion exciting forces and the restoring force and moment that

result from the situation of the ship in the system of waves at any time step during the simulation.

The sea surface elevation is given by the sum of sinusoidal waves in the fixed, $\bar{0}\bar{x}\bar{y}\bar{z}$, coordinate system. The water surface is given by

$$\bar{\eta}(\bar{t}, \bar{x}, \bar{z}) = \sum_{i=1}^N \eta_i(\bar{t}, \bar{x}, \bar{z}) \quad (24)$$

where

$\bar{\eta}$ = the \bar{y} coordinate of the surface,

and

N = the number of wave components (in the present version of the program $0 \leq N \leq 20$).

The component wave amplitude is:

$$\eta_i = A_i \cos(\bar{x}k_i \cos \delta_i - \bar{z}k_i \sin \delta_i + \phi_i - \sigma_i t)$$

where

A_i = the amplitude of the i -th wave,

σ_i = the circular frequency,

ϕ_i = initial phase angle,

$k_i = \sigma_i^2/g$ = wave number,

g = the gravitational acceleration,

and

δ_i = the direction of the wave propagation.

The wave pressure is

$$p(t, \bar{x}, \bar{y}, \bar{z}) = -\rho g \bar{y} + \sum_{i=1}^N p_i(t, \bar{x}, \bar{y}, \bar{z})$$

$$p_i = \rho g e^{k_i \bar{y}} \eta_i$$

where

ρg = the specific weight of the water.

The Froude-Arylev force and moment may be obtained by integrating the pressure over the entire wetted surface of the ship. By applying Gauss' Theorem the force and moment are given by integrals of the pressure gradient over the submerged volume of the ship. The components of the force and moment in the ship coordinate system, $Oxyz$, are

$$\begin{aligned}
 f_1 &= - \iiint \frac{\partial p}{\partial x} dv \\
 f_2 &= - \iiint \frac{\partial p}{\partial y} dv \\
 f_3 &= - \iiint \frac{\partial p}{\partial z} dv \\
 f_4 &= \iiint (z \frac{\partial p}{\partial y} - y \frac{\partial p}{\partial z}) dv \\
 f_5 &= \iiint (x \frac{\partial p}{\partial z} - z \frac{\partial p}{\partial x}) dv \\
 f_6 &= \iiint (y \frac{\partial p}{\partial x} - x \frac{\partial p}{\partial y}) dv
 \end{aligned}
 \tag{26}$$

which may be represented by the generalized force vector, \vec{f} . In equation (26) the volume element is dv ; f_1 , f_2 and f_3 are forces in the x , y , and z -directions; and f_4 , f_5 and f_6 are moments about these x , y , and z -axes. The integrals are taken over all volume up to the instantaneous sea surface within the envelope of the ship.

The ship hull is approximated by a number of polygons representing the stations of the ship. Each polygon is in a plane defined by a constant value of x in the ship coordinate system. A maximum of 24 line segments are used for each closed polygon station in the ship and a maximum of 25 stations may be used. The stations may be unsymmetrical and unequal station spacings are permitted. The position of the center of gravity may be in any fixed position relative to the ship.

The integrals of the pressure gradients, velocities and accelerations over each station made up with straight line segments are evaluated exactly, but with two restrictions on

the angle of pitch. First, the pitch angle must not become so large as to cause the intersection of a station plane and the instantaneous sea surface to define multiple regions or a closed contour in the station plane. Second, the magnitude of a quantity like the product of the pitch angle and the slope of all component waves must be "small". These two restrictions are satisfied for vessels and of usual proportions in waves with realistic slopes.

The two-dimensional forces and moment at each station are evaluated as functions of the form

$$f(x) = V' + \sum_{i=1}^N [C_i \cos(k_i'x) + S_i \sin(k_i'x)] \quad (27)$$

where

V' is obtained from the static ($\rho g \bar{y}$) part of pressure, C_i and S_i result from the sinusoidal pressure fluctuation for the i -th wave component, and

k_i' is a projection of the wave number onto the x -axis of the ship.

The relative magnitude of C_i and S_i depends on the phase of the waves relative to the center of ship coordinates at each instant of time. The integrals and moments of the functions like (27) along the length of the ship are evaluated with the assumption that V' , C_i and S_i vary linearly in x between adjacent stations of the ship.

Wave diffraction, added mass and damping.

Approximations are used for the hydrodynamic forces resulting from the diffraction of the incident waves and motion of the ship. These forces are computed using constant two-dimensional added mass and linear damping coefficients for each station combined with averages of the water acceleration and velocity relative to the stations. The hydrodynamic approximations are not expected to lead to serious errors if the Froude-Krylov force is dominant. This, as noted, is expected to be the case in the most severe capsizing situations in following or quartering seas.

The hydrodynamic force resulting from the diffraction of the waves is approximated in the following manner. Two dimensional added mass and damping coefficients for heave, sway, roll and roll-sway coupling are entered into the program as constants for each station of the ship. Each time the sectional Froude-Krylov forces are computed by integrating the pressure gradient over a station of the ship, average values of vertical, horizontal and "roll" water velocities and accelerations are also evaluated for the station. The "roll" velocity and acceleration components are the first and second time derivatives of the slopes of constant pressure lines in the plane of the station. The two-dimensional coefficients are scaled by the instantaneous submerged area of the station, and the products of the average water velocities and accelerations with these coefficients yield two-dimensional diffraction forces which are added to the two-dimensional Froude-Krylov forces before the longitudinal integrations are performed.

The force resulting from ship velocities in heave, sway, roll, yaw and pitch are computed in the above manner using the scaled damping coefficients and the components of ship velocity at each station. Since the linear and angular accelerations of the ship are unknown when the forces are being computed, the force resulting from the ship acceleration cannot be computed with the same procedure. Instead, a matrix of three-dimensional added mass coefficients is computed using the scaled two-dimensional added mass coefficients. The product of this added mass matrix and the vector of accelerations, gives the required force vector. The generalized acceleration vector, \underline{a} , is defined by equation (21). The hydrodynamic force and moment resulting from this acceleration is

$$\underline{h} = -\underline{A}'' \underline{a} \quad (28)$$

where \underline{A}'' is the added mass matrix. The use of the longitudinal moments of the two-dimensional added mass coefficients leaves the elements, A_{ij}'' , which are related to surge (i or j equal to 1) undefined. They are taken as zero.

In order to use this hydrodynamic force, the momentum equation (23) is rewritten as

$$\underline{A}' \underline{a} = \underline{f}' + \underline{h} \quad (29)$$

where the right hand side is the sum of all forces on the ship. The inertia matrix for the ship is \underline{A}' .

The substitution of equation (28) into equation (29) gives the momentum equation including added mass:

$$\underline{A} \underline{a} = \underline{f}' \quad (30)$$

where

$$\underline{A} = \underline{A}'' + \underline{A}' .$$

Equation (30) is solved to obtain the accelerations required for integration.

Steering system.

The steering system of a typical ship consists of three components--an autopilot, steering machinery and the rudder. The autopilot computes a rudder angle which should correct or prevent errors in the ship's heading. The machinery attempts to rotate the rudder to the angle specified by the autopilot. This rotation is mechanically limited to some maximum rate of rotation and some maximum rudder deflection angles. The rudder acts as a lifting surface in the water which generates forces and moments on the ship which are used to maintain the desired course. The steering system for the numerical simulation incorporates these three components.

The autopilot model computes a required rudder angle which is a linear combination of the yaw rate, the yaw angle (heading error), and the time integral of the yaw angle. The proportionality factor or "gain parameter" for any of these heading functions may be set to zero resulting in a simpler autopilot. For example, the yaw integral gain parameter is zeroed to simulate the autopilots used for the CHALLENGER and SL-7 models that were run on

San Francisco Bay. The yaw angle used for the heading error and yaw integral is the angle ϕ which is always measured about a fixed vertical axis. The yaw rate is measured in the ship coordinates rather than about a fixed vertical axis. This is the same as used in the ship model autopilots but it may differ from that used in some full sized autopilots. Two "dead band" parameters are provided in the simulated autopilot. If the magnitude of the heading error is less than the first dead band parameter, the autopilot will require a zero rudder rather than the value computed using the gain parameters. This type of dead band is typical of the "weather" adjustment on ship autopilots. The other dead band available in the simulation was incorporated in the ship model autopilots. With this form of dead band the magnitude of the required rudder angle is reduced by the value of this dead band parameter.

The steering machinery is modeled with constant values for the rate of rotation of the rudder and limits to the magnitude of rudder deflection. If the autopilot requires a rudder deflection rate that is less than the machinery rate and an angle that is less than the mechanical stops, the machinery simulation sets the rudder to the autopilot angle. Otherwise, the rudder angle lags that computed by the autopilot.

The rudder is simulated by a vertical line (in ship coordinates) through an effective center of the rudder. The average of the water velocity relative to points on this line is computed at each time step. The water velocity across this line is the superposition of the motion of the ship, the motion of the water particles in the waves, and a constant wake velocity. The lift and drag forces on the rudder are assumed to be proportional to the instantaneous submerged rudder area, the square of the average relative water velocity, and to the angle of incidence between the rudder and the average water velocity. Rudder lift is limited by a stall angle. The lift and drag forces are resolved into force and moment components in the ship coordinate system.

Thrust-resistance force.

Surge damping is controlled by a table of resistance versus speed data. The surge retarding or accelerating force is obtained by interpolation in a resistance table. This surge force is equal to the resistance at the desired speed minus the resistance for the instantaneous velocity. The total resistance of the ship as a function of speed is simulated by providing a table of resistance forces, $R(v)$, for several speeds, $v = v_1, v_2, \dots, v_n$. The program is provided with the intended ship speed, v_s . The propulsion system is assumed to provide constant thrust, equal in magnitude to the resistance at the intended mean speed. At each time step the surge force due to any difference between the intended speed and the instantaneous speed is

$$f_x = R(v_s) - R(v_x) . \quad (31)$$

The resistance function, $R(v)$, is assumed to be linear between tabulated speeds.

Wind force and moment.

Certain forces due to wind loading may be included. The simulation provides for a sway force and roll and yaw moments which are proportional to the square of the wind speed and the sine of the angular difference between the instantaneous yaw angle and a constant direction towards which the wind is blowing. Since wind directions are traditionally measured as the direction from which the wind is blowing, these forces are proportional to the sine of the sum of the wind direction and the yaw angle. The force and moments are given by

$$\begin{aligned} f_z &= \omega^2 \cdot D \cdot C_z \cdot \sin(\phi + \phi_\omega) \\ f_\theta &= \omega^2 \cdot D \cdot C_\theta \cdot \sin(\phi + \phi_\omega) \\ f_\phi &= \omega^2 \cdot D \cdot C_\phi \cdot \sin(\phi + \phi_\omega) \end{aligned} \quad (32)$$

where

f_2 is the sway force,

f_θ is the roll moment,

f_ϕ is the yaw moment,

ω is the wind speed,

D is an average drag coefficient per unit area or an average pressure coefficient,

C_z is the projected lateral area of the ship above the waterline,

C_θ is the vertical moment of the projected area above the waterline,

C_ϕ is the longitudinal moment of the projected area above the waterline,

ϕ is the yaw angle,

ϕ_ω is the direction from which the wind is blowing.

The moments, C_θ and C_ϕ , may be taken about the center of gravity of the ship if the hydrodynamic moments about the same origin are supplied for the sway velocities induced by the wind sway force. In practice, the sway force and yaw moments are ignored, and the origin for the roll moment is taken as the center of projected area below the waterline. This corresponds to the Coast Guard's "Weather Criterion" for minimum roll metacentric height above the center of gravity.

Other forces.

An additional damping force may be computed and included for any of the six motion components. Let f_i be one of the components of force or moment in the ship coordination system. Let l_i be the average over the volume of the ship of a component of the linear or angular velocity of the ship relative to the

water, and let q_i be the average of the square of the relative velocity. The force or moment is then computed from

$$f_i = f_i^* - l_i L_i - q_i Q_i \quad (33)$$

where

f_i^* = force or moment due to the waves, wind, propulsion, and steering systems,

L_i = coefficient of linear damping for the particular motion component,

Q_i = coefficient of quadratic damping for the particular motion component.

There are three force and moment equations using these three-dimensional linear and quadratic damping constants, but in practice the only non-zero coefficients used with the simulation are for roll damping.

III. Towing Tank Model Experiments

Mariner model.

Most of the background for the development of the capsize simulator was founded on the observations made during the open bay experiments. In order to properly test the computer program, therefore, it is desirable to conduct experiments in laboratory conditions which are as similar as possible to those of the open bay waters.

The ship model towing tank at the University of California has a usable test length of about one hundred and fifty feet. The tank is eight feet wide and has a water depth of five feet. These tank dimensions restrict the length of the ship models to about six feet. An American Challenger model of this size was not available, however a 1/96 scale model of the Mariner class cargo ship was on hand. The American Challenger and Mariner have similar dimensions and hull form as shown in table A-1 and it was decided that the Mariner model could be used after some minor modifications were made to it. The Mariner above water profile was changed to be identical to the American Challenger. Figure A-1 shows the American Challenger body plan and figure A-2 shows the modified Mariner, "Mariner 77.7", body plan. The depth at the side along the entire length, drafts fore and aft, and the vertical center of gravity are adjusted to give a righting arm curve similar to that of the American Challenger. It is found that, by multiplying the depth and drafts by 77.7/75, the desired shape of the righting arm curve is achieved (see figure III-1). The vertical center of gravity of the Mariner is adjusted so that the Mariner and American Challenger GZ (righting arm) are equal at a heel of forty degrees in smooth water. Note that figure III-1 indicates a GM (metacentric height) of .81 feet for the Mariner. The final Mariner GM of .62 feet, used throughout the experiments, is arrived at by again adjusting the Mariner vertical center of gravity so that the Mariner and American Challenger righting moments are equal for a forty-degree heel in smooth water (see figure III-2).

The transverse and longitudinal radii of gyration of the Mariner model are the same as the American Challenger. A rudder is not installed. An attempt to reproduce the exact sea conditions was not made in the towing tank but rather, simple waves composed of one or two sinusoidal components having the steepness and essential features of the observed open water seas were used.

Motion restraints.

A free running model could not be used for these experiments because of the narrow width of the towing tank. Therefore, it was necessary to suppress sway and yaw motions. Also, surge was suppressed so that a practical towing scheme could be employed. A towing device was constructed which allowed the model complete freedom in roll, pitch and heave, while suppressing surge, sway, and yaw. A description of the towing device is given in appendix B.

In order to make meaningful comparisons between experiments and computations, the computer simulations were made with surge, sway, and yaw motions suppressed. Some computations were made also, to determine the influence of this restriction on the computed motions, and these are discussed in a later section.

Experimental measurements and parameters.

The following data was recorded in the laboratory during experimental runs:

1. Roll angle
2. Pitch angle
3. Heave acceleration
4. Model speed
5. Wave period
6. Wave elevation abeam the model forward perpendicular, longitudinal center of gravity, and after perpendicular.

Appendix B contains a list of the instrumentation and a sketch showing the wave sensor location. Note that the wave sensors were installed so as to be outside the wave field generated by the model.

Model tests were made in regular waves and in wave groups consisting of two superimposed regular waves. The number of wave encounters per group was varied. The wave length was equal to the ship length between perpendiculars for all experimental runs including those made in wave groups, and runs were made for a range of wave amplitudes and model speeds. Table III-1 contains a summary of the experimental conditions and results.

Experimental Results and Observations

The waves generated in the towing tank do not have a perfectly sinusoidal profile, however, the capsize program simulates waves which are sinusoidal. In the laboratory, the wave periods for the one component wave train ("regular" waves) or two component wave train (wave groups) were nearly constant. The amplitudes of individual waves in a wave train deviated, at times, by as much as fifteen percent from the mean wave amplitude (see figures III-5 through III-11). Furthermore, the wave group profiles became more asymmetric as the wave amplitude and distance from the wave maker increased (the highest wave in a group would occur not at the center of the group but instead, closer to the front of the group). This asymmetry is probably a result of nonlinear effects which are discussed in reference [8].

Table III-1 contains a summary of the experimental runs. It can be seen that the model capsized for a certain range of speeds, corresponding to certain wave encounter frequencies, and the range narrowed as wave amplitude decreased.

For example, from Table III-1 it can be seen that model tests made at a speed (ship scale) of 6.9 knots in regular waves of length equal to the model length and amplitude of ten to twelve and one half feet (ship scale) resulted in one out of three runs (33 percent) capsizing. For the same speed but wave amplitude of twelve and one half to fifteen feet, four out of five (80 percent) runs capsized. A simple calculation shown below verifies that the wave encounter frequency for the above cases is nearly twice the natural frequency of roll as determined from free roll decay data. The experimental data used for this calculation is converted to ship scale.

From Table III-1 it is seen that capsizes frequently occurred for a speed U of 6.9 knots (critical speed) where the wave period T_w was 10.24 seconds. Converting U (knots) to U (feet/second) and the wave period T_w to wave frequency ω_w one obtains:

$$U = (6.9 \text{ knots}) (1.689 \text{ feet/second/knot}) = 11.7 \text{ feet/second}$$

$$\omega_w = 2\pi/T_w = 2\pi/10.24 \text{ second} = 0.614 \text{ 1/second.}$$

The wave number K is calculated to be

$$K = \omega_w^2/g = (0.614 \text{ 1/second})^2/32.2 \text{ feet/second}^2 = 0.0117 \text{ 1/feet.}$$

The frequency of wave encounter ω_e experienced by the vessel is calculated using

$$\omega_e = \omega_w - KU .$$

Thus,

$$\begin{aligned} \omega_e &= 0.614 \text{ 1/second} - (0.0117 \text{ 1/feet}) (11.7 \text{ feet/second}) \\ &= 0.477 \text{ 1/second.} \end{aligned}$$

Figure III-16 shows the model free roll decay history in calm water for a forward speed of 7.3 knots which, for practical purposes (since roll decay depends on vessel speed) is close enough to 6.9 knots. In this figure the experimental data have been converted to full scale. A typical roll period T , which is taken as the natural roll period for this calculation, is $T = 26$ seconds. Converting this to frequency, one gets $\omega = 2\pi/T = 2\pi/26$ seconds = 0.242 1/seconds as the natural roll frequency. Note that the natural roll frequency here is about half the wave encounter frequency above.

Several observations of the model behavior are noted when the speed is near the upper and lower limits of the critical speed range.

1. The probability of a capsizing is lower than that for speeds nearer the critical speed.
2. The roll amplitude may build up to the point of nearly capsizing, a change in phase relative to the wave occurs, the roll immediately dies out and then slowly builds up again, repeating the cycle.
3. After the roll motion had developed to near capsizing the model was observed to "hang" at a roll attitude between forty and sixty degrees while a complete wave

cycle passed. The model then sometimes capsized to that side, or sometimes rolled to the other side. An example of this behavior is shown in figure III-7, titled "Mariner Capsize RUN 0905-55J3".

If the speed was somewhat further removed from the critical value, the roll amplitude was observed to increase until it reached a steady value and no further. The magnitude of the steady state amplitude was less the further the model speed was removed from the critical speed.

When the speed was equal to the critical speed and the roll amplitude had reached ten or twenty degrees, a capsize frequently occurred in two to six more roll cycles, provided the wave amplitude was sufficiently high during these subsequent rolls. In the case of regular waves of critical amplitude, the amplitude during these two to six roll cycles, was always sufficient. However, in the case of wave groups, the wave amplitude is not constant and so waves of sufficient amplitude during these two to six roll cycles may not have been present. When the number of wave encounters per wave group was seven or eight, there were only two or three waves having critical amplitudes, therefore, insufficient consecutive waves of sufficient amplitude were present to cause capsizing. When the number of wave encounters per wave group was increased, more consecutive waves of sufficient amplitude were present and thus a capsize was more likely to occur.

At the beginning of an experimental run in regular waves, two to ten waves would pass before the model started rolling. When tested in wave groups, the first or second wave group to pass the model would initiate rolling so that some roll motion would be present as the initial condition upon encounter of the next group. As the next wave group passed, one of three alternative patterns of motion was observed:

1. the roll amplitude increased further in this group until the model capsized,
2. the roll amplitude decreased between the wave groups and built up again during a subsequent group resulting in a capsize or,

3. the roll amplitude continued to decrease and increase as the wave groups passed, possibly resulting in a capsize after several groups.

Comparison of simulations with Mariner experiments.

Before proceeding with a discussion of the comparisons it should be noted that accuracy of the step-by-step numerical integration of the equations of motion depends on both the size of time step used and the number of offset points used to define the ship hull form.

Figure III-3 shows an example of the computed response for time steps one-half, one, and two seconds. It was found by experience that a time step of one second yields reasonably consistent results without excessive use of computer time.

The full table of offsets for the Mariner contains 240 points of each side of the longitudinal centerline and a partial table of offsets contains 79 points. Tables A-2 and A-3 in appendix A list these offsets and figures A-2 and A-3 in the same appendix show the corresponding body plans. The short offsets are arrived at by removing entire stations and some points in the remaining stations from the full offsets. Hydrostatic properties computed with the short table of offsets are within two percent of those computed with the full offsets, if the vertical center of gravity is adjusted so that GM is the same. Figure III-4 shows the outcome of simulations made using both the full and shortened table of offsets where GM is the same for both cases. It is difficult to determine whether one set of offsets is significantly more accurate than the other since slight changes in some numerical coefficients input to the simulation, e.g., the roll quadratic damping coefficient, could overshadow the differences due to the different tables of offsets. The significance of roll damping is discussed more fully in a later section of the report. Since computer time is proportional to the number of offsets used for the computation, the short table of offsets is used for subsequent computations.

The initial conditions for the computer simulations are taken directly from experimental records and can be found in appendix D.

The laboratory records for heave are uncertain and as a consequence the initial heave motion is unknown. Therefore, the heave initial conditions are set to zero. It is expected that this will have little effect on the simulations since heave is relatively strongly damped and, therefore, the transient motion which is further moderated by the starting ramp function will not be pronounced.

It was mentioned earlier that additional linear and quadratic roll damping coefficients may be supplied to the capsize simulator. Quadratic roll damping only was supplied for all the simulations presented here, in addition to the roll hydrodynamic damping calculated by the simulator.

Simulation results for the Mariner.

Figures III-5 through III-11 show time history plots of experimental (solid line) and simulated (*) roll records in the upper figure and in the lower part of the figure are corresponding records of the absolute wave elevation at the longitudinal center of gravity. Where the title is the same for two or more consecutive figures, e.g., "CAPSIZE RUN 0901-41A", the experimental data are the same, but the quadratic roll damping coefficient, "DAMPQ" for the simulator has been changed. "SPEED" is the ship forward velocity in knots. "WAVE AMP" is the approximate experimental wave amplitude in feet and the value supplied to the simulator. In the case of runs made in wave groups (two superimposed regular waves), "WAVE AMP" is the maximum wave amplitude. Note that full scale ship values are used throughout in the labels.

Figure III-5 shows an example of excellent agreement between experiment and simulator. Notice that the experimental wave amplitudes are not constant but that the wave periods are fairly close to the sine wave generated by the simulator. Figure III-6 shows the same run where "DAMPQ" has been increased from $1.6 \times 10^9 \text{ ft}\cdot\text{lbsec}^2$ to 1.8×10^9 . The simulated roll continues for a longer time as expected but the ship does not capsize within the two hundred seconds of simulated time.

Figure III-7 shows a run where the model hangs on one side at a large roll angle while one wave passes, changing the roll phase by one-half period. The simulator output displays a similar behavior but the hanging occurs one roll period sooner. Compare this figure with figures III-8 and III-9 and note the change in "DAMPQ". It can be seen that for this case a small change in "DAMPQ" makes a radical difference in the simulated roll behavior. This suggests a high degree of sensitivity of either the capsizing simulator or of the phenomenon itself to changes in quadratic roll damping.

Figures III-10 and III-11 are runs made in wave groups. In this case the simulated wave train is generated which best fits the experimental wave train. One can see here some apparent discrepancy between the simulated wave (two superimposed sine waves) and the measured wave profiles. In figure III-10 the simulated roll record is nearly the same as the experiment. The roll amplitude increases when higher waves pass, decreases when shorter waves pass, then increases again with higher waves as before. Here the simulator does not give a capsize but the experiment does. In figure III-11 the quadratic roll damping coefficient is adjusted so that both simulator and experiment capsize at the same time. Notice that the roll records are nearly the same except that they are out of phase by one half the roll period.

Factors which influence results.

The hydrostatic restoring forces and moments are a function of:

1. hull form,
2. vertical center of gravity,
3. wave profile and position relative to the ship,
4. position or attitude of the ship, given by pitch, heave, and roll for this three-degree-of-freedom system corresponding to the experiment.

The model hull form was carefully checked against the table of offsets. The measured displacement is 52.29 LB (model scale,

fresh water) or 20, 653 LT (ship scale, fresh water) which differs by four and one half percent of the computed displacement of 21,616 LT (fresh water). See Principal Dimensions table A-1. It was found by experiment that the model righting arm in calm water goes to zero for a heel of about sixty-two degrees but by computation goes to zero for a fifty-eight degree heel.

Carefully controlled inclining experiments were made in the laboratory for determining the metacentric height. Appendix C contains a detailed description of the inclining procedure, table of measured values of GM and a sample plot of inclining arm vs. angle of heel. The GM to beam ratio is only eight tenths of one percent, and this small value resulted in the need for extreme care when making the inclining experiments. The average measured value of GM is $.65 \pm .04$ ft, a variation of six percent. A value of .62 ft is used for the simulator. Figure III-12 shows an example of the effect of variation of GM on the simulation.

The wave elevation at the model longitudinal center of gravity and period were accurately measured in the laboratory. It was pointed out earlier, however, that the wave profile is not accurately modeled with sine waves used by the computer simulator. This can be seen by inspecting figures III-5 through III-11. Figure III-13 shows three simulations where only the wave amplitude has been changed.

Effect of roll damping.

The capsizes simulator inherently computes a linear hydrodynamic damping moment due to wave making by conventional strip theory. An additional quadratic damping coefficient "DAMPQ" may be supplied at the option of the user.

Figures III-14 through III-17 show experimental and simulated roll decay time histories and these plots may be used as an aid in estimating "DAMPQ" for capsizes simulations. The four figures give experimental results for four different forward speeds, and, therefore, show the effect of speed on roll damping. The simulations were made with the same quadratic damping coefficient in all cases, 4.0×10^8 . It was found that moderate changes in the

coefficient DAMPQ do not improve the comparisons. Note also that the value of DAMPQ used to obtain good correlation with the roll decay curves here is substantially less than that which gives the best fit to the motion in waves as may be seen in figures III-5 through III-11.

A necessary condition for capsizing in a longitudinal seaway by the phenomenon previously referred to as "autoparametric excitation", is that roll frequency be near the natural or resonant roll frequency. Then, according to the theory of linear spring-mass dynamic systems, since damping is small relative to critical damping, the roll amplitude is quite sensitive to small changes of damping. Figures III-5 and III-6 show this sensitivity very clearly. These figures also suggest that although a small change in DAMPQ may make a difference between capsizing or not capsizing, large rolling motion is still predicted. An example of this great sensitivity to damping is displayed in figures III-7 and III-8 and III-9 where changes in the fourth or fifth significant digit of the value for DAMPQ results in much different simulations.

Listed below are several sources of damping or energy dissipation for a ship operating in high longitudinal waves and experiencing large roll amplitudes.

1. Wave making: the simulator computes a linear coefficient, however, small roll amplitude and a constant frequency is assumed. For large roll amplitudes, however, this moment takes on a more complicated form, for which a theoretical procedure does not exist at present.
2. Eddy damping: noticeable turbulence was observed during model tests particularly around the bilge and deck edge. Eddy damping depends on viscosity and is certainly non-linear.
3. Viscous or skin friction: frictional damping occurs as a result of water flowing across the hull and deck and depends on, among other things, surface area and relative tangential velocity. The surface area in contact with the water depends on the model position

relative to the wave and is, therefore, dependent on pitch, roll, heave, and the wave profile. The tangential velocity of the water particles is continuously changing in magnitude and direction.

4. Sloshing of water on deck: water sloshing across the deck creates hydraulic jumps.

It should be clear that roll damping at very large angles is not adequately estimated by the simple sum of a linear plus quadratic term with constant coefficients for each. Roll damping has a complicated form and depends not only on roll velocity but also on roll angle and possibly other parameters. The exact theoretical prediction of roll damping for large angles in waves is not, however, possible at present.

Effect of suppression of surge, sway and yaw.

As previously noted, the towing system used in the experiments suppressed the model's surge, sway and yaw motion. In order to test the effect of this suppression on the roll motion of the vessel, source simulations were made allowing six degrees of freedom for the experimental conditions shown in figure III-5. Simulations were carried out using four different values of the quadratic roll damping coefficient and the results are shown in figures III-18 through III-21. The general characteristics of the motion immediately before capsizing are duplicated but some differences are introduced by the additional degrees of freedom as may be seen by comparing figures III-5 and III-18 which have identical quadratic damping coefficients. Here, the final cycle prior to capsize is duplicated closely by the six-degree-of-freedom simulation but the capsize does not occur. By reducing the damping, the computational model may be made to capsize, although the time history of the motion differs somewhat from both the three-degree-of-freedom experiments and simulations.

SEA LAND 7 containership model.

In order to provide a second test of the capsize simulator

using a hull form previously tested in San Francisco Bay, a second series of experiments were conducted with a 1/150 scale model of the Sea Land 7 class containership.

The principal dimensions of the model and the full scale ship are presented in Appendix A and Table A-4. These dimensions were scaled from the model used in the tests in San Francisco Bay and corrected for the fresh water of the towing tank.

In Appendix A also can be found the reduced table of offsets used in the calculations and the initial 100% table of offsets. The reasons for this reduction in the number of points at the table of offsets was discussed in an earlier section which described the Mariner experiments and simulations. A righting arm curve for the SL7 is presented in figure III-22.

It was desired to simulate the more adverse conditions that were observed during the free running ship model tests in San Francisco Bay and, consequently, tank tests were conducted for model and wave conditions which could be expected to lead to capsizing conditions for the model. Summaries of the experimental runs are presented in Table III-2. In this table it is noted that for certain wave conditions combined with a certain model condition the frequency of occurrence of capsizes is higher for a clearly defined range of speed, and thus, for the given sea conditions the ship appears to have a "critical speed" for capsize.

The experiment-simulator comparisons which are illustrated in this section were chosen from the more adverse regions mentioned above.

As in the Mariner experiments and simulations, the model was restricted to three degrees of freedom in heave, pitch and roll.

A description of the location of instrumentation used in the experiments is presented in the Mariner section. For the experimental runs, both regular waves and wave groups, consisting of two superimposed regular waves were used, also as was the case with the Mariner.

Values for the linear and quadratic damping roll coefficients were estimated using data from free roll decay curves for the model.

The value obtained from the model at rest and moving forward, for the full scale ship with GM number 5 are given below.

Forward Speed (knots)	Linear Damping Coefficient	Quadratic Damping Coefficient
0	7.25×10^7 lb-ft/rad/sec	2.00×10^9 lb-ft/(rad/sec) ²
3.1	0.92×10^8	2.60×10^9
9.2	1.15×10^8	7.30×10^9
12.2	1.15×10^8	7.30×10^9

The values used for the capsize simulator were chosen to approximate the above values for the closest forward speed. Thus, for a forward speed 9.8 knots, the linear and quadratic coefficients used in the simulation were DAMPL = 1.70×10^8 and DAMPQ = 6.0×10^9 .

Comparison of simulation with SL-7 experiments.

Table D-2 shows the initial conditions used for each of the simulations that are discussed in this subsection. The ratios of natural roll frequency to frequency of encounter for these runs were calculated as noted previously in the case of the Mariner and the following values were found.

Run Number	Forward Speed (knots)	$\frac{\omega_N}{\omega_e}$	<u>wave length</u> LBP
0409-45	9.8	.44	1.0
0409-46	9.8	.44	1.0
0409-61	1.3	.42	1.5
0409-63	3.7	.44	1.5

In figures III-23 and III-24 excellent agreement between simulation and experiment is obtained for these non-capsizing runs. As mentioned before in the subsection "Damping" the values used for the linear and quadratic roll damping coefficients

were close to the ones determined from free roll decay experiments. It was noted that small changes in both values for the damping coefficients do not appreciably affect the simulation here.

Figures III-25, III-26 and III-27 show two different experimental runs which resulted in capsizes. Capsizes were not, however, obtained for the simulation.

Figure III-25 shows comparison with experiments for run number 0409-45 in which the simulator linear damping coefficient was the same as initially assumed ($DAMPL = 1.15 \times 10^8$) and the quadratic damping coefficient was reduced by 99.6 percent from the initial value as originally obtained from the roll decay experiments. The initial value of $DAMPQ$ was 6.0×10^9 and the reduced value $DAMPQ$ was 2.5×10^7 .

Figure III-26 shows results for run number 0409-45. Here the linear and quadratic damping coefficients were increased by 50% from the initial values. The initial value of $DAMPL$ was 1.15×10^8 , and the increased value of $DAMPL$ was 1.73×10^8 ; the initial value of $DAMPQ$ was 6.0×10^9 and the increased value of $DAMPQ$ was 9.0×10^9 .

Figure III-27 shows results for run number 0409-61 in which the linear damping coefficient was reduced 93% from its initial value (the initial value $DAMPL$ was 7.25×10^7 and the reduced value of $DAMPL$ was 5×10^6). Here the quadratic damping coefficient was reduced by 97 percent from its initial value (initial value $DAMPQ$ was 2.0×10^9 and the reduced value $DAMPQ$ was 5.0×10^7).

The purpose of this study was to ascertain the sensitivity of roll motion to variations in the linear and quadratic damping coefficients. The changes in these values was carried out in steps, and it was observed that reasonably good agreement was obtained between computed and measured roll motion in the initial few oscillations. In some cases, with reductions in the damping coefficients an increase in the roll amplitude and a change in the apparent roll frequency was obtained. This may be seen in comparing figures III-25 and III-26. This increase was larger when the linear roll damping coefficient was reduced by a certain fraction compared with the reduction in roll amplitude due to the

same relative reduction in the quadratic roll damping coefficient. For reasons which are not clear, the attempts to simulate capsizing were less successful with the SL7 than with the Mariner.

Figures III-28 and III-29 show some roll decay simulations in which the agreement between experiment and simulation is quite good. In these simulations, the values for the quadratic damping coefficients were changed substantially from the nominal values discussed earlier in order to test the sensitivity of roll motion to this parameter.

Experimental observations.

The observations and conclusions drawn from the experimental runs are similar to those described in the earlier section. The following observations were made during the SL7 model test.

A higher percentage of capsizes occurred for GM numbers 3 and 5 while for GM number 6 almost no capsizes occurred as can be seen in Table III-2.

It was observed that the model with GM number 5 required an average of 20 to 30 seconds to start rolling. The same observation for GM number 6 shows an average of 40 to 60 seconds to start rolling from the beginning of an experimental run.

The increase in the value of GM from number 3 to number 5 does not reduce the percentage of capsizes by a significant amount, while the change from GM number 5 to number 6 causes the percentage of capsizes to drop almost to zero.

Pacific Coast Crab Boat model.

In order to examine the capability of the capsize simulator to predict behavior of ships of widely varying form, a short series of model tests in following seas was conducted utilizing an existing 1:22 scale model of typical Pacific Coast crab boat. The arrangement and body plan of this model are shown in figures A-5 and A-6 . This model was chosen for several reasons:

1. The hull geometry differs substantially from that of both the Mariner and the SL-7 models used in similar following sea tests. For comparison with these other ships, a table of full-scale offsets and the model test is listed in Table A-9 in the same format discussed in relation to the Mariner offsets.
2. Similar model tests in following seas have been conducted by Hydronautics, Inc., Reference [13] using a 1:11 scale model of the same Pacific Coast crab boat and identified as model #F-34 in the cited report. These experiments provided some data and initial conditions for comparative purposes.
3. The model used in these following sea tests had been tested extensively in beam seas at the University of California Towing Tank over the preceding two years, and a substantial body of useful data on roll damping coefficients versus metacentric heights, and roll radii of gyration had been obtained from free roll decay time histories for various load distributions.
4. Many of the methods used in conducting the aforementioned beam sea experiments and in analyzing the subsequent data were found to be directly applicable to the present following sea tests. These included the following:
 - a. layout, ballasting, and instrumentation of the model,
 - b. instrument calibration techniques, inclining procedures,

and free roll decay experiment procedures; these were identical to those discussed elsewhere in this report for the Mariner model tests,

- c. the use of previously developed computer programs for the purpose of analyzing experimental data with respect to determining metacentric height, transverse roll gyradii, and linear and quadratic roll damping coefficients.

The crab boat model tests in following seas which were conducted at the University of California Towing Tank were subject to the same motion restraints, experimental measurements and parameters as discussed elsewhere for the Mariner model tests. That is, surge, sway, and yaw motions were suppressed by a system of restraining rods similar to that shown for the Mariner model as shown in figures B-4 and B-5, and the model carried neither a rudder nor a propeller during the tests.

The experimental data which were recorded during the course of the experiment included the following:

1. roll and pitch angles from a vertical gyroscope,
2. heave acceleration from a $\pm 1g$ accelerometer,
3. model speed via a digital readout connected to the towing carriage,
4. wave period via a digital readout connected to the wave maker,
5. wave elevations abeam the model at the forward and after perpendiculars and at the longitudinal position of the center of gravity from conductance-type wave sensors; these sensors were located relative to the model so as to minimize interference from the wave field induced by the model motions and by reflections from the wall of the towing tank.

The crab boat experimental results reported in Reference [13] were initially used as the basis for planning the present tests. These included model load conditions, initial metacentric heights, ship model speeds, and wave conditions (i.e. wave heights and wave lengths). The model (and full scale) test conditions are

compiled in Table A-8, while figures III-30 to III-33 show the accompanying full-scale righting arm curves (in calm water and while hydrostatically perched on waves with $\lambda/L = 1.5$ and 2.0) for each of the GM conditions tested. Tables III-3 to III-5 lists all of the model (and full scale) speed and wave parameters used in the various experimental runs. Note that, in the present case, no tests in wave groups of two or more superimposed sinusoidal waves were attempted. This differs from the case for the Mariner model tests, but is consistent with the program of following sea tests reported in Reference [13].

During most of the experimental runs the bulwarks were lowered completely to the level of the main deck between the poop deck and the forecastle deck. This was done to prevent green water from becoming entrapped on deck during the inevitably large roll excursions which occurred during the tests. Although such entrapment is a real occurrence for such vessels while at sea, the capsize simulator presently has no provision to allow for such a contingency. It was therefore deemed important to eliminate this complexity in the interest of obtaining the best agreement between experimental conditions and simulated conditions.

Experimental results and observations.

The results reported in Reference [13] indicate that "extreme rolls" and "capsizes" were recorded at a value of $V/\sqrt{L} = 1.0$ when the metacentric height GM was seven and one-half percent of the ship beam and the full scale ship displacement Δ was 367.0 long tons for a value of wave steepness $\lambda/H_w = 8$. However, testing in such steep waves presented two major problems at the University of California Towing Tank. The first such difficulty was the inability of the wavemaker to produce regular sinusoidal waves of such steepness. In fact, as λ/H_w approached a value near ten or twelve, the tank waves were seen to break at distances far from the wavemaker. A value of $\lambda/H_w \approx 10$

was found to be about the upper limit of wave steepness which could be used in the present tests while still maintaining some degree of data reproducibility.

The second problem in trying to produce steep waves with $\lambda/H_w \leq 10$ was that the induced pitch and heave motions of the model were so large as to exceed the limits of motion freedom allowed by the restraint mechanism. Also, the surge force which was transmitted to the restraining rods was so large as to cause several equipment failures when λ/H_w approached a value near twelve. Therefore, it was decided not to test the crab boat model in waves as steep as $\lambda/H_w = 8$ as was done in Reference [13].

The present research effort was, instead, concentrated in the areas of reasonable ship and wave parameters which might result in either one of the two main modes of ship capsizing in astern seas (excluding broaching) of autoparametric excitation and static capsizing due to a loss of hydrostatic stability as the ship moves in a single wave crest.

In order to narrow the range of ship conditions to be tested, it was decided to conduct all experiments at a full scale displacement of 340 long tons, corresponding to a fully loaded condition. It was found in this condition that none of the possible combination of ship speed and wave steepness resulted in a capsize for values of GM as low as four percent of the ship beam. This is lower than the value of GM of seven and one-half percent of the ship beam reported in Reference [13] for "extreme roll" and capsize" behavior.

On the other hand, it was found for a value of GM = two and one-half percent of the ship beam that the slightest perturbation from upright hydrostatic equilibrium resulted in an immediate static capsize without rolling. Therefore, a value of metacentric height of three and one-half percent of the ship beam was selected as the critical value separating extremely stable behavior from extremely unstable behavior for this model. This value for GM was used throughout all subsequent model tests, and was used as input for all numerical simulations. It should be noted, however,

that full scale ships of this type rarely operate with a GM less than about ten percent of the ship beam, Reference [13], so that the experimental value is probably unrealistically low and was used principally for purposes of providing data to test the capsize simulator.

The experimental effort was first focused on the capsize mode which is termed "autoparametric excitation" (or resonant roll) which was described earlier in the section on the Mariner experiments. This effort introduced the need to make experimental runs at values of ship speed and wave frequency resulting in frequencies of wave encounter relative to the ship's natural roll frequency which are in the ratio $\omega_n/\omega_e = 1/2, 1, 3/2, \dots m/2$ where m is a positive integer.

More precisely, at frequencies of encounter $\omega_e = \omega_w - KU$ (in astern seas) which are equal to $2/m$ times the ship natural roll frequency ω_n , a condition of "autoparametric excitation" may be initiated which may cause increasingly larger roll angles up to capsize. The model values of $\omega_n, \omega_e, \omega_w, K$ and U corresponding to values of $n = \frac{m}{2} = 2, 1$ and $1/2$ are given in Table III-4, where it should be noted that the resultant encounter frequencies for $n = 1/2$ was so high as to cause pitch and surge motions which were too large to be accommodated by the restraint mechanism and consequently, most of the experiments were conducted in the vicinity of $n = 1$.

During the course of these tests, it was observed that the crab boat model did not exhibit the same resonant behavior as is described for the Mariner model in relation to a loss of dynamic stability. That is, no cases of gradually increasing roll angles were observed (or recorded as data) which corresponded to autoparametric excitation of motion as the model travelled from wave trough to wave crest, respectively.

Instead, the mode of capsizing which was observed in the test load condition for the Pacific Coast crab boat model was an apparent pure loss of static stability. That is, the model would execute a large roll to one side (on the order of ten to twenty degrees), remaining in that position for two successive

wave encounters due to insufficient righting energy. Then it would return to an upright position as the next wave trough passed amidships, causing a large roll to the opposite side. This was then followed either by a capsize as the roll motion increased for the next wave encounter, or by a repetition of the cycle to the original side. This behavior is apparent in the model experiment roll records shown in figures III-40 and III-41.

Table III-5 summarizes the capsize results for the experimental runs conducted for the crab boat model with a $GM = 3\frac{1}{2}$ percent of the ship beam. The three runs marked by an asterisk (*) were those which were chosen to be compared to the results of the numerical simulations from the capsize simulator. These runs were chosen as being representative of typical crab boat model motions in the following sea tests. Note that there were two cases in which actual capsizes occurred, while two other runs resulted in "extreme roll" angles very near to capsize values (on the order of twenty to thirty degrees).

Comparison of simulations with experiments.

It has been noted in the discussion of the results for the Mariner that either the simulations or the actual physical phenomena of capsizing in following seas often exhibit extreme sensitivity to the values of the roll damping coefficients which are input to the capsize simulator. In an attempt to circumvent the difficulty of scaling the model experiment results up to full scale values, especially in the case of the damping coefficients, all simulations for the crab boat have been computed in model scale. Through the use of a data analysis program which computes a linear and quadratic roll damping coefficient from model free roll decay data, representative values can be input to the capsize simulator for direct comparison of experimental model roll records and simulated roll motion histories without the need to resort to scaling. The validity of these model scale coefficients, as well as the methods by which they were computed from the free roll decay records, has been discussed by Dalzell in Reference [3] and by Visineau in Reference [15].

It should be noted in examining the accompanying graphs of simulations and experiments for the crab boat that since the results are plotted in model scale the coordinate axes are greatly expanded over those for both the Mariner and the SL7 graphs. That is, the time axis extends for only 20 to 25 seconds (approximately ten natural roll cycles for the crab boat model), while the roll amplitude axis and the wave amplitude axis cover ranges of only ± 40 degrees and ± 0.5 feet, respectively. Therefore, any direct comparison between the crab boat graphs and the Mariner and SL7 graphs must take account of these scaling differences between the respective model and full scale presentations.

In an attempt to further improve the method of selecting the value of roll damping and simulations, an attempt was made to simulate free roll decay records for $V/\sqrt{L} = 0, 0.8$ and 1.0 when $GM =$ three and one-half percent of the ship beam. Figures III-34, III-35 and III-36 show a comparison of the experimental results with the numerical simulation output using values for roll damping coefficients computed directly (and without modification) from the experimental records. Using these comparisons as a starting point, Figures III-37, III-38 and III-39 show similar comparisons using the above roll damping coefficients modified in such a way that the "best" agreement between experiment and simulation was achieved. It is these values for the linear and quadratic roll damping coefficients which were used in the initial capsized simulations with non-zero wave amplitudes and forward speeds.

Upon closer examination, the following comments are suggested concerning the free roll decay records for the crab boat model. In Reference [1], Blagoveshensky suggests that the total roll damping moment may be decomposed into a linear term (dependent on the roll velocity) which is due to wave and vortex damping, plus a quadratic term (dependent on the square of the relative roll velocity) due to frictional resistance. If this decomposition is accepted, then the consistency of the quadratic roll damping coefficients for a range of $V/\sqrt{L} = 0, 0.8$ and 1.0 is explained as nearly constant wetted surface (which is approximately independent of forward speed in otherwise calm water). Contrarily,

the linear roll damping coefficient increases significantly when $V/\sqrt{L} \neq 0$ due to increased wave-making resistance at non-zero forward speed in the absence of incident waves.

Table D-3 is a compilation of the initial conditions (slightly modified from the model records) which were input to the capsize simulator for the purpose of performing the numerical computations so as to match the test results as closely as possible. The values for linear and quadratic roll damping coefficients reflect the changes in the values from the free roll decay simulations which were required to achieve this matching. It should be mentioned that no explicit initial conditions for the heave motions were input to the capsize simulator for the accompanying three degree of freedom simulations (i.e., roll, pitch, and heave). As was mentioned in regards to the Mariner model tests, this was due mainly to an inability to record heave acceleration data which were unaffected by electronic "noise" from the oftentimes violent surge forces. Therefore, it was assumed that classical ship motion theory applied to the crab boat model so that the heave motions could be considered as being uncoupled from the roll motions. Furthermore, since heave and pitch are strongly damped motions, then transient effects should decay rapidly and, therefore, inaccurate initial values would have an effect only on the initial two to four cycles of the simulation.

Figures III-40, III-41 and III-42 show the simulated crab boat model roll amplitude and wave amplitude (***) plotted on the same axes as the actual experimental model records for runs Number 7, Number 8 and Number 20 as described in Table III-5. The first important point to notice is that in the case of run Number 7 (extreme roll to port followed by a capsize to starboard) and run Number 8 (initial extreme rolls followed by steady state), the additional values for the linear roll damping coefficient DAMPL and the quadratic roll damping coefficient DAMPQ were reduced identically to zero from the non-zero values derived from the free roll decay simulations. Nevertheless, the capsize simulator failed to predict the experimental motions

behavior and instead computed regular sinusoidal roll motions over twenty seconds. Although the mean roll amplitudes appeared to agree quite well in both runs, the extreme excursions were not adequately simulated.

In comparison, the simulation of run Number 20 was quite accurate for values of DAMPL and DAMPO near to those derived from the free roll decay comparisons in Figure III-42. Aside from a phase change in the experimental roll record near $t = 6.5$ seconds, the simulated and experimental roll motions agree qualitatively over the entire range of time shown.

A final attempt to rectify the differences between experiments and simulations for run Number 7 and run Number 8 was concerned with the effect of the initial roll angle on the simulated results. That is, it was conjectured that the small value of the roll angle initial condition which was input to the capsize simulator may have had an adverse transient effect on the model scale numerical computations. Figures III-43 and III-44 show two roll motion time histories for run Number 7 with zero additional roll damping for initial roll angles of fifteen and twenty degrees, respectively. Note that for both fifteen and twenty degrees the simulations are rapidly damped out over the first two roll cycles. After that, the mean regular amplitudes are qualitatively the same, except for the large experimental roll excursion at $t = 10$ seconds and the subsequent capsize. Again the simulator appears capable of predicting regular sinusoidal roll motions as long as no extreme excursions or capsizes occur.

Table III-1
Summary of Mariner Experimental Runs

Values given in ship scale.

Interpretation of table: | A/B P | A is the number of runs a capsizes occurred.
B is the number of experimental runs.
 $P = \frac{A}{B} \times 100\%$ = percent of runs which resulted in a capsizes.

Regular waves

one wave component, period = 10.24 sec., $\lambda/LBP = 1.0$

speed (kn)	wave amplitude (ft)									
	7½ - 10		10 - 12½		12½ - 15		15 - 17½		total	
4.9	0/1	0	0/2	0	0/2	0			0/5	0
5.4	0/1	0	0/1	0	0/2	0			0/4	0
5.9	0/1	0	0/1	0	1/4	25	0/1	0	1/7	14
6.4	0/1	0	2/2	100	3/5	60	2/2	100	7/10	70
6.9	0/1	0	1/3	33	4/5	80	1/1	100	6/10	60
7.3	0/1	0	0/2	0	2/5	40	3/3	100	5/11	45
7.8	0/1	0	0/2	0	4/4	100	2/2	100	6/9	67
8.3			0/1	0	4/4	100	1/2	50	5/7	71
8.8			0/1	0	1/4	25	2/2	100	3/7	43
9.3					0/2	0	0/1	0	0/3	0
9.8					0/1	0	0/1	0	0/2	0
10.8							0/1	0	0/1	0
total	0/7	0	3/15	20	19/38	50	11/16	69	33/76	43

Table III-1 (cont.)
Summary of Mariner Experimental Runs

Values given in ship scale.

Interpretation of table:

A/B P

A is the number of runs a capsizes occurred.
B is the number of experimental runs.

$P = \frac{A}{B} \times 100\%$ = percent of runs which resulted in a capsizes.

Wave Groups

(two regular waves superimposed)

$T_1 = 9.65$ sec.

$T_2 = 10.73$ sec.

$T_{ave} = 10.19$ sec.

$\lambda/LBP = 1.0$

Wave amplitudes are the highest wave in a group.

N is the number of wave encounters per group.

speed (kn)	N	wave amplitude (ft)								total	
		12½ - 15		15 - 17½		17½ - 20		20 - 22½			
4.9	11½			0/2	0	1/2	50	0/2	0	1/6	17
5.4	12			0/1	0	0/3	0	0/2	0	0/6	0
5.9	12½	0/1	0	0/1	0	0/2	0	1/3	33	1/7	14
6.4	13	0/1	0	0/2	0	1/2	50	1/3	33	2/8	25
6.9	13	0/1	0	0/2	0	2/2	100	3/4	75	5/9	56
7.3	13½	0/1	0	0/2	0	0/2	0	0/3	0	0/8	0
7.8	14½	0/1	0	1/2	50	0/1	0	1/4	25	2/8	25
8.3	15	0/1	0	0/2	0	2/3	66	2/4	50	4/10	40
8.8	15½	0/1	0	3/3	100	1/2	50	3/7	43	7/13	54
9.3	16½	0/1	0	0/2	0	0/2	0	2/4	50	2/9	22
9.8	17½			0/1	0	1/2	50	2/4	50	3/7	43
10.3	19			0/1	0	2/3	66	2/4	50	4/8	50
10.8	20½					0/2	0	2/3	66	2/5	40
11.3	22½					0/2	0	1/1	100	1/3	33
11.8	25					0/1	0	2/3	66	2/4	50
12.2	27½							0/2	0	0/2	0
12.7	31½							0/1	0	0/1	0
total		0/8	0	4/21	19	10/31	32	22/54	41	36/114	32

Table III-1 (cont.)

Summary of Mariner Experimental Runs

Values given in ship scale.

Interpretation of table:

A/B P

A is the number of runs a capsize occurred.
B is the number of experimental runs.

$P = \frac{A}{B} \times 100\%$ = percent of runs which resulted in a capsize.

Wave Groups

(two regular waves superimposed)

$T_1 = 9.80$ sec.

$T_2 = 10.58$ sec.

$T_{ave} = 10.19$ sec.

$\lambda/LBP = 1.0$

Wave amplitudes are the highest wave in a group.

N is the number of wave encounters per group.

speed (kn)	N	wave amplitude (ft)									
		12½ - 15		15 - 17½		17½ - 20		20 - 22½		total	
4.9	16	0/1	0	0/1	0	0/1	0	0/1	0	0/4	0
5.4	16½	0/1	0	0/2	0	1/2	50	0/1	0	1/6	17
5.9	17	0/2	0	0/2	0	0/2	0	0/1	0	0/7	0
6.4	17½	0/2	0	0/3	0	1/2	50	1/2	50	2/9	22
6.9	18½	1/2	50	1/3	33	1/3	33	0/1	0	3/9	33
7.3	19	0/2	0	0/2	0	1/3	33	2/3	66	3/10	30
7.8	19½	0/2	0	1/3	33	2/3	66	1/4	25	4/12	33
8.3	20½	0/1	0	0/2	0	1/2	50	0/2	0	1/7	14
8.8	21½			1/2	50	1/3	33	1/3	33	3/8	38
9.3	23			2/2	100	1/2	50	0/3	0	3/7	43
9.8	24½			0/2	0	1/1	100			1/3	33
total		1/13	8	5/24	21	10/24	42	5/21	24	21/82	26

Table III-1 (cont.)

Summary of Mariner Experimental Runs

Values given in ship scale.

Interpretation of table:

A/B P

A is the number of runs a capsize occurred.
B is the number of experimental runs.

$P = \frac{A}{B} \times 100\%$ = percent of runs which resulted in a capsize.

Wave Groups

(two regular waves superimposed)

$T_1 = 9.31$ sec.

$T_2 = 11.07$ sec.

$T_{ave} = 10.19$ sec.

$\lambda/LBP = 1.0$

Wave amplitudes are the highest wave in a group.

N is the number of wave encounters per group.

speed (kn)	N	wave amplitude (ft)				total	
		12½ - 15	15 - 17½	17½ - 20	20 - 22½		
4.9	7		0/1 0	0/2 0	0/1 0	0/4 0	
5.4	7½		0/1 0	0/1 0	0/1 0	0/3 0	
5.9	7½		0/1 0	0/1 0	0/1 0	0/3 0	
6.4	8		0/2 0	0/2 0	0/1 0	0/5 0	
6.9	8		0/2 0	1/2 50	0/2 0	1/6 17	
7.3	8½		0/2 0	0/2 0	0/2 0	0/6 0	
7.8	9		0/2 0	0/1 0	0/1 0	0/4 0	
8.3	9		0/2 0	0/1 0	0/1 0	0/4 0	
8.8	10		1/3 33	0/1 0		1/4 25	
9.3	10		1/3 33			1/3 33	
9.8	11		0/2 0			0/2 0	
total			2/21 10	1/13 8	0/10 0	3/44 7	

Table III-2

Summary of SL7 Experimental Runs

Values given in ship scale.

Interpretation of table: | A/B P | A is the number of runs a capsizes occurred.
B is the number of experimental runs.

$$P = \frac{A}{B} \times 100\% = \text{percent of runs which resulted in a capsizes.}$$

Regular waves - GM #3

one wave component; period = 13.25 sec; $\lambda/LBP = 1.0$

speed (kn)	wave amplitude (ft)						TOTAL	
	7½		15		22.5			
6.1	0/2	0	0/2	0	0/2	0	0/6	0
7.3	0/2	0	0/2	0	0/2	0	0/6	0
8.6	0/2	0	0/2	0	4/4	100	4/8	50
9.8	0/2	0	2/3	67	3/4	75	5/9	56
11.0	0/2	0	4/4	100	4/4	100	8/10	80
12.2	0/2	0	4/4	100	4/4	100	8/10	80
13.5	0/2	0	4/4	100	4/4	100	8/10	80
14.7	0/2	0	4/4	100	4/4	100	8/10	80
15.9	0/1	0	1/3	33	4/4	100	5/8	63
17.1			1/3	33	1/3	33	2/6	33
18.4					0/2	0	0/2	0
19.6					0/1	0	0/1	0
20.8					0/1	0	0/1	0
22.0					0/1	0	0/1	0
total	0/17	0	20/31	65	23/40	70	48/88	55

Table III-2 (cont.)

Summary of SL7 Experimental Runs

Values given in ship scale.

Interpretation of table: | A/B P | A is the number of runs a capsize occurred.
B is the number of experimental runs.

$$P = \frac{A}{B} \times 100\% = \text{percent of runs which resulted in a capsize.}$$

Regular waves - GM #3

one wave component; period = 16.23 sec; $\lambda/LBP = 1.5$

speed (kn)	wave amplitude (ft)						TOTAL	
	7½		15		22.5			
0			0/1	0	0/1	0	0/2	0
1.3			0/1	0	2/2	100	2/3	67
2.4	0/1	0	0/1	0	2/2	100	2/4	50
3.7	0/1	0	2/2	100	2/2	100	4/5	80
4.9	0/1	0	2/2	100	2/2	100	4/5	80
6.1	0/1	0	2/2	100	2/2	100	4/5	80
7.3	0/1	0	2/2	100	2/2	100	4/5	80
8.6	0/1	0	2/2	100	2/2	100	4/5	80
9.8	0/1	0	2/2	100	2/2	100	4/5	80
11.0	0/1	0	0/1	0	2/2	100	2/4	50
12.2			0/1	0	2/2	100	2/3	67
13.5					0/1	0	0/1	0
14.7					0/1	0	0/1	0
total	0/8	0	12/17	71	20/23	37	32/48	67

Table III-2 (cont.)

Summary of SL7 Experimental Runs

Values given in ship scale.

Interpretation of table: | A/B P | A is the number of runs a capsizes occurred.
B is the number of experimental runs.

$$P = \frac{A}{B} \times 100\% = \text{percent of runs which resulted in a capsizes.}$$

Regular waves - GM #3

one wave component; period = 18.74 sec; $\lambda/LBP = 2.0$

speed (kn)	wave amplitude (ft)				TOTAL	
	15		22.5			
0	0/1	0	2/2	100	2/3	67
1.3	0/1	0	2/2	100	2/3	67
2.4	0/1	0	2/2	100	2/3	67
3.7	1/2	50	2/2	100	3/4	75
4.9	0/1	0	2/2	100	2/3	67
6.1	0/1	0	0/2	0	0/3	0
7.3	0/1	0	0/1	0	0/2	0
8.6			0/1	0	0/1	0
9.8			0/1	0	0/1	0
total	1/8	13	10/15	67	11/23	48

Table III-2 (cont.)

Summary of SL7 Experimental Runs

Values given in ship scale.

Interpretation of table: | A/B P | A is the number of runs a capsizes occurred.
B is the number of experimental runs.

$$P = \frac{A}{B} \times 100\% = \text{percent of runs which resulted in a capsizes.}$$

Regular waves - GM #5

one wave component; period = 13.25; $\lambda/LBP = 1.0$

speed (kn)	wave amplitude (ft)				TOTAL	
	15		22.5			
2.4			0/1	0	0/1	0
3.7			0/1	0	0/1	0
4.9	0/1	0	0/1	0	0/2	0
6.1	0/1	0	0/1	0	0/2	0
7.3	0/1	0	2/2	100	2/3	67
8.6	1/2	50	2/2	100	3/4	75
9.8	1/2	50	2/2	100	3/4	75
11.0	0/1	0	2/2	100	2/3	67
12.2			0/1	0	0/1	0
13.5			0/1	0	0/1	0
total	2/8	25	8/14	57	10/22	45

Table III-2 (cont.)

Summary of SL7 Experimental Runs

Values given in ship scale.

Interpretation of table: | A/B P | A is the number of runs a capsize occurred.
B is the number of experimental runs

$$P = \frac{A}{B} \times 100\%$$

Regular waves - GM #5

one wave component
period = 16.23; $\lambda/LBP = 1.5$

speed (kn)	wave amplitude (ft)				TOTAL	
	15		22.5			
0	1/1	100	2/2	100	3/3	100
1.3	2/2	100	2/2	100	4/4	100
2.4	0/1	0	3/3	100	3/4	75
3.7	0/1	0	0/1	0	0/2	0
4.9			0/1	0	0/1	0
total	3/5	60	7/9	78	10/14	71

period = 11.48 sec; $\lambda/LBP = .75$

speed (kn)	wave amplitude (ft)				TOTAL	
	15		22.5			
4.9			0/1	0	0/1	0
6.1			0/1	0	0/1	0
7.3	0/1	0	0/1	0	0/2	0
8.6	0/1	0	0/1	0	0/2	0
9.8	0/1	0	0/1	0	0/2	0
11.0	0/1	0	0/1	0	0/2	0
12.2	0/1	0	1/2	50	1/3	33
13.5	0/1	0	0/1	0	0/2	0
14.7			0/1	0	0/1	0
total	0/6	0	1/10	10	1/16	6

period = 18.74; $\lambda/LBP = 2.0$

speed (kn)	wave amplitude (ft)		TOTAL	
	22.5			
0	0/1	0	0/1	0
1.2	0/1	0	0/1	0
2.4	0/1	0	0/1	0
total	0/3	0	0/3	0

Table III-2 (cont.)

Summary of SL7 Experimental Runs

Values given in ship scale.

Interpretation of table: | A/B P | A is the number of runs a capsize occurred.
B is the number of experimental runs.

$$P = \frac{A}{B} \times 100\%$$

Regular waves - GM #6

one wave component; period = 13.25 sec; $\lambda/LBP = 1.0$

speed (kn)	wave amplitude (ft)				TOTAL	
	22.5		30			
0	0/1	0	0/1	0	0/2	0
1.3	0/1	0	0/1	0	0/2	0
1.8	0/1	0	0/1	0	0/2	0
2.4	0/1	0	0/1	0	0/2	0
3.1	0/1	0	0/1	0	0/2	0
3.7	0/1	0	0/1	0	0/2	0
4.3	0/1	0	0/1	0	0/2	0
4.9	0/1	0	0/1	0	0/2	0
5.5	0/1	0	0/1	0	0/2	0
6.1	0/1	0	0/1	0	0/2	0
7.3	0/1	0	0/1	0	0/2	0
8.6			0/1	0	0/1	0
9.8			1/2	50	1/2	50
11.0			0/1	0	0/1	0
total	0/11	0	1/15	7	1/26	4

Table III-2 (cont.)

Summary of SL7 Experimental Runs

Values given in ship scale.

Interpretation of table : $\left| \begin{array}{c} A/B \quad P \end{array} \right|$ A is the number of runs a capsize occurred.
 B is the number of experimental runs.

$$P = \frac{A}{B} \times 100\%$$

Regular waves - GM #6

one wave component

period = 16.23 sec; $\lambda/LBP = 1.5$

speed (kn)	wave amplitude (ft)		TOTAL	
0	0/1	0	0/1	0
1.3	0/1	0	0/1	0
1.8	0/1	0	0/1	0
2.4	0/1	0	0/1	0
3.1	0/1	0	0/1	0
3.7	0/1	0	0/1	0
4.3	0/1	0	0/1	0
total	0/7	0	0/7	0

period = 11.48 sec. $\lambda/LBP = .75$

speed (kn)	wave amplitude (ft)		TOTAL	
2.4	0/1	0	0/1	0
3.7	0/1	0	0/1	0
4.9	0/1	0	0/1	0
6.1	0/1	0	0/1	0
7.3	0/1	0	0/1	0
8.6	0/1	0	0/1	0
9.8	0/1	0	0/1	0
total	0/7	0	0/7	0

Table III-2 (cont.)

Summary of SL7 Experimental Runs

Values given in ship scale.

Interpretation of table: | A/B P | A is the number of runs a capsize occurred.
B is the number of experimental runs.

$$P = \frac{A}{B} \times 100\%$$

Wave groups - GM #5

(two regular waves superimposed)

$$T_1 = 14.38 \text{ sec}$$

$$T_2 = 12.12 \text{ sec}$$

$$T_{av_1} = 13.25 \text{ sec}$$

$$\lambda/LBP = 1.0$$

Wave amplitudes are the highest wave in a group.

speed (kn)	wave amplitude (ft)				TOTAL	
	22.5		30			
4.9	0/1	0	0/1	0	0/2	0
6.1	0/1	0	0/1	0	0/2	0
7.3	0/1	0	0/1	0	0/2	0
8.6	0/1	0	0/1	0	0/2	0
9.8	0/1	0	0/1	0	0/2	0
11.0	0/1	0	1/2	50	1/3	33
12.2			0/1	0	0/1	0
total	0/6	0	1/8	13	1/14	7

Table III-2 (cont.)

Summary of SL7 Experimental Runs

Values given in ship scale.

Interpretation of table: | A/B P | A is the number of runs a capsize occurred.
 B is the number of experimental runs.

$$P = \frac{A}{B} \times 100\%$$

Wave groups - GM #5

(two regular waves superimposed)

$$T_1 = 13.89 \text{ sec}$$

$$T_2 = 12.61 \text{ sec}$$

$$T_{av} = 13.25 \text{ sec}$$

$$\lambda/LBP = 1.0$$

Wave amplitudes are the highest in a group.

speed (kn)	wave amplitude (ft)				TOTAL	
	22.5		30			
4.9			0/1	0	0/1	0
6.1	0/1	0	0/1	0	0/2	0
7.3	0/1	0	0/1	0	0/2	0
8.6	1/2	50	2/2	100	3/4	75
9.8	0/1	0	1/2	50	1/3	33
11.0	0/1	0	1/1	100	1/2	50
12.2			1/1	100	1/1	100
13.5			0/1	0	0/1	0
total	1/6	17	5/10	50	6/16	38

Table III-3

Pacific Coast Crab Boat
Speed and Wave Parameters

V/ \sqrt{L}	V(knots)		U(ft/sec)		λ/L	λ (feet)		H_w/L	H_w (feet)		λ/H_w
	full	model	full	model		full	model		full	model	
0.6	5.556	1.175	9.384	1.984	1.50	128.63	5.75				10
0.7	6.482	1.371	10.948	2.315	1.75	150.06	6.71				11
0.8	7.408	1.566	12.512	2.646	2.00	171.50	7.67				12
0.9	8.334	1.762	14.076	2.976				0.10	8.58	0.38	13
1.0	9.260	1.958	15.640	3.307				0.15	12.68	0.58	14
1.1	10.186	2.154	17.204	3.638				0.20	17.15	0.77	15
1.2	11.112	2.350	18.768	3.968							17.5
1.3	12.036	2.545	20.332	4.299							20
1.4	12.964	2.741	21.897	4.630							

L = 85.75 ft full scale, model scale = full scale/22.368

U = 1.689 V

λ is crest-to-crest wave length

H_w is peak-to-peak wave height

Table III-4
Pacific Coast Crab Boat
Model Frequencies of Encounter

$GM = 3\frac{1}{2}\%$ B, $i_T = 46\%$ B, $T_M = 2.728$ seconds

$\omega_M = m\omega_e$, $\omega_M = \frac{2\pi}{T_M} = 2.303$ rad/sec, Mathieu coefficients $n = 2, 1, 2/3, \frac{1}{2}$

$\omega_e = \omega_w - KU$, $K = \frac{2\pi}{\lambda}$, $\omega_w = \sqrt{gk}$ for linear deep water waves, $U = 1.689$ V

n	λ/L	V(knots)	U(ft/sec)	V/\sqrt{L}	ω_e (rad/sec)
2	1.50	2.589	4.372	1.322	1.152
	1.75	2.742	4.632	1.401	
	2.00	2.878	4.861	1.470	
1	1.50	1.965	3.318	1.003	2.303
	1.75	2.014	3.402	1.029	
	2.00	2.046	3.455	1.045	
$\frac{1}{2}$	1.50	0.717	1.211	0.366	4.606
	1.75	0.558	0.942	0.285	
	2.00	0.381	0.644	0.195	

Table III-5

Pacific Coast Crab Boat
Summary of Experimental Runs

Values given in model scale = full scale/22.368

Interpretation of results: | A/B P | A is the number of runs a
capsize occurred.
B is the number of experimental
runs.

$$P = \frac{A}{B} \times 100\%$$

GM = 2½%B: model too unstable to test.
GM = 4%B: no capsize under any speed and wave conditions.
GM = 7½%B: no capsize under any speed and wave conditions.

Regular Waves
(one wave component)

GM ≈ 3½%, $i_T \approx 46\%B$, $T_N = 2.728$ sec.

Run	V/\sqrt{L}	λ/L	T_w (sec)	H_w/L	λ/H_w	Results	Comments
1	0.9					0/2 0	extreme
2	1.0					0/1 0	roll
3	1.1	1.50	1.060	0.10	15	0/1 0	large roll
4	1.2					0/1 0	
5	1.3					0/1 0	
6	1.4					0/1 0	
7*	0.9					2/2 100%	capsize to
8*	1.0					0/2 0	starboard
9	1.1	1.75	1.145	0.10	17.50	0/2 0	extreme
10	1.2					0/1 0	roll
11	1.3					0/1 0	
12	1.4					0/1 0	
13	0.9						
14	1.0						
15	1.1	1.75	1.145	0.15	11.67	no data	severe heave
16	1.2						and pitch
17	1.3						moments
18	1.4						
19	0.9					2/2 100%	capsize to
20*	1.0					0/2 0	port
21	1.1	2.00	1.224	0.10	20	0/1 0	moderate
22	1.2					0/1 0	roll
23	1.3					0/1 0	
24	1.4					0/1 0	

*indicates simulated runs.

total: 4/23 17%

MARINER 77.7 AND AMERICAN CHALLENGER RIGHTING ARM CURVES

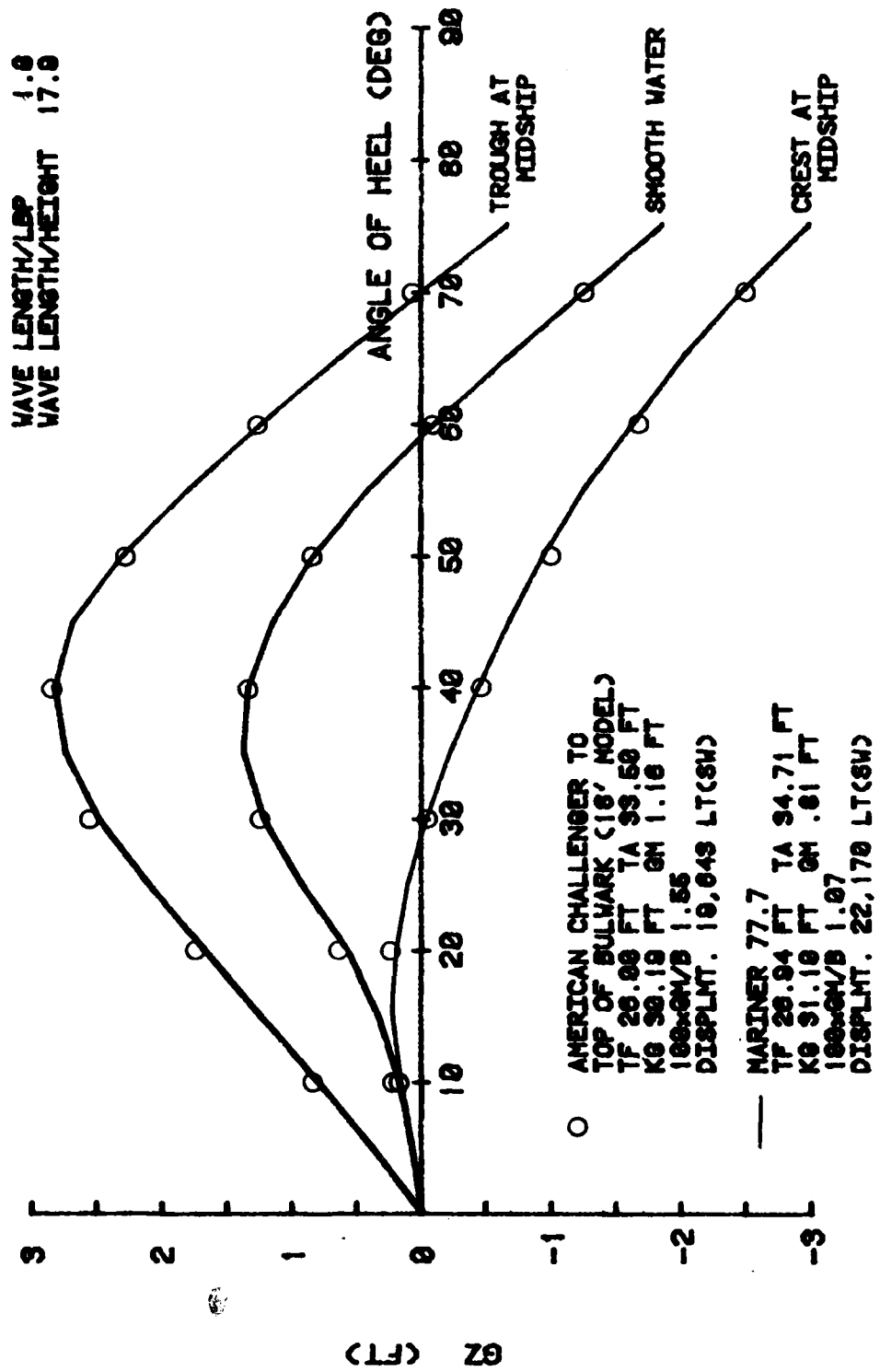


Figure III-1

MARINER 77.7 AND AMERICAN CHALLENGER
RIGHTING MOMENT

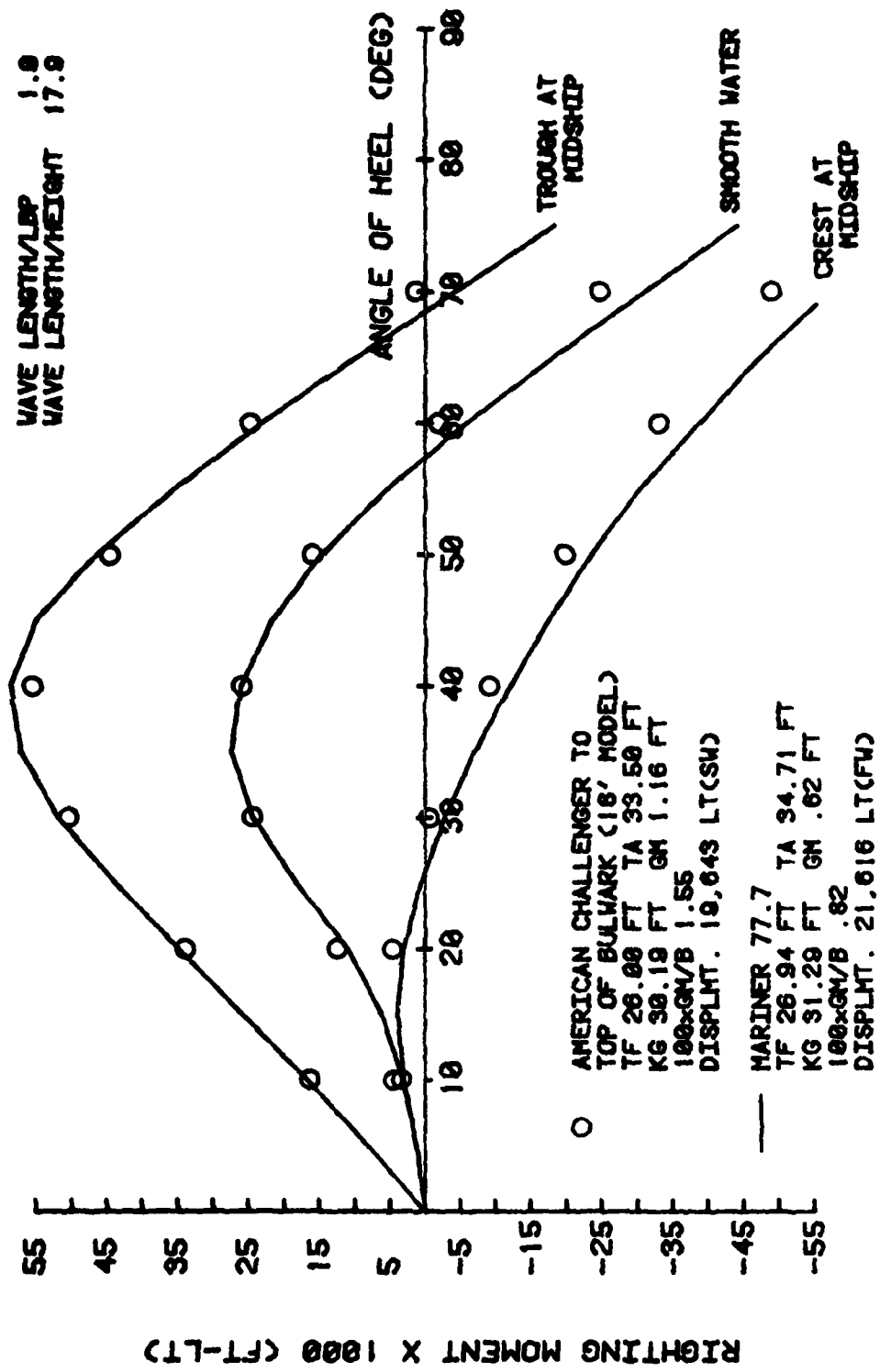


Figure III-2

CAPSIZE: INTEGRATION TIME STEP

SPEED= 6.4 KN WAVE AMP= 16.7 FT DAMPO= 1.4E+9 FT:LB:SEC²

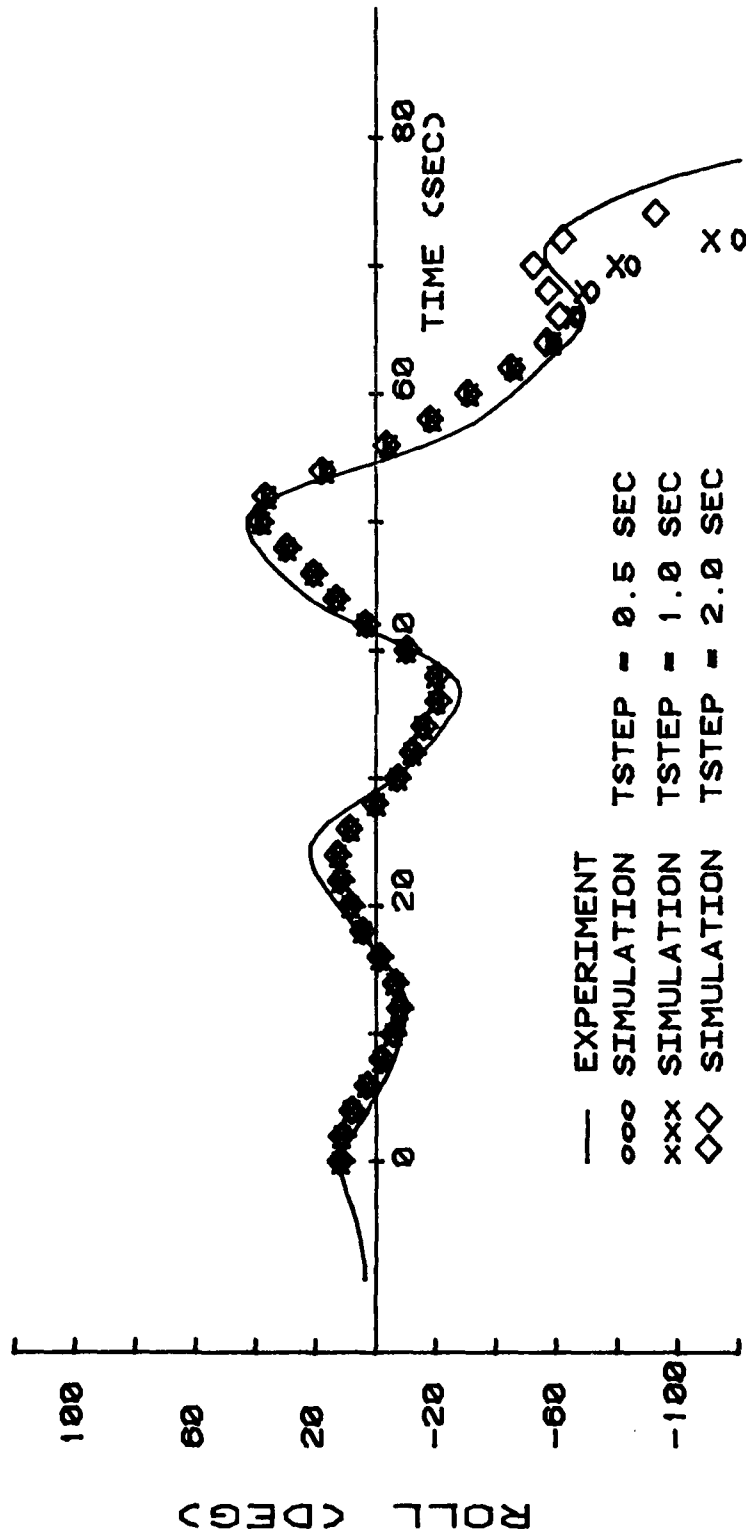


Figure III-3

CAPSIZE: OFFSETS

SPEED= 8.3 KN WAVE AMP= 13 FT DAMPQ= 1.0E+9 FT:LB:SEC²

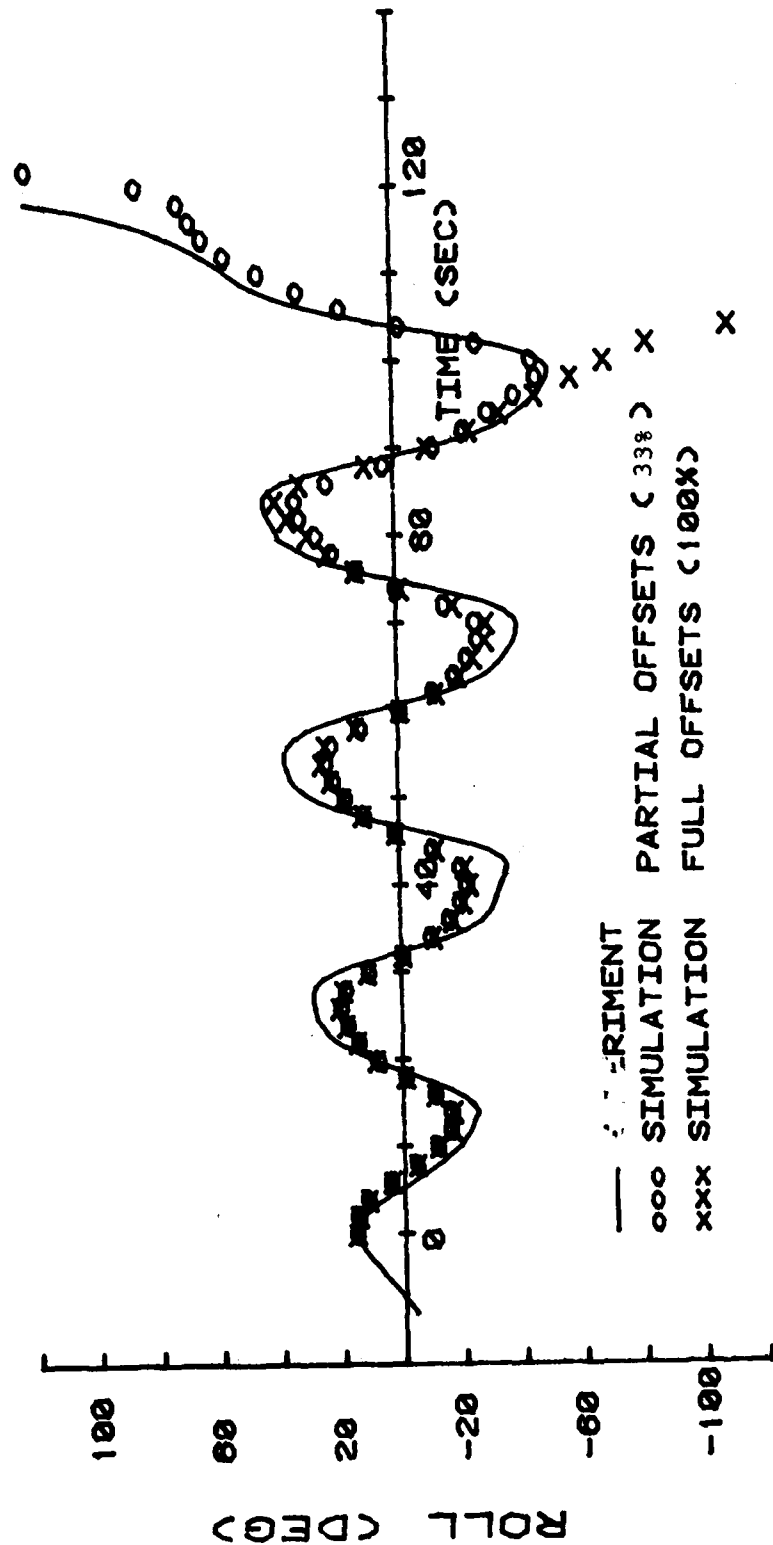


Figure III-4

MARINER CAPSIZE RUN 0901-41A
 SPEED= 7.3 KN WAVE AMP= 17.5 FT DAMPO= 1.6E+9 FT·LB·SEC²

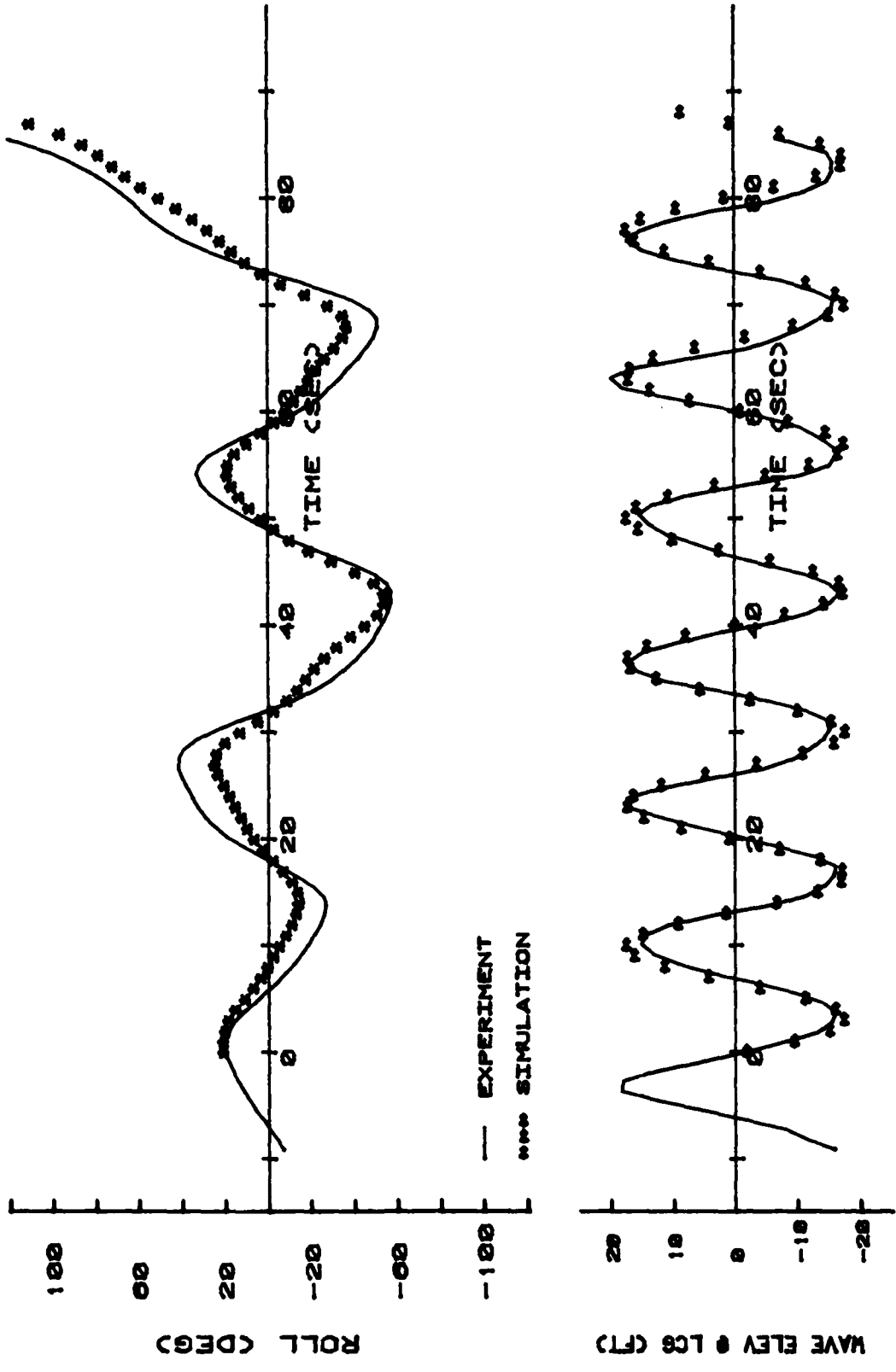


Figure III-5

MARINER CAPSIZE RUN 0901-41A
 SPEED= 7.3 KN WAVE AMP= 17.5 FT DAMPO= 1.8E+9 FT·LB·SEC²

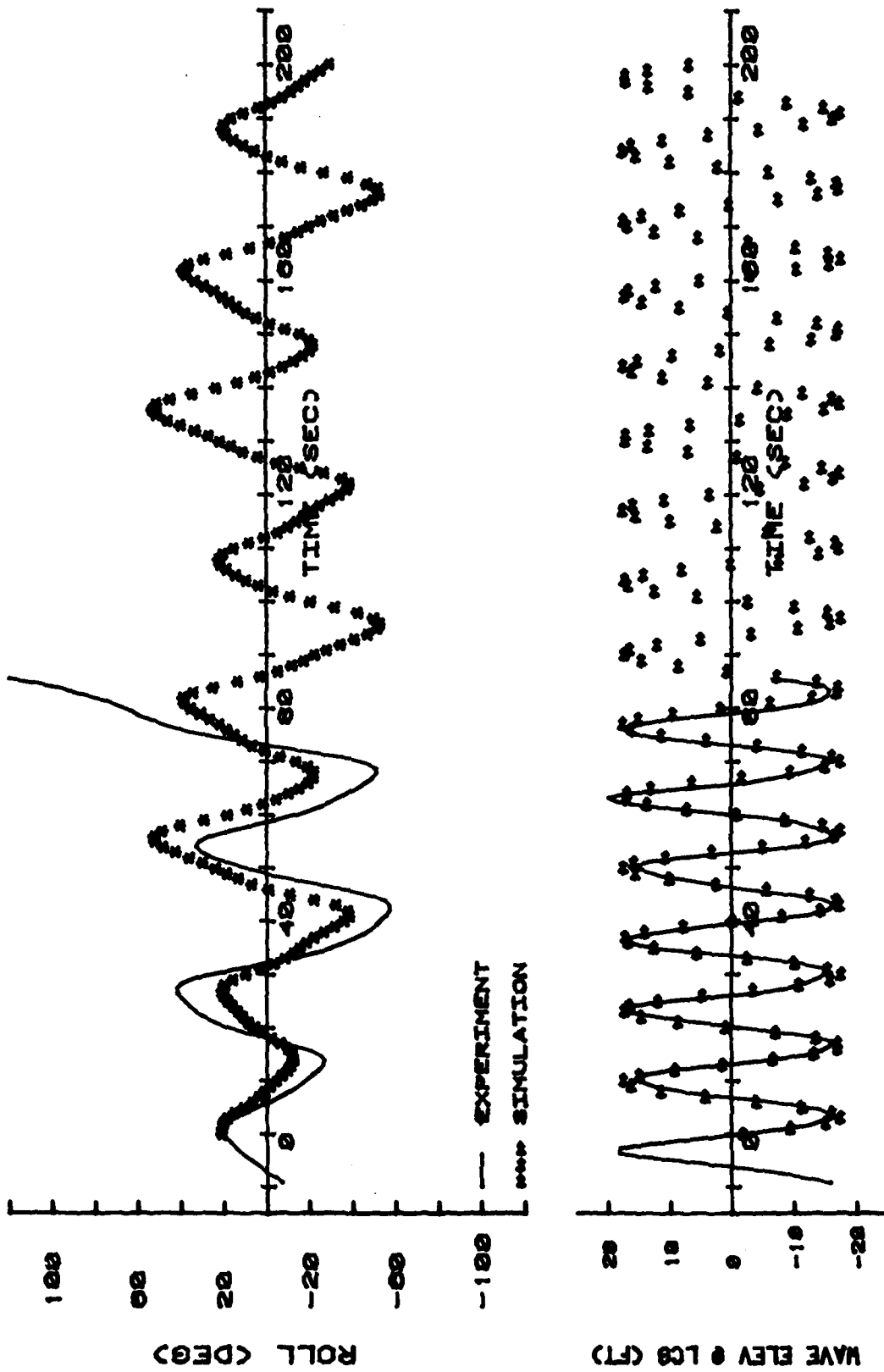


Figure III-6

MARINER CAPSIZE RUN 0905-55J3
 SPEED= 7.8 KN WAVE AMP= 12.8 FT DAMPQ= 1.239E+9 FT·LB·SEC²

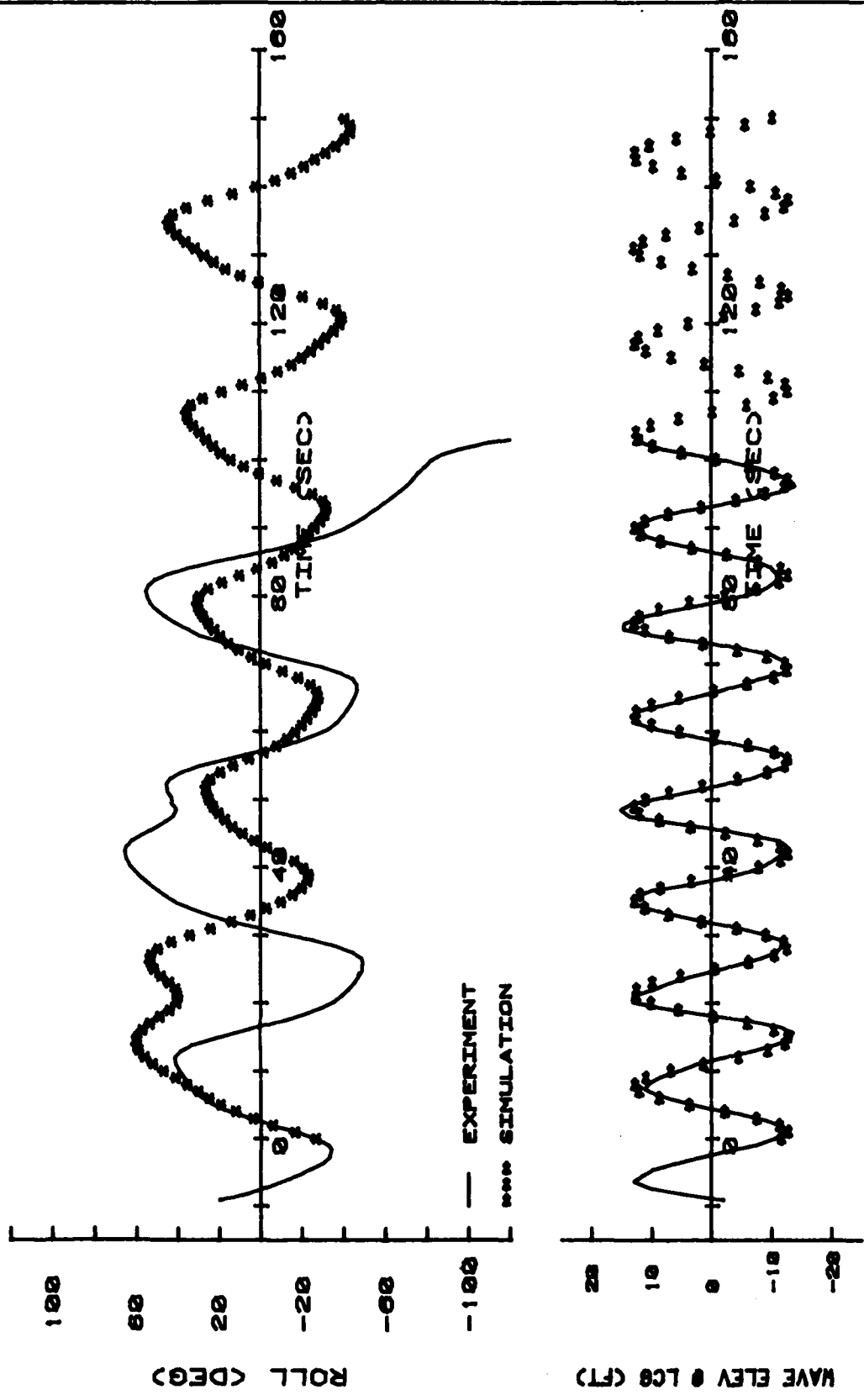


Figure III-7

MARINER CAPSIZE RUN 0905-55J3
 SPEED= 7.8 KN WAVE AMP= 12.8 FT DAMPO= 1.2366E+0 FT:LB:SEC²

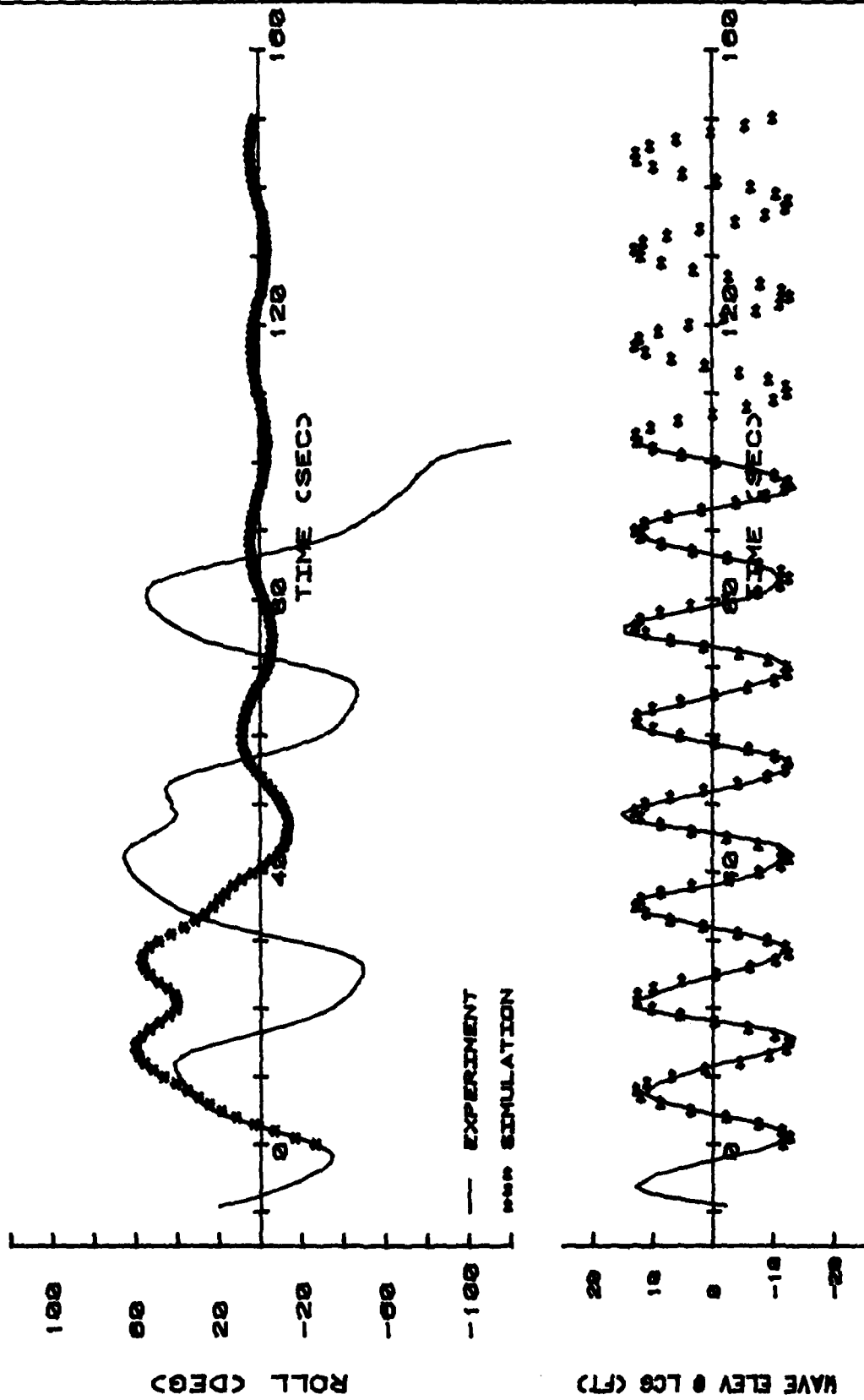


Figure III-8

MARINER CAPSIZE RUN 0905-55J3
 SPEED= 7.8 KN WAVE AMP= 12.8 FT DAMPO= 1.2385E+0 FT·LB·SEC²

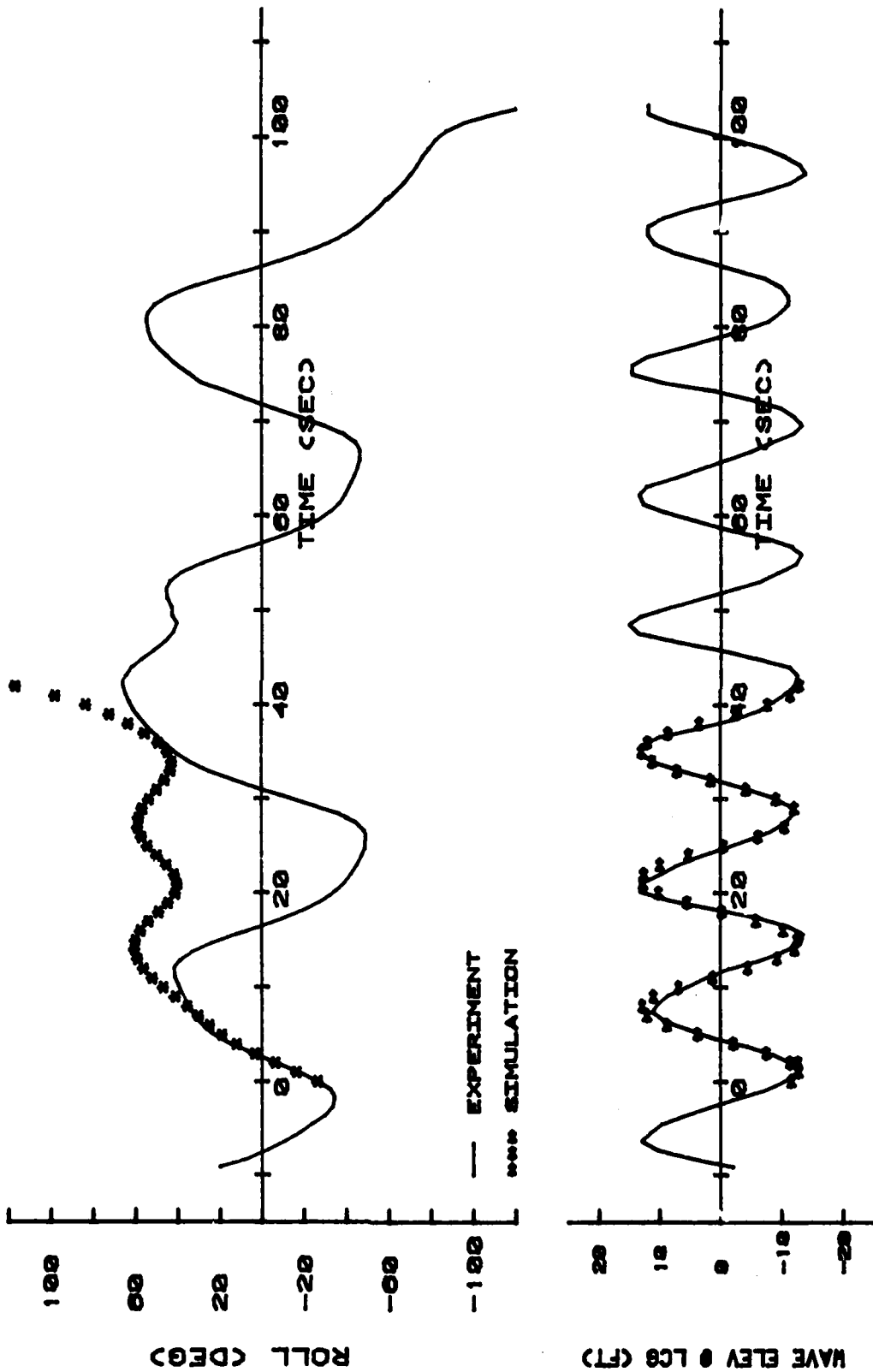


Figure III-9

MARINER CAPSIZE RUN 0911-79B1
 SPEED= 6.9 KN WAVE AMP= 16 FT DAMPQ= 1.18E+9 FT·LB·SEC²

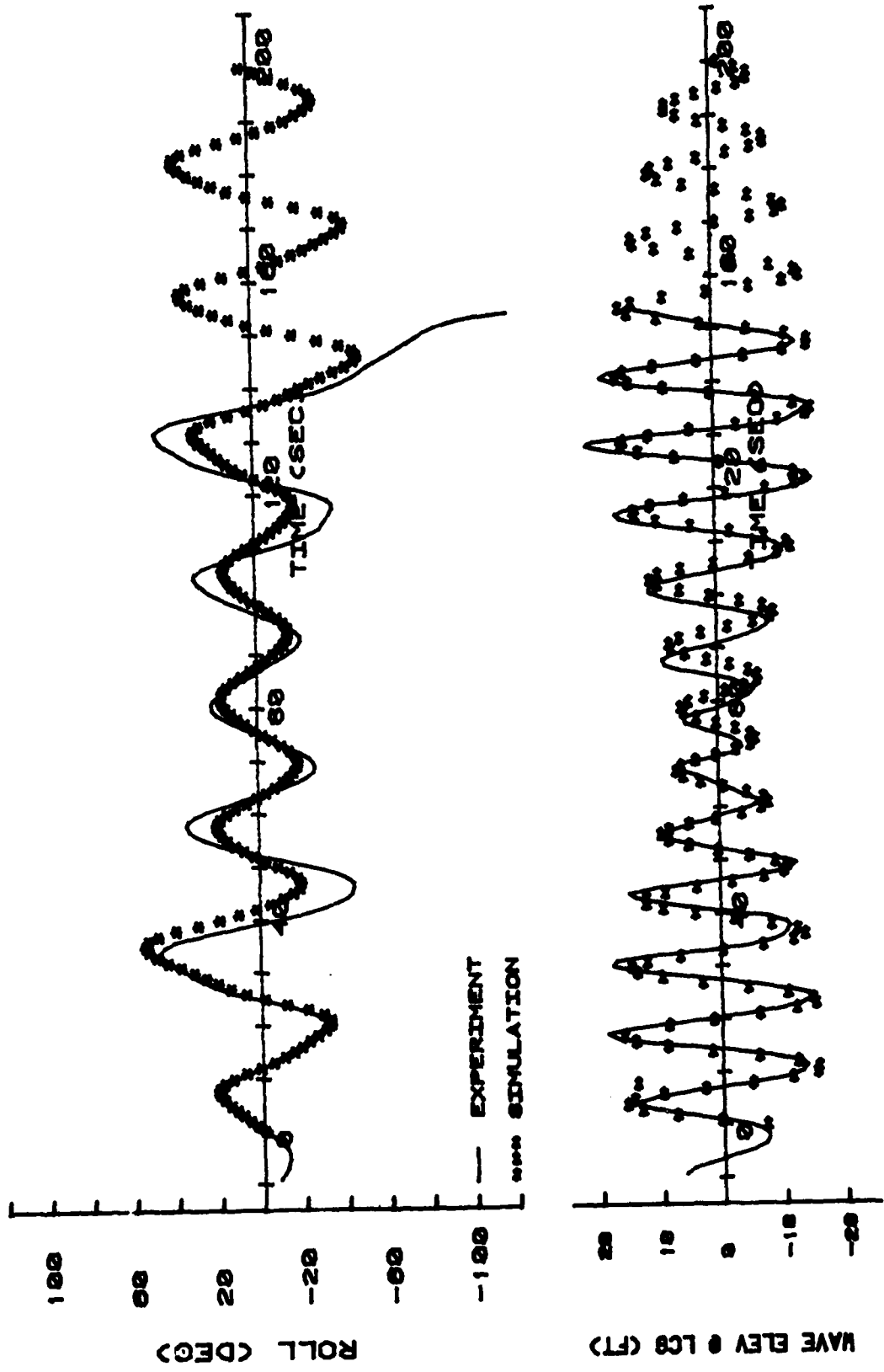


Figure III-10

MARINER CAPSIZE RUN 0911-79B1
 SPEED= 6.9 KN WAVE AMP= 16 FT DAMPO= 1.15E+9 FT:LB:SEC²

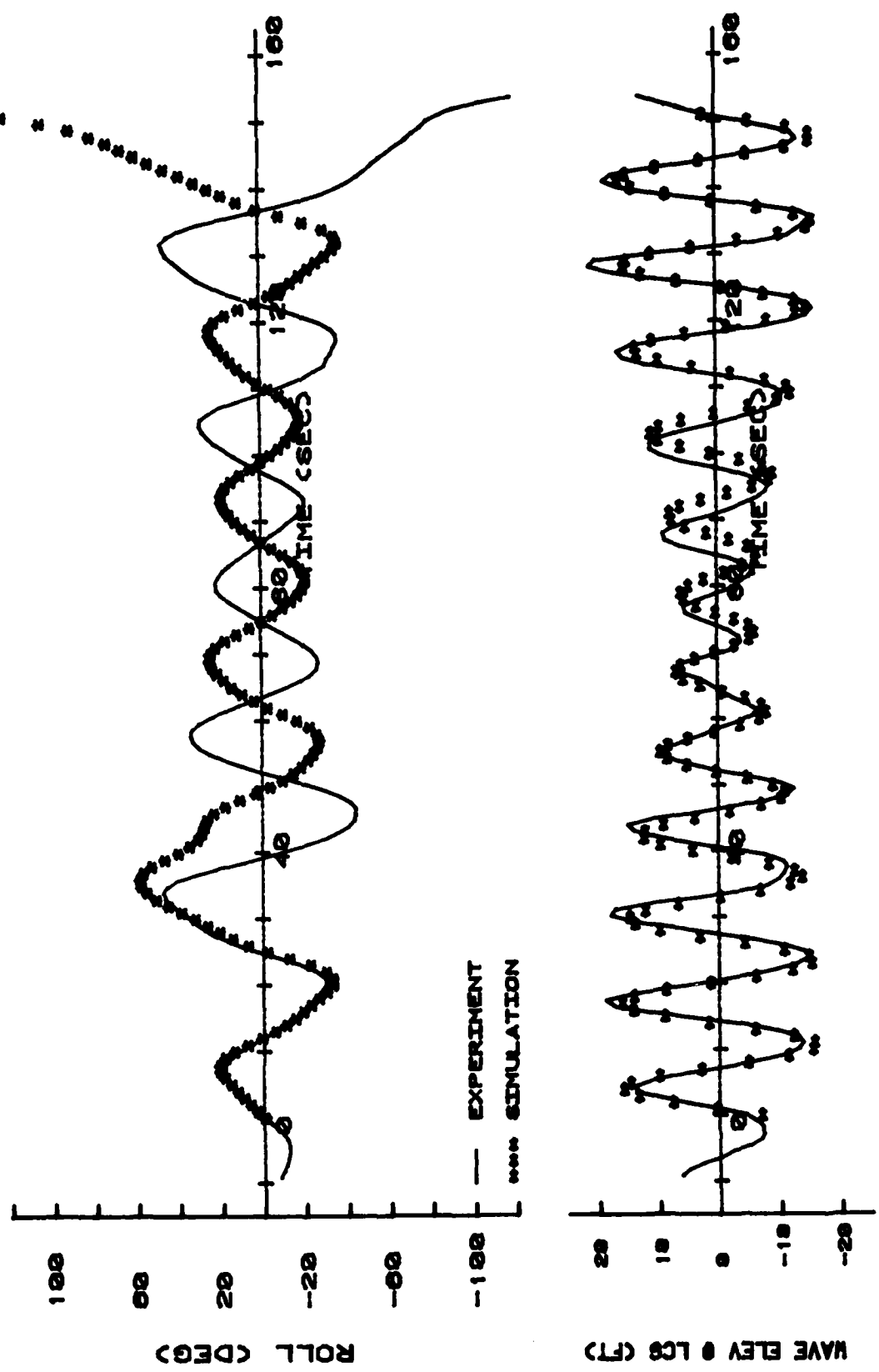


Figure III-11

CAPSIZE: GM

SPEED= 8.3 KN WAVE AMP= 13 FT DAMPO= 1.0E+9 FT:LB:SEC²

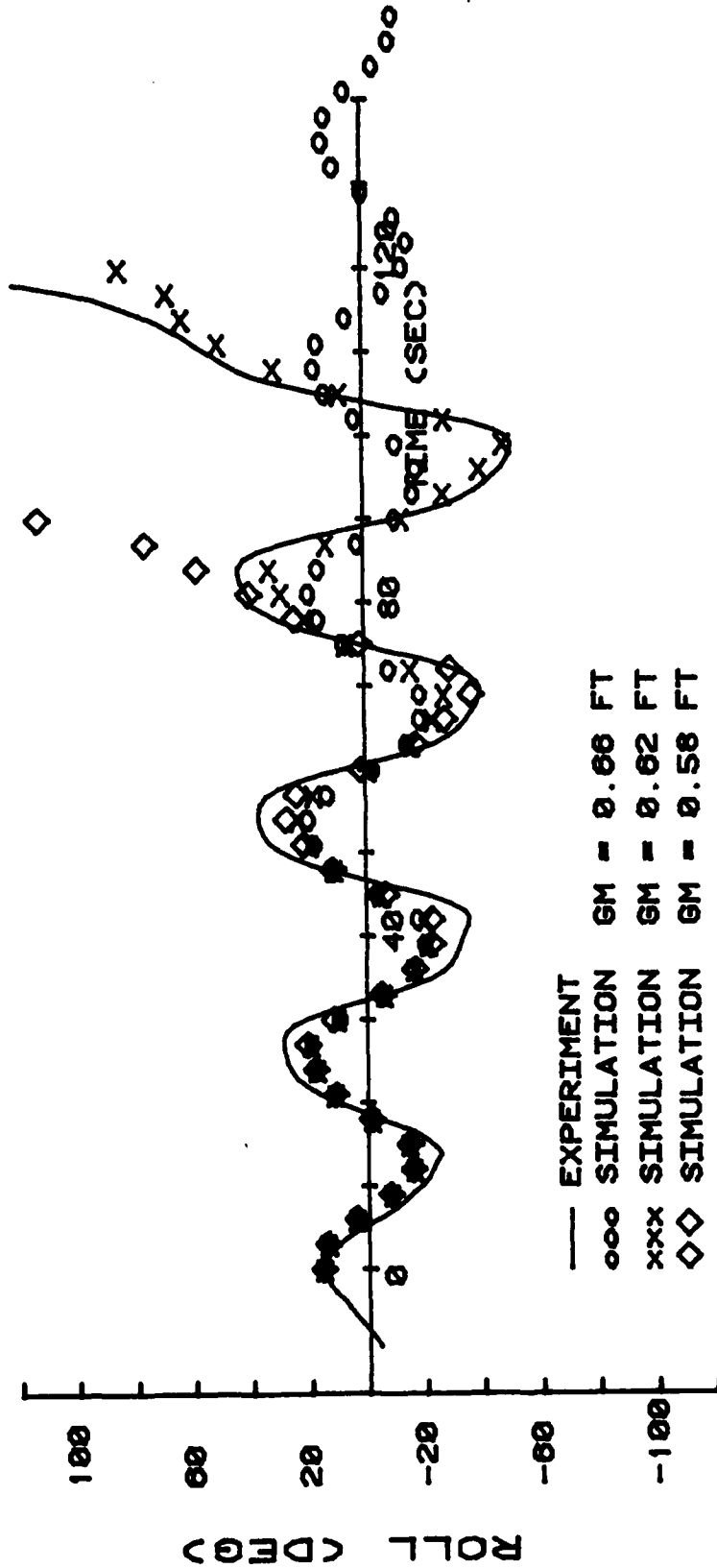


Figure III-12

CAPSIZE: WAVE AMPLITUDE

SPEED= 8.3 KN DAMPQ= 1.0E+9 FT:LB:SEC²

SPEED= 8.3 KN

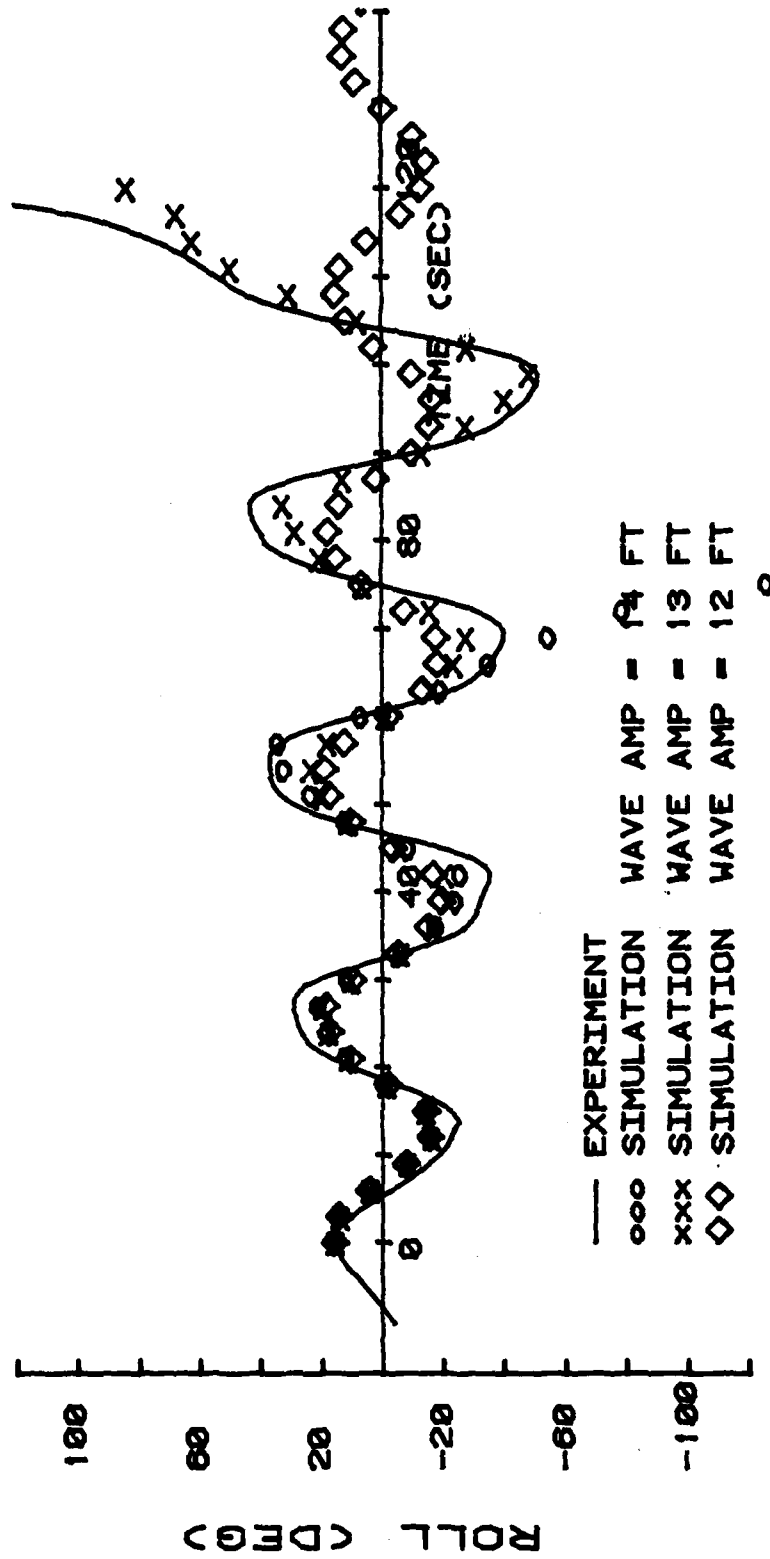


Figure III-13

MARINER ROLL DECAY

SPEED= 0 KN WAVE HEIGHT= 0 FT DAMPQ= 4.0E+8 FT:LB:SEC²

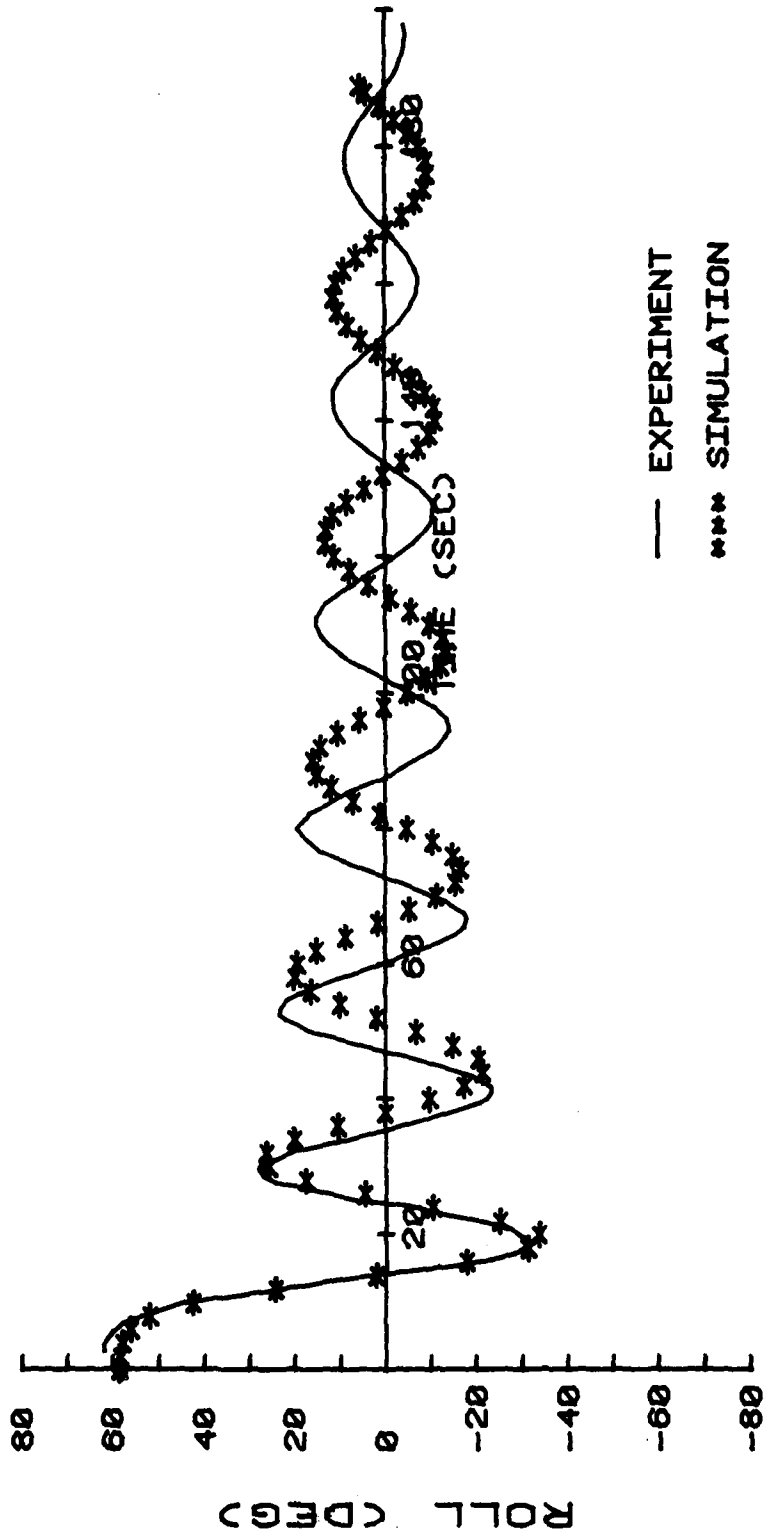


Figure III-14

MARINER ROLL DECAY

SPEED= 4.9 KN WAVE HEIGHT= 0 FT DAMPO= 4.0E+8 FT:LB:SEC²

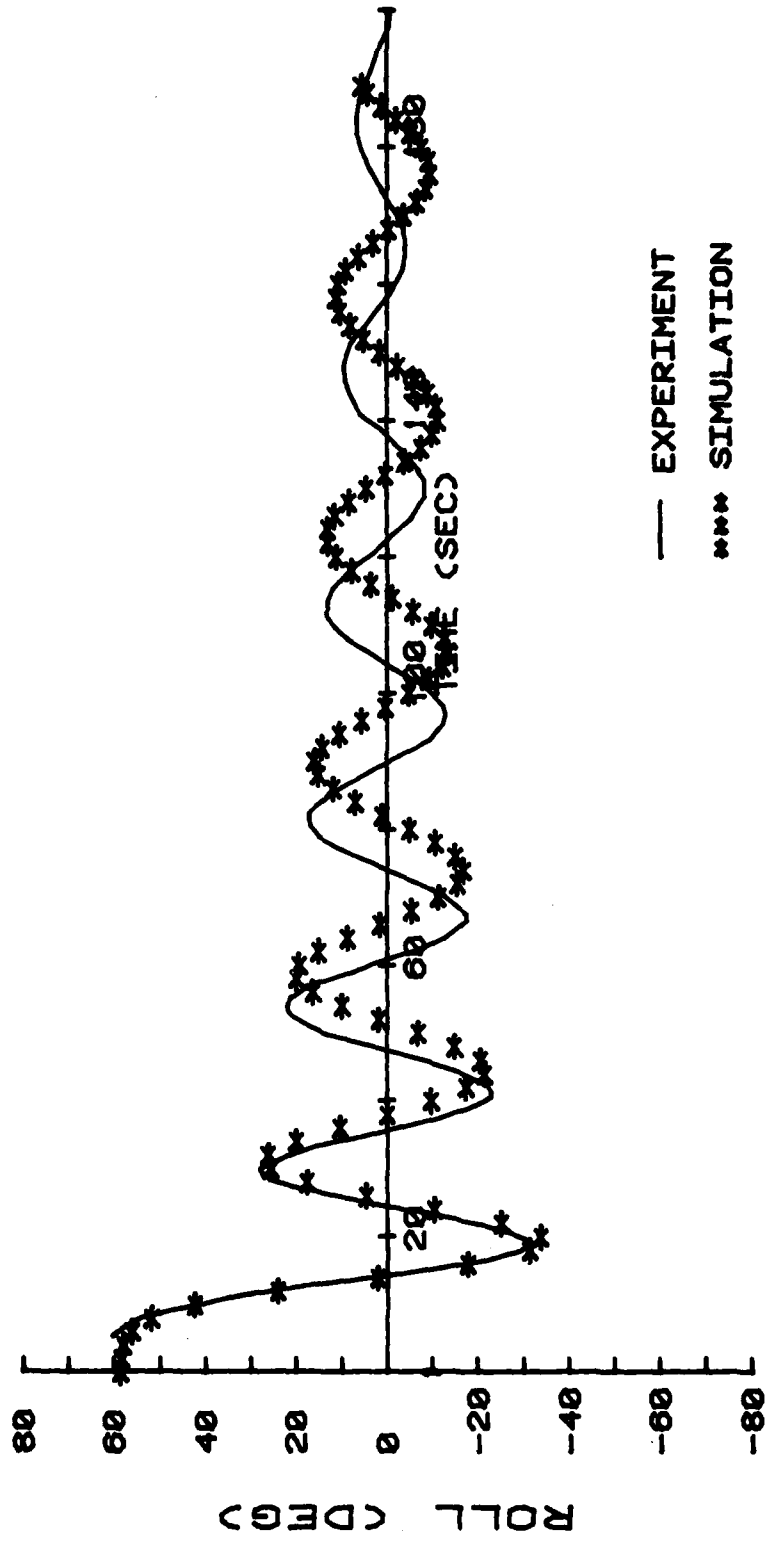


Figure III-15

MARINER ROLL DECAY

SPEED= 7.3 KN WAVE HEIGHT= 0 FT DAMPO= 4.0E+8 FT:LB:SEC²

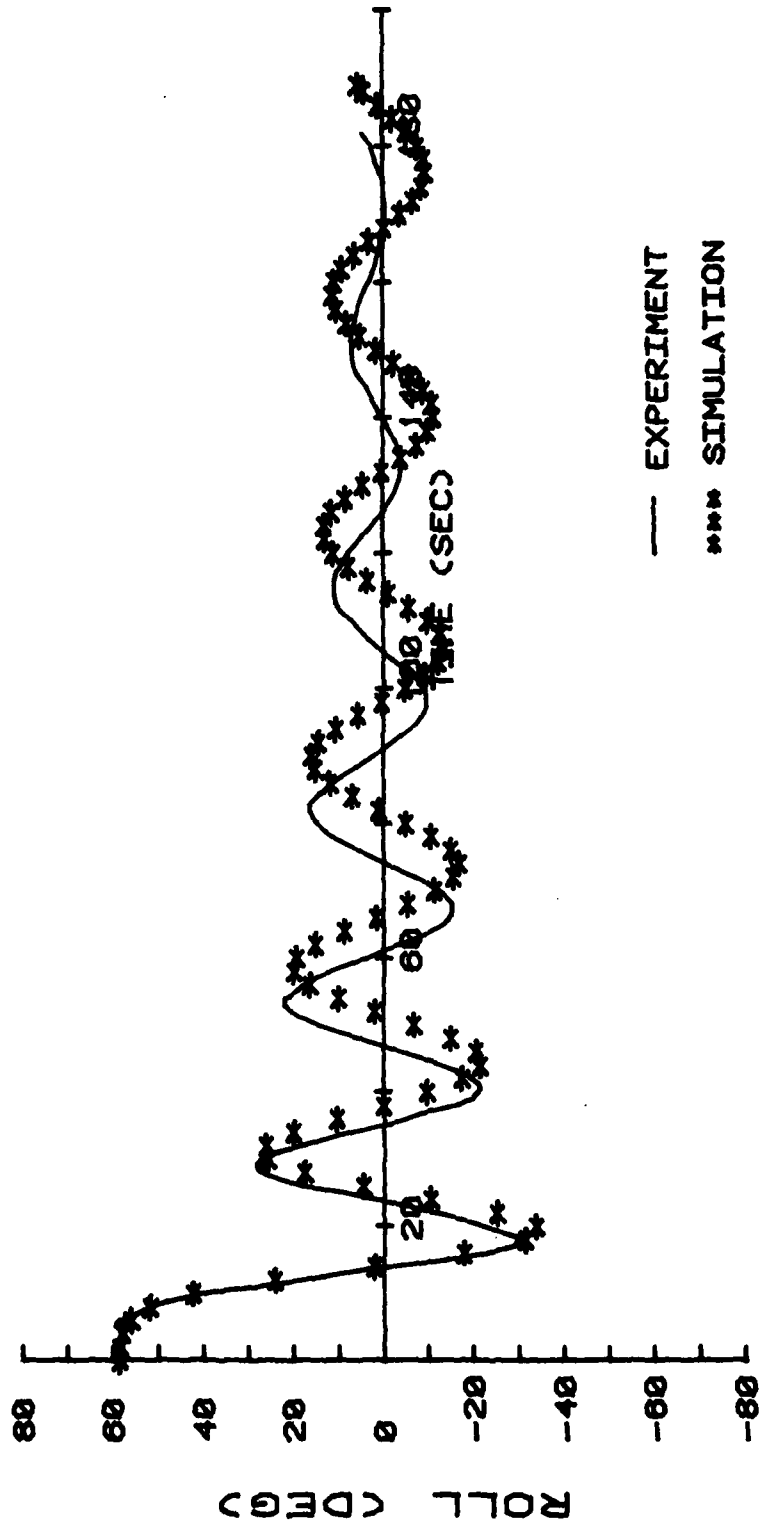


Figure III-16

MARINER ROLL DECAY

SPEED= 9.9 KN WAVE HEIGHT= 0 FT DAMPO= 4.0E+8 FT:LB:SEC²

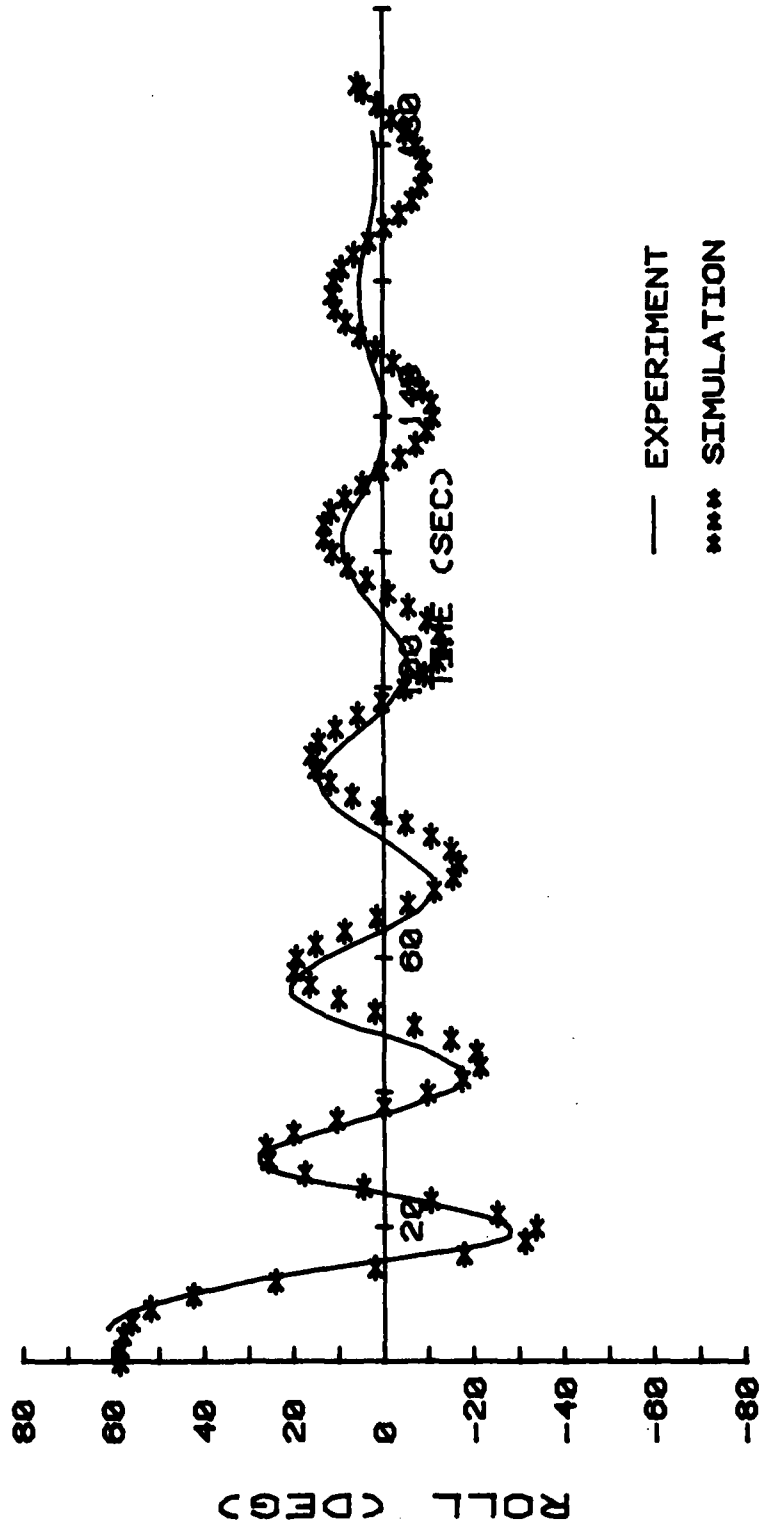


Figure III-17

SPEED= 7.3 KN WAVE AMP= 17.5 FT DAMPQ= 1.6E+9 FT:LB:SEC²
 CAPSIZE RUN 0901-41A SIX DEOF

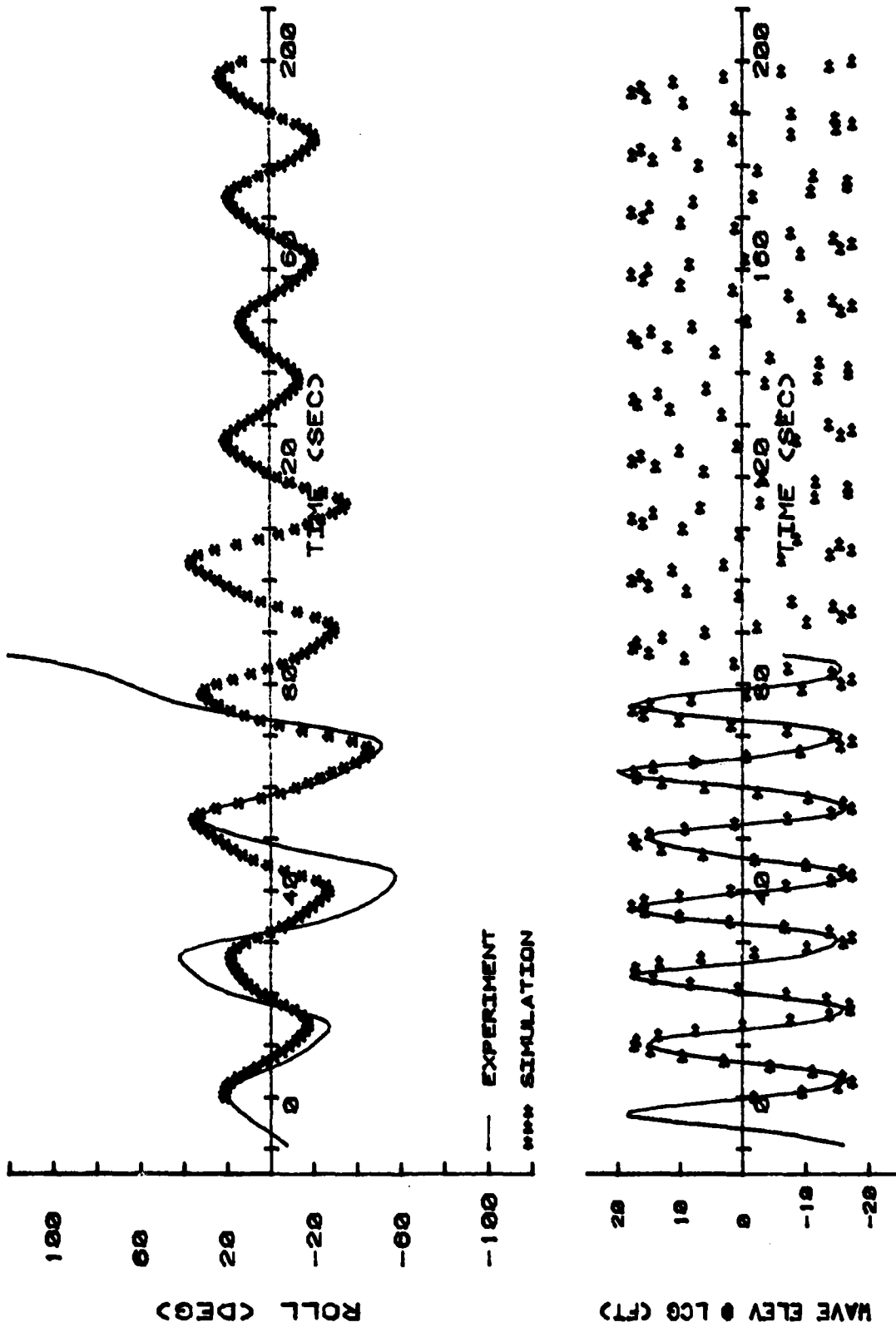


Figure III-18

CAPSIZER RUN 0901-41A SIX DEOF
 SPEED= 7.3 KN WAVE AMP= 17.5 FT DAMPQ= 1.4E+8 FT·LB·SEC²

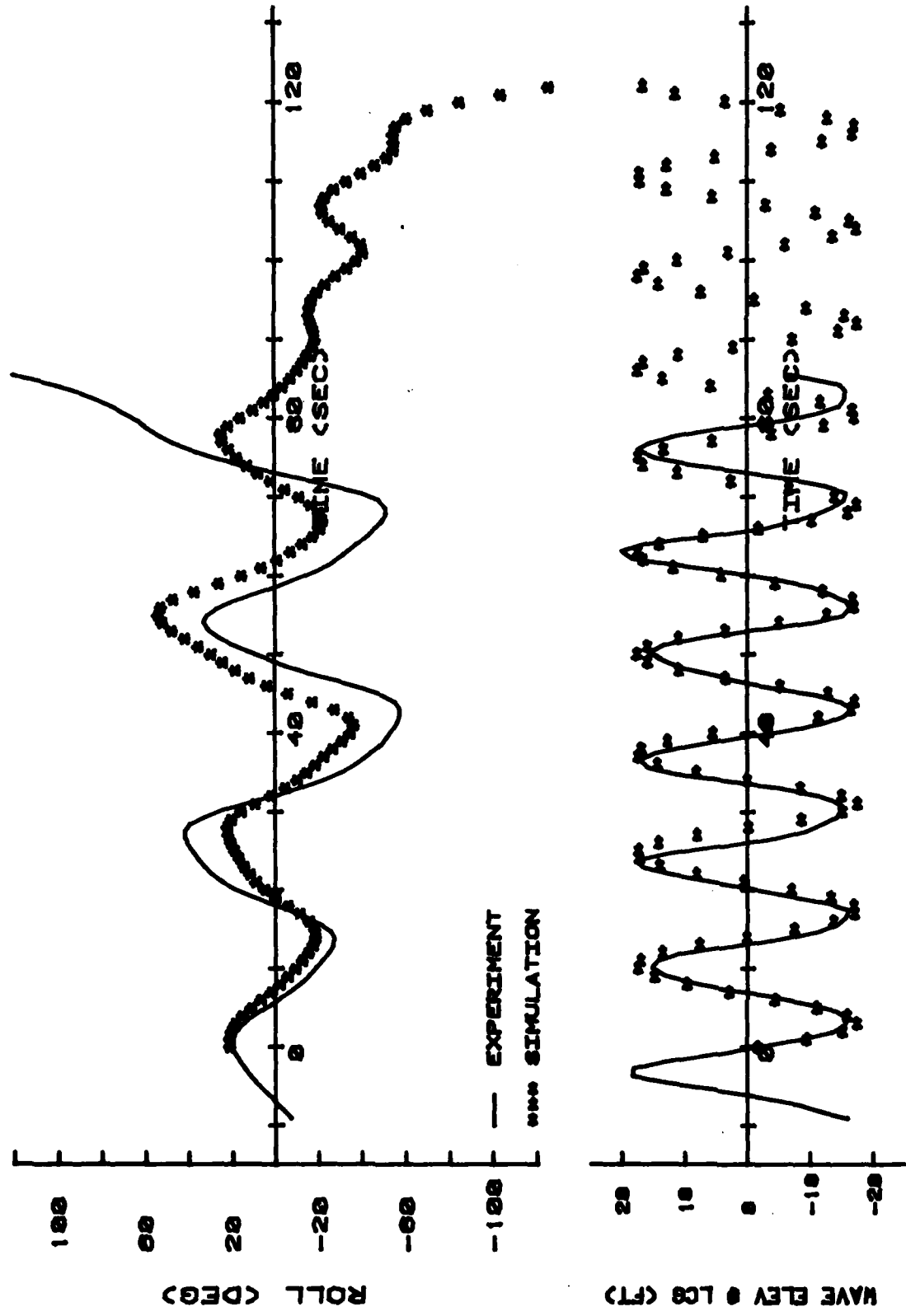


Figure III-19

CAPSIZER RUN 0901-41A SIX DEOF
 SPEED= 7.3 KN WAVE AMP= 17.5 FT DAMPQ= 1.2E+9 FT·LB·SEC²

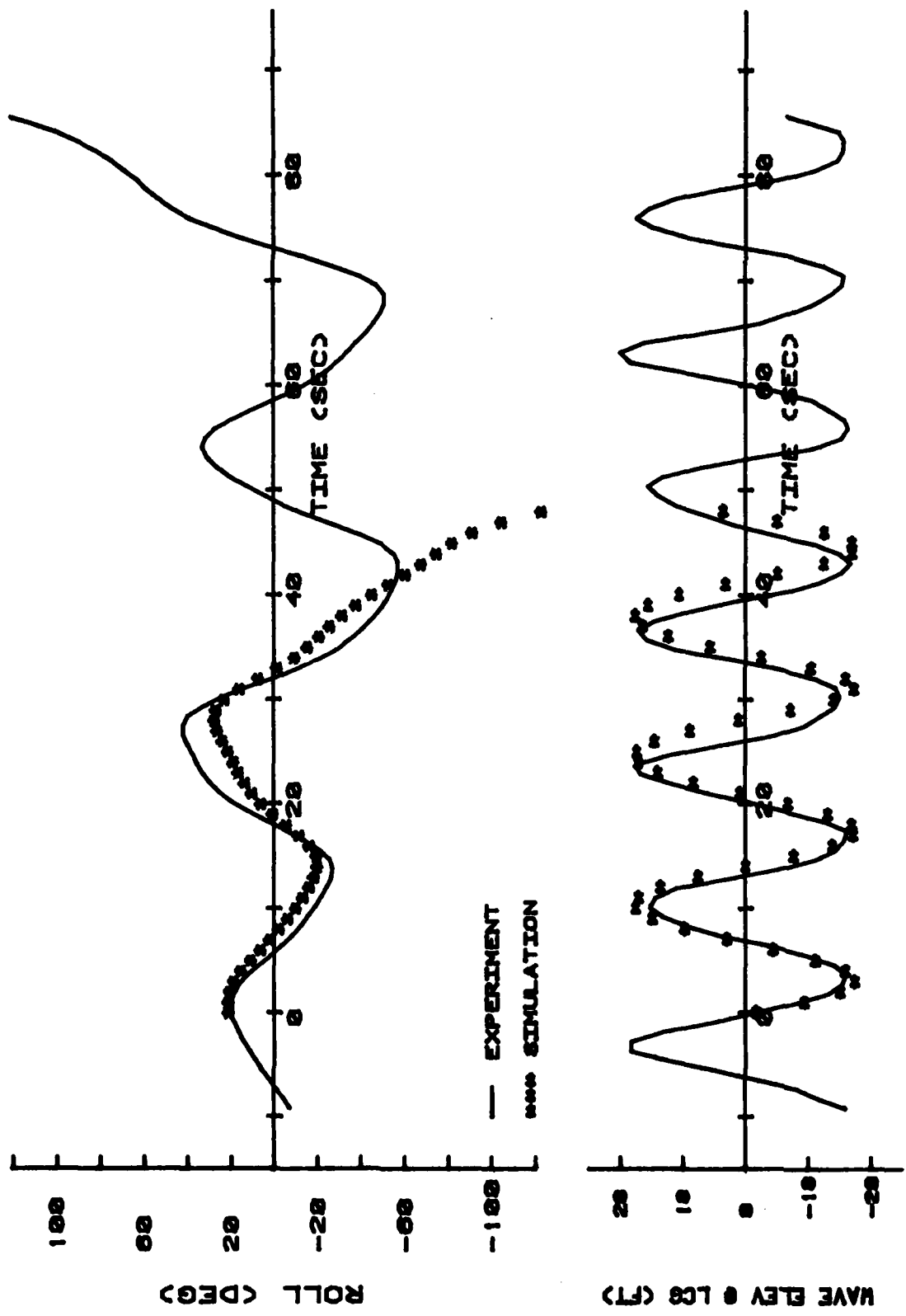


Figure III-20

CAPSIZE RUN 0901-41A SIX DEOF
 SPEED= 7.3 KN WAVE AMP= 17.5 FT DAMPO= 1.0E+0 FT·LB·SEC²

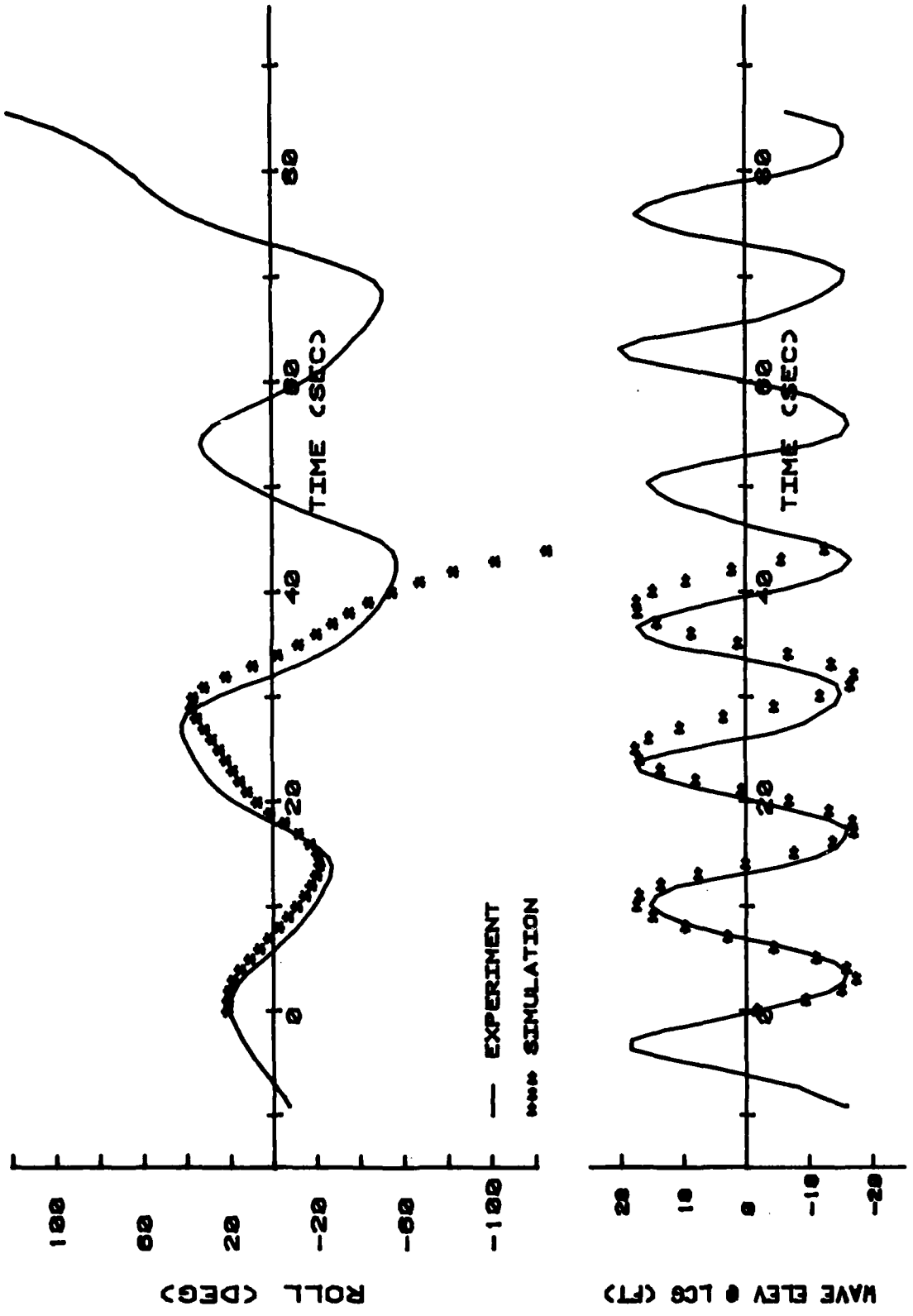


Figure III-21

SEA LAND 7 CONTAINER VESSEL RIGHTING ARM CURVES

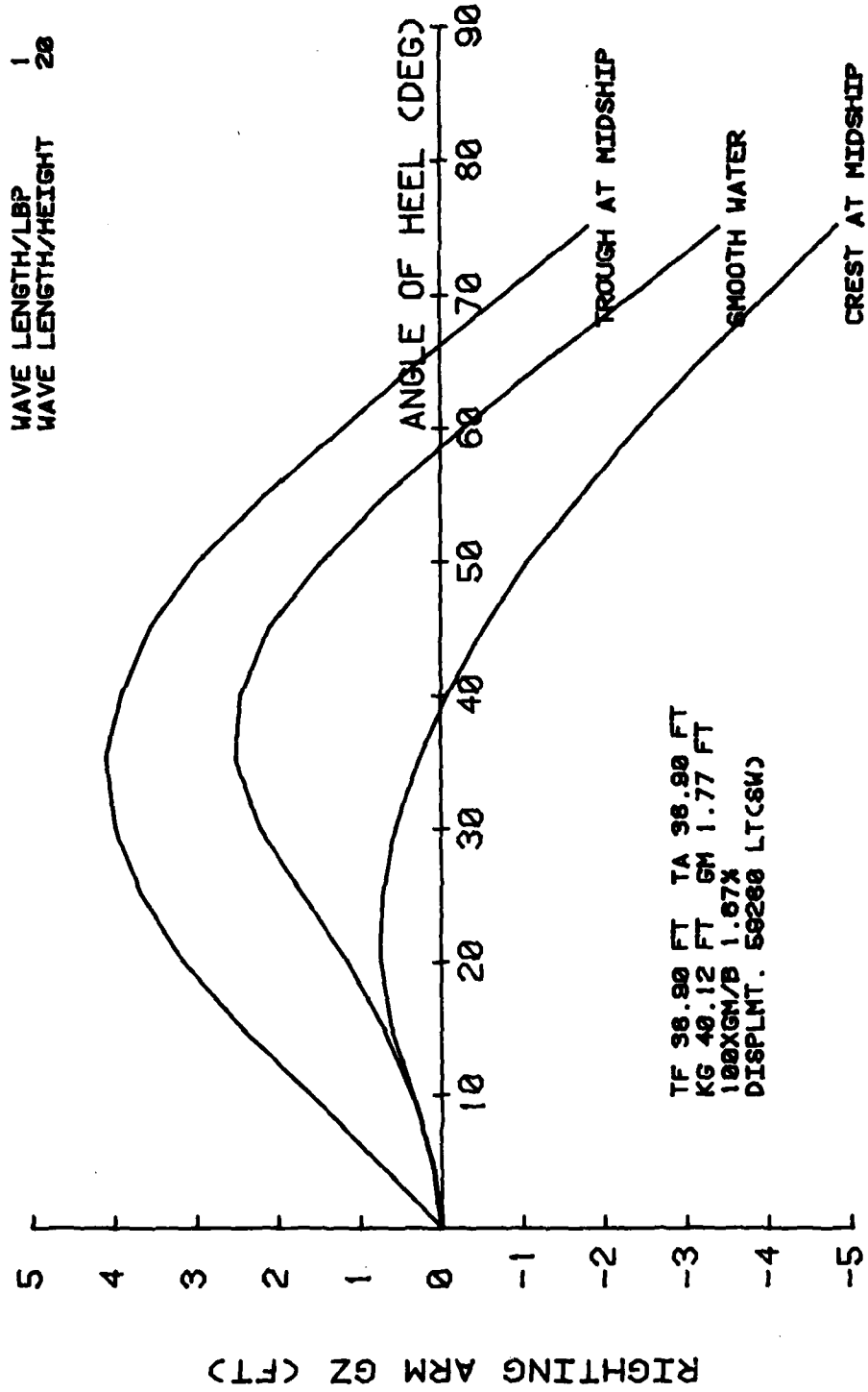


Figure III-22

SL7 CAPSIZE RUN 0409-46LQ 3DEOF
 SPEED= 9.8 KN WAVE AMP= 12.9 FT DAMPQ= 6.0E+9 FT.LB.SEC²
 DAMPL= 1.7E+8 FT.LB.SEC

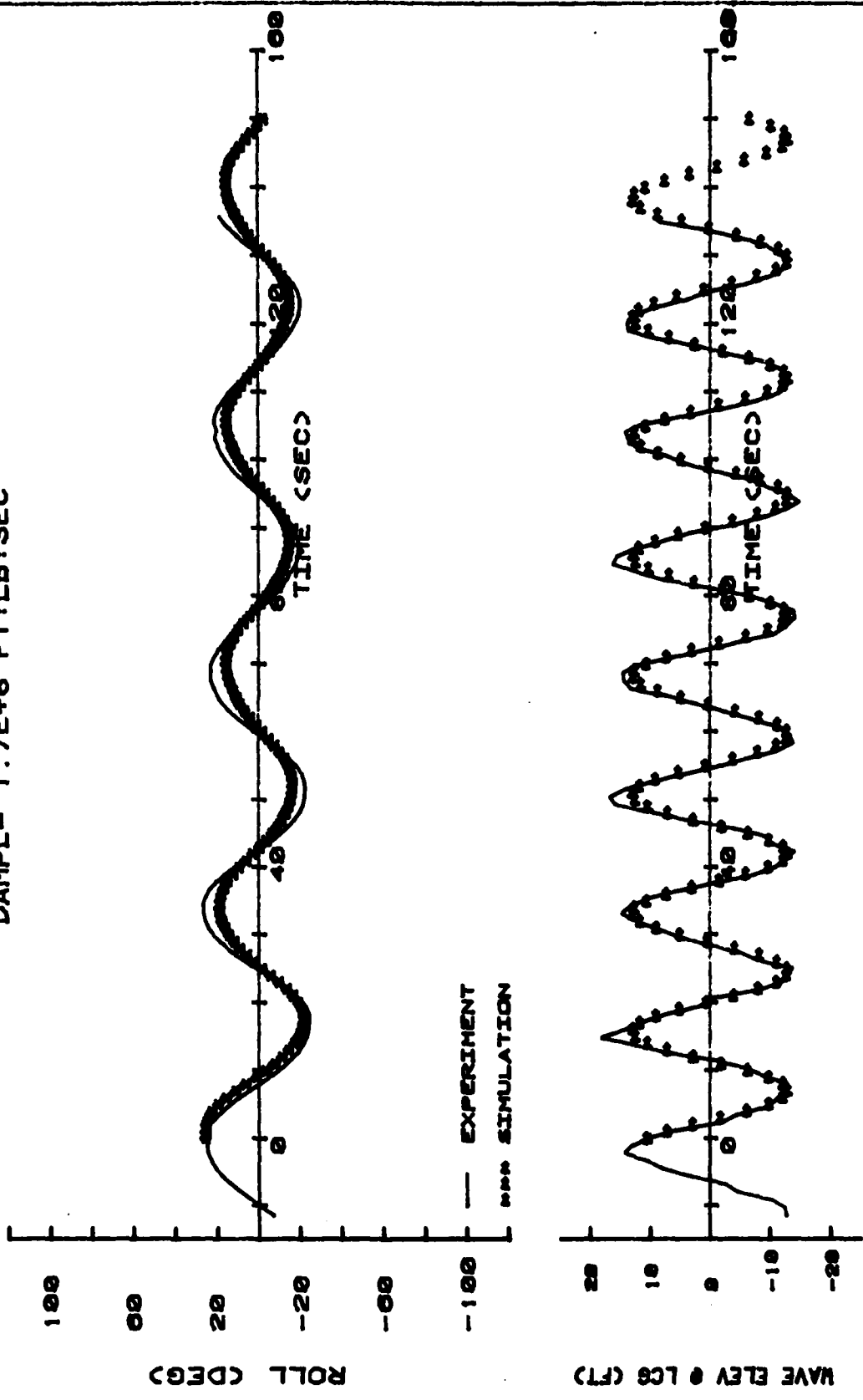


Figure III-23

SL7 CAPSIZE RUN 0409-63LQ 3DEOF
 SPEED= 3.7 KN WAVE AMP= 16 FT DAMPQ= 2.1E+8 FT·LB·SEC²
 DAMPL= 1.1E+8 FT·LB·SEC

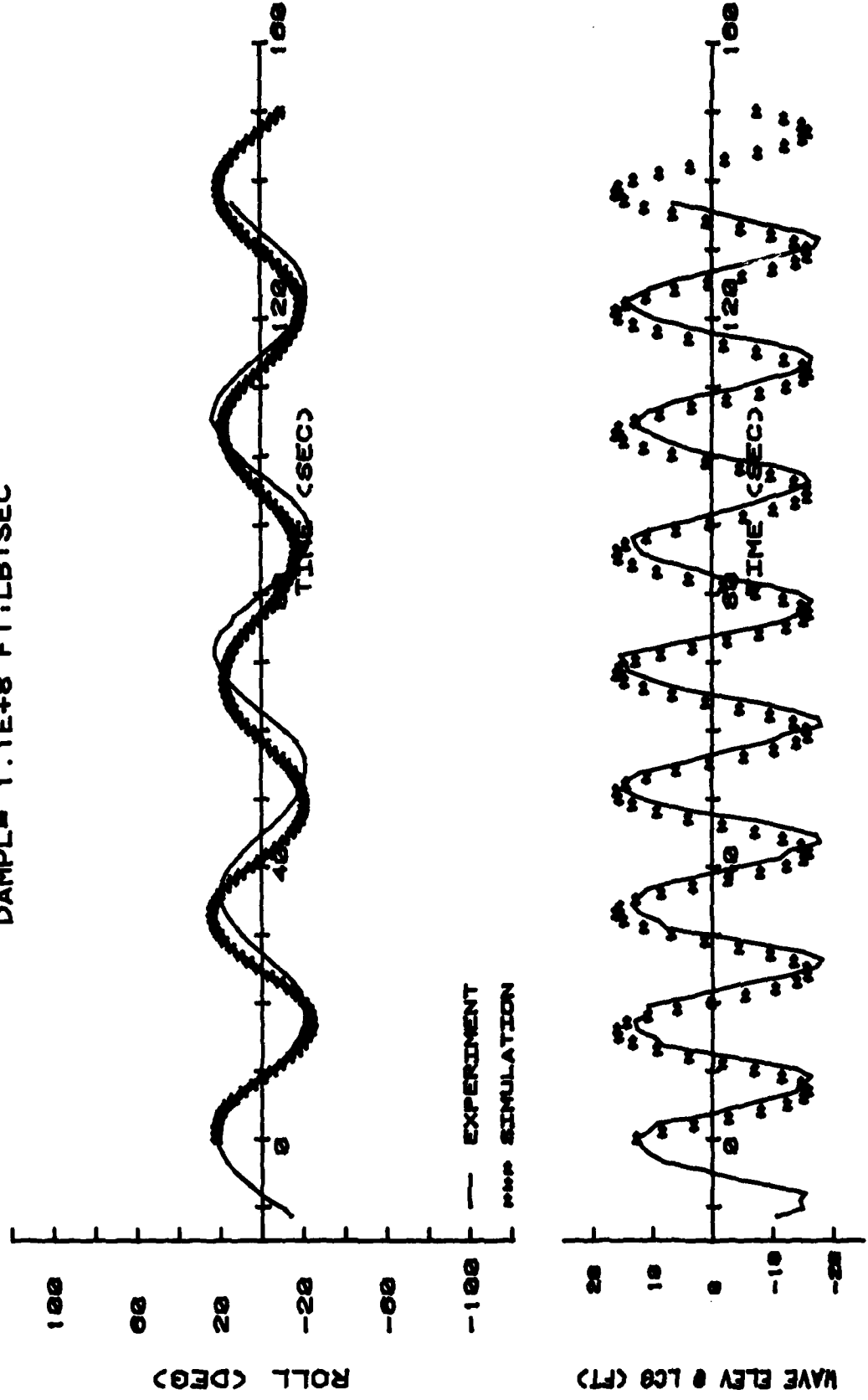


Figure III-24

SL7 CAPSIZE RUN 0409-45LQ 3DEOF
 SPEED= 9.8 KN WAVE AMP= 15.9 FT DAMPQ= 2.5E+7 FT:LB:SEC²
 DAMPL= 1.15E+8 FT:LB:SEC

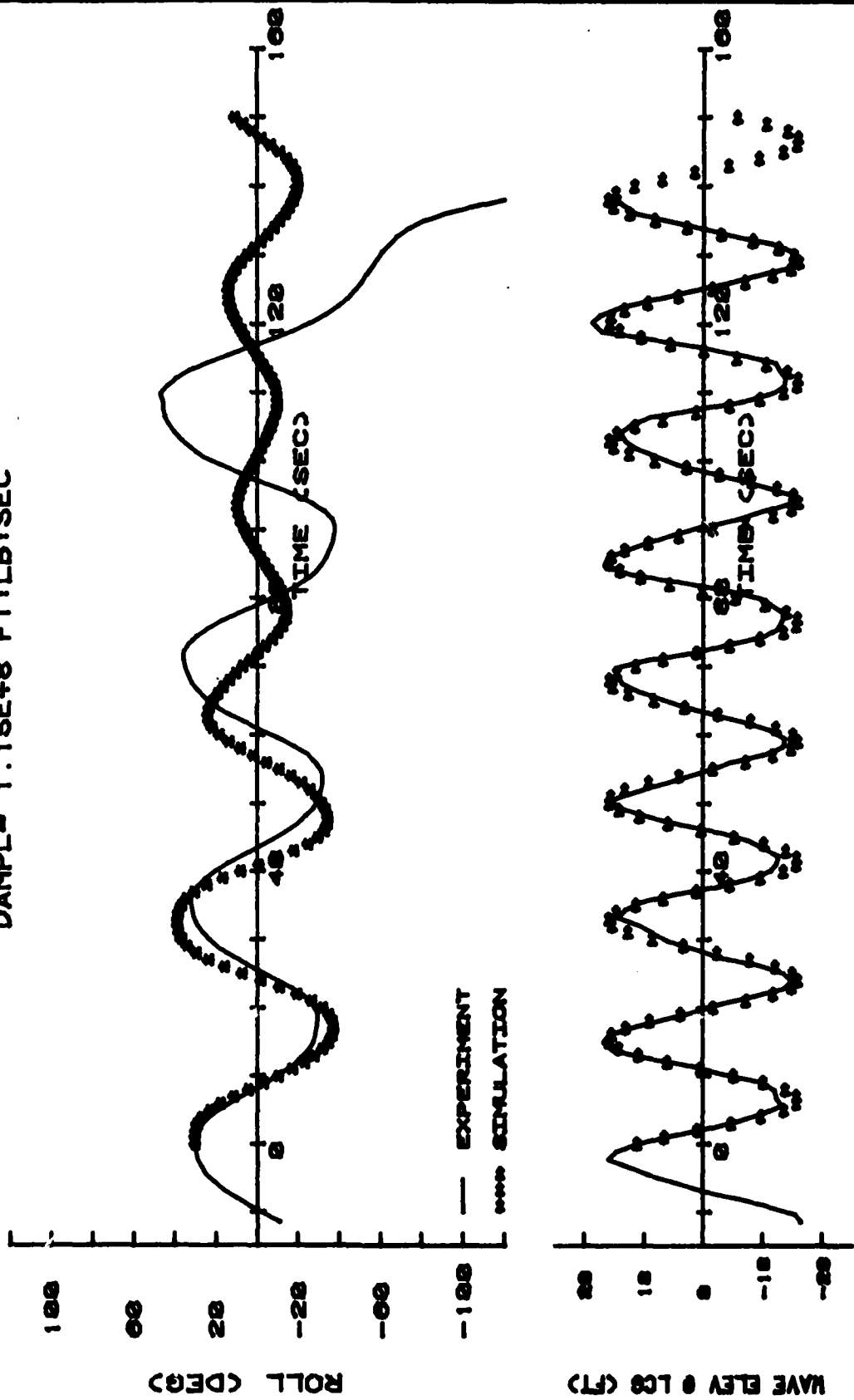


Figure III-25

SL7 CAPSIZE RUN 0409-45LQ 3DEOF
 SPEED= 9.8 KN WAVE AMP= 15.9 FT DAMPO= 9.0E+9 FT.LB.SEC²
 DAMPL= 1.79E+8 FT.LB.SEC

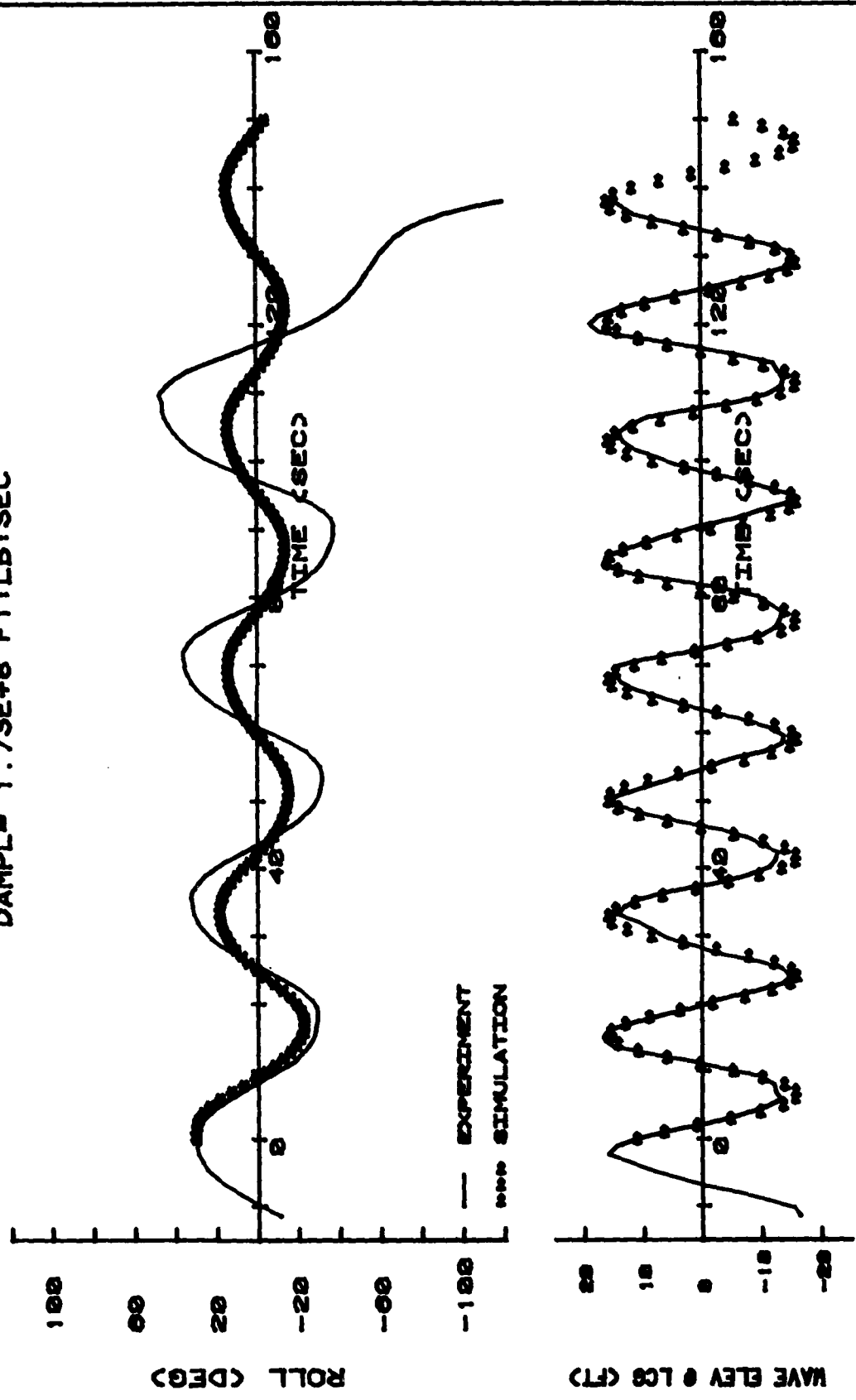


Figure III-26

SL7 CAPSIZE RUN 0409-61LQ 3DEOF
 SPEED= 1.3 KN WAVE AMP= 15.4 FT DAMPO= 5.0E+7 FT.LB:SEC.
 DAMPL= 500000 FT.LB:SEC

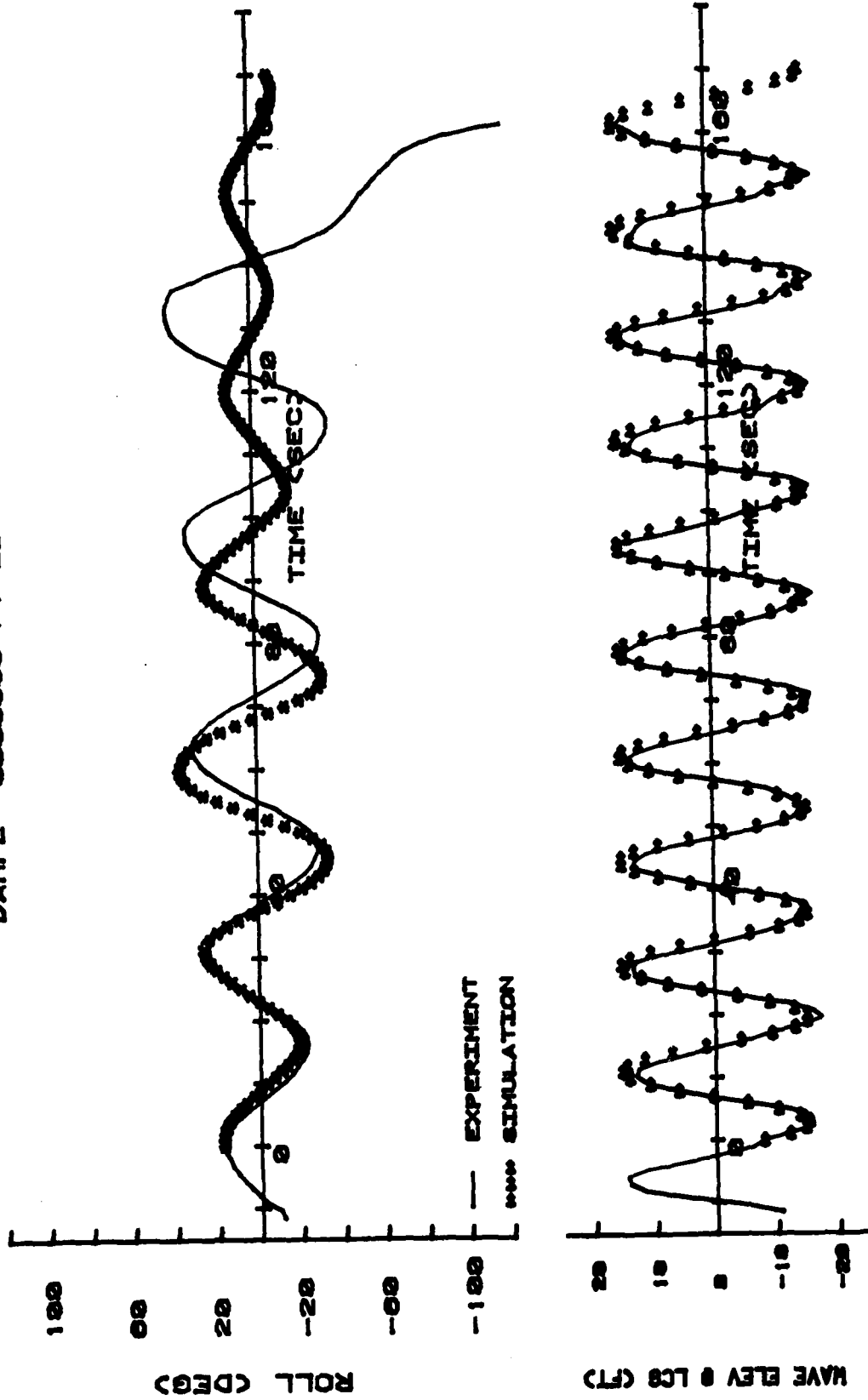


Figure III-27

SL7 ROLL DECAY 3DEOF
 SPEED: 3.1 KTS WAVE AMPLITUDE: 0 FT
 DAMPL: $9.2E+7$ FT*LB*SEC DAMPG: $2.0E+9$ FT*LB*SEC*SEC

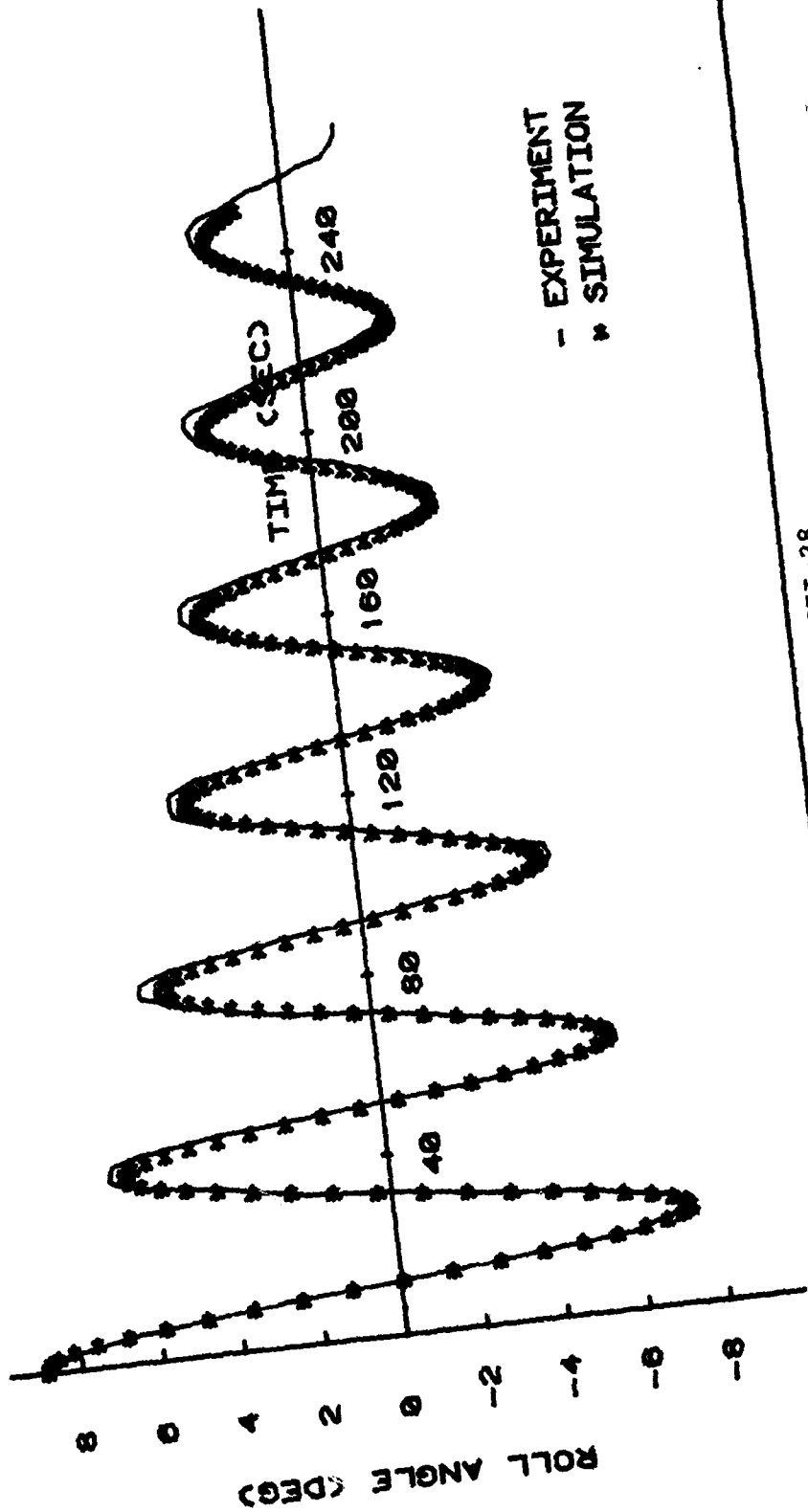
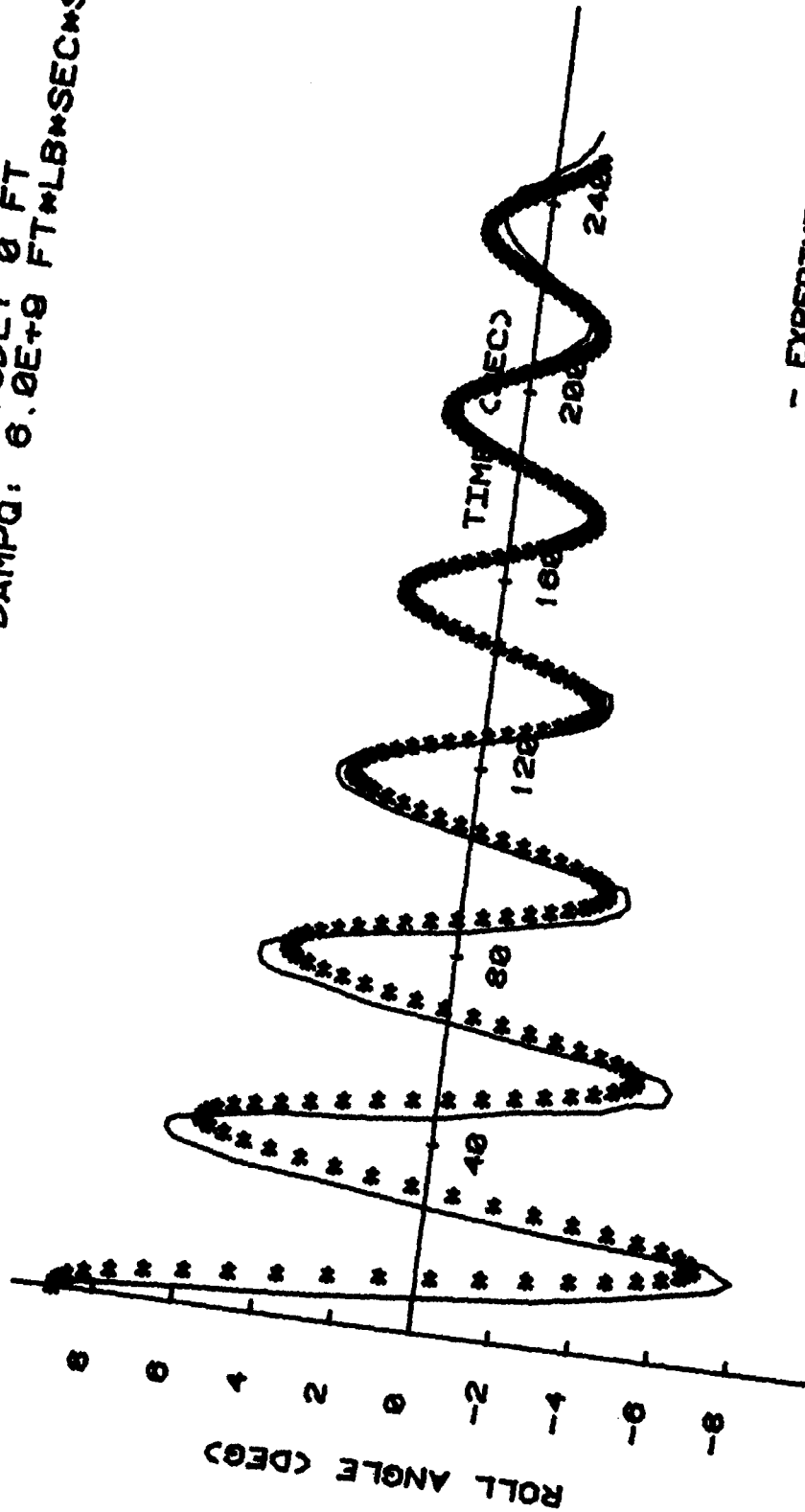


Figure III-28

SL7 ROLL DECAY 3DEOF
 DAMPL: 9.0E+7 FT*LB*SEC WAVE AMPLITUDE: 0 FT
 SPEED: 12.2 KTS DAMPG: 6.0E+9 FT*LB*SEC*SEC



- EXPERIMENT
 * SIMULATION

Figure III-29

PACIFIC COAST CRAB BOAT
 (values in full scale)
 RIGHTING ARM CURVES
 100GM/B = 7.5

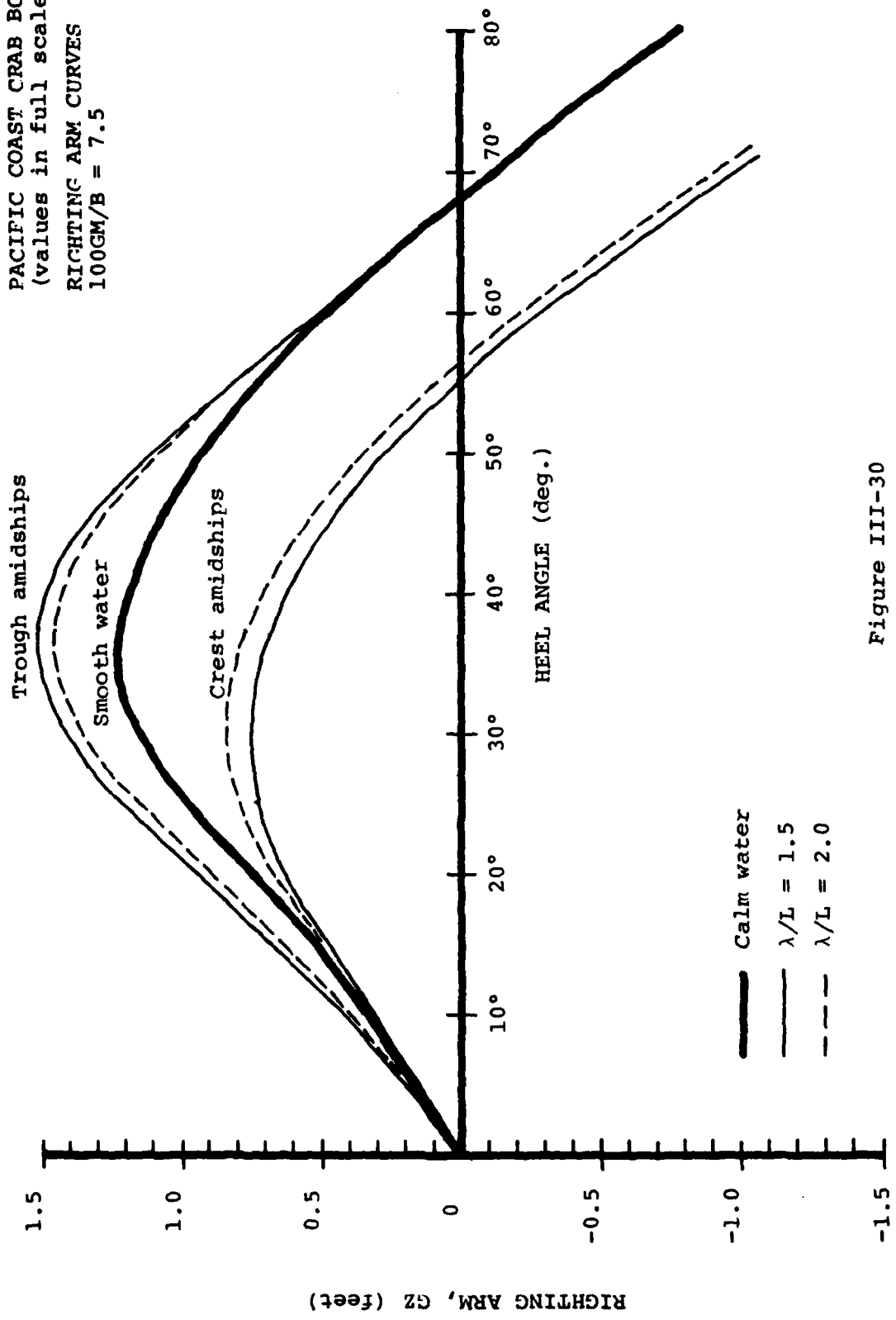


Figure III-30

PACIFIC COAST CPAB BOAT
 (values in full scale)
 RIGHTING ARM CURVES
 100M/B = 4.0

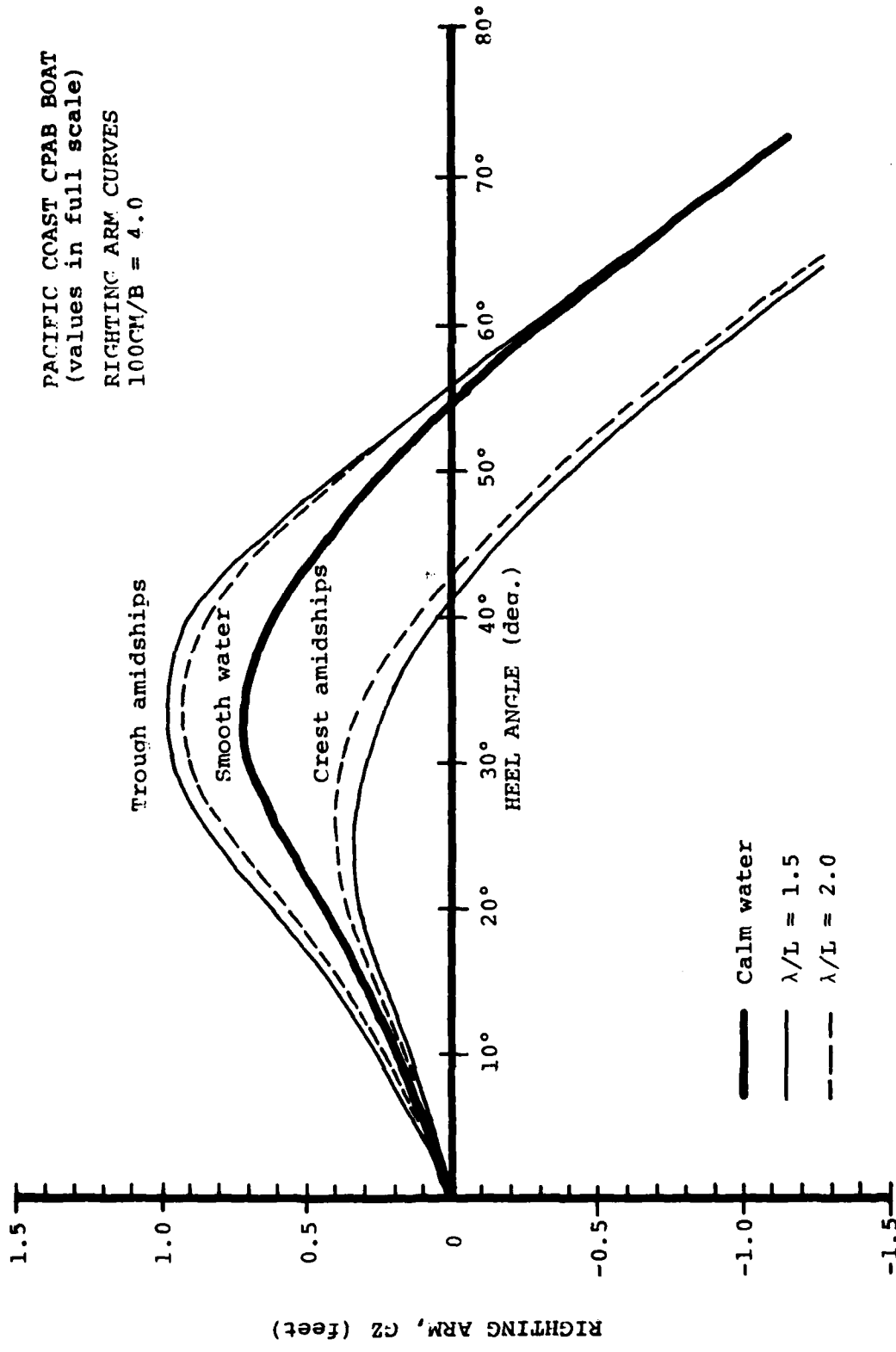


Figure III-31

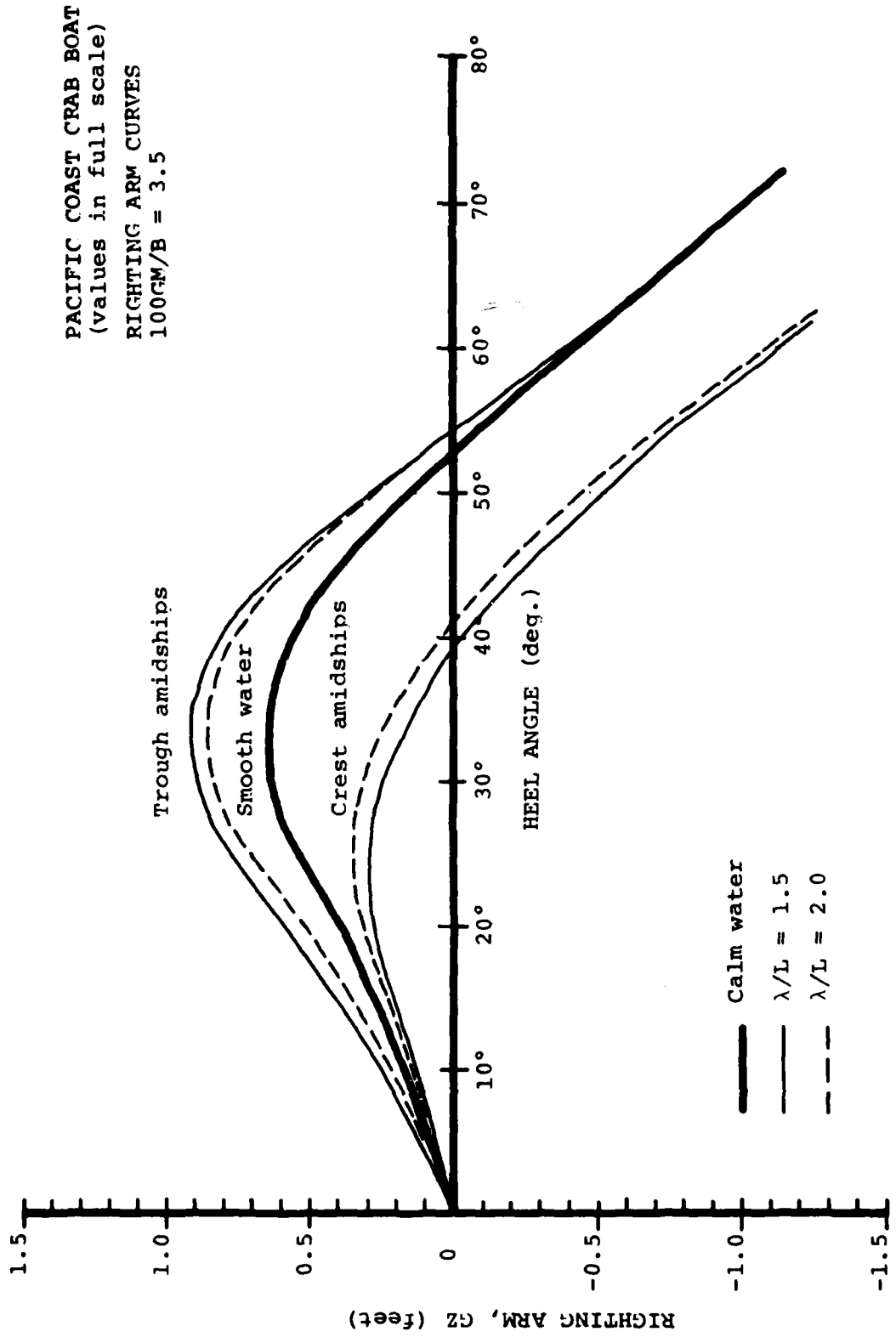


Figure III-32

PACIFIC COAST CFAB BOAT
 (values in full scale)
 RIGHTING ARM CURVES
 100GM/B = 2.5

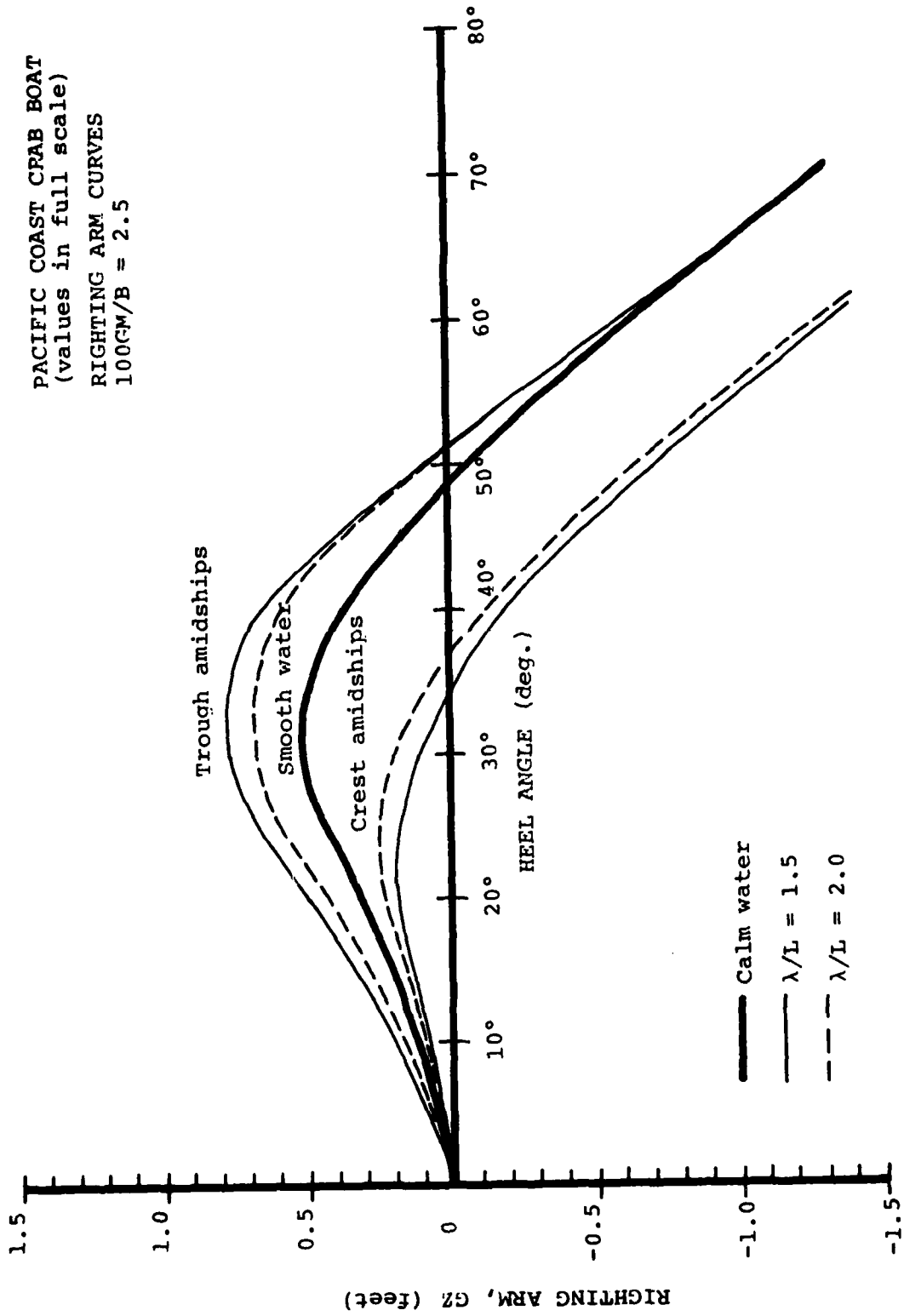
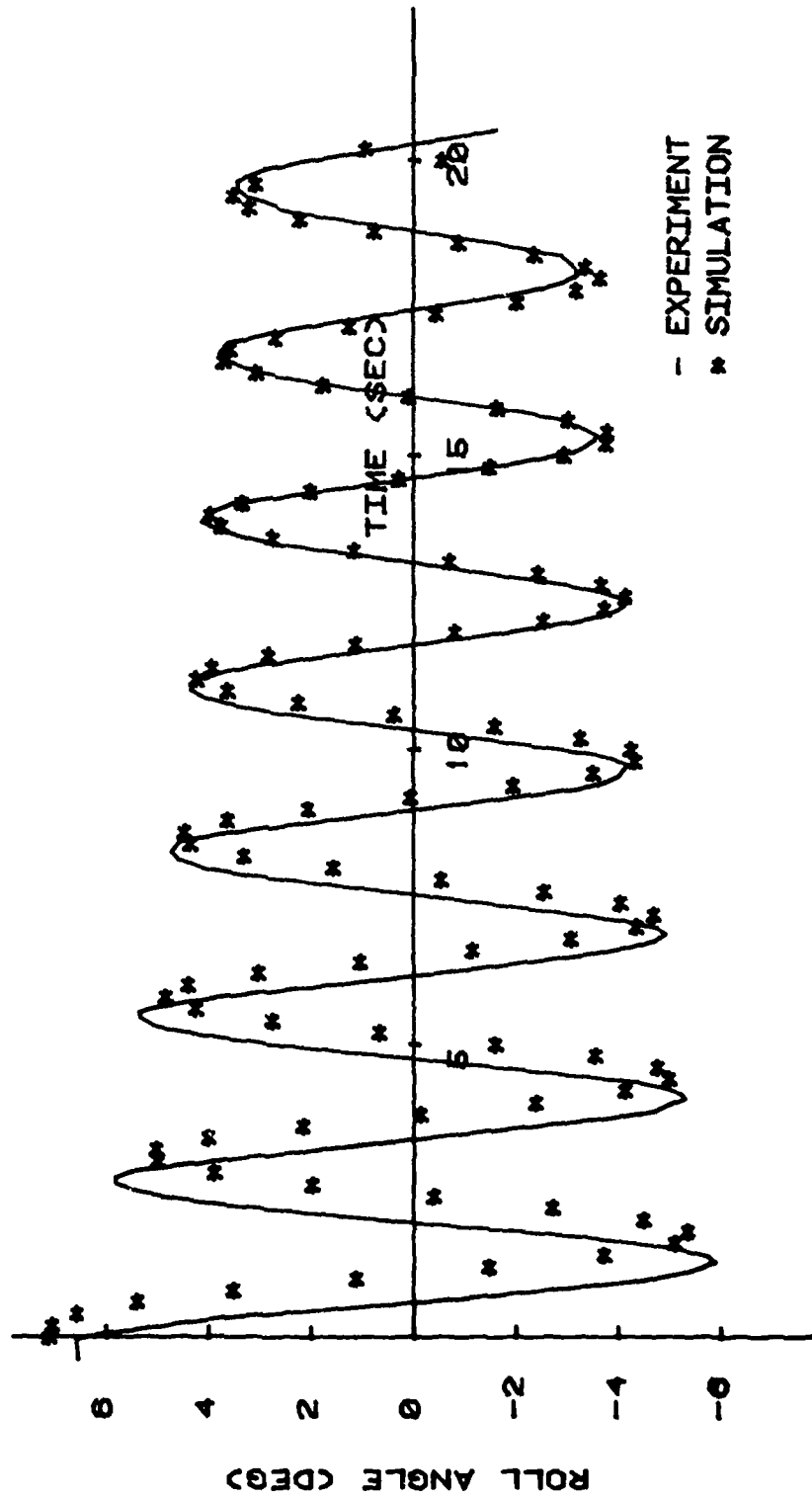


Figure III-33

CRAB BOAT MODEL FREE ROLL DECAY

SPEED: 0 KTS WAVE AMPLITUDE: 0 FT
DAMPL: 0.026 FT*LB*SEC DAMPG: 0.032 FT*LB*SEC*SEC



- EXPERIMENT
* SIMULATION

Figure III-34

CRAB BOAT MODEL FREE ROLL DECAY

SPEED: 1.572 KTS WAVE AMPLITUDE: 0 FT
DAMPL: 0.158 FT*LB*SEC DAMPO: 0 FT*LB*SEC*SEC

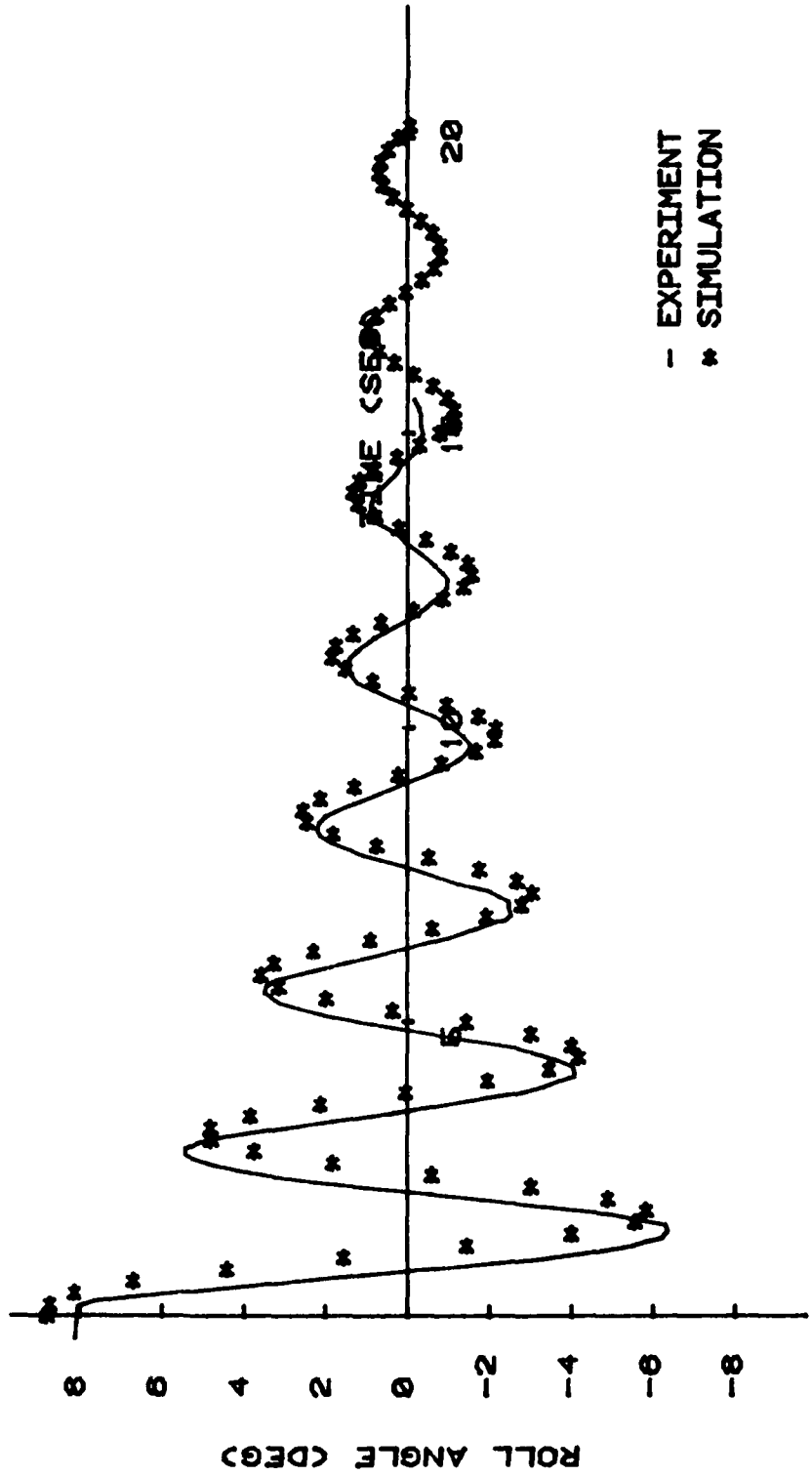


Figure III-35

CRAB BOAT MODEL FREE ROLL DECAY

SPEED: 1.976 KTS
 DAMPL: 0.1762 FT*LB*SEC

WAVE AMPLITUDE: 0 FT
 DAMPO: 0.0309 FT*LB*SEC*SEC

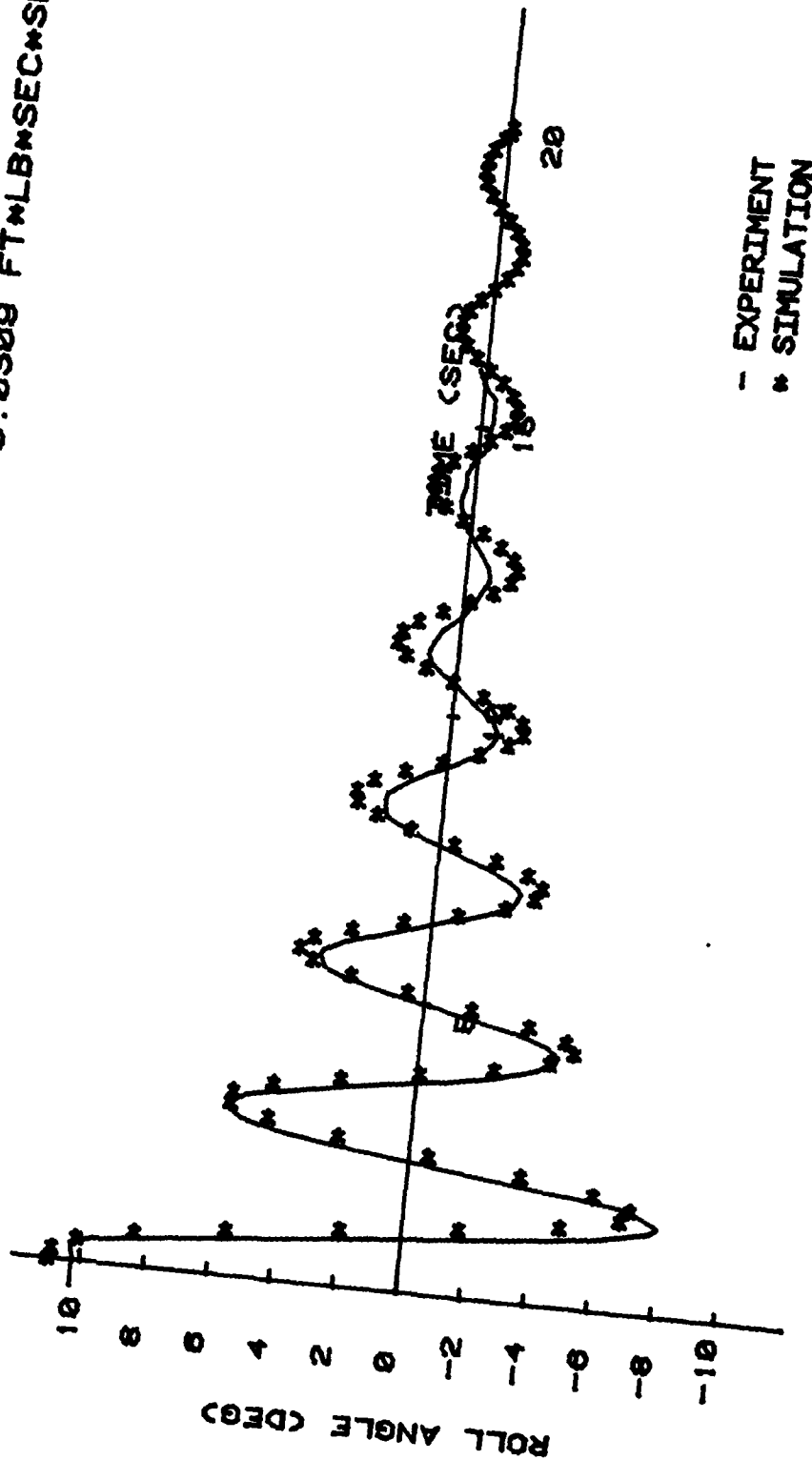


Figure III-36

CRAB BOAT MODEL FREE ROLL DECAY

SPEED: 0 KTS WAVE AMPLITUDE: 0 FT
DAMPL: 0.03 FT*LB*SEC DAMPG: 0.095 FT*LB*SEC*SEC

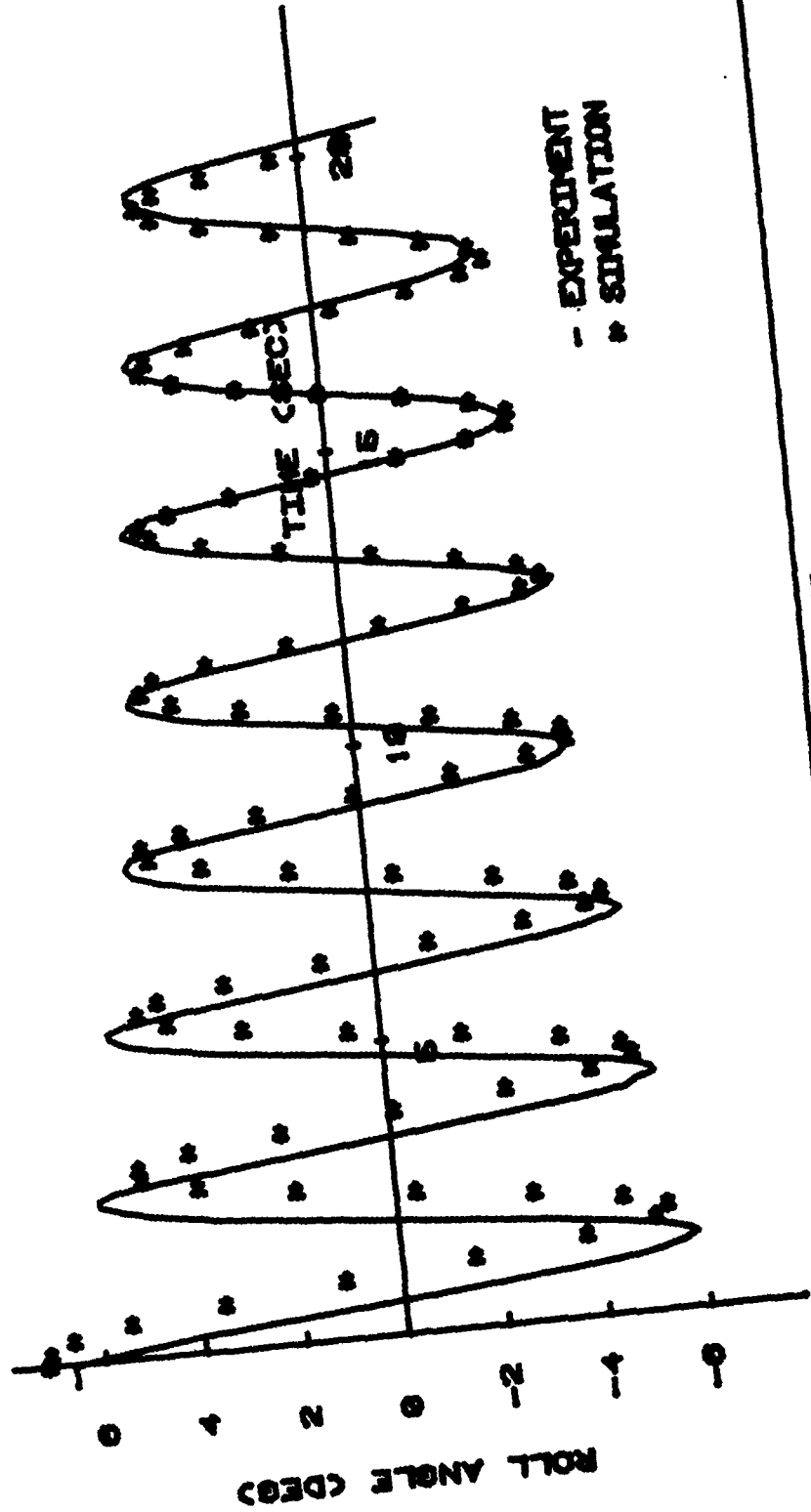


Figure III-37

CRAB BOAT MODEL FREE ROLL DECAY

DAMPL: 0.17 FT*LB*SEC
SPEED: 1.572 KTS

WAVE AMPLITUDE: 0 FT
DAMPQ: 0.03 FT*LB*SEC*SEC

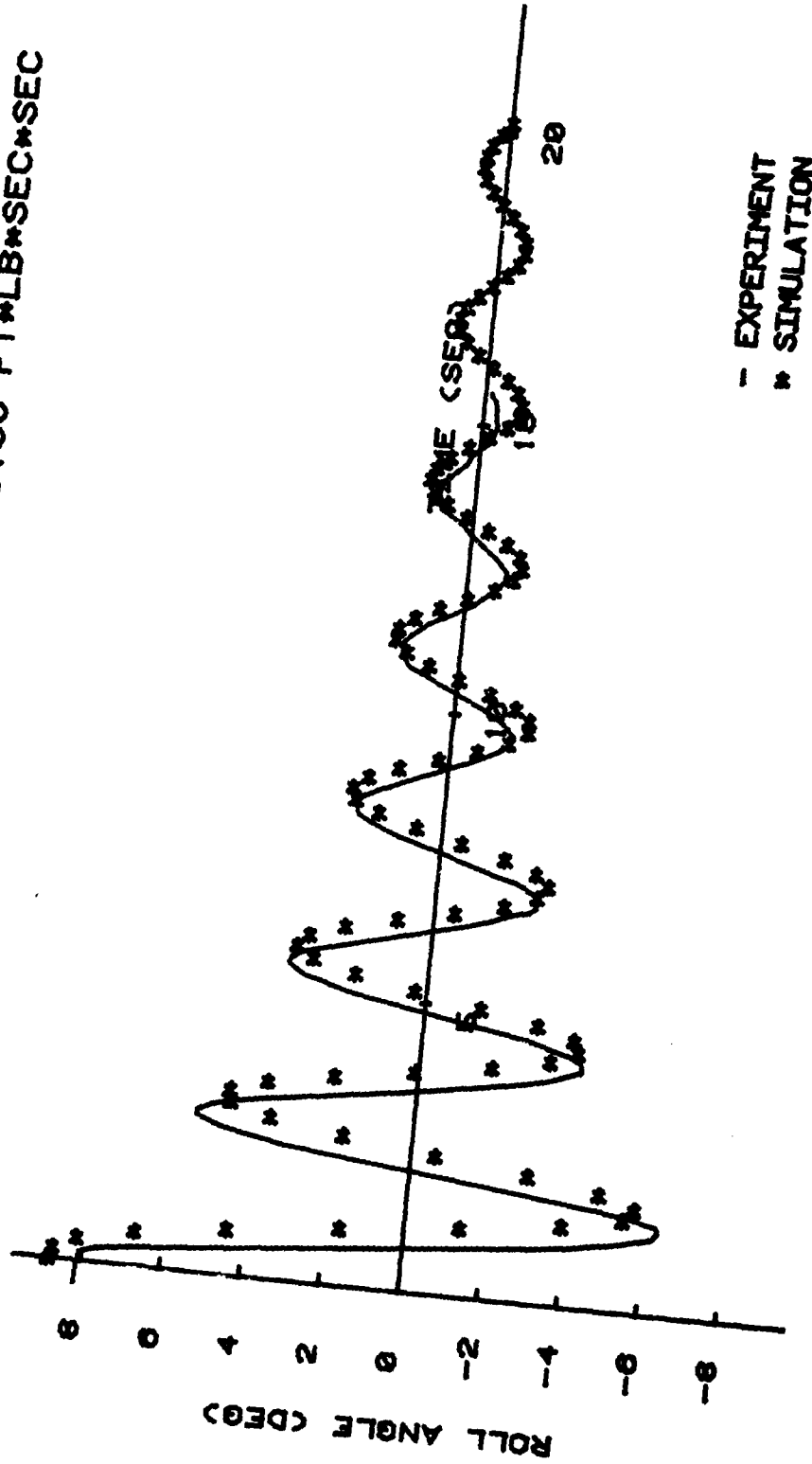


Figure III-38

CRAB BOAT MODEL FREE ROLL DECAY

DAMPL: 0.2 FT*LB*SEC
SPEED: 1.976 KTS

WAVE AMPLITUDE: 0 FT
DAMPQ: 0.06 FT*LB*SEC*SEC

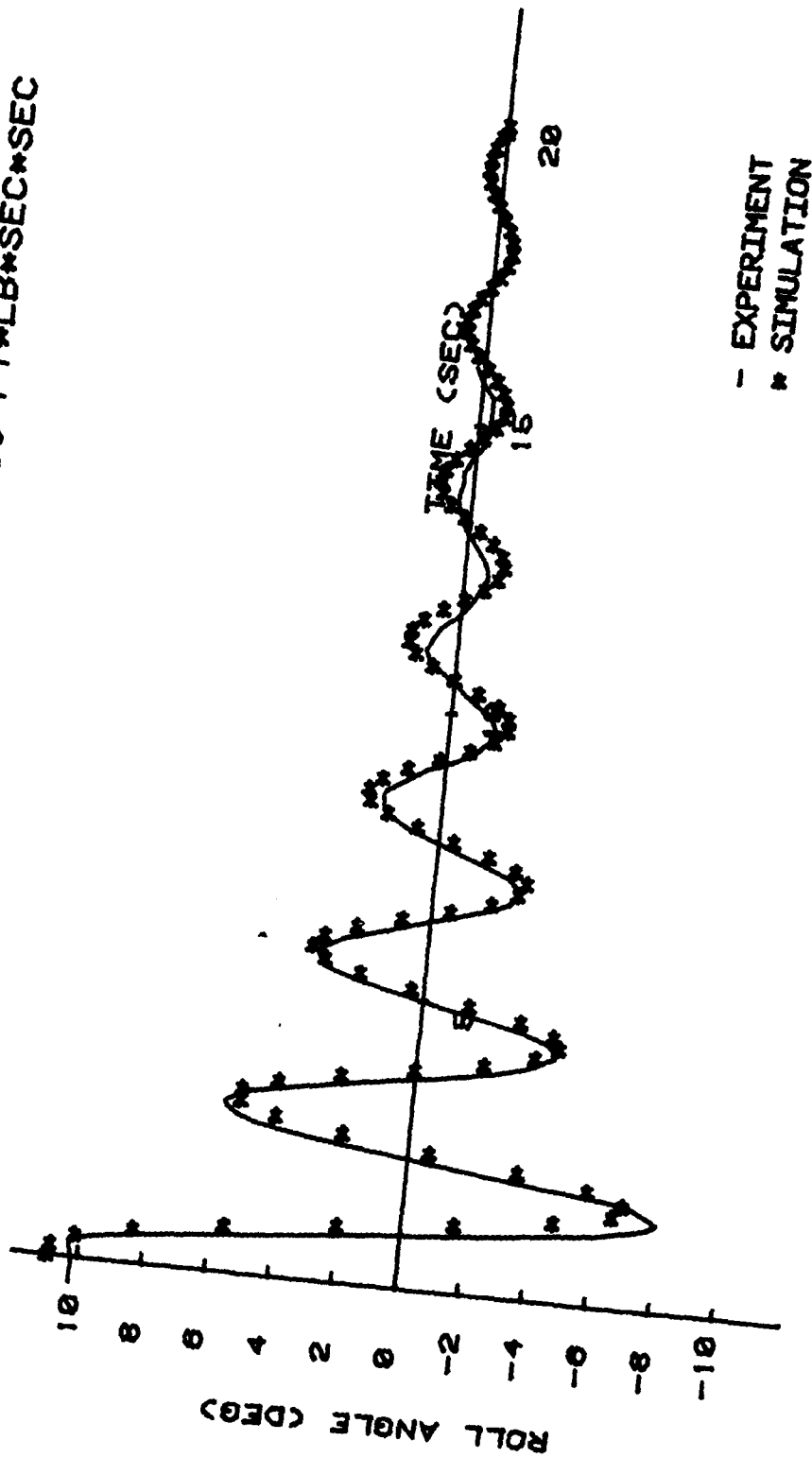


Figure III-39

CRAB BOAT MODEL RUN #7
 SPEED= 1.748 KN WAVE AMP= 0.172 FT DAMPO= 0 FT·LB·SEC²
 DAMPL= 0 FT·LB·SEC

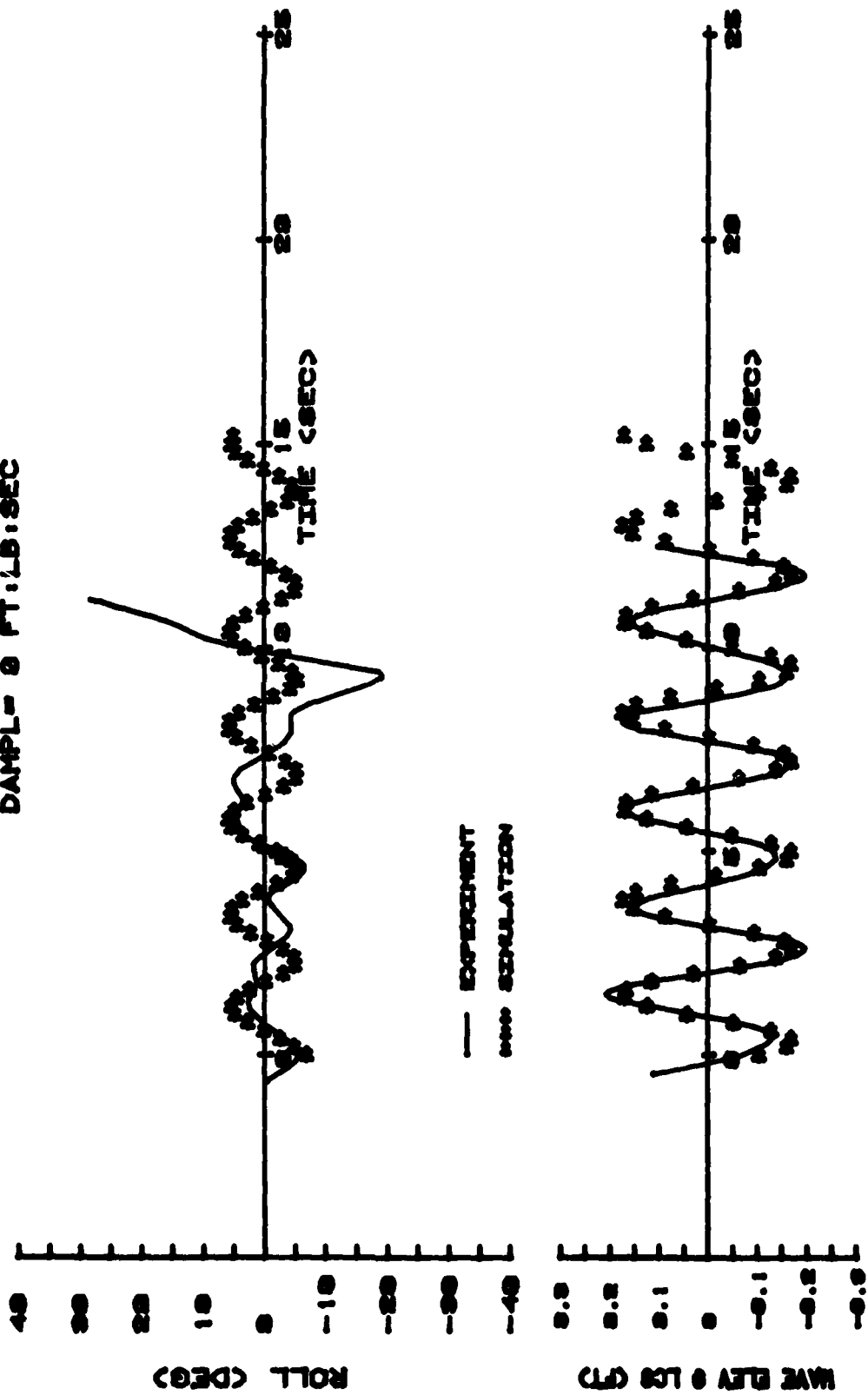


Figure III-40

CRAB BOAT MODEL RUN #8
 SPEED= 1.909 KN WAVE AMP= 0.147 FT DAMPG= 0 FT.LB.SEC²
 DAMPL= 0 FT.LB.SEC

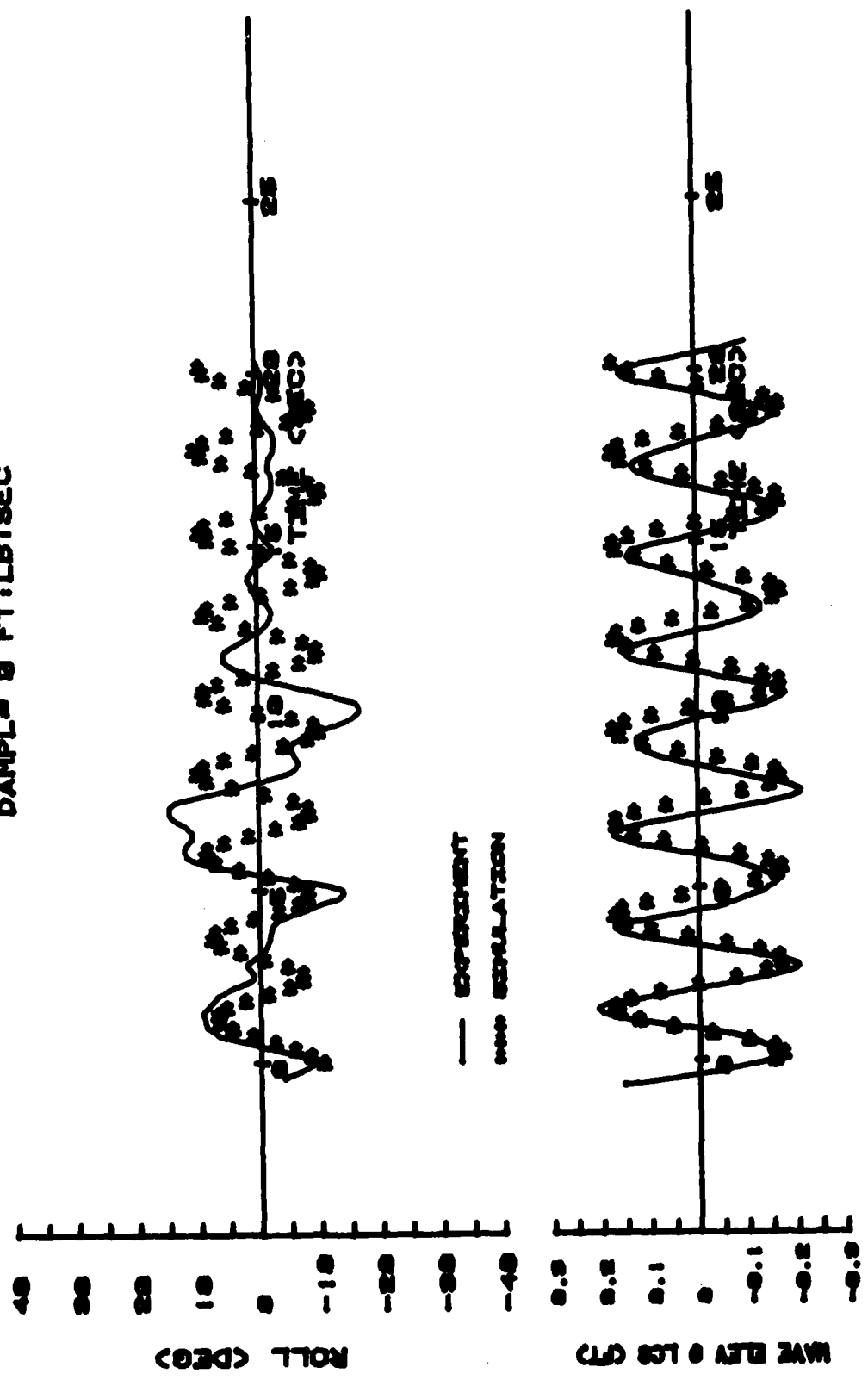


Figure III-41

CRAB BOAT MODEL RUN #20
 SPEED= 2.004 KN WAVE AMP= 0.185 FT DAMPO= 0.023 FT·LB·SEC²
 DAMPL= 0.075 FT·LB·SEC

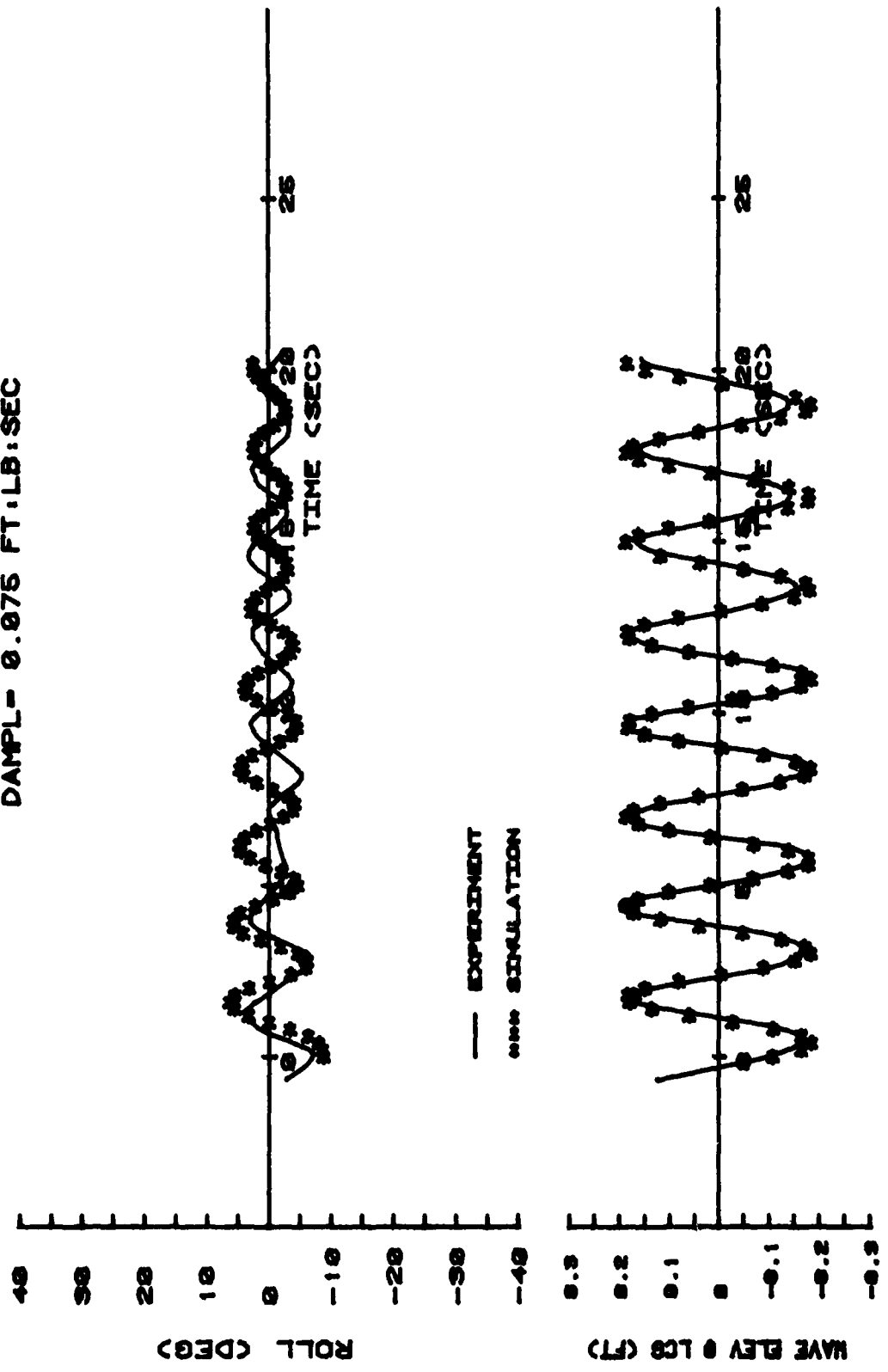


Figure III-42

CRAB BOAT MODEL RUN #7 (15 DEG)
 SPEED= 1.748 KN WAVE AMP= 0.172 FT DAMPO= 0 FT·LB·SEC²
 DAMPL= 0 FT·LB·SEC

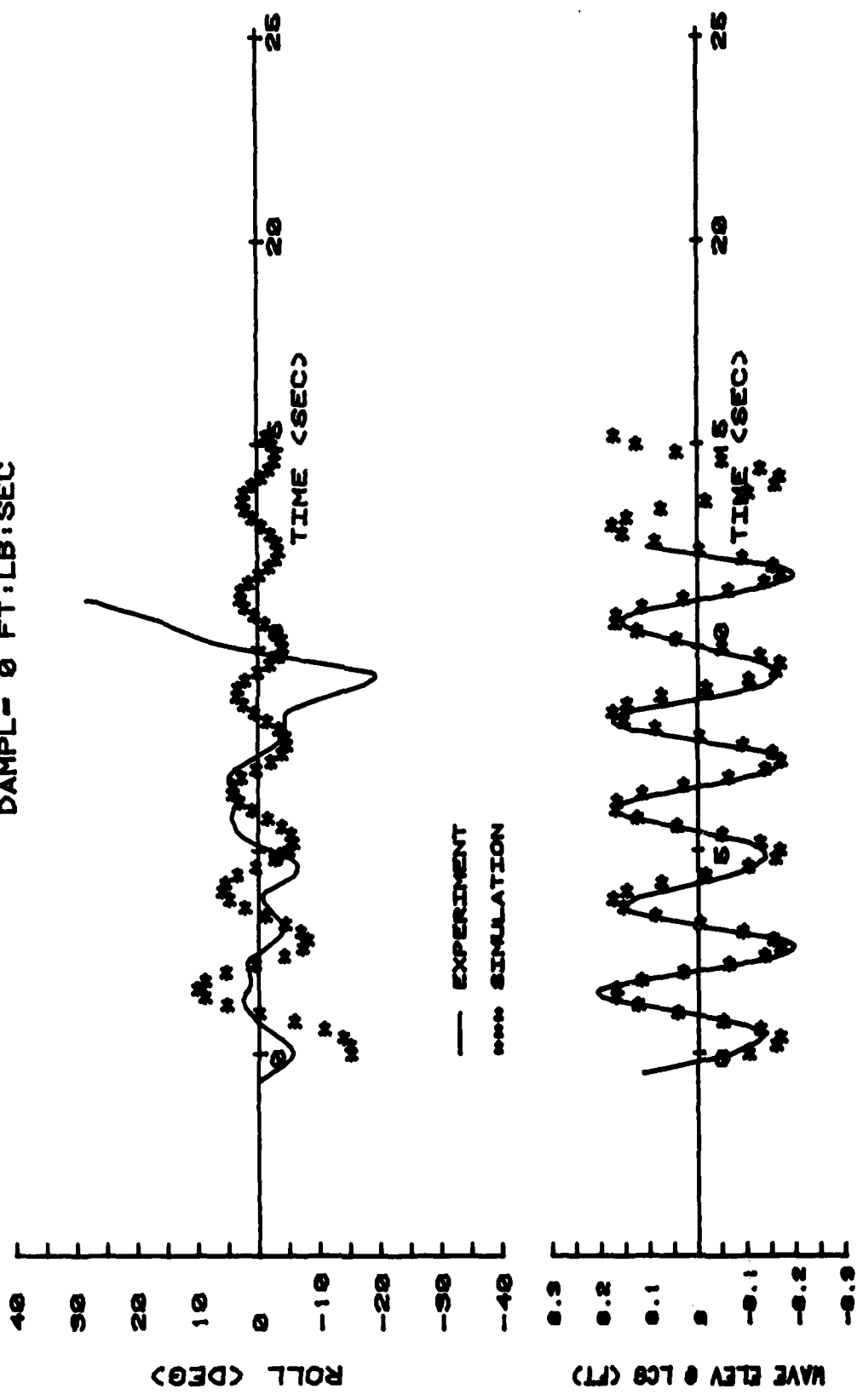


Figure III-43

CRAB BOAT MODEL RUN #7 (20 DEG)
 SPEED= 1.748 KN WAVE AMP= 0.172 FT DAMPO= 0 FT.LB.SEC.²
 DAMPL= 0 FT.LB.SEC

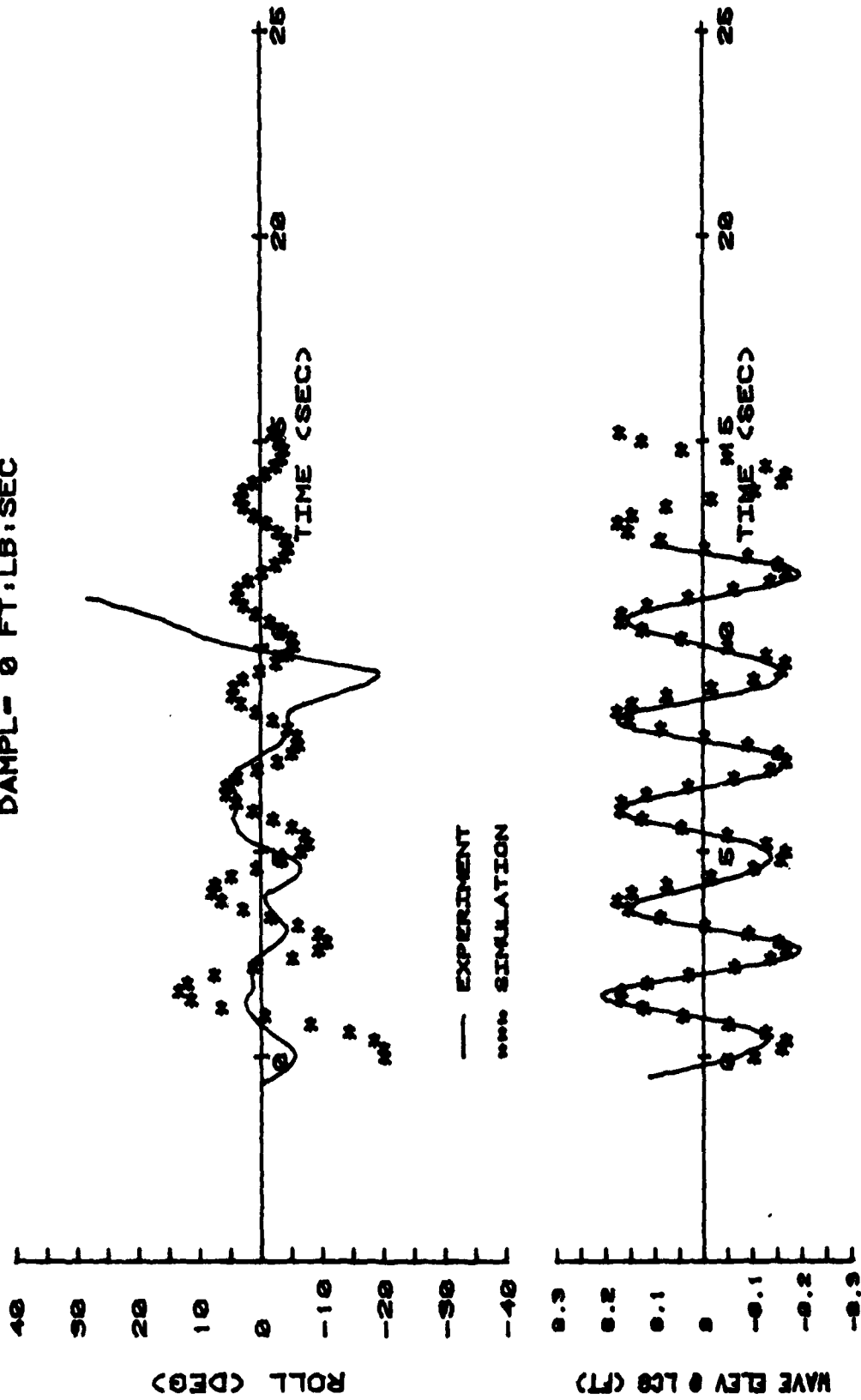


Figure III-44

IV A ONE DEGREE-OF-FREEDOM MODEL OF THE NONLINEAR ROLLING MOTION OF A SHIP IN WAVE GROUPS

Reference [10] contained a brief discussion of the analysis of the rolling motion of a ship moving in following or quartering seas by means of one degree of freedom equation of motion. The nonlinear restoring moment at large angles of heel and nonlinear damping were included in this equation, and the time dependence of the roll restoring moment was approximated for the case of regular waves. The equation of motion was integrated numerically to obtain a time history of the roll motion.

It became apparent during the development of the six degree of freedom capsize simulator program that considerable computing time and expense would be involved in running full simulations, and, in order to use the simulator effectively, a preliminary screening of cases to be run would be desirable in order to eliminate combinations, e.g. of ship speed, heading, and wave characteristics which would not produce severe motions. The one degree of freedom model was considered a possible means of conducting this preliminary screening.

The simple procedure and associated computer program described in Reference [10] had two shortcomings which have now been rectified; It used only an approximation to the time dependent variation of the righting arm curve and it was capable of treating a wave system consisting of only a single regular wave. The current procedure computes the "exact" righting arm at each time step of the numerical simulation and provision is made for including several component waves. This latter feature now permits the determination of the ship response to wave group.

Unfortunately, these modifications have increased the program running time substantially and its usefulness as a screening procedure is somewhat degraded. The results produced do, however, resemble the results of experiments in important respects.

One degree of freedom equation of rolling motion in oblique seas.

The one degree of freedom nonlinear rolling equation among

long-crested waves may be considered in the form:

$$I_x \ddot{\psi} + N(\dot{\psi}) + B(\psi) = F(t) \quad (\text{IV-1})$$

where

- ψ = angle of inclination of the ship from the vertical
- I_x = roll moment of inertia
- $\quad = \frac{\Delta(1 + \mu)}{g} r_x^2$
- μ = added mass coefficient
- r_x = radius of gyration of mass of ship about a longitudinal axis through C.G.
- $N(\dot{\psi})$ = damping function
- $B(\psi)$ = restoring function
- $F(t)$ = roll exciting moment.

The wave is represented by a linear combination of a series of sinusoidal waves and is given by:

$$Z = \sum_{n=1}^N A_n \cos(k_n x - \omega_n t + \theta_n) \quad (\text{IV-2})$$

where

- A_n = amplitude of the n^{th} wave component
- ω_n = frequency of the n^{th} component
- θ_n = phase angle
- $k_n = 2\pi/\lambda_n$
- λ_n = wave length
- N = number of wave components.

From equation (IV-2), the wave slope at any point can be obtained by taking the first derivative of Z with respect to x ,

$$\frac{dZ}{dx} = \sum_{n=1}^N [-A_n k_n \sin(k_n x - \omega_n t + \theta_n)].$$

The effective wave slope at a fixed point becomes

$$\frac{dz}{dx} = \sum_{n=1}^N [A_n k_n \sin(\omega_n t - \theta_n)]. \quad (\text{IV-3})$$

In oblique seas, the wave-induced rolling moment is determined by the effective wave slope and is given approximately by,

$$F(t) = \Delta GM \sin \phi \cdot \sum_{n=1}^N [A_n k_n \sin(\omega_{en} t - \theta_n)] \quad (\text{IV-4})$$

where

- ϕ = angle between the ship's course and the direction of wave motion, as shown in Figure IV-1.
- ω_{en} = encounter frequency
- = $\omega_n - k_n V_s \cos \phi$
- V_s = ship speed.

The restoring function, $B(\psi)$, in equation (IV-1) is a function of the righting moment and can be expressed as:

$$B(\psi) = \Delta GZ(\psi, t)$$

where Δ is the total displacement of the ship. Therefore, the one degree of freedom equation of rolling motion in oblique seas may be written as:

$$I_x \ddot{\psi} + N(\dot{\psi}) + \Delta GZ(\psi, t) = \Delta GM \sum_{n=1}^N [A_n k_n \sin(\omega_{en} t - \theta_n)] \quad (\text{IV-5})$$

Determination of the damping coefficient.

In equation (IV-1) the damping moment, $N(\dot{\psi})$, for a large roll angle is modelled as the sum of a linear term and a cubic term following the procedure of Reference [3]

$$N(\dot{\psi}) = N_{31} \dot{\psi} + N_{33} \dot{\psi}^3. \quad (\text{IV-6})$$

In order to estimate the values of N_{31} and N_{33} , the coefficients r_1 and r_3 are chosen so as to best fit the free roll decay record.

$$-\frac{dY}{dn} = r_1 Y + r_3 Y^3 \quad (\text{IV-7})$$

where $\frac{dY}{dn}$ is the decrease in roll amplitude per cycle. The estimates of N_{31} and N_{33} then are given by the following expressions as shown in Reference [3]

$$N_{31} = \frac{I_x \sigma_n}{\pi} r_1$$

$$N_{33} = \frac{4I_x}{3\pi\sigma_n} r_3$$

where

$$\sigma_n = \sqrt{\frac{\Delta(1+\mu)GM}{I_x}}$$

Determination of the righting moment of a ship in waves.

The method of determining the righting moment on the wave described in Reference [11] is used to calculate the righting arm for the instantaneous position of the ship and wave profile. It was assumed that the hydrostatic pressure distribution yields results which are sufficiently accurate for the present purpose and the hydrodynamic pressure in wave was neglected. Therefore, the total righting moment is given by

$$RM = \int_{\text{bow}}^{\text{stern}} \omega'(x)M(x)dx \quad (\text{IV-9})$$

where

$\omega'(x)$ = effective weight density of water at each section
 = pressure gradient at the depth of centroid of each section

$M(x)$ = moment of the immersed section area about a vertical axis through an assumed C.G.

It is assumed that the ship is in a position of vertical and trim static equilibrium on the wave. This requires that the buoyant force equals the weight, i.e.,

$$\int_{\text{bow}}^{\text{stern}} \omega'(x)A(x)dx = \Delta \quad (\text{IV-10})$$

and the moment of the buoyant force about a transverse axis is equal to the moment of weight of the ship about the transverse axis,

$$\int_{\text{bow}}^{\text{stern}} x\omega'(x)A(x)dx = x_B\Delta . \quad (\text{IV-11})$$

The righting arm, GZ will then be given by

$$GZ = \int_{\text{bow}}^{\text{stern}} M(x)\omega'(x)dx/\Delta .$$

Numerical solution to the problem.

From equation (IV-1) and equation (IV-9) the equation of rolling motion is given by

$$I_x \ddot{\psi} + N_{31} \dot{\psi} + N_{33} \dot{\psi}^3 + \Delta GZ(\psi, t) = F(t) . \quad (\text{IV-12})$$

This differential equation may be transformed into a system of two first-order equations which are integrated numerically by the Runge-Kutta method.

To develop a procedure which can be easily used for a computer solution, we set

$$\begin{aligned} y_1 &= \dot{\psi} \\ y_2 &= \psi . \end{aligned}$$

The original differential equation, therefore, may be transformed into two simultaneous first-order differential equations which are given by:

$$\begin{aligned} \frac{dy_1}{dt} &= -\frac{N_{31}}{I_x}y_1 - \frac{N_{33}}{I_x}y_1^3 - \frac{\Delta}{I_x}GZ(y_2, t) + \frac{F(t)}{I_x} \\ \frac{dy_2}{dt} &= y_1 . \end{aligned} \quad (\text{IV-13})$$

If we set

$$f_1(y_1, y_2, t) = -\frac{N_{31}}{I_x}y_1 - \frac{N_{33}}{I_x}y_1^3 - \frac{\Delta}{I_x}GZ(y_2, t) + \frac{F(t)}{I_x}$$

and $f_2(y_1) = y_1$

then equation (IV-13) may be written as:

$$\begin{aligned} \frac{dy_1}{dt} &= f_1(y_1, y_2, t) \\ \frac{dy_2}{dt} &= f_2(y_1) \end{aligned} \quad (IV-14)$$

If the values of the dependent variables in equation (IV-14) are given at $t = t_n$, we can use the following algorithm to obtain their numerical values at $t_{n+1} = t_n + \Delta t$:

$$(y_1)_{n+1} = (y_1)_n + (\Delta y_1)_n$$

$$(y_2)_{n+1} = (y_2)_n + (\Delta y_2)_n$$

where

$$(\Delta y_1)_n = \frac{\Delta t}{\sigma} (k_0 + 2k_1 + 2k_2 + k_3)$$

$$(\Delta y_2)_n = \frac{\Delta t}{\sigma} (m_0 + 2m_1 + 2m_2 + m_3)$$

and

$$\begin{aligned} k_0 &= f_1[t_n, (y_1)_n, (y_2)_n], & m_0 &= f_2[(y_1)_n], \\ k_1 &= f_1[t_n + \frac{\Delta t}{2}, (y_1)_n + k_0 \frac{\Delta t}{2}, (y_2)_n + m_0 \frac{\Delta t}{2}], & m_1 &= f_2[(y_1)_n + k_0 \frac{\Delta t}{2}], \\ k_2 &= f_1[t_n + \frac{\Delta t}{2}, (y_1)_n + k_1 \frac{\Delta t}{2}, (y_2)_n + m_1 \frac{\Delta t}{2}], & m_2 &= f_2[(y_1)_n + k_1 \frac{\Delta t}{2}], \\ k_3 &= f_1[t_n + \Delta t, (y_1)_n + k_2 \frac{\Delta t}{2}, (y_2)_n + m_2 \Delta t], & m_3 &= f_2[(y_1)_n + k_2 \Delta t]. \end{aligned} \quad (IV-19)$$

The numerical solutions from such a computer simulation are shown in figures IV-2 through IV-7 to compare with the experimental results in three different cases.

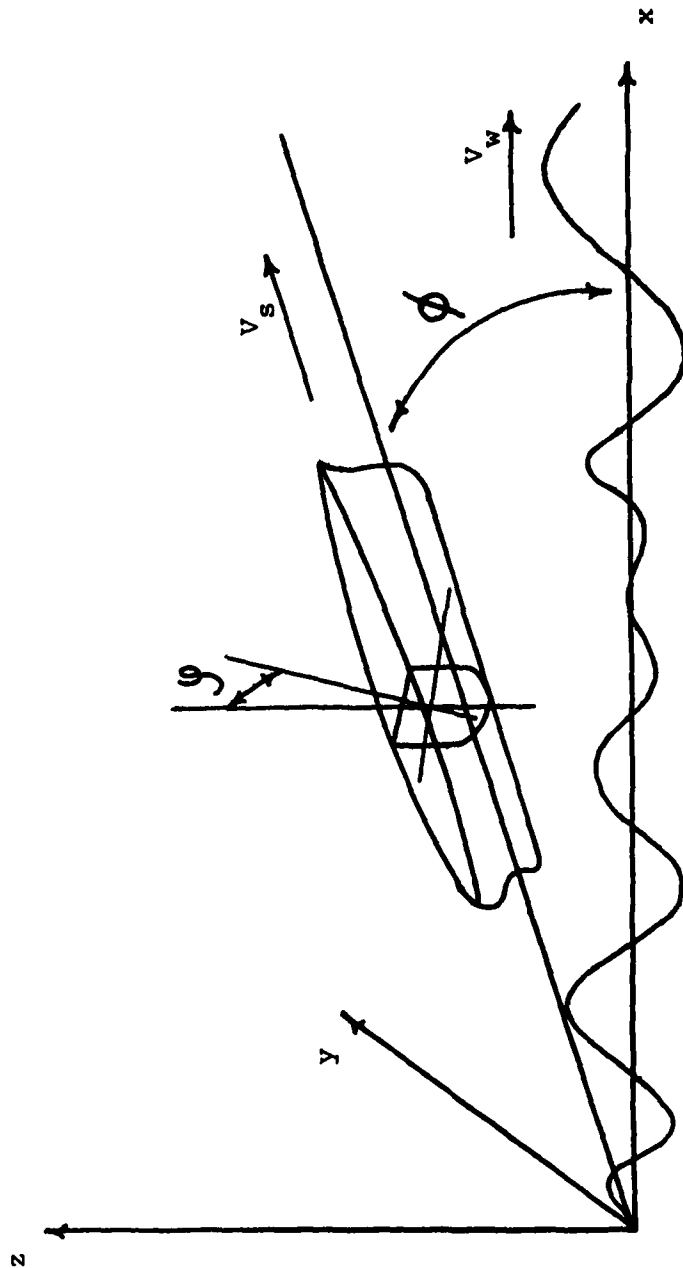
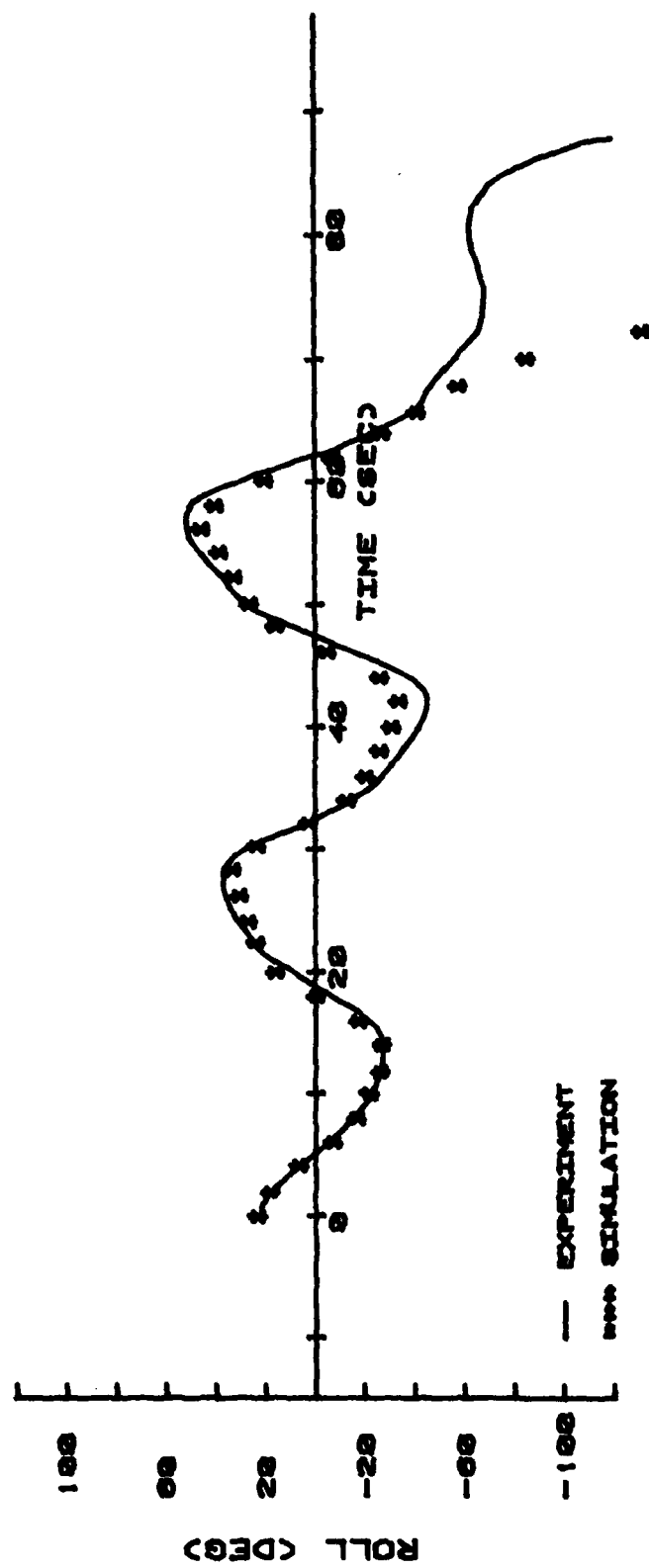


Figure IV-1 Coordinate Systems

MARINER RUN 0918-41A (1 DEOF)



Wave Data

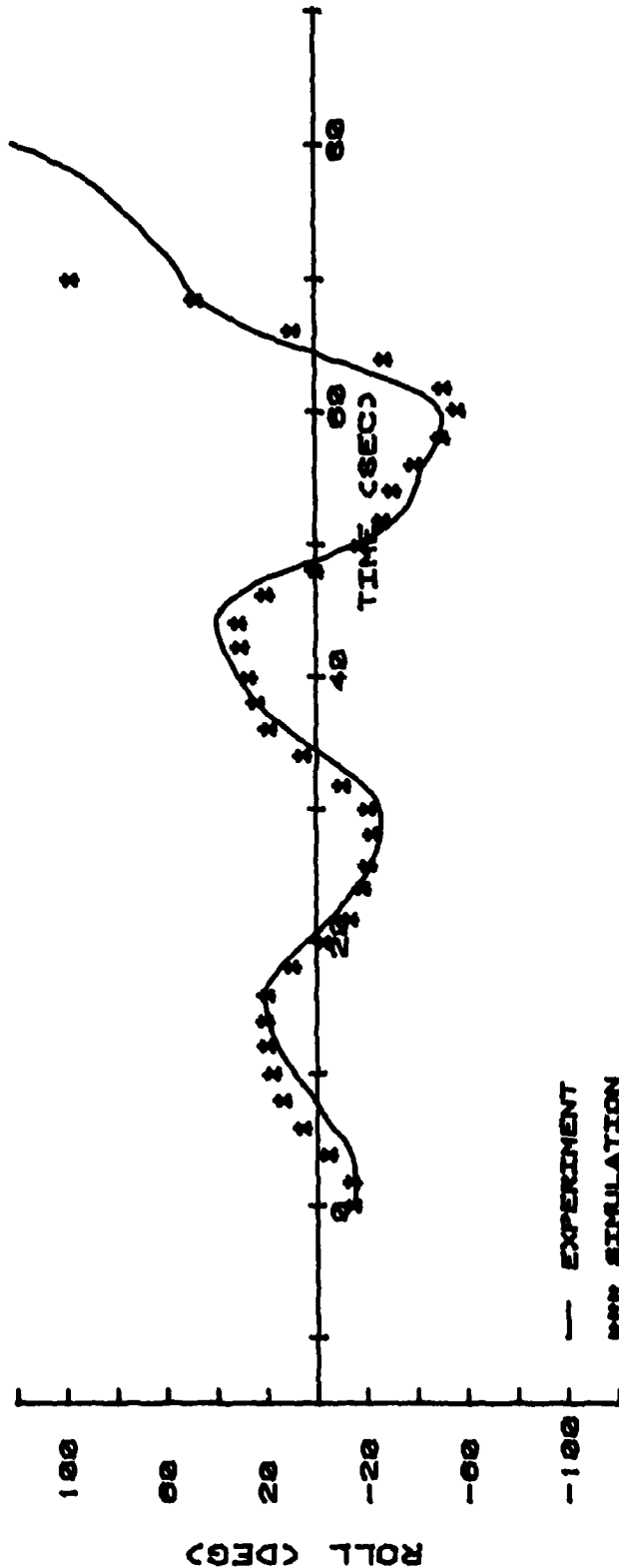
1. Wave Freq: $\omega_1 = 0.586$ RAD/SEC
 $\omega_2 = 0.651$ RAD/SEC
2. Wave Height: $H_1 = 18$ FT
 $H_2 = 18$ FT
3. Phase angle: $\theta_1 = 244.8$ DEG
 $\theta_2 = 276.1$ DEG
4. Direction: $\psi = 180$ DEG

Rolling Experiment Data

1. Ship Speed : $V = 8.8$ KNOTS
2. Initial angle: $= 21.7$ DEG
3. DAMPL : $C_1 = 114,462,208$ FT-LB-SEC
DAMPC : $C_3 = 8,302,700$ FT-LB-SEC³
4. Natural Period: $T_N = 38.028$ SEC
5. $(T_E/T_N)_1 = 0.3866$
 $(T_E/T_N)_2 = 0.3630$

Figure IV-2

MARINER RUN 0918-42A (1 DEOF)

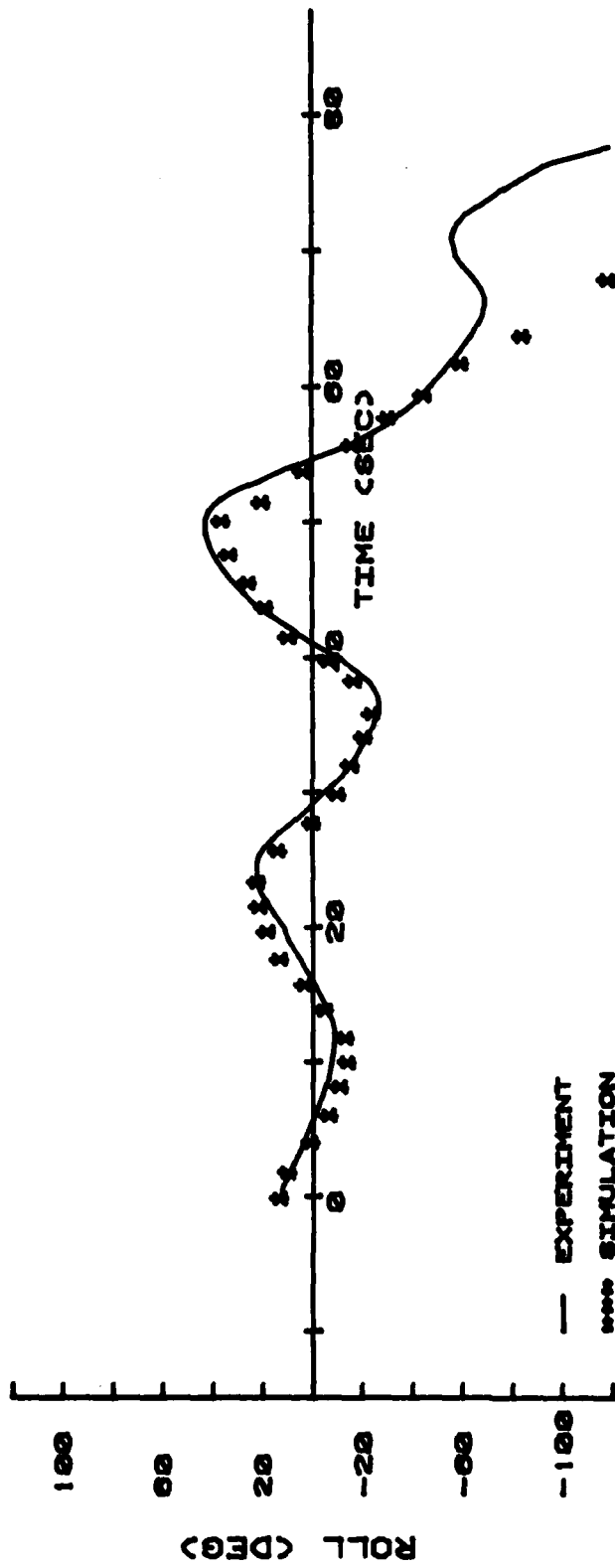


- Wave Data**
1. Wave Freq: $\omega_1 = 0.586$ RAD/SEC
 $\omega_2 = 0.651$ RAD/SEC
 2. Wave Height: $H_1 = 18$ FT
 $H_2 = 18$ FT
 3. Phase Angle: $\theta_1 = 275.70$ DEG
 $\theta_2 = 333.10$ DEG
 4. Direction: $\psi = 180$ DEG

- Rolling Experiment Data**
1. Ship Speed : $V = 8.8$ KNOTS
 2. Initial Angle : -15.9 DEG
 3. DAMPL : $C_1 = 15,347,909$ FT-LB-SEC
DAMPC : $C_3 = 4,607,570$ FT-LB-SEC³
 4. Natural Period: $T_N = 38.028$ SEC
 5. $(T_E/T_N)_1 = 0.3866$
 $(T_E/T_N)_2 = 0.3630$

Figure IV-3

MARINER RUN 0901-45A (1 DEOF)



Wave Data

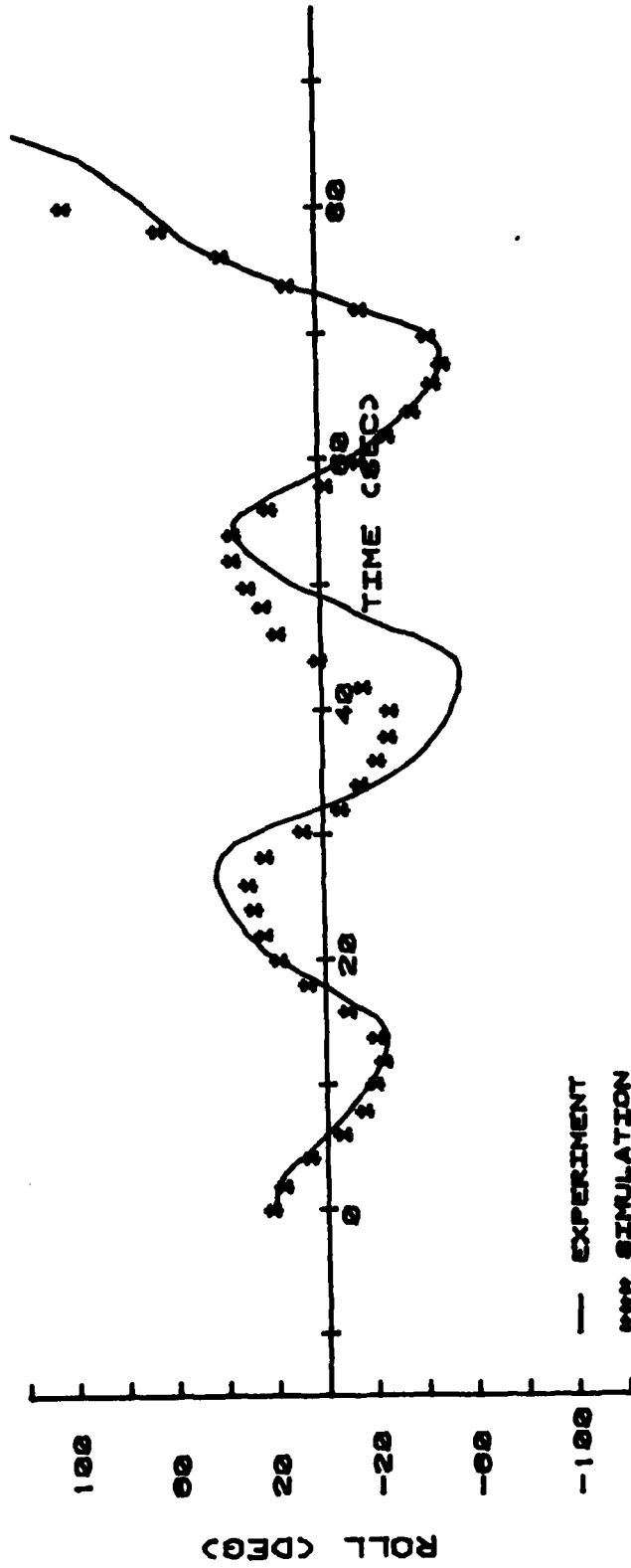
1. Wave Freq : $\omega_1 = 0.614$ RAD/SEC
2. Wave Height : $H_1 = 33.4$ FT
3. Phase angle : $\theta_1 = 217$ DEG
4. Direction : $\psi = 180$ DEG

Rolling Experiment Data

1. Ship Speed : $V = 6.4$ KNOTS
2. Initial angle : $= 11.7$ DEG
3. DAMPL : $C_1 = 96,000,562$ FT-LB-SEC
DAMPC : $C_3 = 41,513,503$ FT-LB-SEC³
4. Natural period: $T_N = 38.028$ SEC
5. $(T_E/T_N)_1 = 0.3390$

Figure IV-4

MARINER RUN 0901-41A (1 DEOF)



Wave Data

1. Wave Freq : $\omega_1 = 0.614$ RAD/SEC
2. Wave Height : $H_1 = 35$ FT
3. Phase Angle : $\theta_1 = 264$ DEG
4. Direction : $\psi = 180.00$ DEG

Rolling Experiment Data

1. Ship Speed : $V = 7.3$ KNOTS
2. Initial Angle : $= 21$ DEG
3. DAMPL : $C_1 = 130,462,302$ FT-LB-SEC
DAMPC : $C_3 = 4,151,350$ FT-LB-SEC³
4. Natural Period : $T_N = 38.028$ SEC
5. $(T_E/T_N)_1 = 0.3519$

Figure IV-5

CAPSIZE RUN 0901-41A (1 DEOF)
 SPEED= 7.3 KN WAVE AMP= 17.5 FT CUBIC DAMP.= 4150000 FT.LB.SEC.³
 LINEAR DAMP.= 1.3E+8 FT.LB.SEC

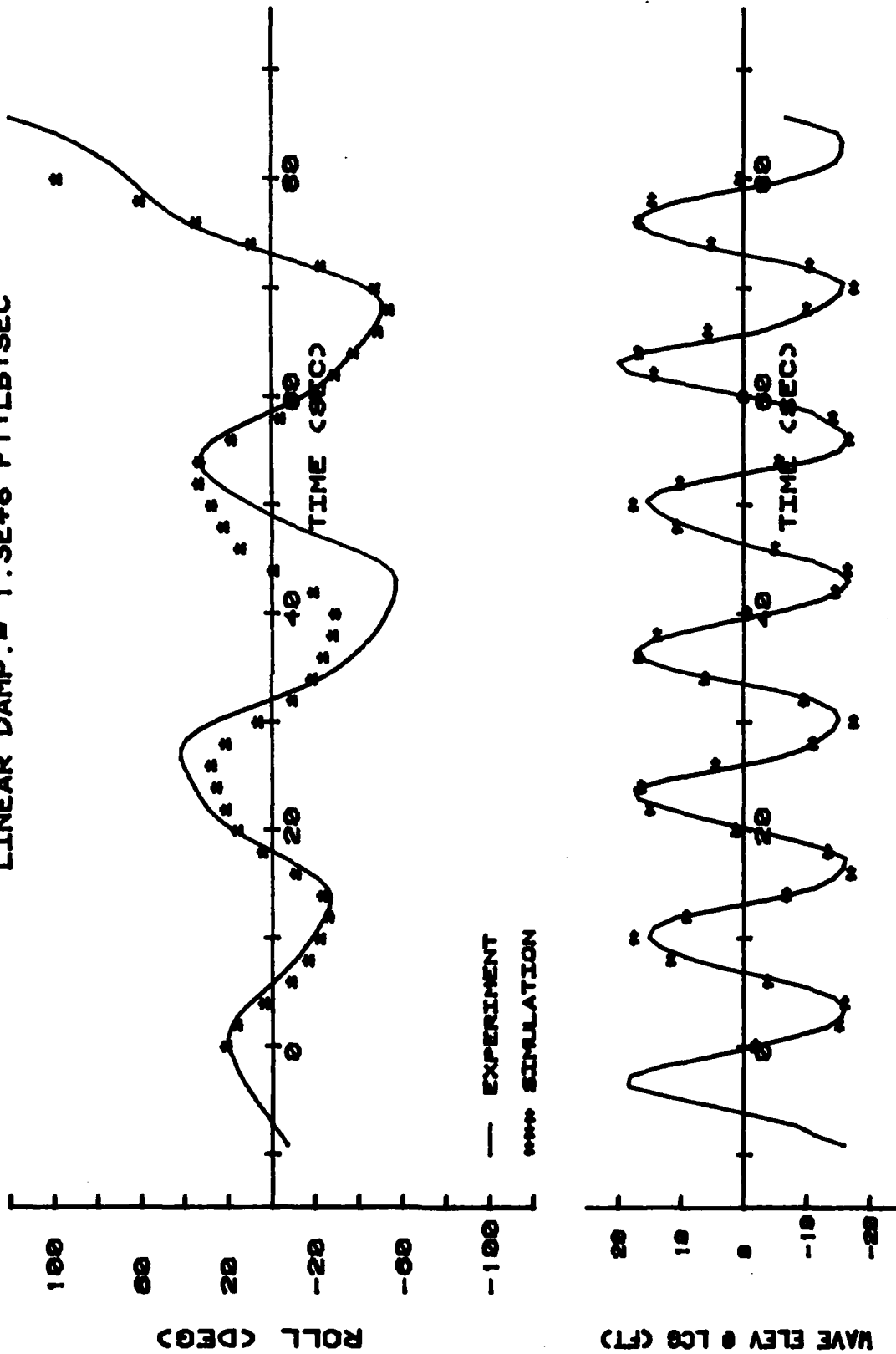


Figure IV-6

CAPSIZE RUN 0905-55J3 (1 DEOF)
 SPEED= 7.8 KN WAVE AMP= 12.8 FT CUBIC DAMP.= 4.15E+7 FT.LB:SEC³
 LINEAR DAMP.= 1.15E+8 FT.LB:SEC

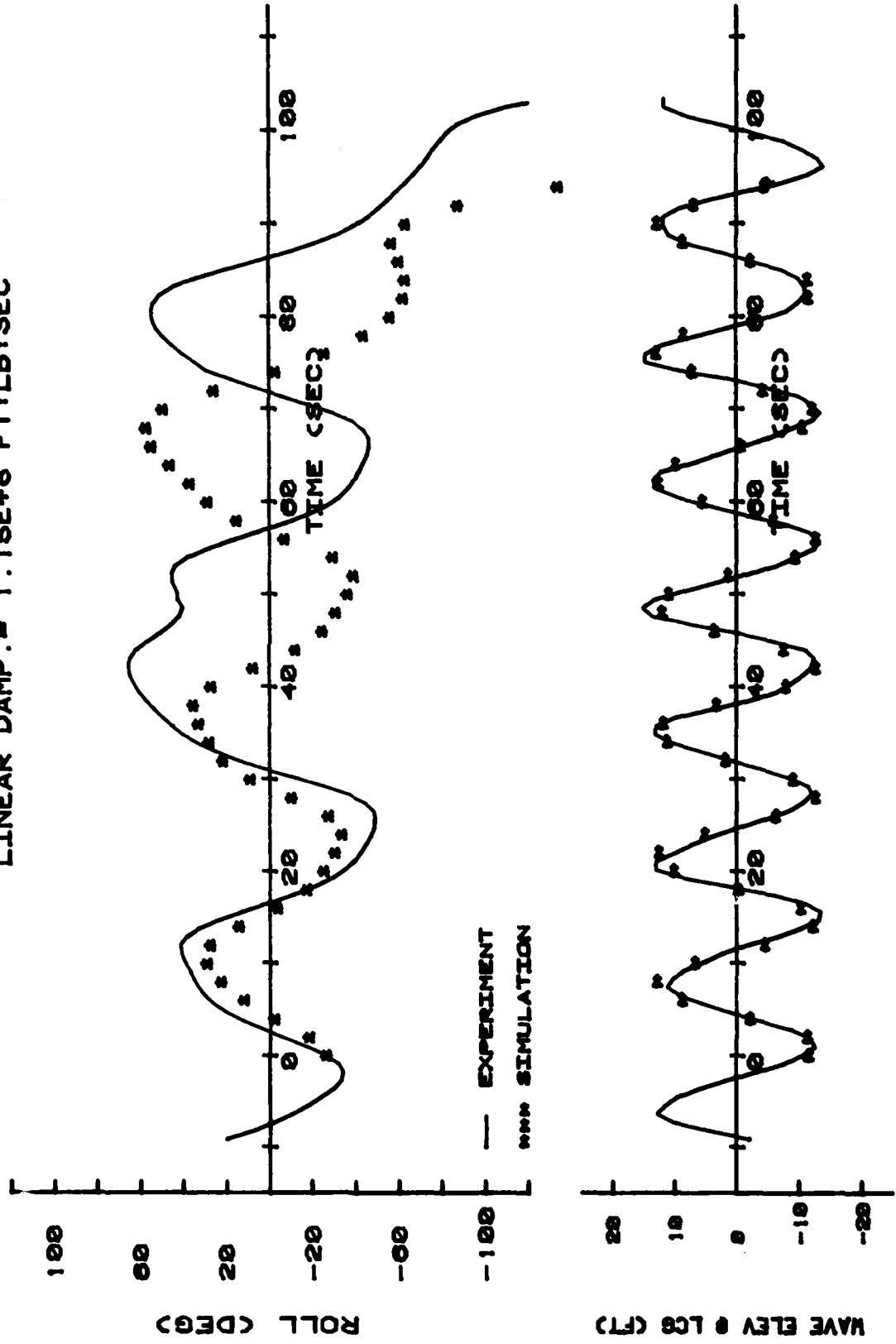


Figure IV-7

CONCLUSIONS

As in virtually all research programs involving new or little understood phenomena, the results which have been obtained from the present study are somewhat less complete than was originally expected. Nevertheless, some important aspects of the ability to simulate by computer the severe rolling motions and capsizing of ships in following seas have been investigated and conclusions may be drawn. The following are the most important of them.

(1) The numerical capsize simulator program has the capability of providing a good representation of the rolling and capsizing motion in following seas for a ship whose proportions and speed are not greatly different from those of an average seagoing merchant ship.

(2) The capability to simulate the motion of a vessel of high volumetric coefficient and high speed is less clearly demonstrated. This is probably a result of the approximations used in the simulation of hydrodynamic forces for such vessels.

The studies whose results are presented here, are insufficient to distinguish clearly the characteristics of the hull forms for which "good" and "bad" simulations may be expected. However, tentatively the following features may be expected to characterize ships for which good results may be expected.

- a. $L/B > 5$
- b. $B/T < 3$
- c. $C_B < 0.7$
- d. $V/\sqrt{L} < 1.0$
- e. A fair hull form without chines or other abrupt discontinuities.

Erratic results may be expected for hull forms which fall outside these criteria. Since the accuracy of the simulation seems especially sensitive to roll damping, hull characteristics which may lead to a strong amplitude dependence of the roll damping must be viewed with caution. Such characteristics are

- a. High B/T
- b. Low F/B (Freeboard/Beam)
- c. Chines or other discontinuities, especially near the waterline.

(3) The occurrence of a capsize and, consequently, the ability to simulate that capsize appears to be quite sensitive to roll damping. The damping coefficient which is obtained by a roll decay experiment in calm water does not always give good results for the simulated motion in following waves.

(4) In the experiments, the occurrence of a capsize was found to be quite sensitive to small variations in wave properties. Thus, even in waves which were nominally regular, slight variations in wave shape caused the motion extremes and capsize occurrence to take on somewhat random qualities.

(5) Capsizes in a following sea which result from low cycle resonance may occur when the model or ship encounters from two to six waves of critical steepness and regularity. The occurrence of capsize is greatest if the frequency of encounter is twice the natural frequency of roll.

(6) In order to obtain reliable results with the use of the simulator, the effective roll damping moment at large angles in waves must be predicted with more precision. This will require new understanding to be developed concerning the mechanism of roll damping and the effect of waves on it.

In the case of extremely steep waves, large roll motions and irregular, full hull forms, the conventional concepts upon which ship motion predictions are based may, in fact, not be sufficiently accurate at all. Specifically, the subdivision of the force and moment system acting on the ship into independent terms referred to as "added mass", "damping", "static restoring" and "wave-exciting" forces, even when a nonlinear relationship is assumed between the force term and the relevant motion variable, may omit vital interactions and other effects which may have profound hydrodynamic effects. It is probably safe to state that hydrodynamic theory alone is not, at present, capable of yielding a satisfactory

solution to the general problem of concern here. Some of the current work in the field of numerical hydrodynamics may shed light on some aspects of the problem. An example is the simulation of breaking waves by direct numerical solution of the equations of motion of the fluid. In order for this type of simulation to be of use in simulating the complete ship capsizing situation, a substantial increase in available computational capability is required.

Initially, it is suggested that experimental studies may be carried out with the objective of pinpointing the important parameters and relationships in the ship wave interaction phenomena. Two types of experiments are suggested:

- a. Forced-roll experiments using a large-amplitude planar motion mechanism. These should be conducted in calm water and in waves.
- b. Free-motion experiments in calm water and waves.

In both cases, the experimental results should be analyzed using system identification techniques coupled with a comprehensive model of the hydrodynamic force system. While the second of the above category of experiments duplicate, in some ways, experiments described in the present report, the emphasis should be placed on the methods and theoretical models used in the analysis in order to shed the most light on the hydrodynamic force relationships. It must be emphasized that the needed basic research work involves a complete departure from conventional methods of ship motion analysis, and the specific methodology and results cannot be foreseen in advance.

(7) The one-degree-of-freedom roll motion simulator, in some cases gave results which were in good agreement with experiments. In order to achieve this capability for composite wave groups, however, the running time of the simulator has been substantially increased over that of earlier versions such that it now approaches that of the six-degree-of-freedom simulator.

REFERENCES

- [1] Blagoveshensky, S. N.
Theory of Ship Motions, Volume I, Dover Publications,
New York, 1962.
- [2] Chou, S. J.; Oakley, O. H.; Paulling, J. R.; Van Slyke, R.;
Wood, P. D.; Zink, P. F.
"Ship Motions and Capsizing in Astern Seas", U.S. Coast
Guard Report No. CG-D-103-75.
- [3] Dalzell, J. F.
"A Note on the Form of Ship Roll Damping", Journal of
Ship Research, Volume 22, Sept. 1978, pages 178-185.
- [4] Frank, W.
"Oscillations of Cylinders In or Below the Free
Surface of Deep Fluids", NSRDC Report No. 2375, 1967.
- [5] Glauz, R. D.
"Adams Method of Integration of Differential Equations",
Computing Services Report No. 13, Aerojet-General,
Sacramento, California, May 12, 1960.
- [6] Haddara, M. R.; Kastner, S.; Magel, L. F.; Paulling, J. R.;
Perez y Perez, L.; Wood, P. D.
"Capsizing Experiments with a Model of a Fast Cargo
Liner in San Francisco Bay", U.S. Coast Guard Project
723 411, Naval Architecture Department, Univ. of Calif.,
Berkeley, Jan 1972.
- [7] Kato, H.
"On the Frictional Resistance to Rolling of Ships",
SNAME, Japan 1958.
- [8] Lake, B. M.; Yuen, H. C.; Rungaldier, H.; Ferguson, W. E.
"Nonlinear Deep Water Waves: Theory and Experiment.
Part 2. Evolution of a Continuous Wave Train", J.
Fluid Mech. (1977), Vol. 83, Part I, pp. 49-74.
- [9] Nayfeh, A.
Perturbation Methods, John Wiley & Sons, New York, 1973.
- [10] Oakley, O. H.; Paulling, J. R.; Wood, P. D.
"Ship Motions and Capsizing in Astern Seas", Tenth
Symposium on Naval Hydrodynamics, Massachusetts Institute
of Technology, Cambridge, Mass., June 1974, pp. 297-350,
ONR Report ACR-204.
- [11] Paulling, J. R.
"The Transverse Stability of a Ship in a Longitudinal
Seaway", Journal of Ship Research, March 1961, pp. 37-49.

- [12] Paulling, J. R. and Rosenberg, R. M.
"On Unstable Ship Motions Resulting from Nonlinear
Coupling", Journal of Ship Research, June 1959, pp. 36-46.
- [13] Pepper and Miller
"Evaluation of Current Towing Vessel Stability Criterion
and Proposed Fishing Vessel Stability Criteria: Task 2
-- Tripping and Seakeeping Tests of Towing and Fishing
Vessels", Prepared for U.S.C.G. by Hydronautics, Inc.,
Report No. CG-D-3-76, Jan. 1976.
- [14] Saunders, H. E.
Hydrodynamics in Ship Design, Volume III, SNAME,
New York, 1957.
- [15] Visineau, G.
"Relative Roll Motion of a Ship in Beam Seas", paper
presented at Northern California Section of SNAME,
San Francisco, California, March 8, 1979.

Appendix A

Principal Dimensions

Body Plans

Tables of Offsets

Table A-1
 PRINCIPAL DIMENSIONS
 OF THE
MARINER AND AMERICAN CHALLENGER

		<u>MARINER 77.7</u>		<u>AMERICAN CHALLENGER</u>	
		ship	model 1/96	ship	model 1/30.189
length between					
perpendiculars	LBP	528.0'	66"	529.0'	17.523'
length for ordinates		520.0'	65"	521.0'	17.258'
breadth, molded	B	76.0'	9.5"	75.0'	2.484'
depth, molded to					
main deck	D	47.7'	5.96"	46.0'*	18.484"
draft, molded to					
design waterline	T	27.0'	3.38"	27.5'	10.931"
 <u>Model Test Condition</u>					
displacement	Δ	21616 LT(FW)	52.29 lb(FW)**	19643 LT(SW)	1600 lb(SW)
draft forward	TF	26.94'	3.37"	26.00'	10.33"
draft aft	TA	34.71'	4.34"	33.50'	13.32"
transverse meta-					
centric height	GM	.62'	.078"	1.16'	.46"
	GM/B %	.82	.82	1.54	1.54
transverse	KM	31.91'	3.989"	31.35'	12.46"
transverse radius					
of gyration (air)	i_t	26.40'	3.30"	25.58'	10.16"
longitudinal rad.					
of gyration (air)	i_l	143.0'	1.49'	140.2'	4.64'
block coefficient	C_b	.636	.636	.582	.582
prismatic coef.	C_p	.648	.648	.592	.592
midship section					
coef.	C_m	.983	.983	.984	.984
	LBP/B	6.95	6.95	7.05	7.05
	B/D	1.59	1.59	1.63	1.63

* The American Challenger model (1/30.189) was built to the top of the bulwarks. Reference [4] gives D as 46.5 feet, however the table of offsets used for computing the righting arm curves has D as 46.0 feet.

** This is a measured value and does not agree with the computed value due to distortion of the Mariner model (1/96) geometry.

AMERICAN CHALLENGER

Body Plan

scale: 1 in. = 10 ft.

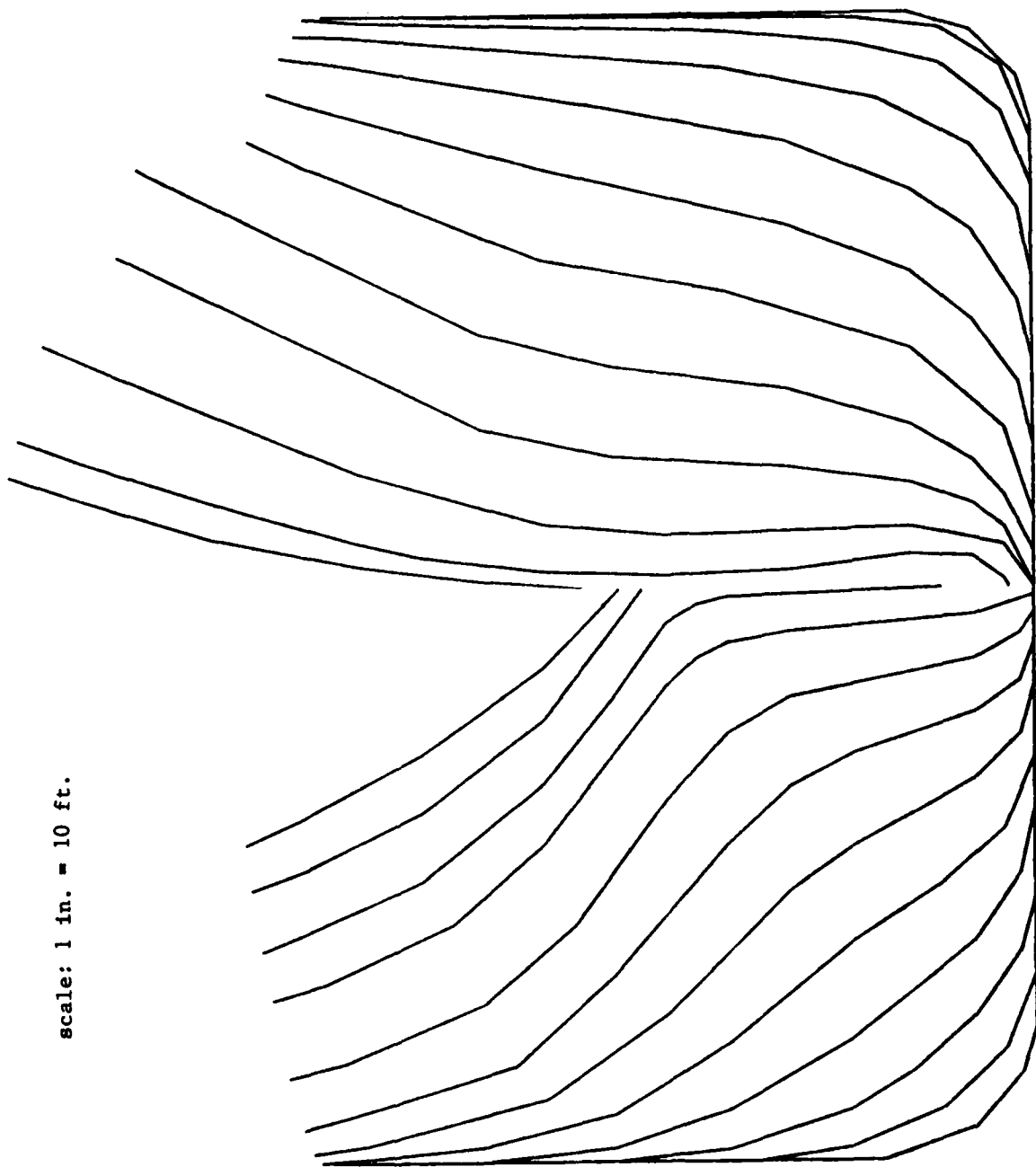


Figure A-1

MODIFIED MARINER: MARINER 77.7 (full offsets)

Body Plan

scale: 1 in. = 10 ft.

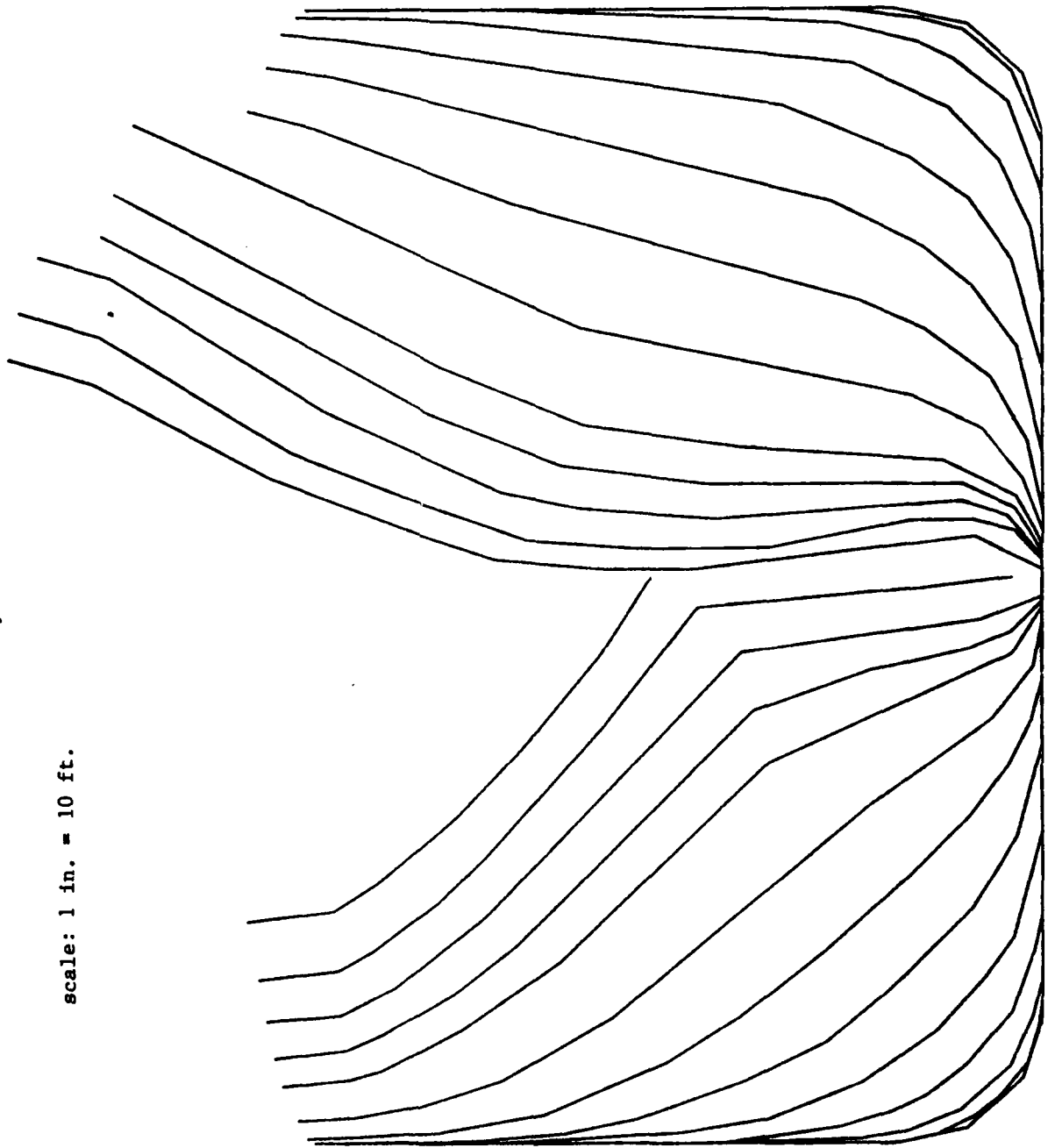


Figure A-2

MODIFIED MARINER: MARINER 77.7 (partial offsets)

Body Plan

scale: 1 in. = 10 ft.

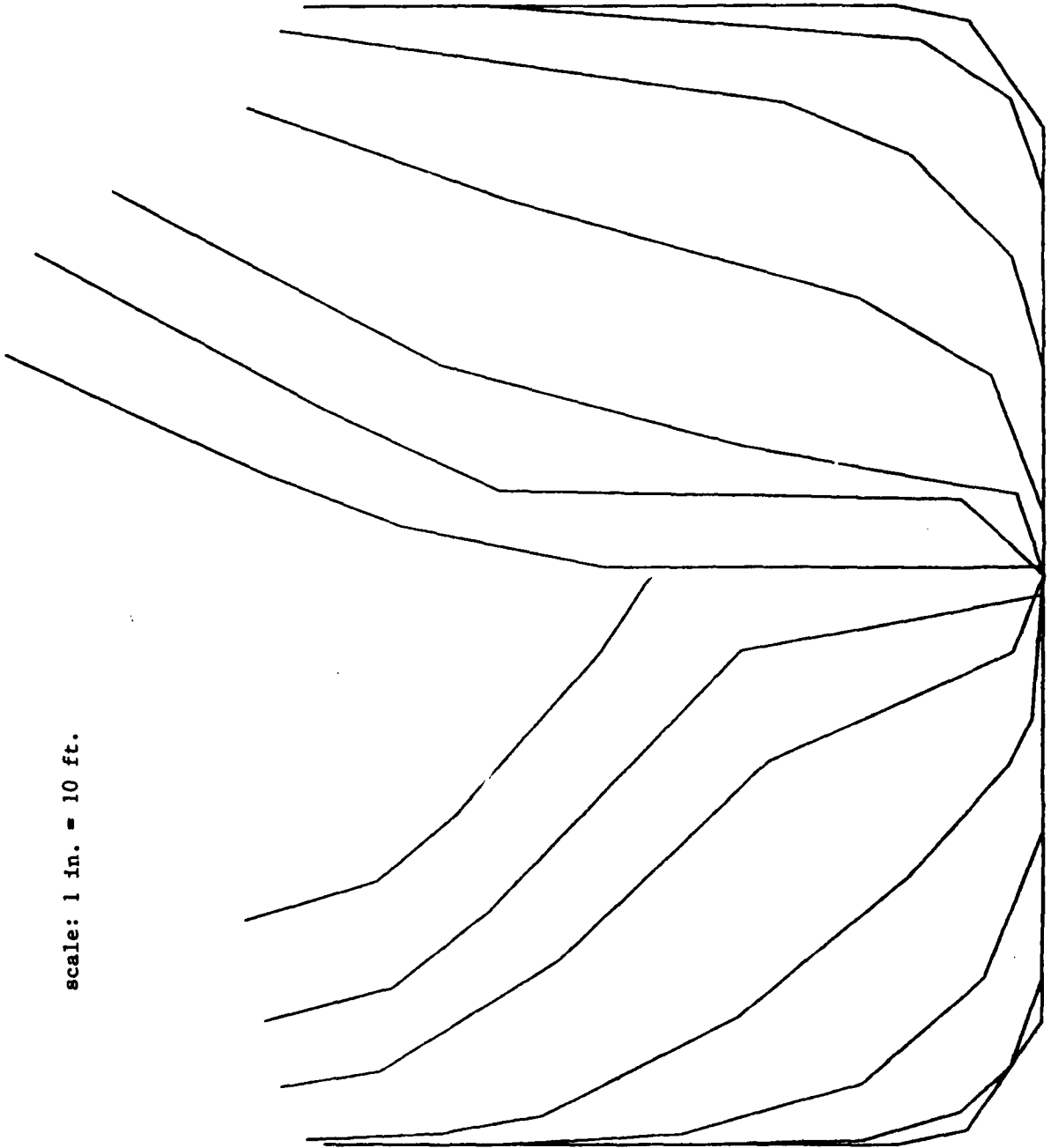


Figure A-3

TABLE OF OFFSETS

The first line of the table of offsets is the title, e.g. "CAPSIZE SIMULATOR: FULL OFFSETS (100%)". The second line is the ship identification, for this example: "MARINER 77.7"; length between perpendiculars: "520.00"; beam: "76.00"; design draft: "27.00". The third line of the table of offsets is the number of stations: "25". Next are the coordinates of the offsets for each station. The first line for each station has the number of points on one side of the symmetric station (for the first station of the example this is 10) and the distance of that station aft of the forward perpendicular (for the first station of the example this is 4.00 ft). This is followed by the coordinates of each point in the transverse plane. The first column has the distance in feet above the keel (for the first station first point of the example, this is 0, and for the last point of the first station this is 68.70). The second column has the distance in feet abeam the vertical centerline (for the same example, first point, this is 0, and last point is 14.80). All of the remaining stations have the same format.

Table A-2 (cont.)
Mariner Full Table of Offsets (cont.)

CAPSIZE SIMULATOR: FULL OFFSETS (100%)

11	338.00	10	442.00	7	520.00
0.	0.	0.	0.	26.00	0.
0.	22.60	0.	2.80	29.29	5.10
.54	25.00	.60	6.00	34.60	11.50
2.00	29.18	3.30	9.46	38.90	16.00
5.00	32.70	11.58	15.35	44.20	20.50
7.70	34.75	28.65	29.55	47.20	22.40
10.10	35.90	36.00	33.80	52.90	23.10
13.45	36.90	41.40	35.53		
21.20	38.00	45.70	36.30		
44.75	38.00	49.50	36.50		
47.70	38.00	9	468.00		
11	364.00	0.	0.		
0.	0.	0.	2.00		
0.	17.00	2.00	5.10		
1.90	24.20	18.20	12.40		
3.85	26.90	32.00	25.70		
7.00	30.40	38.62	30.35		
12.00	33.90	44.00	33.15		
18.30	36.40	46.10	33.75		
24.00	37.30	50.60	34.20		
36.00	38.00	11	481.00		
44.90	38.00	0.	0.		
47.70	38.00	0.	1.60		
12	390.00	2.10	3.65		
0.	0.	4.90	4.78		
0.	11.20	11.41	6.20		
1.70	17.40	19.20	8.90		
4.60	22.20	34.90	24.65		
10.10	27.60	39.25	28.00		
14.40	31.20	44.00	30.76		
20.00	33.90	46.35	31.75		
27.00	36.40	51.10	32.30		
31.80	37.35	9	494.00		
37.35	37.85	0.	0.		
45.10	38.00	0.	1.30		
48.40	38.00	4.15	2.85		
13	416.00	7.58	3.30		
0.	0.	20.00	5.00		
0.	6.80	36.95	22.70		
.75	9.60	43.10	27.56		
2.30	12.70	46.70	29.40		
4.80	16.05	51.60	29.80		
8.80	20.00	9	507.00		
14.40	25.00	2.00	0.		
20.15	29.50	8.00	.70		
25.00	32.55	22.90	2.00		
33.20	36.10	29.20	10.00		
40.20	37.30	36.95	18.70		
45.40	37.60	40.20	21.80		
48.90	37.70	44.55	25.10		
		46.90	26.40		
		52.20	27.00		

Table A-4

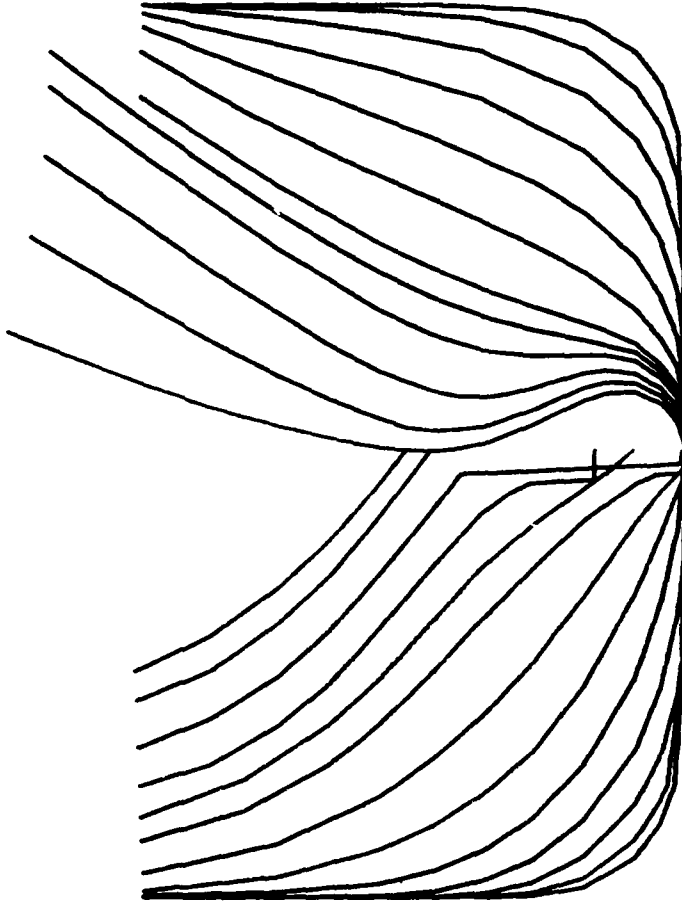
Principal Dimensions
SEALAND 7 Containership

	Abbrev.	Fresh Water	
		Ship	Model (1:150)
Length between perpendicular	LBP	900.0'	6.00'
Breadth (molded)	B	105.5'	8.44"
Depth (molded)	D	64.0'	4.90"
Draft (molded)	T _Ø	38.9'	3.11"
Displacement	Δ	57,797 LT	38.36 lbs
Draft forward	T _F	38.9'	3.11"
Draft aft	T _A	38.9'	3.11"
Transverse metacentric height			
#3 - heavy	GM	.92'	.0736"
#5 - heavy	GM	1.76'	.141"
#6 - heavy	GM	2.19'	.175"
Transverse	KM	44.88'	3.59"
Transverse radius of gyration (air)	i _T	47.0'	3.76"
Longitudinal radius of gyration (air)	i _L	219.0'	1.46'
Block coefficient	C _B	.561	.561
Prismatic coefficient	C _P	.593	.593
Midship section coefficient	C _m	.946	.946
Waterplane coefficient	C _w	.718	.718
Transverse metacentric height			
#3 - heavy	GM/B x 100%	0.87%	0.87%
#5 - heavy	GM/B x 100%	1.67%	1.67%
#6 - heavy	GM/B x 100%	2.08%	2.08%
Ratio of length to breadth	LBP/B	8.53	8.53
Ratio of length to draft	LBP/T	23.14	23.14
Ratio of breadth to draft	B/T	2.71	2.71

N A GRAPH 4.1C 15.98.22. 10/11/78 1

SL7

BODY PLAN (100%)



SCALE: 1 IN = 20 FT DATE: 10/11/78

Figure A - 4

Table A-5
Sea Land 7 Full Table of Offsets

SEALAND CONTAINER VESSEL	SL-7	26 STATIONS	
SEA LAND 7 CONT VES	900.00	105.50	32.00
26			
17	0.		
	0.		
	1.00		
	3.00		
	6.00		
	9.00		
	12.00		
	18.00		
	24.00		
	27.00		
	30.00		
	33.00		
	36.00		
	42.00		
	48.00		
	56.00		
	64.00		
	80.00		
17	45.00		
	0.		
	1.00		
	3.00		
	6.00		
	9.00		
	12.00		
	18.00		
	24.00		
	27.00		
	30.00		
	33.00		
	36.00		
	42.00		
	48.00		
	56.00		
	64.00		
	77.33		
16	90.00		
	0.		
	0.		
	1.00		
	3.00		
	6.00		
	9.00		
	12.00		
	18.00		
	21.00		
	24.00		
	27.00		
	30.00		
	36.00		
	42.00		
	56.00		
	75.50		
	0.		
	1.76		
	5.36		
	7.60		
	9.20		
	9.60		
	9.28		
	7.52		
	6.80		
	6.40		
	6.56		
	7.20		
	9.52		
	12.64		
	21.44		
	35.04		
	0.		
	3.60		
	5.84		
	7.04		
	6.96		
	6.00		
	3.20		
	.88		
	.32		
	0.		
	.24		
	.48		
	1.60		
	3.04		
	5.28		
	8.00		
	14.24		
	45.00		
	0.		
	4.48		
	6.72		
	8.08		
	8.24		
	7.52		
	4.96		
	2.88		
	2.56		
	2.48		
	2.88		
	3.92		
	6.16		
	8.96		
	13.12		
	17.68		
	25.52		
	90.00		
	0.		
	0.		
	1.00		
	3.00		
	6.00		
	9.00		
	12.00		
	18.00		
	24.00		
	30.00		
	36.00		
	42.00		
	48.00		
	56.00		
	75.00		
	160.05		
	0.		
	0.		
	1.00		
	3.00		
	6.00		
	12.00		
	18.00		
	24.00		
	30.00		
	36.00		
	42.00		
	48.00		
	56.00		
	75.00		
	160.05		
	0.		
	0.		
	1.00		
	3.00		
	6.00		
	12.00		
	18.00		
	24.00		
	30.00		
	36.00		
	42.00		
	48.00		
	56.00		
	64.50		
	0.		
	0.		
	1.00		
	3.00		
	6.00		
	12.00		
	18.00		
	24.00		
	30.00		
	36.00		
	42.00		
	48.00		
	56.00		
	64.50		
	0.		
	0.		
	1.00		
	3.00		
	6.00		
	12.00		
	18.00		
	24.00		
	30.00		
	36.00		
	42.00		
	48.00		
	56.00		
	64.50		
	0.		
	0.		
	1.00		
	3.00		
	6.00		
	12.00		
	18.00		
	30.00		
	42.00		
	52.00		
	64.08		
	0.		
	.25		
	1.00		
	3.00		
	6.00		
	12.00		
	24.00		
	36.00		
	48.00		
	64.00		
	0.		
	5.04		
	10.00		
	13.52		
	16.88		
	21.20		
	24.48		
	29.72		
	35.28		
	40.16		
	47.28		
	270.00		
	0.		
	0.		
	6.40		
	13.60		
	18.40		
	22.96		
	28.24		
	31.92		
	37.12		
	41.84		
	45.52		
	50.24		
	315.00		
	0.		
	13.12		
	18.80		
	24.96		
	29.92		
	35.52		
	41.60		
	45.28		
	48.16		
	51.84		

Table A-5 (cont.)
Sea Land 7 Full Table of Offsets

11	360.00	10	540.00	11	720.00
0.	0.	0.	0.	0.	0.
.25	13.20	.25	13.20	0.	2.40
.33	21.20	.50	26.40	3.00	9.76
1.00	25.84	2.17	39.60	6.00	16.88
3.00	32.24	3.00	41.44	12.00	27.84
6.00	36.88	6.00	46.08	18.00	35.60
12.00	42.24	12.00	50.56	24.00	40.72
24.00	47.28	18.00	52.24	30.00	44.48
36.00	49.68	24.00	52.80	36.00	47.12
48.00	51.20	64.00	52.80	48.00	50.40
64.00	52.80	11	585.00	64.00	52.08
13	405.00	0.	0.	11	765.00
0.	0.	.25	13.20	0.	0.
.25	13.20	.48	24.80	0.	1.76
.33	21.20	1.00	28.80	3.00	4.80
.50	26.40	3.00	36.16	6.00	8.64
1.00	32.40	6.00	41.92	12.00	17.20
3.00	38.40	12.00	48.00	18.00	25.04
6.00	42.88	18.00	51.04	24.00	31.44
12.00	47.60	24.00	52.40	30.00	36.64
18.00	49.84	30.00	52.80	36.00	40.88
24.00	51.12	64.00	52.80	48.00	46.48
36.00	52.16	12	630.00	64.00	50.00
48.00	52.48	0.	0.	13	810.00
64.00	52.80	.25	12.80	0.	0.
11	450.00	1.00	19.44	0.	2.56
0.	0.	3.00	28.00	2.00	2.64
.25	13.20	6.00	35.60	3.58	2.72
.33	21.20	12.00	43.68	6.00	4.00
.50	26.40	18.00	48.32	12.00	8.16
1.00	37.60	24.00	50.88	18.00	13.76
3.00	43.36	30.00	52.16	24.00	19.92
6.00	47.20	36.00	52.64	30.00	26.40
12.00	50.80	48.00	52.80	36.00	32.24
18.00	52.24	64.00	52.80	42.00	37.12
30.00	52.80	11	675.00	52.00	42.56
64.00	52.80	0.	0.	64.25	46.16
10	495.00	1.00	9.28	10	832.50
0.	0.	3.00	18.00	6.25	0.
.25	13.20	6.00	26.88	9.00	2.40
.50	26.40	12.00	37.20	12.00	4.48
1.25	39.60	18.00	43.44	18.00	8.64
3.00	44.08	24.00	47.36	24.00	13.68
6.00	48.24	30.00	49.76	30.00	20.32
12.00	51.68	36.00	51.20	36.00	26.88
18.00	52.56	48.00	52.16	42.00	32.40
24.00	52.80	64.00	52.64	52.00	38.88
64.00	52.80			64.33	43.36

Table A-5 (cont.)
Sea Land 7 Full Table of Offsets

13	855.00	15	0.	0.
10.75	0.	1.50	9.60	
10.75	3.44	6.00	16.08	
12.00	3.44	8.25	16.88	
15.00	3.60	12.00	14.24	
18.45	3.76	18.00	7.04	
21.00	5.12	24.00	1.92	
24.00	7.28	30.00	0.	
30.00	13.84	36.00	.40	
36.00	20.88	42.00	1.92	
42.00	27.60	48.00	4.16	
48.00	32.48	56.00	7.92	
56.00	37.12	64.00	12.24	
64.42	39.68	72.00	17.12	
12	877.50	81.75	23.44	
.50	0.	11	0.	-71.12
.50	1.50	3.00	3.00	-69.44
10.75	2.00	6.00	6.00	-67.68
18.00	2.32	10.75	10.75	-64.96
24.00	2.56	12.00	12.00	-19.44
26.50	2.72	25.00	25.00	-19.44
30.00	7.20	30.00	30.00	0.
36.00	14.40	33.00	33.00	12.24
42.00	21.28	42.00	42.00	13.92
48.00	26.64	64.83	64.83	17.92
56.00	31.68			
64.67	35.20			
6	900.00			
30.00	0.			
36.00	7.60			
42.00	14.80			
48.00	20.40			
56.00	26.00			
64.83	29.60			
6	915.00			
33.00	0.			
36.00	3.76			
42.00	10.56			
48.00	16.08			
56.00	21.84			
64.92	26.08			

Table A-6
Sea Land 7 Partial Table of Offsets

SEALAND CONTAINER VESSEL	SL-7	14 STATIONS
SEA LAND 7 CONT VES	900.00 105.50 32.00	
14		
9	0.	
0.	0.	6 450.00
6.00	7.04	0.
12.00	6.00	.50 26.40
18.00	3.20	3.00 43.36
24.00	.88	6.00 47.20
30.00	0.	18.00 52.24
36.00	.48	64.00 52.80
64.00	8.00	6 540.00
80.00	14.24	0.
10	90.00	.50 26.40
0.	0.	3.00 41.44
0.	1.76	12.00 50.56
3.00	7.60	24.00 52.80
6.00	9.20	64.00 52.80
12.00	9.28	6 630.00
18.00	7.52	0.
24.00	6.40	3.00 28.00
30.00	7.20	6.00 35.60
36.00	9.52	18.00 48.32
75.50	35.04	30.00 52.16
9	160.00	64.00 52.80
0.	0.	4 720.00
0.	3.44	0.
3.00	9.68	18.00 35.60
6.00	11.76	36.00 47.12
18.00	14.48	64.00 52.08
30.00	18.32	7 810.00
42.00	24.56	0.
56.00	33.52	2.00 2.64
75.00	47.36	6.00 4.00
7	225.00	12.00 8.16
0.	0.	42.00 37.12
0.	5.04	52.00 42.56
3.00	13.52	64.25 46.16
6.00	16.88	6 877.50
18.00	24.48	.50 0.
52.00	40.15	.50 1.50
64.25	47.28	26.50 2.72
5	315.00	42.00 21.28
0.	0.	48.00 26.64
.25	13.12	64.67 35.20
6.00	29.92	4 900.00
24.00	41.60	30.00 0.
64.00	51.84	42.00 14.80
6	360.00	48.00 20.40
0.	0.	64.83 29.60
.33	21.20	4 915.00
6.00	36.88	33.00 0.
12.00	42.24	42.00 10.56
24.00	47.28	48.00 16.08
64.00	52.80	64.92 26.08

Table A-7
Pacific Coast Crab Boat
Principal Dimensions

		Full Scale	Model scale: 1/22.368
Design displacement	Δ_o	260 LT(SW)	52.00 lb(SW)
Length between perpendiculars of design LWL	LBP	85.07'	3.8033'
Breadth, molded to design LWL	B	24.79'	1.1083'
Depth, molded to main deck	D	14.18'	0.6339'
Draft, molded to design LWL	T	12.00'	0.5365'

Table A-8

Pacific Coast Crab Boat

Test Conditions

		Full Scale	Model Scale, 1/22.368
Displacement	Δ	340 LT(SW)	67.95 lb(SW)
Length	L	85.75'	3.8336'
Beam	B	27.71'	1.1494'
Mean draft	T	13.58'	0.6071'
Trim (+by bow)		0	0
Transverse metacentric height	GM	1.93', 1.03' 0.90', 0.64'	0.0862', 0.0460', 0.0402', 0.0287'
Transverse metacentric height	100GM/B	7½%, 4%, 3½%, 2½%*	7½%, 4½%, 3½%, 2½%*
Transverse metacenter	KM	16.20'	0.7242'
Transverse radius of gyration (air)	i_t	11.93'	0.5332'
Transverse radius of gyration	100 i_t /B	46%**	46%**
Longitudinal radius of gyration (air)	i_L	36.04'	1.6113'
Longitudinal radius of gyration	100 i_L /L	42%***	42%***

Form Coefficients

Block coefficient	C_b	0.443
Prismatic coefficient	C_p	0.653
Midship coefficient	C_m	0.679
Length-beam ratio	L/B	3.335
Beam-depth ratio	B/D	1.813
Beam-draft ratio	B/T	1.893
Displacement-depth ratio	$\Delta / (0.01L)^3$	540

*These values for 100GM/B are less than the representative value of $GM \geq 10\%B$ for fishing vessels given by Saunders in [14].

**This value for 100 i_t /B is at the upper end of the representative value of $47\% B \geq i_t \geq 40\%B$ for fishing vessels given by Saunders in [14].

***This value for 100 i_L /L exceeds that of $25\%L \geq i_L \geq 23\%L$ suggested by Saunders in [14]. This was an unavoidable consequence of having to place the vertical gyroscope at the bow under the forecastle deck, and of counterbalancing this large weight with ballast at the stern under the poop deck in order to maintain zero trim.

Table A-9
CRAB BOAT - Table of Offsets

PACIFIC COAST CRAB BOAT: TABLE OF FULL SCALE OFFSETS
 U.S.C.G.#48246526512 85.75 25.71 13.58

16					
7	0.00				68.45
12.00	0.00				0.00
14.00	0.81	2.24	9	17.11	0.15
16.11	1.71	2.24		0.00	0.15
18.70	3.00	3.82		0.34	6.85
20.52	4.14	5.00		0.47	9.29
22.03	5.25	6.00		2.93	15.64
23.90	6.82	7.00		4.49	19.22
12	4.28	8.00		5.83	6
6.66	0.00	8.65		6.80	0.00
6.66	0.05	20.68		7.38	0.00
8.00	0.75		10	11.75	0.00
9.00	1.21	2.09		21.39	7.66
10.00	1.68	2.09		0.00	10.14
12.00	2.52	3.09		0.34	15.81
13.24	3.00	3.63		0.47	19.14
14.00	3.37	4.65		3.00	4
16.00	4.38	5.00		3.85	8.76
18.00	5.53	6.00		5.70	10.92
18.92	6.00	7.00		7.50	16.05
22.31	8.10	8.00		8.84	19.66
13	8.56	16.19		11.05	4
4.94	0.00	20.24		12.07	10.90
4.94	0.05		9	25.67	11.81
6.00	1.26	1.89		0.00	16.33
7.00	2.12	1.89		0.34	19.97
8.00	2.80	3.35		0.47	7
8.83	3.00	4.33		3.00	11.11
9.00	3.36	5.59		6.00	11.74
10.00	3.91	6.00		6.93	12.00
12.00	4.85	7.43		9.78	12.95
14.00	5.78	16.05		11.86	14.00
16.00	6.77	19.83		12.29	16.68
18.00	7.85		6	34.22	20.24
22.00	10.40	1.53		0.00	8
15	12.83	1.53		0.34	2.24
2.00	0.00	3.08		0.47	-17.11
2.80	0.33	6.07		11.10	-12.83
4.25	0.35	15.58		12.68	-8.56
5.00	1.49	19.18		12.56	-4.28
6.00	2.91		6	42.78	-2.11
6.10	3.00	1.21		0.00	-0.91
7.00	4.03	1.21		0.34	0.00
8.00	4.85	2.98		0.47	5.22
9.00	5.54	6.66		11.51	7
10.00	6.00	15.37		0.00	-11.48
12.00	6.36	18.95		6.00	-11.16
14.00	7.72		6	8.26	-10.25
16.00	8.57	0.84		11.09	-0.24
18.00	9.55	0.84		16.83	2.98
21.34	11.25	3.39		17.83	2.98
		7.04		20.35	0.56
		15.33			
		18.89			
			6	59.89	
		0.48		0.00	
		0.48		0.34	
		4.93		1.45	
		7.59		11.41	
		15.32		12.80	
		18.94		12.45	

PACIFIC COAST CRABBER

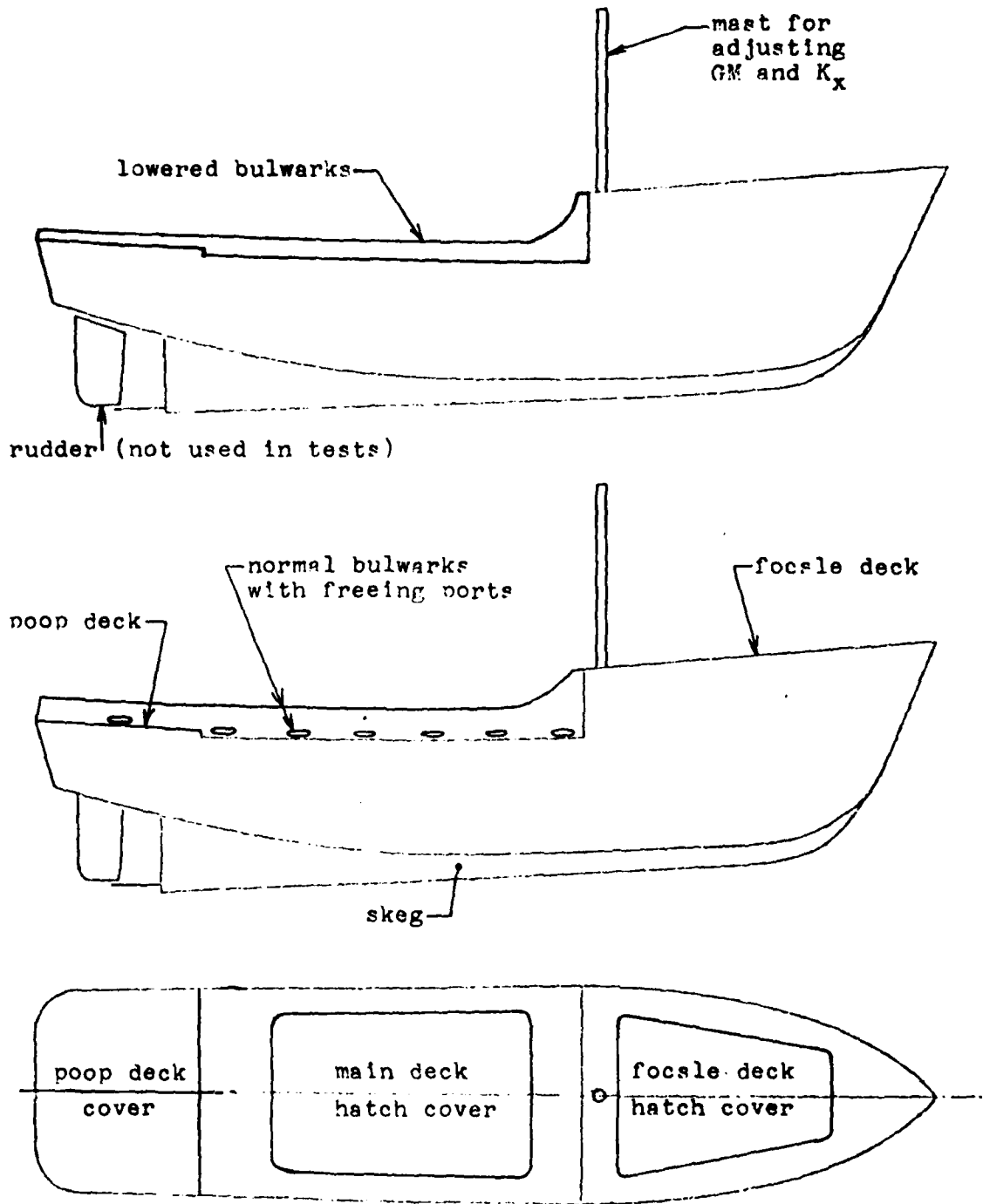
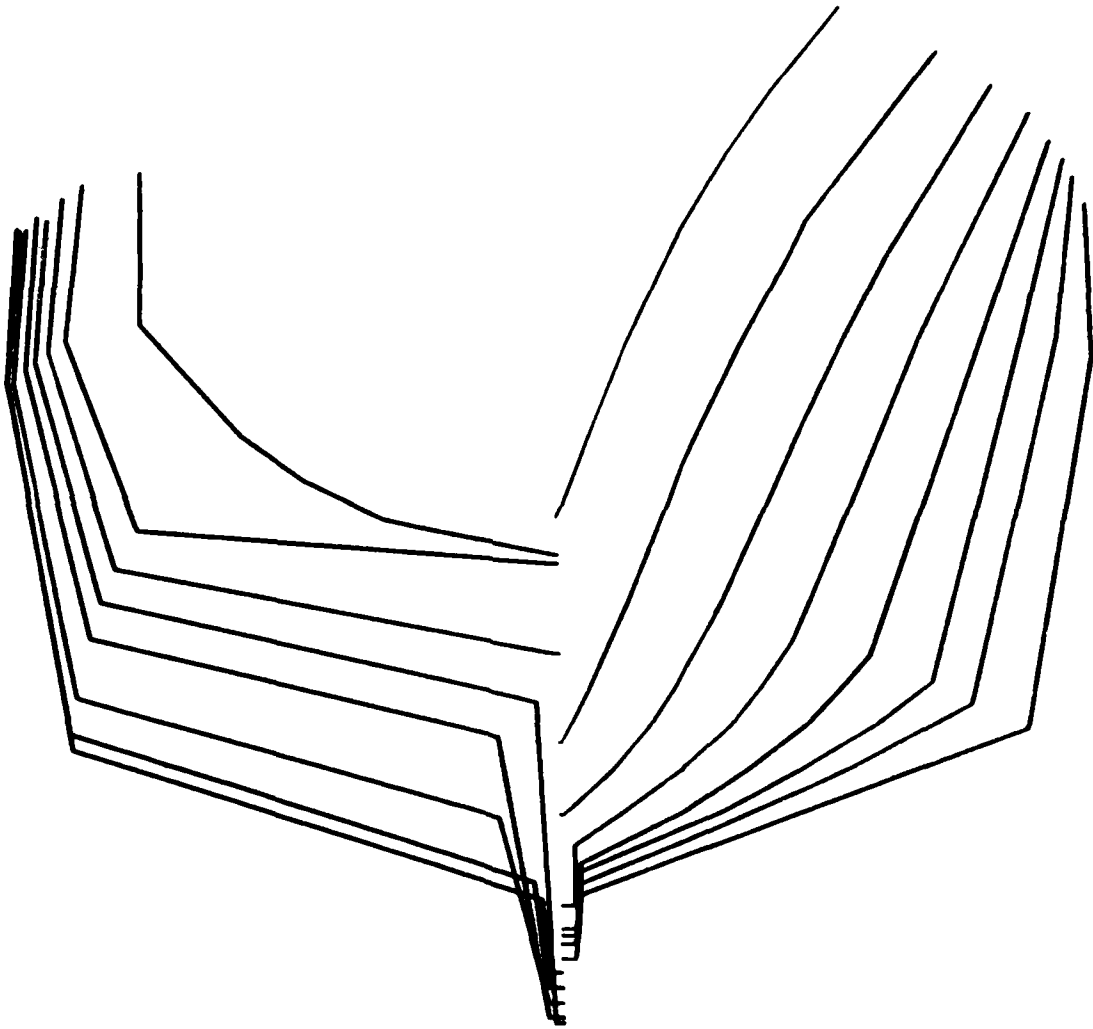


Figure A-5: Ship Plans and Profiles (no scale)

PACIFIC COAST CRAB BOAT
BODY PLAN



SCALE = 1:48

Figure A-6

Appendix B

Motion Restraint Mechanism

Model Arrangement

Instrumentation

LABORATORY ARRANGEMENT

Motion restraint mechanism

The motion restraint mechanism allows for freedom in roll, pitch, and heave while completely restraining yaw, sway, and surge. Refer to figure B-1 during the following description. Figures B-3, B-4, and B-5 show the model in the towing tank ready for experimental runs. A stainless steel rod, designated as "A" in figure B-1, is rigidly attached to the bow of the model with its axis parallel to the keel and longitudinal centerline and passing through the vertical center of gravity. About six inches of the rod extends forward of the hull. Rod "B" is attached at the stern in the same way. Two stainless steel vertical rods "C" whose axis are parallel and in the same transverse plane are rigidly attached to the carriage so that rod "A" passes between rods "C" with a small clearance between rods "A" and "C". Two rods "D" are arranged in the same way at the stern. The longitudinal position of the model is maintained by a pair of oval teflon cylinders ("E" and "F") attached to the horizontal rod at the bow of the model, one forward and one aft of the vertical guide rods "C".

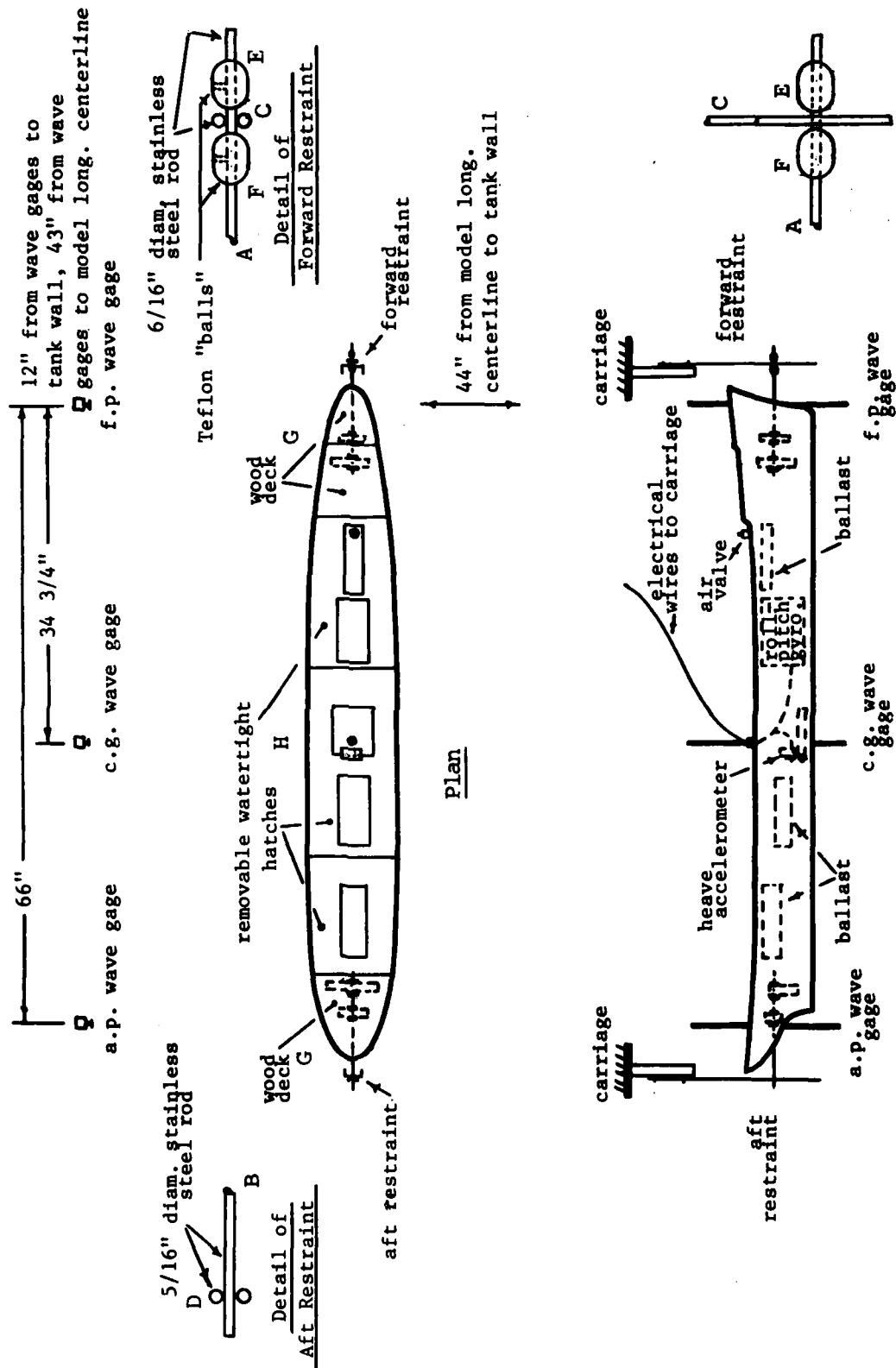
The effect of the restraint mechanism on roll was investigated. When the model was given a large initial roll angle in smooth water with a forward speed, smooth and continuous rolling motion was recorded as shown in the roll decay plots, figures 14 through 17. Also, the roll motion in waves was smooth and continuous even though the contact of vertical rods "C" would alternate between the forward teflon cylinder "E" and the after teflon cylinder "F" as the model tended to surge and at the same time contact of horizontal rods "A" and "B" would oscillate between the port or starboard vertical rods "C" and "D" as the model tended to yaw and sway. By keeping the clearances small, these effects were controlled and felt to have a negligible effect on roll.

Model arrangement

Located on the model at the bow and stern are permanent watertight wooden deck sections, designated as "G" in figure B-1. Three removable plexiglass sections "H" used for the remainder of the deck provide easy access to instrumentation inside the model and insure watertightness. Figure B-6 is a detail of the plexiglass hull connection. Note that bulwarks are not present and the deck has no camber. The deck has a watertight penetration near midships for electrical wires which provide gyroscope power and transmit signals from the instruments inside the model (figures B-1 and B-3). The air valve provides a means of checking for leaks. This is accomplished by spreading soapy water around the deck edges and pumping air into the model. Any leaks will be detected by the presence of soap bubbles. The air pressure inside the model is reduced to atmospheric before proceeding with experimental runs.

Located inside the model are ballast, a vertical gyro which measures pitch and roll angles, and an accelerometer for measuring heave acceleration (figure B-1). Three wave gauges attached to the carriage are aligned parallel to and 43 inches to port of the model centerline so as to be out of the wave field generated by the model. One wave gauge is abeam the forward perpendicular, another is abeam the model longitudinal center of gravity, and the last is abeam the after perpendicular. Roll, pitch, heave and wave data were recorded on an eight channel strip chart recorder and simultaneously on digital magnetic tape. Speeds were read from the tachometer located on the carriage. Wave periods were read from a device on the wave maker. Table B-1 contains a list of the instrumentation.

Figure B-1
 Mariner 77.7 Model General Arrangement



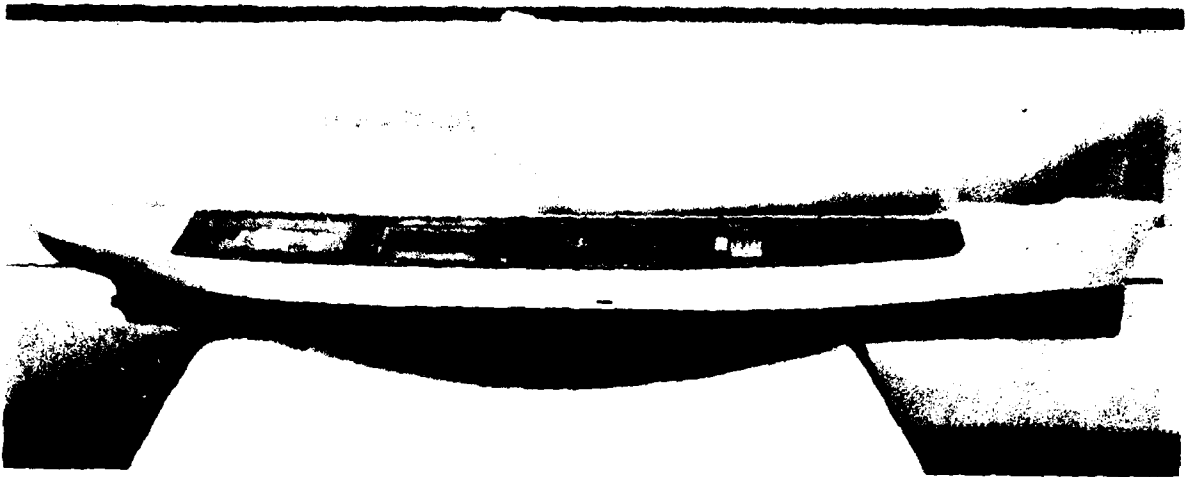


Figure B-2 Mariner Model

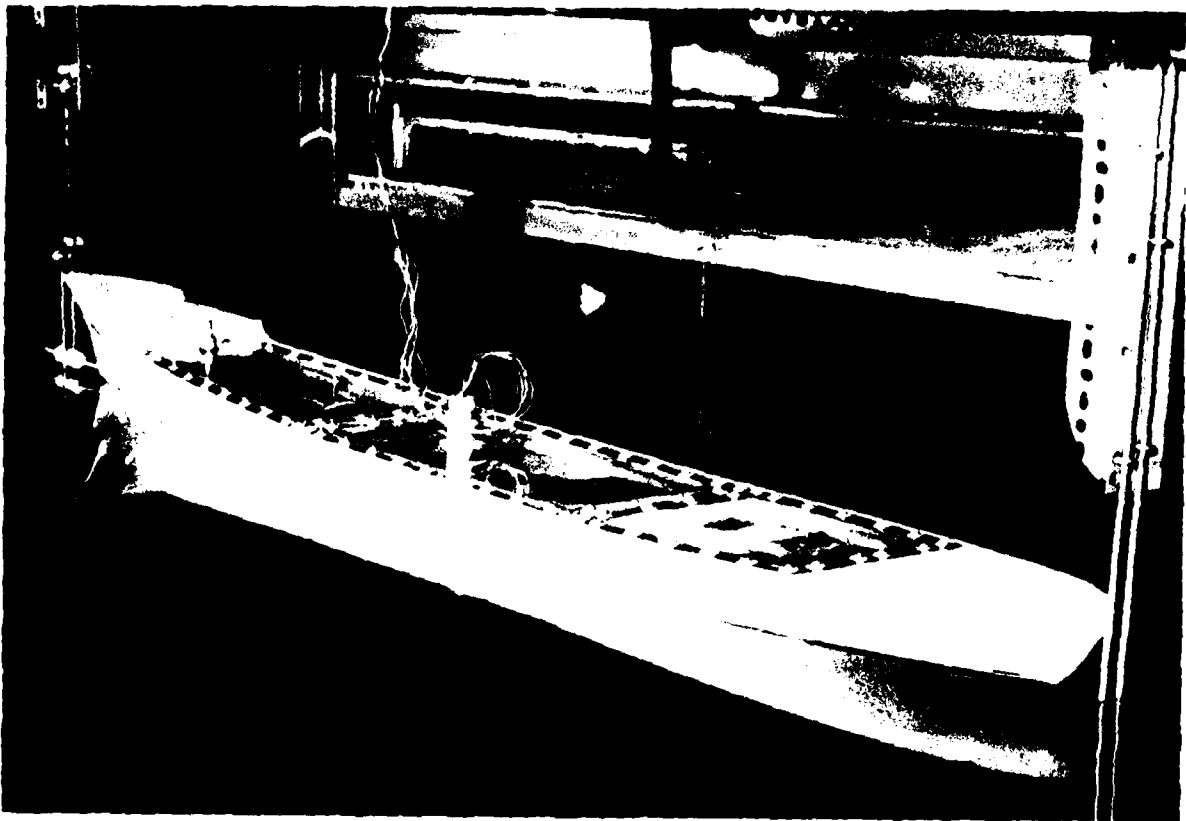


Figure B-3 Towing Arrangement

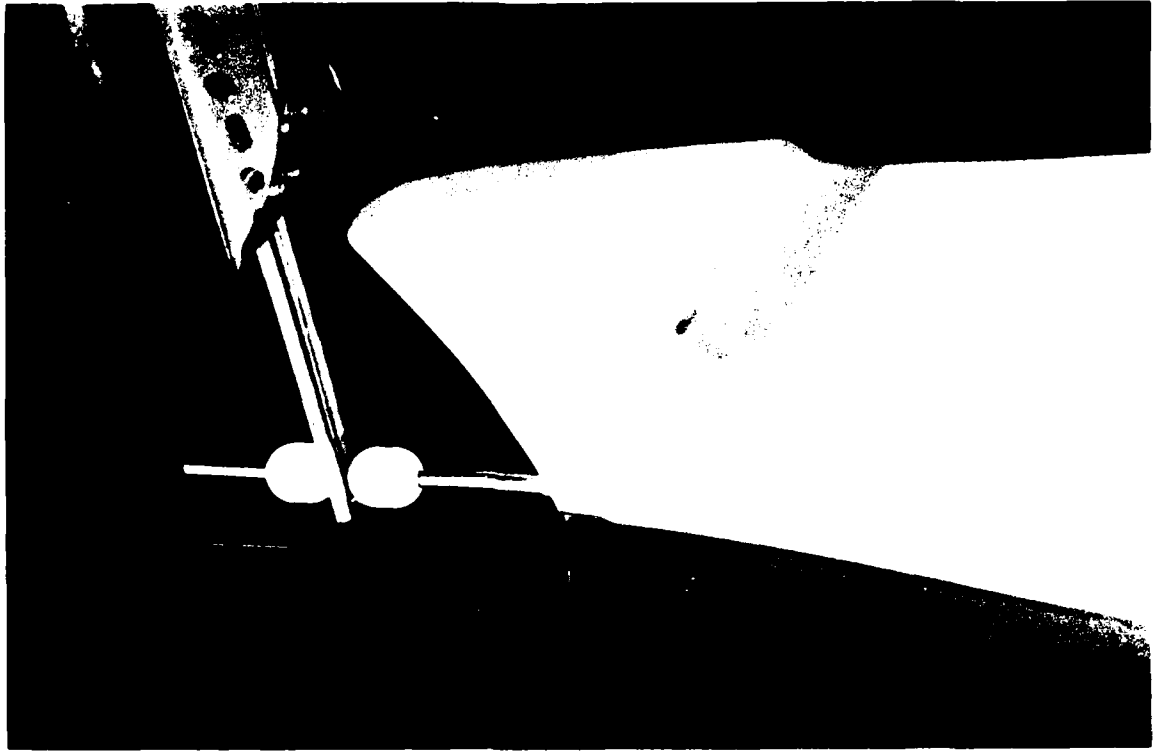


Figure B-4 Forward Restraint

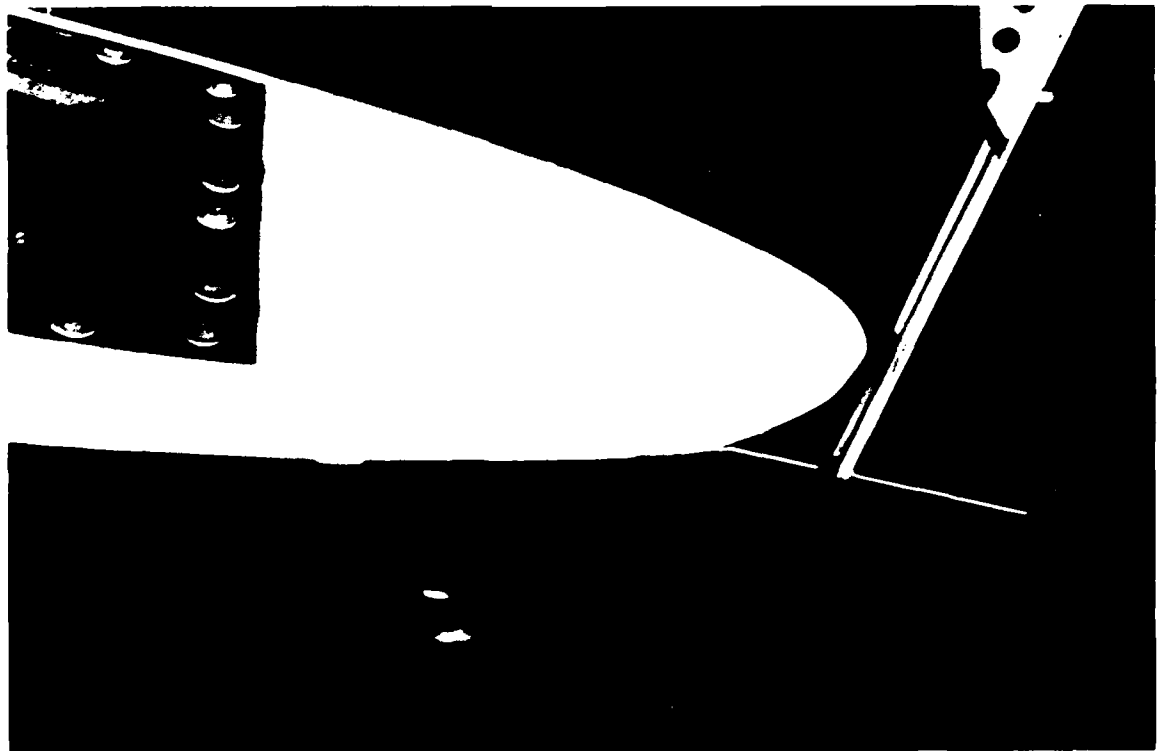
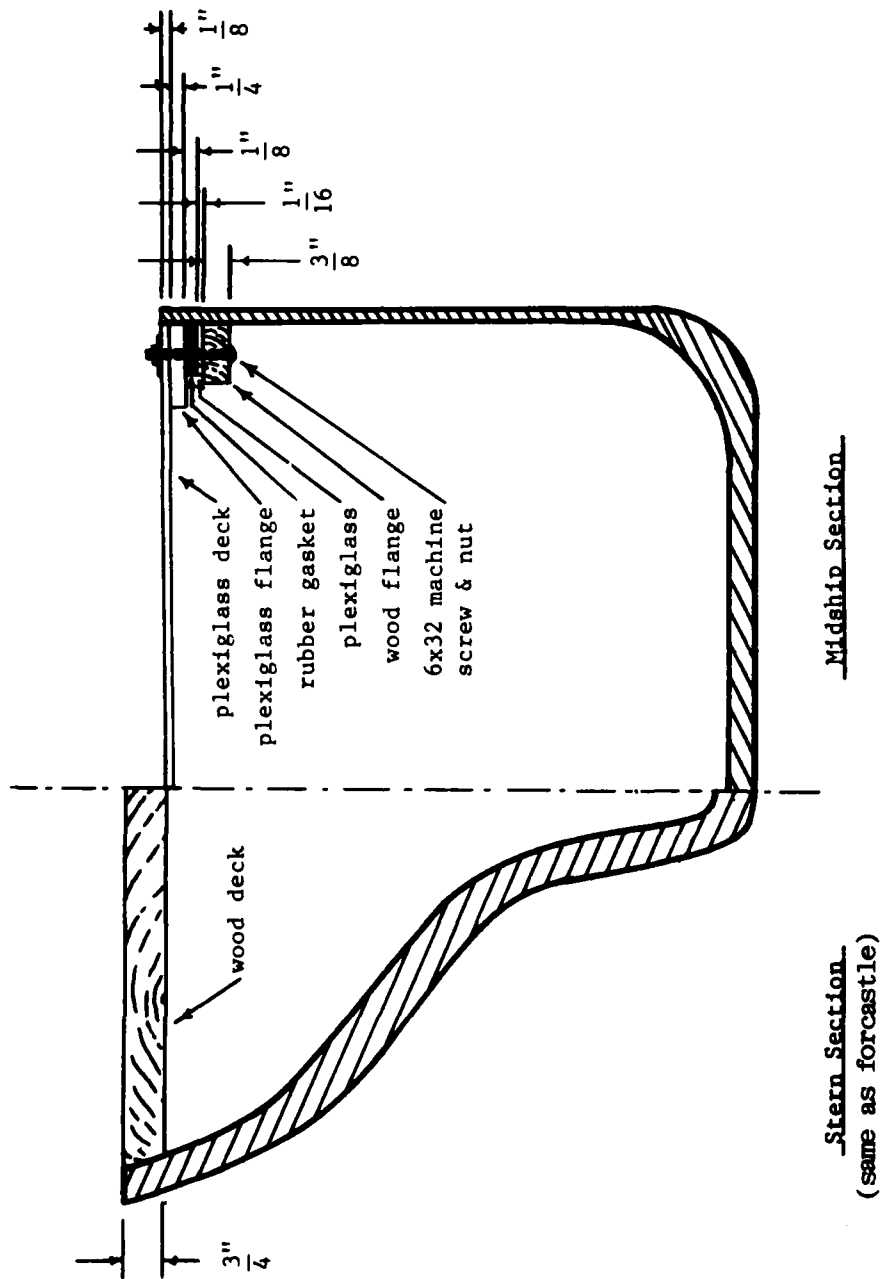


Figure B-5 After Restraint

Figure B-6
Mariner 77.7 Model Deck Attachment



APPENDIX C

Inclining Experiment Procedure

Table of Measured Metacentric Heights

Procedure for Measuring Moments of Inertia

INCLINING EXPERIMENT PROCEDURE

An inclining experiment for measuring the metacentric height (GM) was performed almost every day before proceeding with experimental runs. Table C-1 gives these values. Since GM was small, only 0.8% of the beam or .078 inch (model scale), the inclining had to be carefully executed to obtain acceptable results. Because the electrical wires which are attached to the deck cause adverse heel when the model drifts during the inclining, the inclining experiments were made with the model positioned in the restraint mechanism. Also the wires were separated and spread apart from each other near the model to minimize their affect.

Inclining was performed in the usual manner. The model was given several different known heeling moments while the angle of heel was measured. The heeling moment was obtained by placing a known weight at various known transverse locations. Each time the weight was moved to a new location the model was made to roll freely with an initial two or three degree amplitude and this motion was recorded. The mean roll angle was taken as the angle of heel for that particular weight location. This method eliminates any error due to the coarseness of the windings in the roll potentiometer. GM was taken as the slope of the graph of the inclining moment vs. angle of heel. Figure C-1 shows an example of such a graph for one of the inclining experiments.

Mariner Model (1/96) Inclining Experiment

Sept. 5, 1978

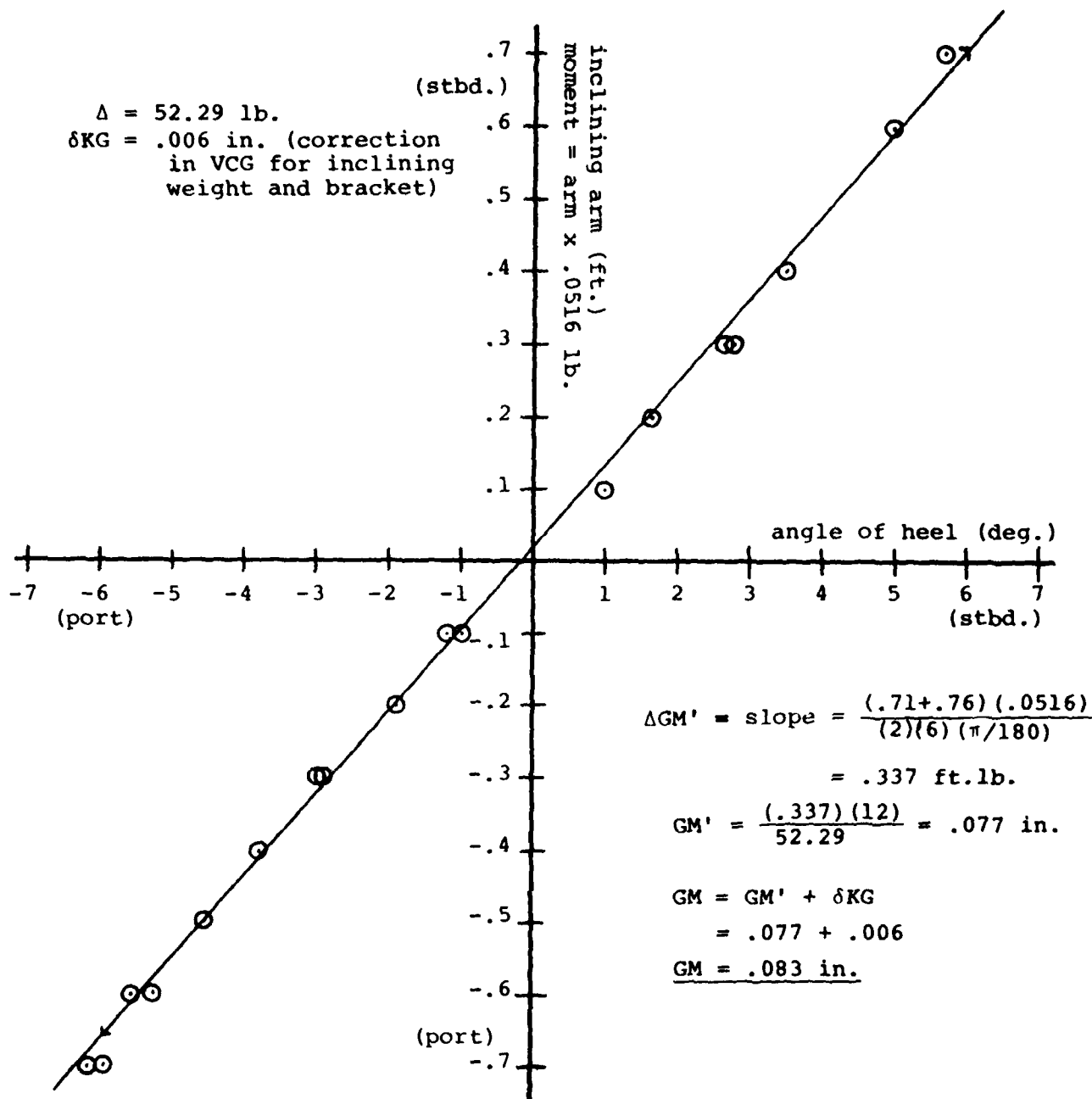


Figure C-1

Table C-1
MARINER 77.7
MEASURED METACENTRIC HEIGHT (GM)

<u>Date</u>	<u>GM (model)</u>	<u>GM (ship)</u>
9/1/78	.079 in.	.63 ft.
9/5/78	.083 in.	.66 ft.
9/6/78	--	--
9/7/78	.085 in.	.68 ft.
9/11/78	.084 in.	.67 ft.
9/13/78	.084 in.	.67 ft.
9/15/78	.076 in.	.67 ft.
<u>AVERAGE</u>	.0818 in.	.65 ft. + .04 ft.

PROCEDURE FOR MEASURING MOMENTS OF INERTIA

Roll and pitch moments of inertia in air were determined by suspending the model a certain distance above the center of gravity as a bifilar pendulum and noting the period of swing. Details and formulas can be found in Sharp [16].

APPENDIX D

Initial Conditions for Capsize Simulator

Table D-1

MARINER 77.1Initial Conditions for Capsize Simulator

(values given in ship scale)

figure	run	speed (kn)	roll angle (deg)	roll ang. vel. (deg/sec)	pitch angle (deg)	pitch ang. vel. (deg/sec)	wave amp. (ft)		wave freq. (rad/sec)		wave phase (deg)		additional quad. damping coef. (ft·lb·sec ²) dampq
							a ₁	a ₂	ω ₁	ω ₂	φ ₁	φ ₂	
III-5	0901-41A	7.3	21.0	0	1.35	1.0	17.5	—	.614	—	264.	—	1.6 x 10 ⁹
III-6	0901-41A	"	"	"	"	"	"	—	"	—	"	—	1.8 x 10 ⁹
III-7	0905-55J3	7.8	-26.2	10.0	-0.68	-0.55	12.8	—	.614	—	205.	—	1.239 x 10 ⁹
III-8	0905-55J3	"	"	"	"	"	"	—	"	—	"	—	1.2386 x 10 ⁹
III-9	0905-55J3	"	"	"	"	"	"	—	"	—	"	—	1.2385 x 10 ⁹
III-10	0911-79B1	6.9	-43	3.32	-2.26	.05	11.0	5.0	.665	.576	-232.2	-267.	1.18 x 10 ⁹
III-11	0911-79B1	"	"	"	"	"	"	"	"	"	"	"	1.15 x 10 ⁹

Table D-2
Initial Conditions for Capsize Simulator for the SL7

(values given in ship scale)

Figure	Run	Speed (kn)	Roll Angle (deg)	Roll Angle Veloc. (deg/sec)	Pitch Angle (deg)	Pitch Angle Veloc. (deg/sec)	Pitch Ang. Veloc. (deg/sec)	Wave Ampl. (ft)	Wave Freq. (rad)	Wave Phase (deg)	Damp Coef. Linear (ft · lbs · sec)	Damp. Coeff. Quadratic (ft · lbs · sec ²)
III-23	0409-46	9.8	25.39	0.	.84	.83	12.9	.410	324.1	1.7 x 10 ⁶	6.0 x 10 ⁹	
III-24	0409-63	3.7	21.7	0.	.12	1.18	16.0	.375	321.8	1.1 x 10 ⁶	2.1 x 10 ⁹	
III-25	0409-45	9.8	30.21	0.	.46	.85	15.9	.410	314.4	1.15 x 10 ⁶	2.5 x 10 ⁷	
III-26	0409-45	9.8	30.21	0.	.46	.85	15.9	.410	314.4	1.73 x 10 ⁶	9.0 x 10 ⁹	
III-27	0409-61	1.3	17.14	0.	3.45	-.28	15.4	.382	239.2	5.0 x 10 ⁶	5.0 x 10 ⁷	

Table D-3
Pacific Coast Crab Boat

Initial Conditions for Capsize Simulator

(values given in model scale = full scale/22.368)

Figure	Run	Forward Speed		Roll Motion		Pitch Motion		Waves			Additional Roll Damping	
		V (knots)	V/\sqrt{L}	Angle (deg)	Angular velocity (deg/s)	Angle (deg)	Angular velocity (deg/s)	Amplitude (feet) a	Frequency (rad/s) ω	Phase (deg) ϕ	Linear damp (ft-lb-s)	Quadratic damp (ft-lb-s ²)
III-34	FRD*	0	0.0	7.125	0	0	0	-	-	-	0.026	0.032
III-35	FRD	1.572	0.8	8.810	0	0	0	-	-	-	0.158	0
III-36	FRD	1.976	1.0	11.000	0	0	0	-	-	-	0.1762	0.0309
III-37	FRD	0	0.0	7.125	0	0	0	-	-	-	0.030	0.035
III-38	FRD	1.572	0.8	8.810	0	0	0	-	-	-	0.17	0.03
III-39	FRD	1.976	1.0	11.000	0	0	0	-	-	-	0.20	0.06
III-40	7	1.748	0.9	-6.725	10.0	4.35	11.25	0.172	5.487	2327	0	0
III-41	8	1.993	1.0	-10.250	10.0	4.25	0.00	0.147	5.487	206.3	0	0
III-42	20	2.004	1.0	-8.850	0	4.85	3.50	0.185	5.133	234.3	0.075	0.023

*FRD indicates a free roll decay simulation.

Wave amplitude, a, is one-half H_w = peak-to-peak wave height.

Wave frequency $\omega = 2\pi/T_w$, where T_w = wave period.

Wave phase, ϕ , is the angular advance of a wave crest ahead of a positive roll peak.

Roll angle is measured positive to starboard.

Pitch angle is measured positive bow up.

Appendix E-1

User Manual for Program CAPSIZE

USER MANUAL FOR PROGRAM CAPSIZE

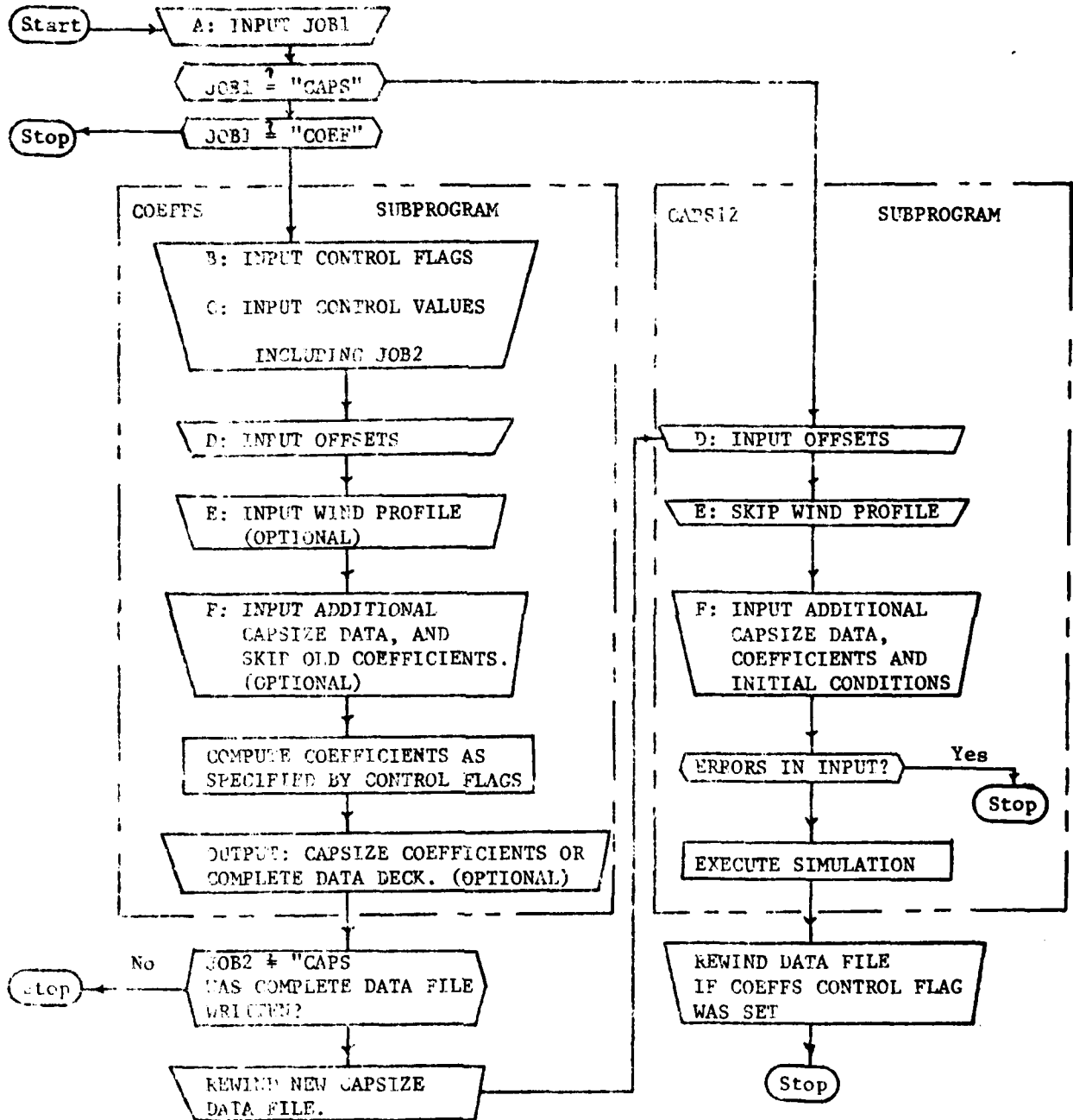
Capsize is a FORTRAN program which simulates ship motions and capsizing in astern seas by means of a time-domain numerical integration of the equations of motion. The CAPSIZE program consists of two subprograms, COEFFS and CAPSIZ. The motion simulation is performed by the CAPSIZ subprogram. The COEFFS subprogram is provided as an aide to the preparation of the input data record for the CAPSIZ subprogram. The primary function of COEFFS is to compute and output two-dimensional hydrodynamic added mass and damping coefficients for the data deck that must be prepared for CAPSIZ. In addition to coefficient generation, COEFFS may be used to update an existing CAPSIZE input file by inserting new displacement and center of gravity values as well as the new coefficient tables. The use of the COEFFS subprogram is optional. Any source of coefficient data in the same format may be used for CAPSIZ. The two subprograms may be executed in the same run, or they may be executed in different runs on the computer. For example, the COEFFS routine may be executed to create an input file for the CAPSIZ subprogram, but the actual simulation may be deferred until the output listing has been examined for possible errors in some of the parameters. After the user has checked the output, the CAPSIZ simulation routine may be executed.

In many cases it is possible to execute the COEFFS routine once saving the CAPSIZE data file. Then several CAPSIZE executions may be made by simply changing the initial conditions, or wave height, or any of the other parameters which do not change the two-dimensional coefficients or location of the center of gravity within the ship. The method of editing the CAPSIZE data file is to be selected by the user. The method which will work on most computers is to punch the data file onto cards. Parameters may be changed by manually replacing the affected cards. Most computer systems also provide a file editing system which may be used.

INPUT

The inputs to both the CAPSIZ and COEFFS subprograms are described below. The notation is similar to FORTRAN, but unit

CAPSIZE PROGRAM



numbers and FORMAT statement numbers are not shown. The notation shows statements that are equivalent to those in the program, but they are not necessarily identical. In addition to the data items specified below, the CAPSIZE simulator reads and lists the contents of columns 73 through 90 of each line (columns 73 through 80 for cards). These columns may be used for comments or sequencing, and any characters which may be represented by the processor are acceptable. All integer values are read using the I5 FORMAT conversion. With the exception of the optional SHCP compatible offset format all real values are read using the F10.2 conversion. All character data--titles and line sequencing--are read using A1 conversion. The directives calling for the execution of either the coefficient generation or the capsiz execution are read using A4 conversion.

The real values represent physical quantities, and the user must provide the numerical values in a consistent system of dimensional units. The length, time and either the mass or the force units are arbitrary. The time unit is usually selected as seconds. Linear velocities are measured in units of length per unit of time. All angles and directions are measured in degrees for input and output purposes. Angular velocities are measured in degrees per unit of time. Circular frequency is used for the waves and this is expressed in radians per unit of time.

A. Selection of subprograms to be executed

When execution of the program begins, one line of data is read by the program. This line identifies the sub-program which is to be executed first. The COEFFS subprogram may be specified to prepare data for the capsiz simulation or the CAPSIZ sub-program may be specified to carry out the simulation. This line is read from unit 5.

```
READ (...)          JOB1
FORMAT (A4)
```

The only valid values for JOB1 are "COEF" or "CAPS". If "COEF" is input, the COEFFS subprogram is executed. If "CAPS" is input,

the CAPSIZE simulator is executed. If "COEF" is specified, input items B and C below must appear in the input file. When COEFFS writes a complete data file for CAPSIZE, the first line contains "CAPSIZE".

B. Input and output control flags for COEFFS only.

One line of data is read by COEFFS to control the remainder of its input and output operations. This line is read from unit 5.

```
READ (...) INPUT1, INPUT2, INPUT3,  
        LIST1, LIST2, LIST3, LIST4, LIST5,  
        LIST6, LIST7, LDATA, LCOEFF,  
        IREWIN, LREWIN  
FORMAT (14I5)
```

If zero is specified--or the field is blank--for any of these items, the program will provide a default value for the item. If a negative value is specified the corresponding input or output operation is suppressed. If a positive value is specified, the operation is specified and the value is the input or output unit number to be used. Note that unit numbers are subject to processor restrictions. The list items are described below.

<u>Item</u>	<u>Description</u>
INPUT1	Unit number for the next four lines of COEFFS control values. The default is INPUT=5. This input may not be suppressed.
INPUT2	Unit number for the table of offsets. The default is either the specified or default value for INPUT1. This input may not be suppressed.
INPUT3	Unit number for additional data which is used by CAPSIZE. The default is

either the specified or default value for INPUT2. If this input is suppressed, LDATA is also suppressed by the program.

- LIST1 Unit number for comments and error messages written by COEFFS. The default is LIST1=6. This output listing may not be suppressed.
- LIST2 Unit number for a listing of the table of offsets. The default is LIST2=6.
- LIST3 Unit number for a listing of hydrostatic values computed from the table of offsets for the specified drafts and center of gravity. The default is LIST3=6.
- LIST4 Unit number for a listing of two-dimensional added mass, damping and coupling coefficients. This output listing is suppressed by default.
- LIST5 This is not used.
- LIST6 Unit number for a listing of the two-dimensional added mass, damping and coupling coefficients that are computed for use by the CAPSIZE simulator. The default is LIST6=6.
- LIST7 Unit number for a listing of the data produced by either of the LDATA or LCOEFF options. This listing is suppressed by default. If it is selected, IREWIN is selected by the program.

LDATA Unit number for a complete data deck to be written for CAPSIZ . This output is suppressed by the program if INPUT3 is suppressed by the user. The default is LDATA=1. If LDATA is specified, LCOEFF is also specified.

LCOEFF Unit number for a data deck to be written containing only the hydrodynamic coefficients required by CAPSIZ . This unit is specified only when LDATA is suppressed. The default is LCOEFF=1.

IREWIN Specifies an initial rewind of the LCOEFF or LDATA unit. If specified by any positive value, the unit is rewound after the data are written. This allows both COEFFS and CAPSIZ to be run in the same computer job. This rewind is suppressed by default.

LREWIND Specifies a final rewind of the LCOEFF or LDATA unit. If specified by any positive value, the unit is rewound after the data are written. This allows both COEFFS and CAPSIZ to be run in the same computer job. This rewind is suppressed by default.

If CAPSIZ is executed in the same run, the data written by COEFFS will be rewound before CAPSIZ is executed regardless of the LREWIND parameter. The records generated by the LIST1 through LIST7 options are formatted for listing on devices having at least 132 print positions on each line. The first character of each line is intended to control the vertical spacing (carriage control)

of the printed lines using the standard FORTRAN convention. The data written by the LDATA and LCOEFF options are formatted with up to 80 characters on a line, and these lines are suitable for punching. The records generated by LDATA are in a form that may be read directly by CAPSIZE.

C. Control values for COEFFS only.

Four more lines of data are ready by COEFFS to specify the condition for which coefficients are to be computed. These lines are read from the unit specified by INPUT1 (default is unit 5).

C1. Optional scale factors and origin translation are read. This transformation applies only to the table of offsets which is described in section D, below. If this transformation is not desired a blank line may be used.

```
READ (...) XSCALE, YSCALE, ZSCALE,  
          XORIG, YORIG  
FORMAT (5F10.2)
```

<u>Item</u>	<u>Description</u>
XSCALE	If non-zero, all x-coordinate values (longitudinal) of the original offsets are multiplied by XSCALE.
YSCALE	If non-zero, all y-coordinate values (vertical) of the original offsets are multiplied by YSCALE.
ZSCALE	If non-zero, all Z-coordinate values (transverse) of the original offsets are multiplied by ZSCALE.
XORIG	Specifies the new position of X=0.0. Note that X is positive forward. The

X-coordinate of the new origin is measured before XSCALE is applied.

YORIG

Specifies the new position of Y=0.0. Note that Y is positive upwards. The Y-coordinate of the new origin is measured before YSCALE is applied.

FLAG

C2. The drafts to the baseline (Y=0.0) at the forward and after perpendiculars and the optional metacentric height, GM, are specified.

```
READ(xxx) TF, TA, XPPERP,  
          XAPERP, GM, CGFLAG  
FORMAT (6F10.2)
```

<u>Item</u>	<u>Description</u>
TF	Draft to baseline at forward perpendicular. The value is positive if the baseline lies below the water surface at the perpendicular.
TA	Draft to baseline at after perpendicular. The value is positive if the baseline lies below the water surface at the perpendicular.
XPPERP	Specifies the X-coordinate of the forward perpendicular. Note that X is measured positive forward of the origin of the table of offsets. See XAPERP.
XAPERP	Specifies the X-coordinate (measured

forward of the origin of offsets) of the after perpendicular. If XPPERP and XAPERP are not specified, the program assumes that the perpendiculars are located at the first and last stations of the offset deck.

GM Specifies the metacentric height, GM, for the ship. If GM is non-zero, the Y-coordinate of the center of gravity will be set to the value that results in the specified GM. The X-coordinate of the center of gravity will be set to the position of the X-coordinate of the center of buoyancy.

CGFLAG Is specified as a non-zero value if $GM=0.0$ is required. If both GM and CGFLAG are zero, the coordinates of the center of gravity specified on the INPUT3 data (if any) are used.

C3. A line containing the optional specification of water density, gravitational constant, and some geometry parameters is read.

```
READ (...) RHO, G, YMAX, ZMAX,  
           WMAX, NWL  
FORMAT (5F10.2, I5)
```

<u>Item</u>	<u>Description</u>
RHO	Specific mass of the water. This specification of the mass per unit volume must be in consistent units with the rest of the data. If RHO is not specified (here or on INPUT3)

it is taken to be 0.000886... which corresponds to sea water at 59 degrees Fahrenheit, lengths in feet and displacement (force) in long tons.

G

Gravitational acceleration. Units must be consistent with other data. If not specified here, it is read from INPUT3. If not specified, it is taken to be 32.17 which corresponds to length in feet and time in seconds.

YMAX

ZMAX

Specify the maximum desired vertical (YMAX) and horizontal (ZMAX) separation between adjacent offset points for calculation of two-dimensional hydrodynamic coefficients. If both YMAX and ZMAX are positive values, interpolated offset points (straight line) will be added before computing coefficients using the method developed by W. Frank (1967).

WMAX

A "deck" on the interior waterline has been added to the geometry of each station which is surface piercing to avoid "irregular" frequencies. The default is to use only one segment for this, but a positive WMAX will allow multiple segments each with a maximum length of WMAX.

NWL

Specifies the number of interior waterline segments to be used to avoid "irregular" frequencies. The default is to use one segment, and this is

selected if NWL is zero. A negative value (not recommended) will suppress the modification to Frank's procedure which eliminates irregular frequencies.

C4. The encounter frequency for coefficient calculation and an error flag value are read.

```
READ (...) SIGMA0, ERRO
FORMAT (2F10.2)
```

<u>Item</u>	<u>Description</u>
SIGMA0	If a positive value is specified, the coefficients will be computed for that frequency. If SIGMA0=-1.0, the coefficients are computed for zero encounter frequency. If SIGMA0=-2.0, the coefficients are computed for infinite encounter frequency. SIGMA0=-1.0 and SIGMA0=-2.0 are not recommended. If SIGMA0 is not specified, averages of the coefficients for all encounter frequencies resulting from the SPEED and wave specifications on the INPUT3 unit is used. The average is weighted by wave amplitude. (If INPUT3 is suppressed and SIGMA0 is not specified, zero frequency is assumed.)
ERRO	Specifies the minimum absolute value that the determinants of the matrices of influence coefficients may assume when computing coefficients. Messages are issued for smaller absolute valued determinants. The default is ERRO = 1.0E-50.

C5. A flag for CAPSIZ execution is input next. This flag is a single line of data read from unit 6:

```
READ (...)          JOB2
FORMAT (A4)
```

If JOB2 contains "CAPS", the CAPSIZ simulator is executed after COEFFS. If it is blank only the COEFFS routine is executed.

D. Table of offsets for COEFFS and CAPSIZ.

Several lines of data are used to define the hull form for both the COEFFS and CAPSIZ sub-programs. The first line of the table of offsets is the eighth line for COEFFS and the first for CAPSIZ. CAPSIZ reads its data from unit 5 unless COEFFS is executed in the same run. If COEFFS and CAPSIZ are executed in the same run, the input unit for CAPSIZ is specified by LDATA in the COEFFS input. This defaults to unit 1.

COEFFS reads the offsets from the unit specified by INPUT2 (the default is unit 5). Two types of offset formats are available in the COEFFS subprogram. Section D1, below, is common to both types. The ship identification line, D2, determines whether type one or type two offsets are to be processed by COEFFS. Only type one offsets are processed by CAPSIZ, but the offset data written by COEFFS is converted to type one format.

D1. A title begins the offset deck. It consists of 72 columns of text (columns 73 through 80 or 90 may also be used if sequencing is not assigned to these columns).

```
READ(...) (TITLE(I), I=1, 72)
FORMAT (72A1)
```

D2. The ship is identified by the next line.

```
READ (...) (SHIP(I), I=1, 20), SHIPL,
           SHIPB, SHIPT, MSTA
FORMAT (20A1, 3F10.2 I5)
```

If all 20 characters in the identification, SHIP, are blank, type two format is used for the remainder of the offset data. Please see section D5 through D7 for type two format.

The following, through D4, refer to the type one offset format.

If MSTA, the number of stations, is not specified on the above line it is read from an additional line.

```
If (MSTA .EQ. 0) READ(...)MSTA
FORMAT (I5)
```

<u>Item</u>	<u>Description</u>
SHIP	Identification name or number of the ship. Any 20 characters representable by the processor may be used. This must contain at least one nonblank character.
SHIPL	Characteristic length of the ship. This is not used for calculations by either program.
SHIPB	Beam of the ship. This is not used for calculations by either program.
SHIPT	Draft of the ship. This is not used for calculations by either program.
MSTA	Number of stations. This is restricted to: $1 \leq \text{MSTA} \leq 25.$

D3. The offsets for each station follow in a loop that is repeated for the MSTA stations. The stations are numbered by the control variable J from the bow to the stern.

```

DO ... J=1, MSTA
  READ (...) N, NASYM, XOFF(J)
  FORMAT (2I5, F10.2)
  LPTS(J)=N
  READ (...) (XOFF(I,J), ZOFF(I,J), I=1,N)
  FORMAT (2F10.2)
... CONTINUE

```

<u>Item</u>	<u>Description</u>
N	Number of offset points defining the station. The station of the ship is represented by a polygon and the offset points are the vertices. For each station, the offset points are numbered by the control variable I in a counter-clockwise direction when viewed from the stern. This is restricted to $2 \leq N \leq 25$.
NASYM	If $NASYM > 0$, an unsymmetrical station is specified. The offset points are required for both sides of the ship for an unsymmetrical section. The first and last offsets for the unsymmetrical section should be coincident. For the symmetrical sections, only the offsets on the starboard side of the centerplane are specified. $NASYM > 0$ is not allowed for the COEPPS program.
XOFF(J)	Distance of station J aft of the center of the ship coordinates. Note that all other X-coordinates are positive forward of the origin.
ZOFF(I,J)	Height of point I for station J. This

is measured positive upwards from the baseline.

ZOFF(I,J)

Half breadth of Z-coordinate of point I for station J. This is measured positive to starboard of the center-plane.

D4. After all station data are read the profile of the ship is defined.

```
READ (...) NFWD
FORMAT (I5)
IF (NFWD.NE.0)READ(...) (YFWD(I), XFWD(I), I=1, NFWD)
FORMAT (2F10.2)
READ (...) NAFT
FORMAT (I5)
IF (NAFT.NE.0)READ(...) (YAFT(I), XAFT(I), I=1, NAFT)
```

<u>Item</u>	<u>Description</u>
NFWD	Number of forward profile points. This is restricted to $0 \leq \text{NFWD} \leq 25$. These points are numbered by the control variable I in a counterclockwise direction when viewed from the starboard side.
YFWD(I)	Height of point I of the forward profile measured forward of the first station.
XFWD(I)	Distance of point I of the forward profile measured forward of the first station. If NFWD=1, XFWD(1) is defined to be the forward most point of the

submerged hull.

NAFT Number of after profile points. This is restricted to $0 \leq \text{NAFT} \leq 25$. These points are numbered by the control variable I in a clockwise direction when viewed from the starboard side.

YAFT(I) Height of point I of the after profile.

XAFT(I) Distance of point I of the after profile measured aft of the last (MSTA) station. If NAFT=1, XAFT(1) is defined to be the after most point of the submerged hull.

The profile points are assumed to be the intersection of the centerplane and the ship's hull. The profile is assumed to be a polygon defined with vertices at the profile data points. The profile data are used to find the end points for the integration of various hydrostatic and hydrodynamic quantities along the length of the ship.

D5. Please go to section E if type one offsets (D2 through D4) have been used. Section D5 through D7 describe the type two offset format. This is the same format that is used by the Ship Hull Characteristics Program (SHCP) developed by the U.S. Navy and documented in "Ship Hull Characteristics Program - SHCP, Users Manual" (January 1976). This type of offset format may not be submitted directly to the CAPSIZE subprogram. However, the COEFFS routine will automatically convert this format to type one format for CAPSIZ.

Type two offsets are processed by COEFFS if the ship identification name, SHIP, is blank in the section D2 data. This corresponds to a blank "work list" for SHCP (SHCP card type B). The description below begins with the same input as was described

in D2, above.

```
READ (...) (SHIP(I), I=1,20), SHIPL  
      SHIPB, SHIPT, MSTA  
FORMAT (20A1, 3F10.2, I5)
```

<u>Item</u>	<u>Description</u>
SHIP	All 20 characters must be blank. This cooresponds to a blank card type "B" for SHCP.
SHIPL	Ignored.
SHIPB	Ignored.
SHIPT	Ignored.
MSTA	Ignored.

If all 20 characters in SHIP are blank, the following type two offsets are read, and the SHIP identification for output is taken from columns 5 through 36 of the title line (D1).

D6. SHCP card type "C".

The SHCP work list, D5 (or ship identification line) is followed by SHCP card type "C".

```
READ (...) SPACE, ZSCAL, YSCAL, SHIPL,  
      NAPN, KINDO  
FORMAT (4F10.3, 13X, I2, I5)
```

<u>Item</u>	<u>Description</u>
SPACE	The station spacing is input as SPACE. This is actually a multiplier of the X-values that are input. If SPACE is read as zero, it is redefined by the program as one.

ZSCAL The vertical offset coordinates are multiplied by 0.005/ZSCAL as they are read into the program. If ZSCAL is input as zero it is changed to 0.005 by the program.

YSCAL The horizontal offset coordinates are multiplied by 0.005/YSCAL as they are read. If YSCAL is read as zero, it is changed to the ZSCAL value by the program.

SHIPL Characteristic length of the ship. This is not used by either COEFFS or CAPSIZ.

NAPN The number of appendages must be zero.

KINDO The kind of SHCP offsets must be either zero or two.

Please note that the scale factors and origin translation specified by the C1 input items XSCALE, YSCALE, ZSCALE, XORIG, YORIG are applied after the SPACE, ZSCAL and YSCAL multipliers are applied.

D.7 SHCP card type "D".

The offset coordinates are specified on a series of SHCP card type D inputs.

```

READ (...) STATN, Y1, Z1, JTEST
FORMAT (F6.3, 2F7.0, I6)
IF (JTEST is not 99999) repeat the READ

```

<u>Item</u>	<u>Description</u>
STATN	The real distance from the station to the origin is the product of STATN and SPACE. The STATN values must be the same for all offsets on the same

AD-A100 306

CALIFORNIA UNIV BERKELEY DEPT OF NAVAL ARCHITECTURE F/G 20/4
MODEL TESTS AND NUMERICAL SIMULATION OF SHIP CAPSIZING IN FOLLO--ETC(U)
JAN 80 W J FALLON, Y HWANG, J L LIGUORI DOT-CG-64601-A
USCG-D-08-81 NL

UNCLASSIFIED

3-3

1-1

1-1

END

DATE

FILMED

7 81

DTIC

station. STATN values should be in a non-decreasing order.

Y1 The half breadth of the offset point is the product of Y1 and YSCAL. The offsets for each station should be ordered from the bottom toward the uppermost parts of the station.

Z1 The height of the offset point is the product of Z1 and ZSCAL.

JTEST The "breakpoint" indicator 77777 is ignored. The last offset on each station is signified by JTEST = 88888. The last offset on the last station is signified by JTEST = 99999. JTEST values other than zero (or blank) 77777, 88888 or 99999 are illegal.

The offsets for each station must be grouped together. The maximum number of offsets on a station is 25. The maximum number of STATIONS is 25. Each section is assumed to be a polygon with straight line segments between the offset points. After all offsets are read, the scale factors and origin translation (Section C1) are applied, and the signs of the station coordinates are reversed to form X-coordinate values.

E. Table of wind profile offsets for COEFFS (ignored by CAPSIZ).

Several lines of data are used to define the profile of the ship which is used to compute the forces and moments on the ship resulting from beam winds. The first line of data in this section indicates the number of wind profile data points. This group of data follows the last after profile offset line for the first type of offset data, or it follows the last offset line (SHCP card type

D with end sentinel equal to 99999) for the second type of offset data. These data lines are used by COEFFS and they are skipped by CAPSIZE. This input is read by COEFFS from the input unit specified by INPUT3.

```
READ (...) NPROF
FORMAT (I5)
IF (NPROF.GT.0)
    READ(...) (YPROF(I), XPROF(I), I=1, NPROF)
FORMAT (2F10.2)
```

<u>Item</u>	<u>Description</u>
NPROF	Number of profile points for wind force. If NPROF is negative, the wind forces and moment coefficients are not changed by the program. If NPROF is zero, or if it is positive, the heeling moment coefficient is computed and the coefficients of sway force and yaw moment are set to zero. If it is zero, the profile is defined by the highest point on each station. (The forward and after profile data for type one offsets are used only to define the intersection of the waterline and the ends of the polygon). If NPROF is one, the profile calculated as a rectangle above the baseline with height, YPROF(1), and length from the forward end of the waterline to the after line. If NPROF is greater than one the projected area for wind forces is taken as a polygon consisting of the waterline and segments joining these profile coordinates, taken in order from the forward end to the after end of the waterline. The maximum

value for NPROF is 25.

YPROF(I) Height of point I above the baseline.

XPROF(I) Distance of profile point aft of the center of ship coordinates. Note that this is measured in the same direction as the station spacing, XOFF(J), but that it has the opposite sign of other X-coordinate values.

F. Additional data required by the CAPSIZE simulator (optional for COEFFS).

The table of offsets is followed by additional data for the CAPSIZE simulator. It is optional input for COEFFS where it is specified by INPUT3. If COEFFS is not executed it is read from unit 5 by CAPSIZ.

F1. The water density and gravitational constant are read.

```
READ (...) RHO, G
FORMAT (2F10.2)
```

<u>Item</u>	<u>Description</u>
RHO	Specific mass of the water. This specification of the mass per unit volume must be in units which are consistent with the rest of the data. The value is required by CAPSIZ, but it is optional for COEFFS.
G	Gravitational acceleration. Units must be consistent with other data. The value is required by CAPSIZ, but it is optional for COEFFS.

If the values for RHO and G are not specified here when

COEFFS is executed, values are inserted by COEFFS as described in section C3.

F2. The coordinates of the center of gravity are next.

```
READ (...) XCG, YCG, ZCG
FORMAT (3F10.2)
```

<u>Item</u>	<u>Description</u>
XCG	Longitudinal position of the center of gravity. This is measured positive forward of the origin of coordinates. This value is required by CAPSIZ , but it is optional for COEFFS. COEFFS will set this value for CAPSIZ based on the "C2" input.
YCG	Vertical center of gravity. This is measured positive upwards from the baseline or origin of coordinates. This value is required by CAPSIZ , but is optional for COEFFS. COEFFS will set this value for CAPSIZ based on the "C2" input.
ZCG	Distance of center of gravity to starboard of centerplane. This value must be zero for COEFFS.

F3. The displacement of the ship and added mass factors for surge, heave and sway follow the center of gravity data.

```
READ (...) DISPL, AMX, AMY, AMZ
FORMAT (4F10.2)
```

<u>Item</u>	<u>Description</u>
DISPL	Displacement of the ship (weight units). This value is required by CAPSIZ , and

it may be computed by COEFFS.

AMX Added mass factor for surge. This is the surge added mass, divided by the actual mass of the ship.

AMY Added madd factor for heave. This is the heave added mass, divided by the actual mass of the ship. This should normally be zero since the CAPSIZE simulator computes the heave added mass from the two-dimensional coefficients.

AMZ Sway added mass factor. This is similar to AMY.

F4. The radii of gyration (in air) follow the displacement and optional added mass data.

```
READ (111) (RADII(I),I=1,6)
FORMAT (6F10.2)
```

<u>Item</u>	<u>Description</u>
RADII(1)	Radius of gyration for roll, ρ_{xx} .
RADII(2)	Radius of gyration for yaw, ρ_{yy} .
RADII(3)	Radius of gyration for pitch, ρ_{zz} .
RADII(4)	Radius of gyration, ρ_{xy} . The products of inertia are computed as, $I_{xy} = I_{yx} = \rho_{xy} \cdot \rho_{xy} \cdot m$ where m is the mass of the ship.
RADII(5)	Radius of gyration, ρ_{xz} .
RADII(6)	Radius of gyration, ρ_{yz} .

F5. The desired or average ship speed and an optional table of resistance data follow the radii of gyration data.

```
READ (...) SPEED, NSPEED
FORMAT (F10.2, I5)
IF (NSPEED.NE.0) READ (...) (RSPEED(I),
    RESIST(I) , I=1, NSPEED)
FORMAT (2F10.2)
```

<u>Item</u>	<u>Description</u>
SPEED	Intended speed of the ship. Units are length per unit of time.
NSPEED	Number of data points defining the resistance curve. The resistance curve is assumed to be linear between data points. The resistance table is limited to $0 \leq \text{NSPEED} \leq 20$.
RSPEED(I)	Speed for resistance data point I.
RESIST(I)	Resistance value for data point I.

F6 The rudder and steering system data comprise three lines following the speed and optional resistance table. All angles are measured in degrees.

```
READ (...) RX,RY(1),RY(2),RAREA
FORMAT (4F10.2)
READ (...) RSTOP,RLIFT,RDRAG,RWAKE
FORMAT (4F10.2)
READ (...) RGAIN(1),RGAIN(2),RGAIN(3),
    RDEAD(1),RDEAD(2),RRATE
FORMAT (6F10.2)
```

<u>Item</u>	<u>Description</u>
RX	Longitudinal coordinate of center of rudder force.

RY(1) Height of the bottom of the rudder.
 RY(2) Height of the top of the rudder.
 RAREA Area of rudder.
 RSTOP Angle of rudder stops in degrees.
 RLIFT Derivative of rudder lift coefficient.
 The lift force, L , is given by

$$L = RLIFT * FACTOR * ANGLE$$
 and

$$FACTOR = 0.5 * RHO * AREA * U ** 2.$$
 where
 ANGLE is the angle of attack of the rudder in degrees and U is the average water speed over the rudder.

RDRAG Derivative of the rudder drag coefficient.
 The drag force, D , is given by

$$D = RDRAG * FACTOR * ANGLE.$$

RWAKE Velocity relative to rudder of ships wake in way of the rudder. This is positive when the rudder is in the propeller race, otherwise negative.

RGAIN(1) Autopilot yaw rate gain. Positive for a stable steering system.

RGAIN(2) Autopilot yaw angle (proportional) gain. Positive for a stable steering system.

RGAIN(3) Autopilot yaw integral gain.

RDEAD(1) Autopilot dead band. If the absolute yaw error is less than RDEAD(1), no rudder angle is ordered.

RDEAD (2) Autopilot dead band. This angle is subtracted from the rudder angle computed from the yaw rate, angle, and integral and the corresponding gain factors.

RRATE Mechanical rudder rate in degrees per unit time.

F7. The table of two-dimensional added mass and damping coefficients follows the rudder and autopilot data. The following READ statement is repeated until I is read as zero.

```
READ (...) J,I,C1,C2,C3,C4
FORMAT (2I5, 4F10.2)
IF (I.EQ.0) exit coefficient loop
IF (I.EQ.1) process added mass
IF (I.EQ.2) process damping coefficients
repeat READ operation.
```

<u>Item</u>	<u>Description</u>
J	Station index number.
I	Flag value: I=0 - - end of coefficients I=1 - - added mass coefficients I=2 - - damping coefficients.
C1	Coefficient (added mass or damping) for heave at station J.
C2	Coefficient for sway at station J.
C3	Coefficient for roll at station J.
C4	Coefficient for coupling between roll and sway at station J.

The two-dimensional coefficients may be in any order, and the coefficient input is terminated by a zero value for I. Any coefficients not entered are set to zero by the program. Each coefficient is the dimensional added mass or damping coefficient per unit length of the ship, and each coefficient is divided by the area of the station for which it is calculated.

F8. Three dimensional linear and quadratic damping constants follow the table of two-dimensional coefficients. This damping is in addition to that given by the two-dimensional coefficients.

```

READ (...) (DAMPL(I), I=1,6)
FORMAT (6F10.2)
READ (...) (DAMPQ(I), I=1,6)
FORMAT (6F10.2)

```

<u>Item</u>	<u>Description</u>
DAMPL(1)	Linear surge damping.
DAMPL(2)	Linear heave damping.
DAMPL(3)	Linear sway damping.
DAMPL(4)	Linear roll damping.
DAMPL(5)	Linear yaw damping.
DAMPL(6)	Linear pitch damping.
DAMPQ(1)	Quadratic surge damping.
DAMPQ(2)	Quadratic heave damping.
DAMPQ(3)	Quadratic sway damping.
DAMPQ(4)	Quadratic roll damping.
DAMPQ(5)	Quadratic yaw damping.

DAMPO(6)

Quadratic pitch damping.

F9. The wave (COSINE) description follows the damping data.

```
READ (...) N WAVES
FORMAT (I5)
IF (N WAVES.NE.0) READ (...) (WVAMP (K),
    WVFRE (K), WVDIR (K), WVPHA (K),
    K=1, N WAVES)
FORMAT (4F10.2)
```

<u>Item</u>	<u>Description</u>
N WAVES	Number of sinusoidal waves. This is restricted to $0 \leq \text{N WAVES} \leq 20$.
WVAMP (K)	Amplitude of wave component K.
WVFRE (K)	Circular frequency of wave component K.
WVDIR (K)	Direction of wave K in degrees. Zero degrees is following.
WVPHA (K)	Phase angle in degrees at time equal zero of wave component K.

F10. The wind speed, direction, density, and coefficients of sway force, roll moment and yaw moment are read from one line. These items are ignored by COEFFS input. They are written by COEFFS for input to CAPSIZ.

```
READ (...) WSPEED, WDIR, WRHO, WSWAY,
    WROLL, WYAW
FORMAT (6F10.2)
```

<u>Item</u>	<u>Description</u>
WSPEED	The wind speed measured in length units per unit of time. The wind force and

moment coefficients are multiplied by the square of WSPEED.

- WDIR The direction from which the wind is blowing. This is measured clockwise in degrees from the positive x-direction. Zero degrees is a head wind. Ninety is wind from the starboard beam.
- WCOEFF Effective wind drag coefficient for beam wind. See description on next page.
- WSWAY Coefficient of wind induced sway force.
- WROLL Coefficient of wind induced roll moments.
- WYAW Coefficient of wind induced yaw moments.

The wind sway force, roll and yaw moments are computed as:

$$ZF = \sin(\phi + WDIR) * WSWAY * WCOEFF * WSPEED ** 2$$

$$XM = \sin(\phi + WDIR) * WROLL * WCOEFF * WSPEED ** 2$$

$$YM = \sin(\phi + WDIR) * WYAW * WCOEFF * WSPEED ** 2$$

where:

ϕ is the yaw angle.

COEFFS computes the roll moment coefficient as the vertical moment of an area projected to the wind. Typical values of WCOEFF are given in the table below.

<u>WCOEFF</u>	<u>LENGTH UNIT</u>	<u>FORCE UNIT</u>	<u>WIND SPEED UNIT</u>
0.0035	feet	pounds	knots
0.00123	feet	pounds	feet/second
1.56E-6	feet	tons	knots
5.48E-7	feet	tons	feet/second

F11. The initial condition of the simulation follows the wave data.

```
READ (...) (POSIT(I),I=1,6)
FORMAT (6F10.2)
READ (...) (VELOC(I),I=1,6)
FORMAT (6F10.2)
```

<u>Item</u>	<u>Description</u>
POSIT(1)	Initial X-coordinate of mass center.
POSIT(2)	Initial Y-coordinate of mass center.
POSIT(3)	Initial Z-coordinate of mass center.
POSIT(4)	Initial roll angle in degrees.
POSIT(5)	Initial yaw angle in degrees.
POSIT(6)	Initial pitch angle in degrees.
VELOC(1)	Initial speed.
VELOC(2)	Initial heave velocity.
VELOC(3)	Initial sway velocity.
VELOC(4)	Initial roll rate.
VELOC(5)	Initial yaw rate.
VELOC(6)	Initial pitch rate.

The position values are specified with respect to the wave coordinate system fixed on the earth. The velocities are with respect to the ship coordinate system.

F12. The initial condition is folled by the specifications for integration timing.

READ (...) TO,TSTART,TSTOP,
TOUTPT,TSTEP,ERR
FORMAT (6F10.2)

<u>Item</u>	<u>Description</u>
T0	Initial time for the integration. This is the time of the initial conditions.
TSTART	Time at which the actual simulation is to start. All forces are multiplied by a ramp function that increases linearly in time from a value of zero at T0 to one at TSTART. This ramp is used to avoid transients caused by arbitrary initial conditions.
TSTOP	Time at which the simulation is to end if there is no capsizing. A roll angle exceeding two radians in absolute magnitude is considered a capsizing and halts the simulation.
TOUTPT	Interval at which the ship position and velocity are to be output.
TSTEP	Integration time step.
ERR	This value is not used.

Appendix E-II

CAPSIZE Program Description

CAPSIZE PROGRAM DESCRIPTION

CAPSIZE main program.

The main program is divided into a number of program units, both subroutines and function subprograms. The program is divided into two main parts. One part is provided as an aide to the preparation of the data necessary to simulate ship motions. This part is called the COEFFS subprogram. The other part of the program actually simulates the ship motions. This is called the CAPSIZ subprogram. These two subprograms may be executed in separate computer runs or they may be executed in the same run. For the convenience of the user, these two subprograms are combined into a single Fortran program.

Block diagrams showing the principal segments and logical flow of the program are given in Figures E1, E2 and E3. Figure E1 contains the first parts of the program, CAPSIZE. Figure E2 contains the hydrodynamic coefficient computation COEFS, and Figure E3 contains the simulator program CAPSIZ.

The Program code, itself, has been extensively documented internally with comments which serve two principal functions.

- (1) They define the most important variables which appear in either input/output lists or in COMMON blocks.
- (2) The function performed by a subroutine or a segment of a subroutine is described.

In the following sections are given brief descriptions of individual subroutines, and these descriptions, when read in conjunction with the block diagrams Figs E2 and E3, a program listing, and the theory presented in the first part of this report, should enable a person who is reasonably proficient in FORTRAN to follow the program logic.

The main program serves to read a line of input, and then to call either the COEFFS subprogram or the CAPSIZ subprogram. As an option, both subprograms may be executed in the same run. At the beginning of the execution, the program reads a line of data. If the first four characters of the input are "CAPS", only the CAPSIZ subroutine is called to execute the CAPSIZ subprogram.

If these letters are "COEF", the COEFFS subroutine and subprogram is called. Any other characters stop the program.

When COEFFS is executed, a variable, JOB2 in COMMON/JOB/ is returned to the main program. If this variable contains the characters "CAPS", the CAPSIZ subprogram is executed after the COEFFS routine has finished. The contents of JOB2 depend on the user's input to the COEFFS subprogram. The user must include the "CAPS" directive in the input, but the COEFFS routine may cancel this if it detects any errors.

Subroutine COEFFS.

The COEFFS subroutine is the main routine in the COEFFS subprogram. Its purpose is to call the various subroutines used to prepare input for the CAPSIZ simulation subprogram. The subroutines are called in the order listed below.

CONTRL is called to input several lines of data which control the execution of the various options available in the subprogram. In addition to setting variables which control the COEFFS routines, the JOB2 variable in COMMON/JOB/ is set by CONTRL to indicate to the main program whether or not the CAPSIZ simulation subprogram is to be executed in this run.

OFFSETS is called to input the table of offsets which defines the shape of the ship. The dimensions of the ship may be scaled and the origin of ship coordinates may be relocated. This routine also inputs the wind profile data.

INPUT is called to read the remainder of the data and to skip the old two-dimensional added mass and damping coefficients.

DRAFT sets the ship at the specified draft and trim. An internal table of offsets for the hull below the waterline is generated. The displacement and location of the ship's mass center may be determined by this routine. An optional listing of the tables of offsets is available.

WINDF computes coefficients of wind heeling moments.

HSTRIP computes the two-dimensional added mass, damping and hydrodynamic motion coupling coefficients for the ship.

OUTPUT writes a file which may be all or part of the input data for the CAPSIZ simulation subprogram. This routine also generates an optional listing of this file.

In addition to calling these subroutines, the COMMON blocks which contain data which must be communicated between these routines is referenced by this subroutine. This is required by standard Fortran to allow execution on an overlaid or segmented system.

Subroutine CONTRL.

The CONTRL subroutine is called by COEFFS to read six lines of data which control the optional calculations and output listings of the COEFFS subprogram. A flag controlling the optional execution of the CAPSIZ subprogram is also set.

The first line read by CONTRL is from the logical unit specified by INPUT1 in the /IOFILE/ common block. This is initialized as unit 5 by the BLOCK DATA subprogram. This line defines fourteen variables in the /IOFILE/ common block. The first twelve variables control optional input and output from the subprogram, and the last two control the positioning of the output data file at the beginning and end of the execution of the program. To allow for values to be defined by the program as well as changed by the user, the following logic is defined. If an input value is zero (or blank), the default value, defined by the program, is set in the corresponding /IOFILE/ variable set to zero. If an input value is positive, the value is set in the /IOFILE/ variable. A negative value of the variable causes the corresponding input or output to be suppressed by the remainder of the program. A positive value is assumed to be the logical unit number for input or output.

Subroutine HSTRIP.

This subroutine utilizes the Frank Close Fit procedure, Ref [4], and much of the code has been adopted directly, with some modifications, from the NSRDC two-dimensional program. HSTRIP calls a series of auxiliary subroutines which initialize data arrays or perform specialized parts of the computation, as follows.

- * STATN revises the station offsets by inserting additional points in order to optimize the hydrodynamic computations and to suppress anomolous behavior which sometimes occurs at certain "singular frequencies". INSERT is called by STATN as part of this process.
- * GIRL computes certain frequency-independent coefficients which are used in the two-dimensional hydrodynamic computations.
- * BEER computes the two-dimensional hydrodynamic coefficients for the special cases of zero or infinite frequency. It calls the simultaneous linear equation solver LINEQT.
- * WINE performs the computation of the two-dimensional hydrodynamic coefficients for finite nonzero frequencies. It calls several subroutines for special operations. WOMEN computes some of the interaction between segments of the section. SONG performs the integration of pressures around the section. ROMEO evaluates the exponential integral with complex argument. JULIET is a simultaneous linear equation solver for certain sets of equations in HSTRIP.

Subroutine CAPSIZ.

The CAPSIZ subroutine is the main routine in the simulation subprogram. This program unit calls the three major subroutines required to execute the time domain motion simulation. These subroutines are called in the order listed below.

READ is called to input all of the data required for the simulation. The input file may be created by the COEFFS subprogram in the same execution of the CAPSIZE program. It is also possible to use a previously generated file written in the same format. If READ discovers any errors such as too many data points, it will stop the execution of the program. It calls THRUST to initialize the surge force.

PRFC is called to convert input values to internal values and to initialize various variables and arrays for the motion simulation. Typical of the conversions are the angular measurements

which are input in degrees, but which must be converted to radians for calculation purposes.

RUN is called to execute the simulation by means of the time domain integration of the equations of motion. Execution is terminated if a capsizes occurs. If the simulated time reaches a user specified stopping point, control returns to the CAPSIZE main program where execution is terminated.

In addition to calling these subroutines, this program unit references all common blocks which contain information which must be communicated between READ, PREP and RUN. This allows the Fortran program to be executed on a computer system which uses segmentation or overlaying of subroutines in memory.

Subroutine READ.

The READ subroutine performs all input for the CAPSIZ subprogram. This input is described in appendix E-1.

After the main program reads the "CAPSIZE" command line, the CAPSIZ subprogram is entered at subroutine CAPSIZ. CAPSIZ then calls READ to input all data lines beginning with the title line. As each line or card is read, it is listed on the output file with the line count and a short description of the assumed contents of the line.

As the input proceeds, errors such as the specification of too few or too many data points are checked, and appropriate messages listed. After all input is complete, the control returns to the calling routine if no errors are detected. If any input errors are detected, the program will stop.

The input lines are read in the following order:

Title line

Table of offsets and profile data

Water density and gravitation of acceleration

Center of gravity coordinates

Displacement

Radii of gyration

Ship speed and optional resistance data

Rudder geometry and autopilot parameters

Sectional added mass and damping coefficients

Linear and quadratic damping constants
Wave components
Wind force
Initial conditions
Numerical integration parameters.

Input format conversion used F10.2 for all real values and I5 for all integers. Only the first seventy columns or less are used for numerical inputs. Columns 73 through 90 of each line are listed for comments or sequence information.

Subroutine PREP.

The PREP subroutine is called to prepare data for the capsizing simulation. It is called to convert external values input by READ to internal values required by the RUN subroutine. The various conversions are collected into this routine in order not to complicate the READ subroutine and in order to avoid repeated conversion during the simulation.

The major conversions are described here:

1. The center of offset coordinates is moved to coincide with the center of gravity, and the x-coordinates of stations are established by reversing the signs of the input values.
2. The forward and after profile data are consolidated into a single array.
3. Rudder coordinates are referred to the center of gravity, and rudder angles and rates are converted from degrees to radians. The algebraic signs of the autopilot gain parameters are reversed.
4. If a table of speed versus resistance data are used, the slopes of the segments are computed for use when interpolations are required during the simulation. The resistance force of the ship at the intended speed is added algebraically to the resistance values so that there will be no additional thrust or resistance on the ship when it is at the intended speed. The program will stop if the resistance values are not in increasing

order of speed.

5. Moments and products of inertia are computed from the specified radii of gyration.
6. Wave numbers of the component waves are computed. The maximum wave elevation is computed as the sum of the absolute values of wave component amplitudes.
7. Wind direction and initial condition directions are converted from degrees to radians.
8. The initial velocity condition is converted from ship coordinate directions to fixed coordinate directions.

Subroutine RUN.

The RUN subroutine is called to execute the motion simulation. The time domain simulation is accomplished by a numerical integration of the equations of motion. The equations of motion are a system of twelve first order ordinary differential equations. If the autopilot model requires a rudder control which is proportional to the integral of the course error (yaw angle), the number of equations is increased to thirteen to include yaw angle integration.

The simulation is carried out by executing a loop consisting of:

- a. Call SAMPLE to output the position and velocity.
- b. Call TEST to stop execution if a capsize has occurred.
- c. Increment the dependent variable limit to the next output time.
- d. Call RK4 to numerically integrate the 12 or 13 differential equations. The integration runs through one or more time stops until output time value is reached. Then control returns to RUN.
- e. If the TIME variable is less than TSTOP, the user specified limit, this loop repeats from "a" above.
- f. If TIME has reached or exceeded TSTOP, SAMPLE is called to output the final position, and FINAL is called to output statistics concerning the behavior of the numerical integration. The control is returned to the calling routine.

Subroutine FINAL.

The FINAL subroutine is the last routine called in the motion simulation. This is called to output the statistics concerned with the behavior of the numerical integration of the equations of motion. It was originally intended to study the automatic step size control used by some numerical integration routines. FINAL is called by TEST if a capsizes is detected, or it is called by RUN if no capsizes is detected at the end of the simulation time.

Subroutine TEST.

The TEST subroutine is called periodically by RUN to test for a capsizes. The test is very simple in the present version of the program. If the absolute value of the roll angle is less than 2.0 radians, TEST returns control to the calling routine. If the absolute roll angle is greater than or equal to this value, the message "CAPSIZE" is output and the program is stopped after a call to FINAL. FINAL prints the statistics concerning the numerical integration. A more detailed capsizes test may be substituted if necessary, but the present test seems to work well for most vessels.

Subroutine RK4.

The RK4 subroutine is called to numerically integrate the equations of motion. A fourth order Runge-Kutta method is used. The derivative of the dependent variable vector are evaluated four times for each time step. The RHS subroutine is called to compute the derivative values by evaluating the right hand sides of the equations of motion. The RK4 routine is called to integrate over each time interval between output operations.

The formal parameters of the RK4 subroutine are listed below.

TIME is the independent variable. It is set to the initial value before the subroutine is called. The value is increased by RK4 as the integration proceeds.

Y is the dependent variable array. This subroutine will handle up to 13 equations or elements of Y. Before RK4 is called, the variables in Y must be set to their initial values. As the integration proceeds, the Y values are updated by RK4.

TNEXT is the limit of integration for the present call to RK4. When the independent variable, TIME, reaches this value, execution returns to the calling routine. This allows the output procedures to be executed. The integration may be continued by increasing TNEXT and calling RK4 again.

NEQS is the number of equations. The maximum is 13. The CAPSIZE program uses either 12 or 13 for NEQS. Thirteen equations are used when the autopilot model includes yaw error integral control.

STEP is the time step. The independent variable, TIME, is incremented by STEP for each integration.

The parameters, ERR and RR4S are not used by RK4.

Three arrays are used internally by RK4. YY is a temporary dependent variable array. YA and YB are used for the derivatives of the dependent variables.

Subroutine RHS.

The RHS subroutine is called by the numerical integration routine each time the right hand side of the equations of motion (15, 16, 17 and 18) are required. This subroutine is called with the value of the independent variable, time, and with values in the dependent variable vector supplied by the calling routine. The derivatives with respect to time of the dependent variables are returned as a vector. This subroutine is called with three parameters, TT, YY, and YYDOT. Time is set by the calling routine in TT. The estimated values of the dependent variables are set by the calling routine in the various elements of the YY vector. Before RHS executes its RETURN statement, the time derivatives of YY are set in the corresponding elements of the YYDOT vector.

Upon entry to the RHS routine certain statistics concerning the program's execution are recorded in the /STATS/ common block. Then the actual computations to evaluate YYDOT begin. The forces acting on the ship at time TT with dependent variables prescribed in YY are evaluated with a call to the FORCE2 subroutine. Then the derivatives of the dependent variables are evaluated as the right hand sides of the equations:

$$\frac{d}{dt} \underline{\tilde{x}} = \underline{\tilde{v}}$$

$$\frac{d}{dt} \underline{\alpha} = \underline{\tilde{B}}^{-1} \underline{\omega}$$

$$\frac{d}{dt} \underline{\tilde{v}} = \frac{1}{m} \underline{\tilde{f}}$$

$$\frac{d}{dt} \underline{\omega} = \underline{\tilde{I}}^{-1} [\underline{g} - \underline{\omega} \times \underline{\tilde{I}} \underline{\omega}]$$

The system of linear equations represented by the last two equations above are evaluated by the LNEOF routine using Gaussian elimination.

Subroutine FORCE2.

The FORCE2 routine is called to evaluate the forces and moments acting on the ship at a specific time with the position and velocity specified by the calling routine. The routine is called with two parameters, TT and YY. Time is specified by TT and the position and velocity vectors are specified by the YY vector. The computed forces and some other data are returned as values in labeled common blocks.

This subroutine first calls the ROTATE subroutine to set values in the matrices used to transform rotational coordinates and to resolve the specified velocity into ship coordinates. Next the six components of the FORCE vector are initialized to zeroes. Calls to other subroutines then add force components to this vector. The forces are evaluated in the ship coordinate system.

The forces involving any unbalance between the instantaneous buoyancy and the ships weight and other force terms requiring integrals over the submerged portion of the hull are computed by the FROUDE subroutine. The propulsion system is modeled by the THRUST subroutine. The autopilot and steering system are modeled by the STEER subroutine.

Simple force components are computed within the FORCE2 program unit. These include the wind generated sway force, roll and yaw moments. The ramp-function multiplier used for simulations beginning with some possibly incorrect initial conditions is applied to the forces by this subroutine.

Subroutine ROTATE.

The ROTATE routine is called to resolve the linear velocity into the ship coordinate system. It is called with one parameter, YY. This is a vector. The directional orientation of the ship coordinates is specified by YY(4), YY(5) and YY(6) which are the Eulerian angles θ , ϕ and ψ . The linear velocity components are YY(7), YY(8) and YY(9) in the \bar{x} , \bar{y} and \bar{z} directions of the fixed coordinate system.

The values in the labeled common blocks, /C/, /CT/, /TRIG/ and /V/ are set by this subroutine. The linear velocity in the ship coordinate directions is set in the /V/ common block as the variables VX, VY, and VZ. Matrices used for rotational transformations are assigned to the /C/ and /CT/ blocks. Sines and cosines of the Eulerian angles are stored in the /TRIG/ block.

Subroutine FROUDE.

- A. Computes force components involving integrals over the submerged volume of the ship.
1. Froude-Krylov forces and moments.
 2. Forces and moments resulting from relative (2-D) velocity.
 3. Forces and moments resulting from acceleration components of wave motion.
 4. Added mass and inertia matrix (since ship acceleration is unknown until all forces are computed).
 5. Forces and moments resulting from rotating coordinates.
 6. Forces and moments resulting from relative (3-D) v^2 .
- B. Procedure:
1. Initialize variables and arrays.
 - a. Zero integration accumulators
 - b. Project wave numbers into calculation coordinate system. (Yawed and Pitch but not rolled). Compute x-coordinates of reference wave crests.
 2. Generate table of "wet" offset points and summed wave elevations above each point. Find intersections with water surface. Find ends of wet portion of hull (uses profile data if available).

3. Resolve ship velocity vector into yawed and pitched coordinates.
4. If ship is out of water go to 6.
5. Loop over all stations between first and last.
 - a. Call KRYLOV to compute sine and cosine components of two-dimensional integrals over each wet station.
 - b. Integrate over length between stations assuming 2-D functions are linear between stations or product of linear function and sinusoid between stations.
6. Finalize results of integrations
 - a. Combine force components
 - (1) Wave depth pressure attenuation
 - (2) Buoyancy minus weight
 - (3) Coordinate acceleration
 - b. Set up A matrix of mass, added mass.
 - c. Resolve forces and moments into ship coordinate system (yawed and pitched and rolled).
7. RETURN

Subroutine KRYLOV.

The KRYLOV routine is called by FROUDE to compute two-dimensional integrals over each submerged station of the ship. The integrations assume that the station is represented by a polygon with vertices located at the submerged offset points and any intersections with the wave surface.

The subroutine is called with the formal parameters, J, which is the index of the station for which the integrals are being performed. Loops for wave components use K for the control variable. The offset point is indicated with I as the subscript and control variable for the loop over the offset points.

The input arrays in block common are described in the description of the FROUDE subroutine.

The following integrals are evaluated by the KRYLOV routine for the station represented by J.

$$\begin{aligned}
\text{AREA} &= \iint dy dz \\
\text{ZMOM} &= \iint z dy dz \\
\text{YMOM} &= \iint y dy dz \\
\text{ZC0}(k) &= \iint \cos(K_y y + K_z z) e^{k_i \tilde{c}_{22} y} dy dz \\
\text{ZS0}(k) &= \iint \sin(K_y y + K_z z) e^{k_i \tilde{c}_{22} y} dy dz \\
\text{ZCY}(k) &= \iint y \cos(K_y y + K_z z) e^{k_i \tilde{c}_{22} y} dy dz \\
\text{ZSY}(k) &= \iint y \sin(K_y y + K_z z) e^{k_i \tilde{c}_{22} y} dy dz \\
\text{ZCZ}(k) &= \iint z \cos(K_y y + K_z z) e^{k_i \tilde{c}_{22} y} dy dz \\
\text{ZSZ}(k) &= \iint z \sin(K_y y + K_z z) e^{k_i \tilde{c}_{22} y} dy dz.
\end{aligned}$$

For convenience, the following integrals are evaluated for each wave component and offset point. The integrals are from the offset point to the wave surface intersection above the point in the plane of the station.

$$\begin{aligned}
\text{YC0} &= \int \cos(K_y y) e^{k_i \tilde{c}_{22} y} dy \\
\text{YS0} &= \int \sin(K_y y) e^{k_i \tilde{c}_{22} y} dy \\
\text{YCY} &= \int y \cos(K_y y) e^{k_i \tilde{c}_{22} y} dy \\
\text{YSY} &= \int y \sin(K_y y) e^{k_i \tilde{c}_{22} y} dy.
\end{aligned}$$

The two dimensional integrals are evaluated in the following form within the KRYLOV routine.

$$\begin{aligned}
\text{ZC0}(k) &= \int \text{YC0} \cdot \cos(K_z z) dz - \int \text{YS0} \cdot \sin(K_z z) dz \\
\text{ZS0}(k) &= \int \text{YS0} \cdot \cos(K_z z) dz + \int \text{YC0} \cdot \sin(K_z z) dz \\
\text{ZSY}(k) &= \int \text{YCY} \cdot \cos(K_z z) dz - \int \text{YSY} \cdot \sin(K_z z) dz \\
\text{YCZ}(k) &= \int \text{YSY} \cdot \cos(K_z z) dz + \int \text{YCY} \cdot \sin(K_z z) dz \\
\text{ZSZ}(k) &= \int \text{YS0} \cdot z \cos(K_z z) dz + \int \text{YC0} \cdot z \sin(K_z z) dz.
\end{aligned}$$

Function ETAF.

The coordinate of the water surface in the yawed and pitched coordinates is returned by this function. The \tilde{y} coordinate of the surface is $\tilde{\eta}$. For the superposition of N wave components the following holds

$$\tilde{c}_{12}\tilde{x} + \tilde{c}_{22}\tilde{\eta} + y_G = \sum_{i=1}^n A_i \cos[...]$$

where

$$[...] = [(x_G + \tilde{c}_{11}\tilde{x} + \tilde{c}_{21}\tilde{\eta} + \tilde{c}_{31}\tilde{z})k_i \cos\delta_i - (z_G + \tilde{c}_{13}\tilde{x} + \tilde{c}_{23}\tilde{\eta} + \tilde{c}_{33}\tilde{z})k_i \sin\delta_i + \phi_i - \sigma_i t] .$$

Let

$$a = \tilde{c}_{21}\tilde{\eta} k_i \cos \delta_i - \tilde{c}_{23}\tilde{\eta} k_i \sin \delta_i$$

$$b = (x_G + \tilde{c}_{11}\tilde{x} + \tilde{c}_{31}\tilde{z})k_i \cos \delta_i - z_G + \tilde{c}_{13}\tilde{x} + \tilde{c}_{33}\tilde{z})k_i \sin \delta_i + \phi_i - \sigma_i t .$$

then

$$[...] = a + b$$

and

$$\tilde{c}_{22}\tilde{\eta} = -\tilde{c}_{12}\tilde{x} - y_G + \sum A_i (\cos a \cos b - \sin a \sin b) .$$

The terms comprising a have a magnitude which is like the product of the pitch angle, ψ , and the wave slope, $\tilde{\eta}k_i$. For surface vessels of interest these terms may be assumed to be small:

$$|\tilde{c}_{21}\tilde{\eta}k_i \cos\delta_i| = |-\cos\phi \sin\psi \tilde{\eta}k_i \cos\delta_i| \ll 1$$

$$|\tilde{c}_{23}\tilde{\eta}k_i \sin\delta_i| = |\sin\phi \sin\psi \tilde{\eta}k_i \sin\delta_i| \ll 1$$

This allows the small argument approximations for sine and cosine:

$$\sin(\epsilon) \approx \epsilon \quad \text{and} \quad \cos(\epsilon) \approx 1$$

for $\epsilon \ll 1$ -- to be substituted in the expression for wave elevation: This yields

$$\begin{aligned} \tilde{c}_{22}\tilde{\eta} = & -\tilde{c}_{12}\tilde{x} - y_G \\ & + \sum A_i \{ -(\tilde{c}_{21}\tilde{\eta}k_i \cos\delta_i \\ & - \tilde{c}_{23}\tilde{\eta}k_i \sin\delta_i) \sin b \\ & + \cos b \} \end{aligned}$$

which can be solved for the wave height. The formula for wave height,

$$\tilde{\eta} = \frac{-\tilde{c}_{12}\tilde{x} - y_G + \sum A_i \cos b}{\tilde{e}_{22} \sum A_i (\tilde{c}_{21}k_i \cos\delta_i - \tilde{c}_{23}k_i \sin\delta_i) \sin k}$$

is evaluated by the function subprogram.

Within the program unit, the variable A is used for the numerator, and the variable B is used for the denominator as the above expression is evaluated. The value returned by the function is $\tilde{\eta}$. The formal parameter, ZT, is the horizontal coordinate, \tilde{z} of the offset point. The value of this parameter and the values in the /ETA/ and /CT/ common blocks must be set before the function is referenced. Also arrays CZK and CYK in blank common must be assigned values before the function is used.

Subroutine STEER.

The STEER routine is called to compute the forces and moments resulting from the rudder of the ship. If the area of the rudder is zero, the subroutine simply executes a RETURN statement without any calculations. If the simulation includes a steering system, this routine computes the rudder angle that would be ordered by an autopilot, the actual rudder angle that the steering machinery would achieve and the forces and moments generated by the rudder.

The autopilot model includes proportionality factors (also called gain parameters) for yaw rate, yaw angle (or course error) and integral of yaw angle. The maximum rudder angle (or rudder stop angles) are included. Two types of deadband parameters (or weather adjustments) are provided in the model.

The rudder machinery is simulated as being able to rotate the rudder at a specified maximum rate or slower if that is required by the autopilot. The rudder is simulated as a vertical line segment in the ship's coordinate system. A single rudder on the ship's centerline is assumed. The area of the rudder, is assumed to be uniformly distributed along this line segment. The simulation includes the possibility of only part of the rudder being submerged. Lift and drag forces on the rudder are computed using constant lift and drag coefficients and instantaneous relative flow velocity averaged over the submerged part of the rudder line. The flow velocity includes wave motion, ship motion, and a wake velocity which is a constant in the ship coordinate system. The drag force is proportional to the absolute angle of attack and the square of the average velocity. A lift stall angle of one half radian is built into the subroutine. If the magnitude of the angle of attack is greater than the stall angle it is reduced to the stall angle. Lift is proportional to this limited angle of attack and the square of the average velocity.

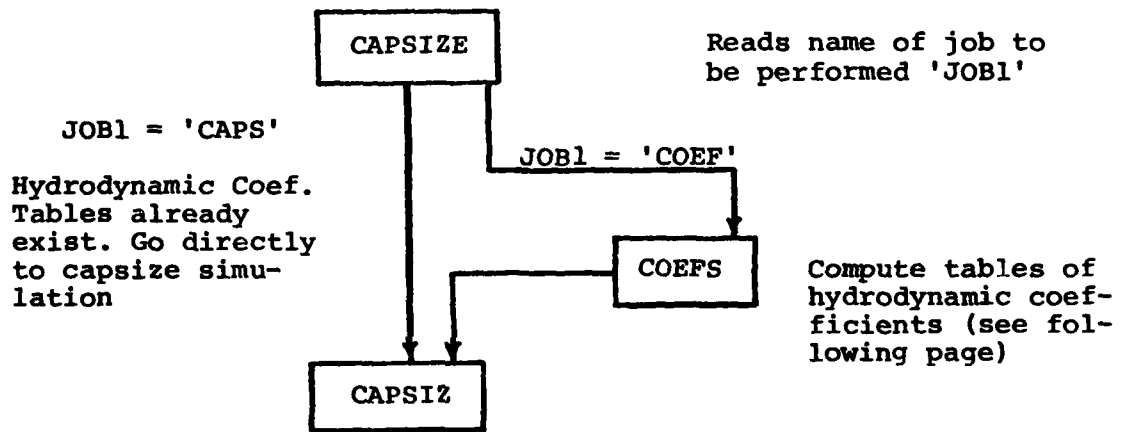
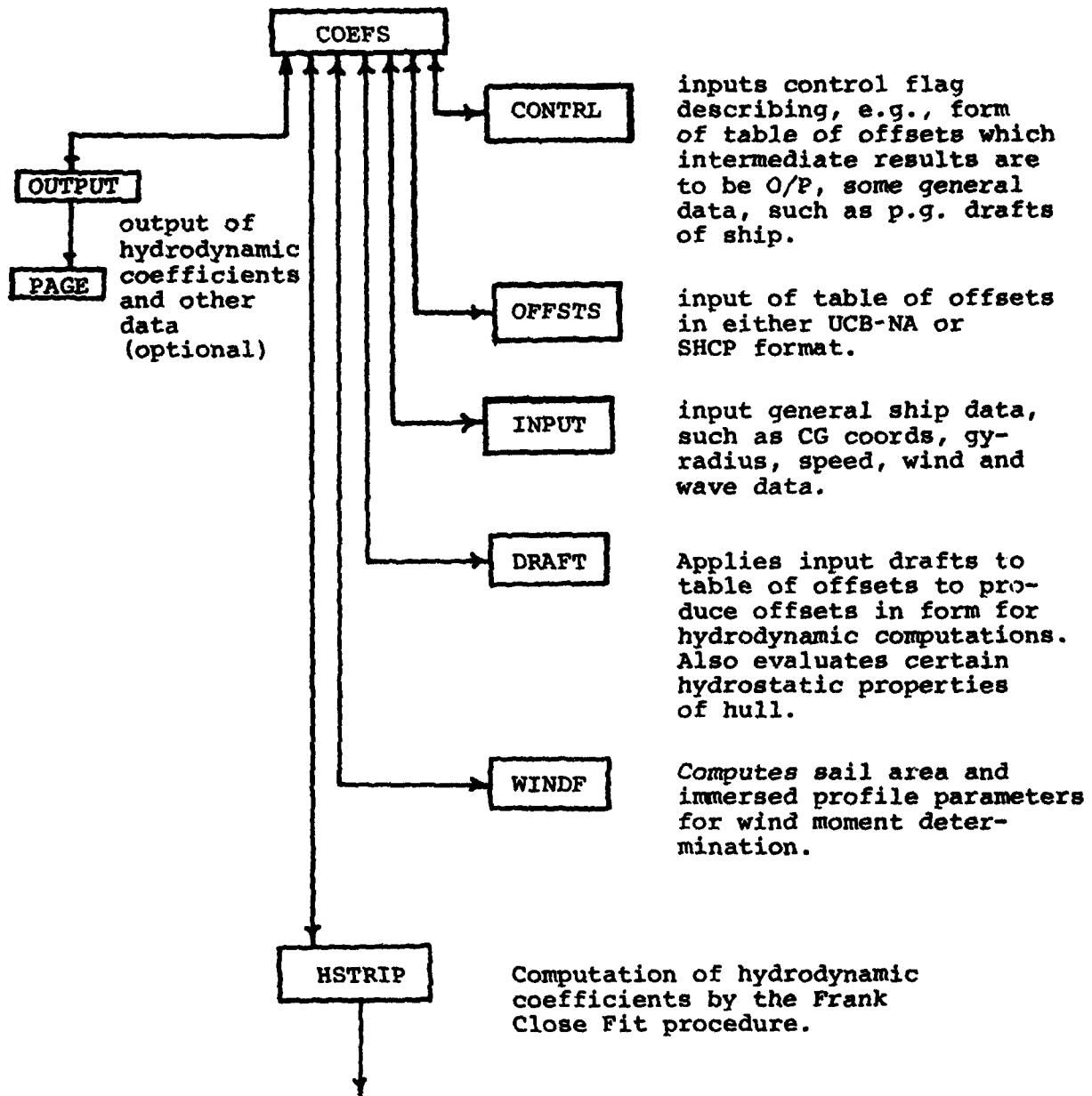


Figure E-1 Block diagram showing principal segments of program CAPSIZE.



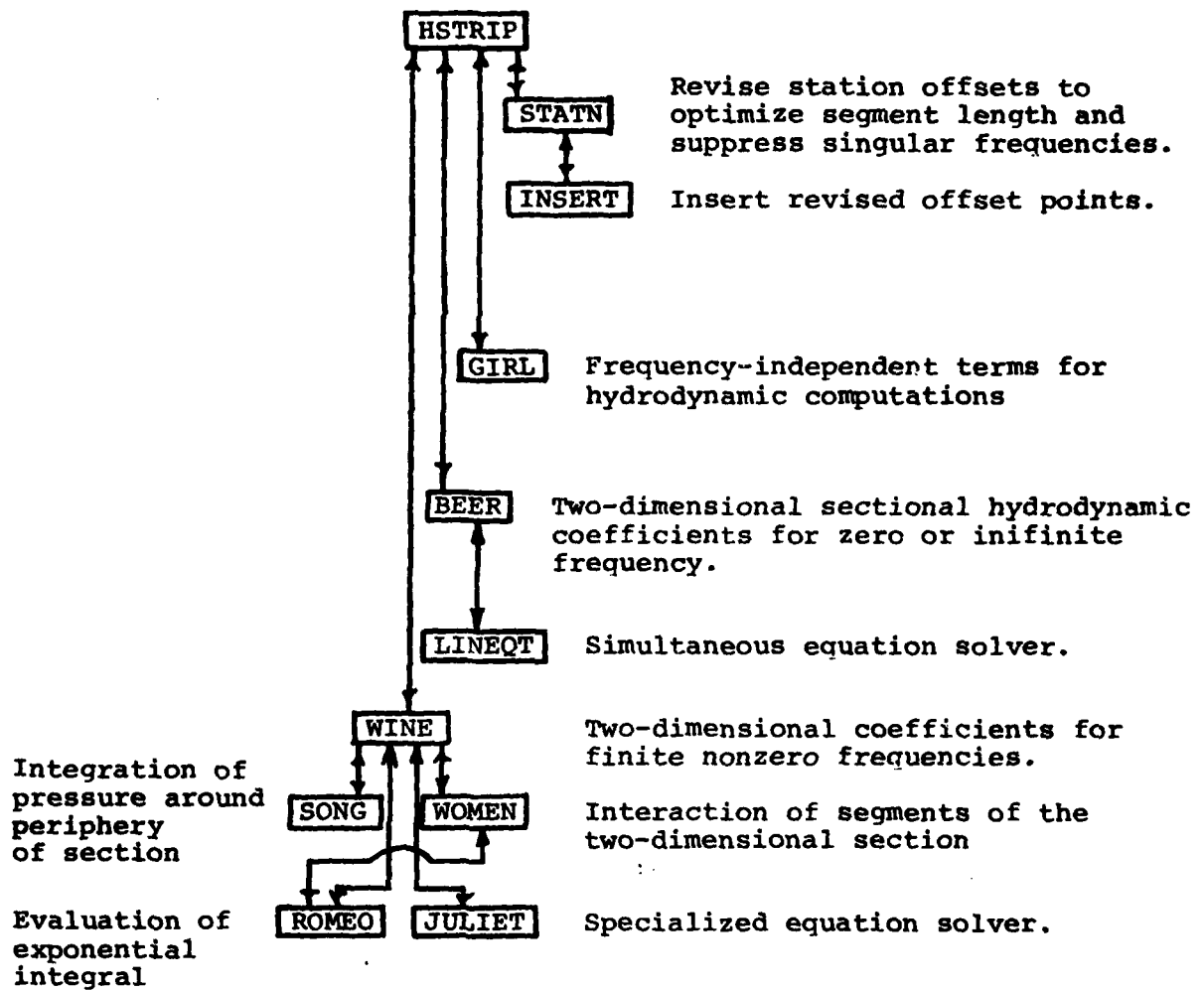


Figure E-2 Block diagram of principal segments of subroutine systems COEFS

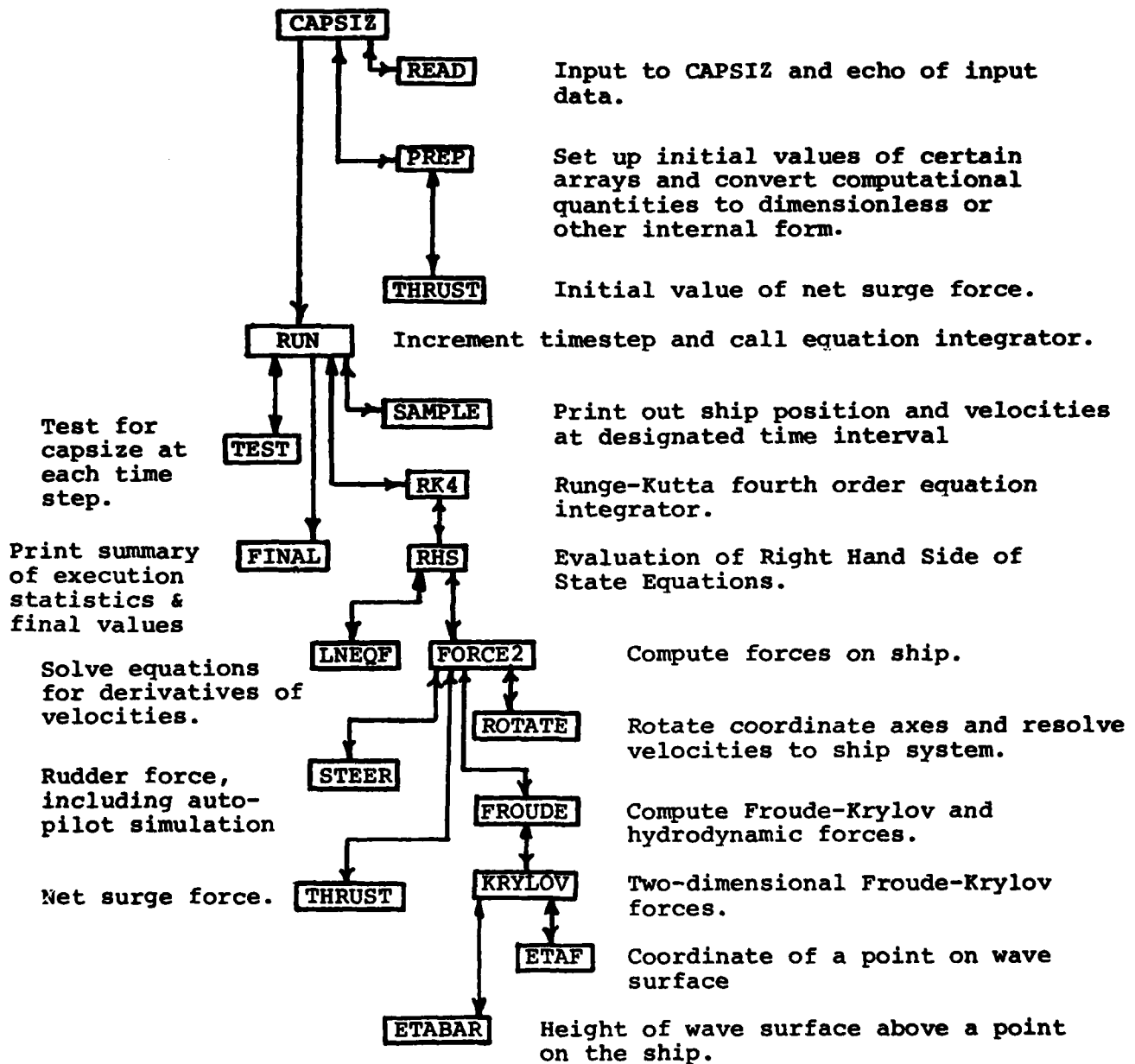


Figure E-3 Block diagram showing principal segments of subroutine system CAPSIZ

**DATA
FILM**